NASA CR108465

Submitted By:

W. J. Everett

Project Engineer

28 November 1964

Pioneer Parachute Company, Inc.

Projects E-2038 and E-2067

National Aeronautics and

Space Administration Contract NAS 9-1157

FACILITY FORM 602

N70-74729

(ACCESSION NUMBER)

237

(PAGES)

CR-108465

(NASA CR OR TMX OR AD NUMBER)

(THRU)

None

(CODE)

(CATEGORY)

FINAL TECHNICAL REPORT

PARA-SAIL EVALUATION AND DEVELOPMENT

VOLUME II

DESIGN AND TESTING OF

A LARGE PARA-SAIL PARACHUTE

DISTRIBUTION

NASA, Manned Spacecraft Center Procurement and Contracts Division General Research Procurement Office Houston 1, Texas Attn: Jack H. Goldstein	(1) Copy
Maj. James E. Ballweg (FTOP) Hdqs. AFFTC, Plans & Programs Division Edwards Air Force Base, California	(1) Copy
Mr. James V. Waite, (FTLGR) 6511th Test Group (P) El Centro Naval Air Station El Centro, California	(1) Copy
NASA, Manned Spacecraft Center Houston, Texas Attn: Marvin F. Matthews Patent Counsel	(1) Copy
NASA, Manned Spacecraft Center Mechanical System Branch Building 13 Clear Lake City Houston, Texas Attn: Leland Norman	(6) Copies
University of Minnesota Department of Aeronautics and Engineering Mechanics Minneapolis 55, Minnesota Attn: Dr. Helmut G. Heinrich	(2) Copies
Pioneer Parachute Company, Inc.	
Sales Department	(3) Copies
Engineering Department	
Manchester	(3) Copies
Minneapolis	(1) Copy

F O R E W A R D

This report was prepared under National Aeronautics and Space Administration Contract NAS 9-1157. The performance of the development effort of this contract was under the supervision of Mr. J. W. Kiker, Mr. J. K. Hinson and Mr. L. C. Norman of the Manned Space Craft Center, Mechanical Systems Branch, Houston, Texas. The technical contributions of these persons in the development of the Para-Sail parachute is gratefully acknowledged.

The author wishes to express his appreciation to personnel at the Joint Parachute Test Facility, El Centro, California, especially to the Project Officer, Mr. J. V. Waite, for the performance of the testing, data acquisition and reduction, and excellent photographic coverage.

Dr. H. G. Heinrich and staff of the Department of Aeronautics, University of Minnesota contributed immeasurably to the success of this program through experimental wind tunnel efforts and by many significant technical recommendations for improvement in design.

The author also extends his gratitude to Mr. E. A. Gimalouski of Pioneer Parachute Company for his consultatory assistance, to Mr. E. D. Vickery for coordinating the field tests and to Mr. W. R. Mueller for his efforts in design and aid in preparation of this report. The assistance of other members of this organizations Engineering and Technical Services Departments in data reduction, analysis, presentation of graphic material and preparation of the manuscript of this report is gratefully acknowledged.

ABSTRACT

A series of drop tests were performed with a large gliding parachute termed the Para-Sail. In the course of this testing, significant deployment and inflation difficulties were overcome and the performance and opening characteristics established. The aerodynamic coefficients determined in full size drop tests indicate good agreement with values from wind tunnel model studies.

From the test data an analysis is performed on the final configuration developed with regard to canopy stresses, inflated profile, and planform. An empirical opening shock relation is also established for the available range of data.

CONTENTS

Section	Title	Page
1.0	Summary	1
2.0	Introduction	3
3.0	Approach	9
3.1	Description of Test Items	10
3.2	Description of Test Programs	30
3.3	Data Acquisition	49
3.4	Data Evaluation	55
4.0	Test Results and Discussion of Data	67
4.1	Steady State Performance	67
4.2	Opening Characteristics	70
4.3	Observed Results	72
5.0	Design Analysis of the Final Configuration	95
5.1	Basic Canopy Shape	95
5.2	Determination of Nominal Diameter	96
5.3	Porosity and Area Distribution	97
5.4	Basic Engineering Geometry	98
5.5	Fabrication and Materials Studies	99
5.6	Para-Sail Component Strength	102
5.7	Determination of Stress	103
5.8	Weight and Volume of the Para-Sail	109
5.9	Planform and Profile	110
5.10	Opening Shock Factor	112
6.0	Conclusions and Recommendations	137

CONTENTS (CONT'D.)

Title	Page
References	140

APPENDIXES

A Derivation of Equations

B Materials Investigations

C Static Test Results

D Damage Charts

E Force Histories

F Drag Area Histories

G Lift/Drag Histories

ILLUSTRATIONS

Figure	Title	Page
1	The Para-Sail as an Ascending Canopy Under Tow -	6
2	Para-Commander - Deployable Personnel Para-Sail	6
3	Slot Arrangement and Nomenclature of an Ascending Para-Sail - - - - - - - - - - - - - -	7
4	Schematic Diagram of Aerodynamic Forces Acting on Para-Sail in Flight- - - - - - - - - - - - -	8
5	Para-Sail with Stabilizers and Centerline - -	18
6	Configuration 80L-1 - - - - - - - - - - - - - -	19
7	Configuration 80L-2 - - - - - - - - - - - - - -	20
8	Configurations 80L-3, 80L-4 - - - - - - - - - -	21
9	Configurations 80A-1, 80A-3 - - - - - - - - - -	22
10	Configuration 80A-2 - - - - - - - - - - - - - -	23
11	Configuration 80A-4 - - - - - - - - - - - - - -	24
12	Configuration 80A-5 - - - - - - - - - - - - - -	25
13	Configurations 80A-6, 80A-7, 80A-8, 80A-9 - -	26
14	a) Stabilizer Sleeves - Configuration 80A-4	
	b) Hesitator Bag - Configuration 80A-4 - - -	27
15	Schematic Arrangement of Deployment Aids on Reefed Para-Sail- - - - - - - - - - - - - - - -	28
16	Method of Inducing Canopy Roll Moment About a Vertical Axis - - - - - - - - - - - - - - - - -	29
17	Malfunction of Para-Sail Configuration 80L-1 During Preliminary Functional Tests - - - - -	62

ILLUSTRATIONS (CONT'D.)

Figure	Title	Page
18	Para-Sail Without Stabilizers Test No. 13 - -	63
19	Para-Sail as Damaged in Test No. 15 - - - - - -	64
20	Test of 24 Foot Diameter Para-Sail With Stabilizer Sleeves and Hesitator Bag- - - - -	65
21	Weight Bomb Vehicle With Para-Sail Attached -	66
22	Cylindrical Vehicle on Extraction Sled- - - -	66
23	Effective Drag Coefficient Vs. Canopy Loading	78
24	Effective Drag Coefficient Vs. Rate of Descent	79
25	Average Lift/Drag Vs. Canopy Loading - - - -	80
26	Average Lift/Drag Vs. Rate of Descent - - - -	81
27	Average Drag Coefficient Vs. Canopy Loading -	82
28	Average Lift Coefficient Vs. Canopy Loading -	83
29	Lift Coefficient Vs. Drag Coefficient - - - -	84
30	Turn Rate Vs. Time- - - - - - - - - - - - - -	85
31	Schematic Cording Diagram for 79.4 Foot Diameter Para-Sail- - - - - - - - - - - - - -	86
32	Typical Force Vs. Time History- - - - - - - -	87
33	Typical Trajectory Data - - - - - - - - - - - -	88
34	Proportionate Reefed Drag Area Vs. Canopy Loading - - - - - - - - - - - - - - - - - - -	89
35	Reefed Filling Time Vs. "C" Factor- - - - - -	90
36	Disreefed Filling Time Vs. "B" Factor - - - -	91
37	Reefed Opening Force Vs. System Momentum- - -	92
38	Disreefed Opening Force Vs. System Momentum-	93
39	Internal Parachute Inflation Characteristics-	94

ILLUSTRATIONS (CONT'D.)

Figure	Title	Page
40	Basic Canopy Shape for a Large Para-Sail - -	122
41	Typical Gore Pattern for 79.4 Foot D_o Para-Sail, Ident. No. 80A-9 - - - - - - - - - - - -	123
42	General Geometry 79.4 Foot D_o Para-Sail, Ident. No. 80A-9 - - - - - - - - - - - - - - -	124
43	Para-Sail 79.4 Foot D_o Engineering Planview, Ident. No. 80A-9 - - - - - - - - - - - - - - -	125
44	Cross Sectional Views of Seam Constructions Studied- - - - - - - - - - - - - - - - - - - -	126
45	Results of Destructive Static Tests of Para-Sail Components- - - - - - - - - - - - - - - -	127
46	Opening Force Vs. Filling Time - - - - - - -	128
47	Diameter Ratio Vs. Filling Time- - - - - - -	129
48	Calculated Weight and Volume for Para-Sail Recovery Parachutes- - - - - - - - - - - - - -	130
49	The Effect of Canopy Loading on Major and Minor Axes of Para-Sail Planform - - - - - - -	131
50	The Effect of Canopy Loading on Semi-Minor Axes of Para-Sail Planform - - - - - - - - - -	131
51	Inflated Profile of 79.4 Foot Diameter Para-Sail -	132
52	Gore Curvature, Arc/Chord Ratio Vs. Gore Length -	133
53	Center of Pressure, Para-Sail 80A-9- - - - - -	134
54	Disreefed Opening Shock Factor - - - - - - - -	135

ILLUSTRATIONS (CONT'D.)

Figure	Title	Page
55	Reefed Opening Shock Factor - - - - - - - - -	135
56	Reefing Line Diameter Ratio Vs. Drag Area Ratio -	136

Photo Credits

National Aeronautics and Space Administration
Manned Spacecraft Center, Pages 18, 62.

U. S. Naval Parachute Facility, El Centro, Calif.*
- Broom, Frontispiece, Neg. No. 013736
- Sphar, Page 63, Neg. No. 12936
- Calkins, Page 66, Neg. No. 11710
- Francouer, Page 66, Neg. No. 12625

Cameron, L. C., Page 64

Pioneer Parachute Company, Inc., Pages 6, 7, 27, 65

* Official U. S. Navy Photographs - Not for publication unless officially released.

TABLES

Table	Title	Page
I	Test Program Plan, El Centro Project L1C-9211	59
II	Comparison of Lift/Drag Ratios Computed From Rawin Balloon and Drift Chute Data - - - - - -	60
III	Comparison of Average Effective Drag Areas and Coefficients Based on Density and Time - - - -	61
IV	Steady State Forces on Individual Risers - - -	74
V	Opening Forces on Individual Risers- - - - - -	75
VI	Inflation Characteristics of a 10 Foot Diameter Ribless Guide Surface Internal Chute - - - - -	76
VII	Para-Sail Test Data Summary- - - - - - - - - - -	77
VIII	Area and Porosity Distribution in Para-Sail 80A-9- -	115
IX	Characteristics of Materials Investigated for Application in the Para-Sail Parachute - - - -	116
X	Summary of Seam Test Investigations- - - - - -	117
XI	Calculation of Canopy Cloth Stress - - - - - -	118
XII	Para-Sail Weights and Volumes- - - - - - - - -	119
XIII	Comparison of Specific Drag Areas for Large Parachutes - - - - - - - - - - - - - - - - - -	120
XIV	Summary of Opening Shock Variables - - - - - -	121

LIST OF SYMBOLS

NOTE: Primed symbols, A', B', C', etc., refer to Figures 41, 42 and 43 and are related to the dimensional geometry of the configuration.

A - A parametric factor relating to opening shock. Equal to $\frac{2W}{C_D S \rho t_f g V}$

$\bar{A}$ - The area under the velocity density curve.

a - The major axis of Para-Sail planform.

$\bar{a}$ - Linear acceleration.

B - A parametric factor relating to disreefed filling time. Equal to $\frac{D_o}{V_{DR} W} \cdot \frac{\rho}{\rho_o}$

b - The minor axis of Para-Sail planform.

C - A parametric factor related to reefed filling time. Equal to $\frac{D_{R_1}^2}{V_{LS} W} \cdot \frac{\rho}{\rho_o}$

c - 1.055 strength loss factor related to convergence angle.

C_D - Aerodynamic drag coefficient.

$C_{D_{eff}}$ - Effective drag coefficient, based on vertical velocity.

C_L - Aerodynamic lift coefficient.

$C_{D_{eff}} S$ - Effective drag area, based on vertical velocity.

$(C_D S)_o$ - Drag area of fully opened canopy, equivalent to $C_{D_{eff}} S$.

$(C_D S)_R$ - Drag area of reefed canopy.

D - Aerodynamic drag force.

D_F - Diameter of the fully opened reefed canopy.

D_o - Nominal diameter, based on canopy area.

D_p - Projected diameter.

D_{R_1} - Reefing line circle diameter.

D_{R_o} - Projected diameter of fully opened Para-Sail (average of major and minor axes).

e - .95 factor related to strength loss due to abrasion.

F - Opening force - general.

F_c - Centrifugal force.

F_I - Internal parachute opening force.

F_o - Disreefed opening force.

F_R - Reefed opening force.

F_{RL} - Force in the reefing line.

F_{RR} - Force applied to the reefing ring.

F_{SL} - Force applied to a suspension line.

F_{ult} - Ultimate force at which failure occurs.

g - Local acceleration of gravity.

H - A factor equivalent to $\sqrt{\frac{2W}{C_{D_{eff}} S}}$

h - Altitude, vertical distance.

h_a - Initial altitude.

h_b - Final altitude.

j - 1.5 safety factor.

K - Factor indicating the relationship between various parachute canopy types.

k - .95 factor related to strength loss due to fatigue.

L - Aerodynamic lift force.

L_S - Cloth stress in the canopy fabric.

l - Distance between skirt of internal canopy and primary canopy skirt in deflated condition.

M - Mass.

N - Number of gores.

n - Number of spaces between reefing rings.

o - .95 factor related to strength loss due to water absorption.

P - Gore curvature chord length.

Q - Gore curvature arc length.

q - Dynamic pressure, general.

q_i - Dynamic pressure at time of full inflation.

q_{SE} - Dynamic pressure at skirt emergence from deployment bag.

q_{DR} - Dynamic pressure at disreef.

q_{SL} - Dynamic pressure at line stretch.

R - Vertical resultant of lift and drag forces.

S - Reference area of canopy.

S_o - Area of canopy based on representative gore.

T - Thrust.

t - Time.

t_f - Filling time general.

t_a - Initial time.

t_b - Final time.

t_{f_1} - Reefed filling time.

t_{f_2} - Disreef to full open filling time.

u - .8 factor related to strength loss due to sewing.

V_A - Total velocity with respect to the air mass - wind corrected.

V_{DR} - Total velocity at disreef - wind corrected.

LIST OF SYMBOLS (CONT'D.)

V_H - Horizontal velocity component, not wind corrected.

V_{LS} - Total velocity at line stretch, wind corrected.

V_T - Total velocity, not wind corrected.

V_{TP} - Tangent plane velocity, equivalent to V_H wind corrected.

V_V - Vertical velocity.

$\overline{V_e}$ - Average vertical velocity.

W - Total weight, parachute and load.

x - Decreasing shock factor.

y - Semi-minor axis, forward planform ellipse.

z - Semi-minor axis, rear planform ellipse.

α - Angle between Para-Sail centerline and front center suspension lines.

β - Angle between Para-Sail centerline and rear center suspension lines.

Δ - A difference or change in quantities.

δ - Reefing line diameter ratio.

θ - Airfoil angle of attack (chord line with respect to direction of flow).

λ_m - Air permeability - (mechanical porosity).

ρ - Atmospheric density.

ρ_a - Initial density.

ρ_b - Final density.

ρ_{DR} - Density at time of disreef.

ρ_{LS} - Density at time of line stretch.

ρ_o - Sea level density.

ϕ - Stable angle of attack (parachute centerline with respect to flow).

1.0 SUMMARY

This report traces the development of a large Para-Sail parachute for application as a gliding decelerator for the recovery of heavy space craft where maneuverability during final descent through the atmosphere is required. This effort was performed by the Pioneer Parachute Company, Inc., under National Aeronautics and Space Administration Contract NAS 9-1157.

The design of such a Para-Sail originated with a small personnel sized version which was capable of lifting attached individuals into the air when towed behind a vehicle or boat. This phenonomen was achieved by virtue of the high lift/drag ratio of the canopy which was shown in wind tunnel tests to be in the order of .8.

Based on the successful principles of the smaller canopy, a Para-Sail of approximately 80 feet in diameter was designed and test programs initiated.

Numerous deployment and inflation problems insued with the large canopy, traceable to many of the unconventional features which were responsible for the high steady state performance evidenced in tests. As a result of these difficulties, numerous modifications were made to the original design including a change in gore shape, elimination of the center suspension line, changes in slot geometry and the introduction of an internal parachute to improve inflation.

The end product of this development program was a Para-Sail of 79.4 feet in diameter which was capable of successful deployment at 154 knots (dynamic pressure of 80 PSF) with a 4,750 pound weight. Opening forces were in the order of 15,000 pounds. Lift/drag ratios averaging 1.13 were developed at canopy

loadings of 0.96 lbs./ft.^{2}, corresponding to a glide angle with respect to the horizontal of 41.5 degrees. An effective drag coefficient, based on vertical velocity, of 1.47 was established at the above value of canopy loading. Fixed turn rates of 18.5 degrees per second were obtained by inverting radial slots on one side of the canopy.

An analysis was performed of the strength of structural components with an empirical study of the stress in these parts being made also. The results of this work indicated the need for improvement of strength in certain areas.

Opening shock factors are established and data relating to canopy planform and profile presented.

It will be concluded that the capabilities of the developed Para-Sail successfully met the requirements and objectives of the program. Recommendations are made regarding improvement in fabrication, materials, design geometry, deployment aids, packaging and the need for additional investigations.

2.0 INTRODUCTION

In January of 1963, Pioneer Parachute Company, Inc., under National Aeronautics and Space Administration Contract NAS9-1157, undertook a program of evaluation and development of a large Para-Sail Parachute capable of recovering heavy payloads and providing a significant degree of gliding and maneuvering characteristics. In March 1964 all test work under this contract was successfully completed.

In the course of this program the principle aerodynamic coefficients for this type of parachute were established in wind tunnel tests. Utilizing the wind tunnel as an investigative tool, studies were made of methods to improve upon these coefficients and to establish better inflation characteristics. These efforts were performed by the University of Minnesota, Department of Aeronautics and Mechanics, and are reported in Volume I of this document, entitled "Aerodynamic Investigations of Para-Sail Parachutes".

The results of the wind tunnel experiments were validated by a series of full scale developmental drop tests with a Para-Sail of approximately 80 feet in diameter. These tests were conducted at the Joint Parachute Test Facility, El Centro, California and are described in this volume together with test results and design aspects of the developed Para-Sail.

The Para-Sail Parachute was invented in France by Monsieur Pierre Lemoigne. The United States patent rights to this parachute were acquired by the Pioneer Parachute Company, Inc. which has since continued with the development of this item. The Para-Sail, as originally conceived, was intended as

a novelty parachute which by virtue of its relatively high lift/drag ratio (approximately .8) and inherent stability, was capable of lifting attached personnel into the air when the parachute was towed behind a vehicle, as is shown in Figure 1. The original configuration served as a basis for the design of a deployable version of the same size (approximately 25 feet in diameter) for use in sport parachuting. This particular version was trade named the Para-Commander and is illustrated in the photograph of Figure 2. The next step in the development of deployable Para-Sails was concerned with the subject canopy of this report.

In addition to the 25 and 80 foot diameter Para-Sails mentioned above, other designs of 12, 40, 51 and 70 foot diameter have since been fabricated and tested successfully. Para-Sails have been used for various purposes such as the accomplishment of point landings by remote control, sport parachuting, towing as an ascending parachute for personnel and aerial target practice, and various recovery projects. Through these efforts considerable experience has been gained in towing techniques, deployment methods, turn control, lift/drag modulation and design characteristics.

The gliding capability of the Para-Sail is due in part to the controlled exhaust of internal air pressure through strategically placed slots and louvers in the surface of the canopy, as shown in Figure 3. In addition, airflow over the non-porous leading surface induces a lift force which further increases horizontal velocity and decreases vertical velocity. The aerodynamic forces are portrayed schematically in the diagram of Figure 4.

The development of the program under Contract NAS 9-1157 has proceeded with the ultimate objective of establishing the Para-Sail parachute as a reliable and efficient gliding decelerator capable of recovering large manned spacecraft, where maneuverability during descent through the atmosphere is desired.

A series of preliminary requirements for such a parachute are defined in Reference 1 and are summarized as follows:

Payload Weight	-	4,750 Lbs.
Deployment Speed	-	154 KEAS
Lift-Drag Ratio	-	1 or better
Canopy Turn Rate	-	10 Deg./Sec.
Rate of Descent	-	30 FPS Maximum
Deployment Altitude	-	10,600 Ft.

The technical approach utilized in fulfilling the above requirements is discussed in Section 3. Section 4 deals with specific results of the test program and Section 5 presents a design analysis of the final configuration. Conclusions and recommendations are included in the final section.

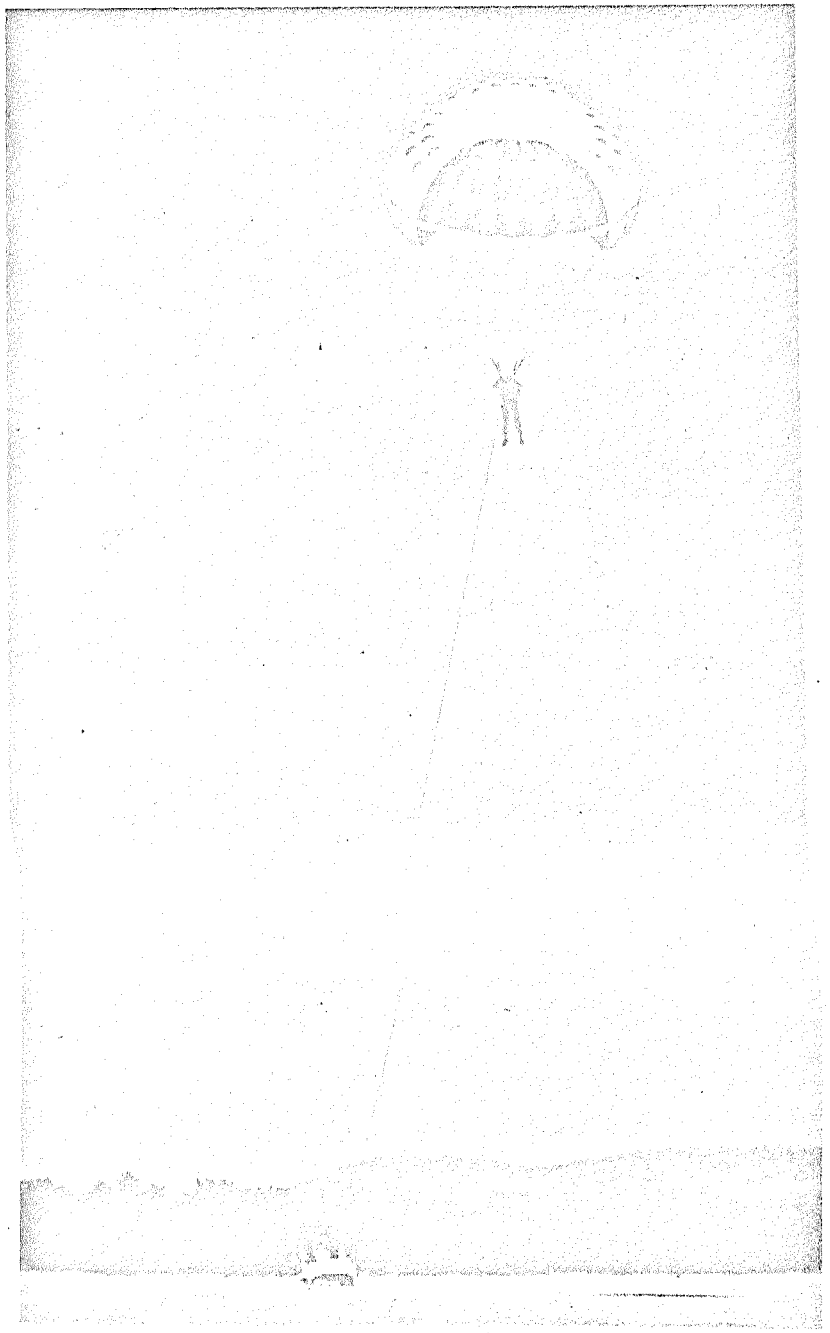

Figure - 1 -
The Para-Sail as an Ascending
Canopy Under Tow

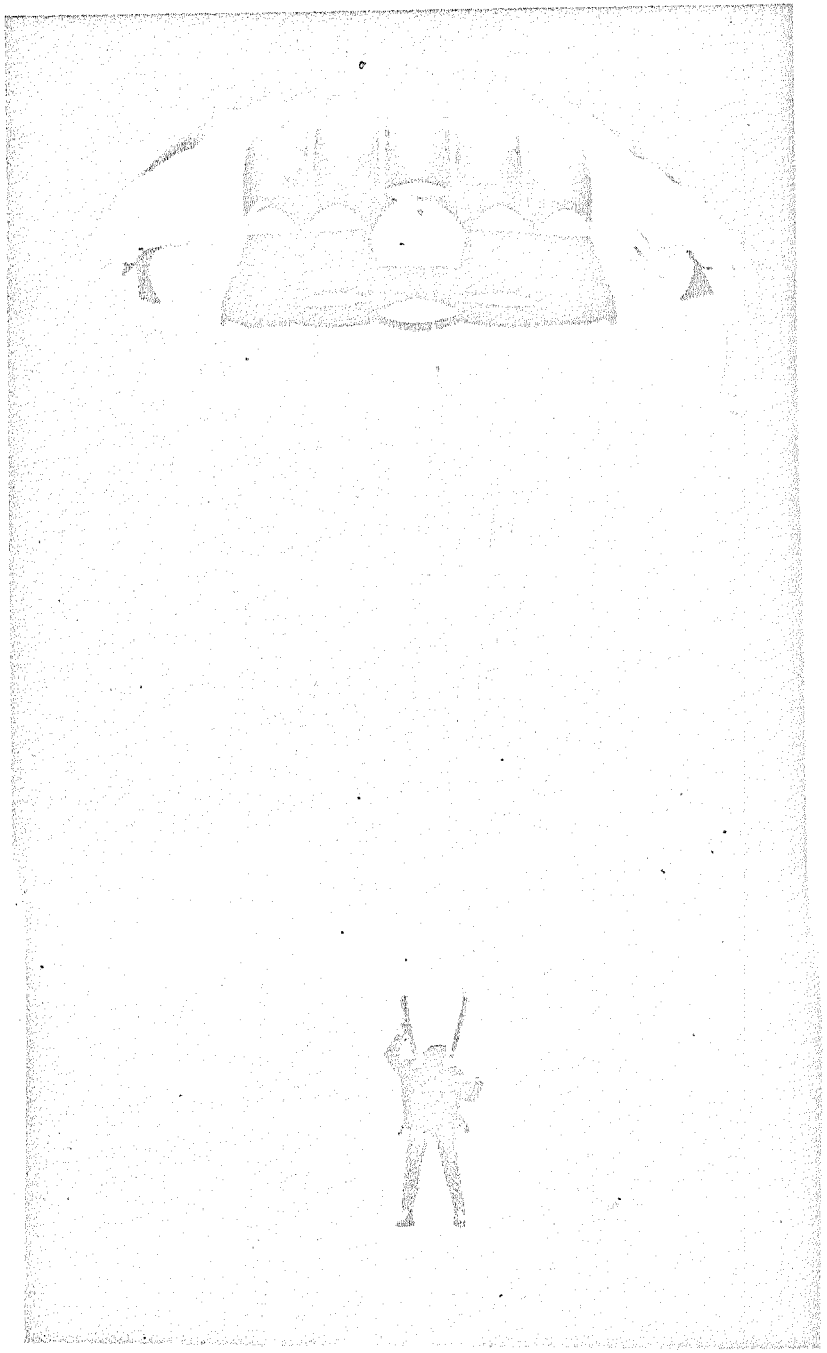

Figure - 2 -
Para-Commander - Deployable
Personnel Para-Sail

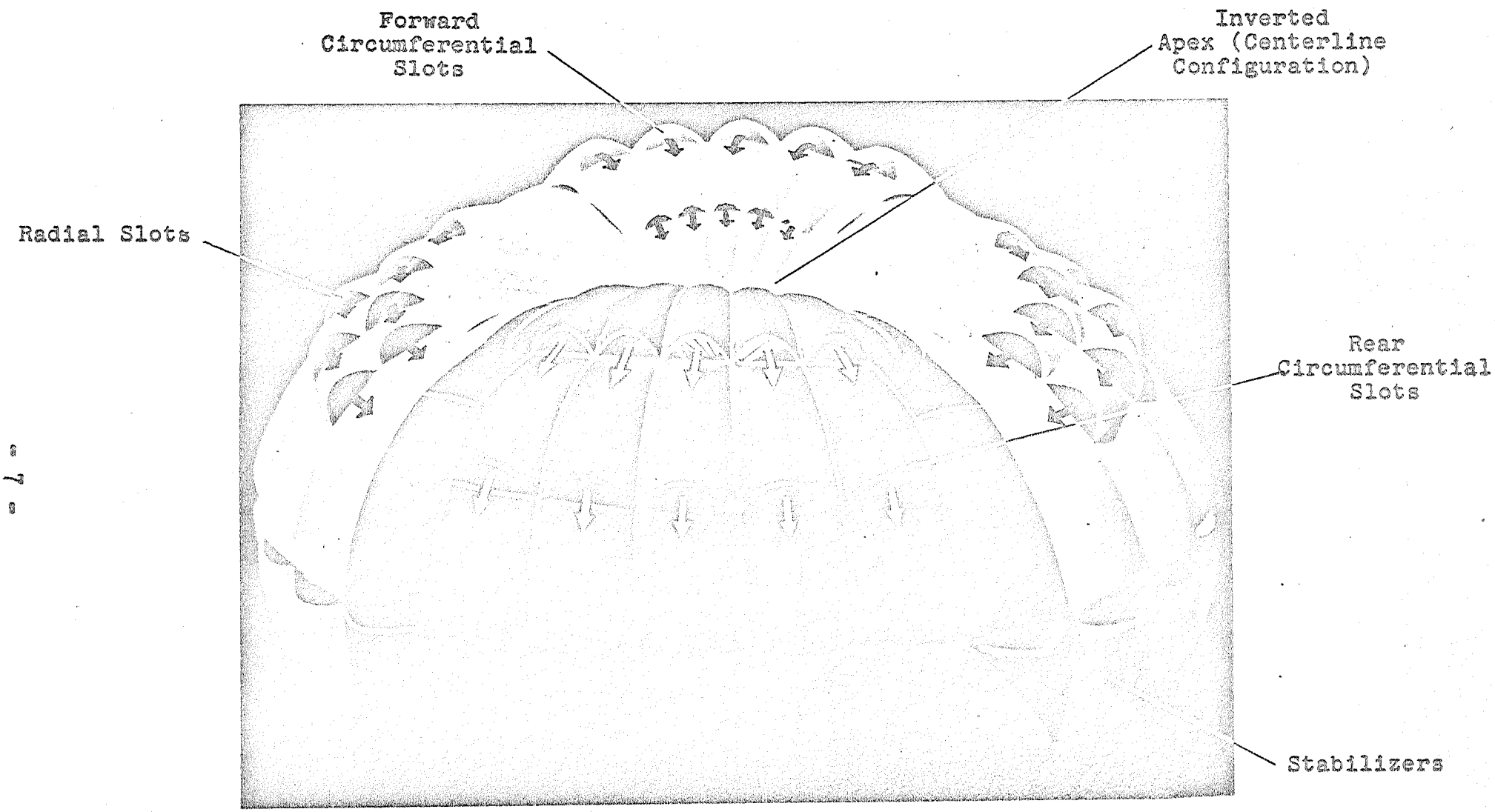

Slot Arrangement and Nomenclature
of an Ascending Para-Sail

Figure - 3 -

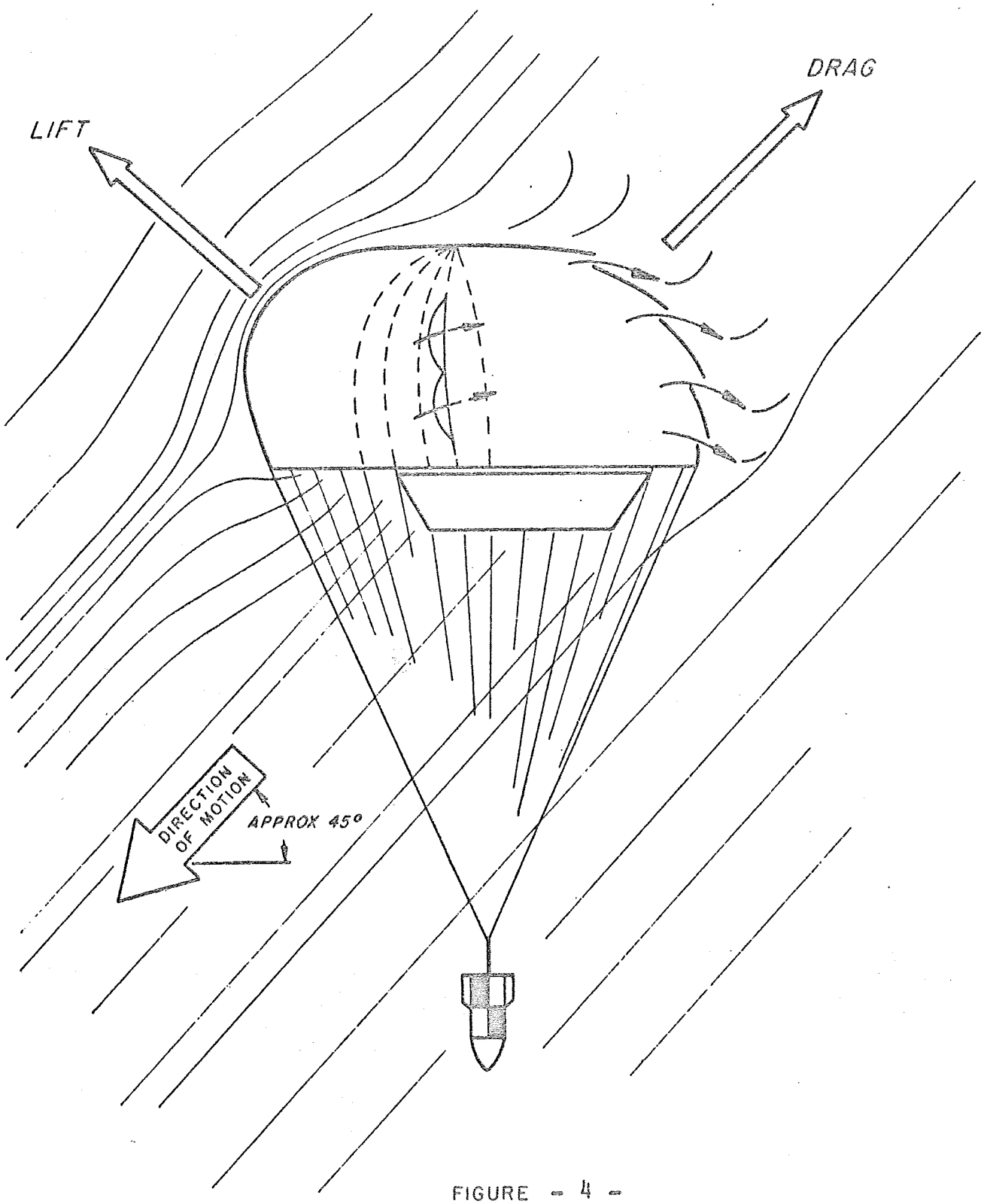

FIGURE - 4 -
SCHEMATIC DIAGRAM OF AERODYNAMIC
FORCES ACTING ON PARA-SAIL IN FLIGHT
(VIEWED IN CROSS SECTION)

3.0 APPROACH

The objectives of this program were approached primarily through actual drop testing of the full sized Para-Sail. This effort was augmented by a wind tunnel program for the purpose of establishing and improving the aerodynamic characteristics of the Para-Sail parachute and aided by a series of standby wind tunnel projects which provided technical guidance when development problems arose.

Initial design work on the full size Para-Sail was performed by the inventor, Monsieur Lemoigne, serving as a consultant at the contractor's facility. The geometric configuration of the parachute, including appropriate dimensions and materials were indicated. From this information a complete design was developed and fabrication commenced on a Para-Sail of approximately 80 feet in diameter.

Numerous modifications to this design resulted after deployment and inflation difficulties were encountered in early functional drop tests conducted by the National Aeronautics and Space Administration, Manned Space Craft Center, Houston. To an extent these difficulties were solved, at least in such a manner that recovery of the test vehicle could be anticipated, and testing was therefore initiated at the Joint Parachute Test Facility, El Centro, California, as originally planned. Throughout this program deployment and inflation problems persisted which were solved by modifications to the previous configuration. Variations of canopy geometry were investigated as well as rigging procedures and deployment aids.

This report will describe only briefly the efforts and modifications produced prior to commencement of the primary

developmental testing at El Centro, but shall deal in more detail with both the configurations and the related testing which occurred during these tests. The following sub-sections will deal with a description of the test items, the test programs, and the methods of data acquisition and evaluation.

3.1 Description of Test Items

3.1.1 Configuration 80L-1 (see foldout Figure 6).

This configuration constituted the initial design effort under this program. A realistic stress analysis was not possible with this unit since little or no information was available regarding load and stress distribution, or opening characteristics. Consequently, structural design was generally based on practices current with standard parachutes of the same size and application.

However, one feature of the selected construction was based on experience gained with the Para-Commander personnel parachute, which utilized what is termed a butt seam. In this construction the radical main seams are formed by butting adjacent panels together, rather than overlapping and locking, thereby supporting circumferential stress via the filling threads of the main seam tape. Although something of a deviation from standard parachute construction, it was felt that certain advantages were offered through reduction of material for seam allowance and greater ease of fabrication.

Seam tests were performed, and although efficiency was not as high as with similar lock seams, it was considered adequate due to the apparent over-strength of the material. Seam construction representative of configuration 80L-1 may be seen in Figure 44I of Section 5.5.2.

Another significant construction feature of this first design was the formation of panels on the straight of the goods as is normally done with Ring Slot canopies. The trapezoidal panel shape dictated by canopy geometry necessitates this type of construction for economical use of cloth.

Canopy materials of a sufficiently low porosity (nearly zero) were quite limited in availability and consequently a nylon taffeta cloth which had been used successfully in both the smaller towable and deployable Para-Sails was utilized for the major portion of the canopy. This material actually serves as a base fabric in military pneumatic mattress applications and is covered by specification MIL-M-10747D.

A number of particularly novel features of the smaller Para-Sails were retained in the design of the 80 foot diameter Para-Sail, among these being a centerline which inverted the canopy apex in the inflated condition, and stabilizer panels arranged below the skirt, as shown in Figure 5.

An 8 foot diameter ribless guide surface parachute was used as pilot chute and a deployment bag provided to allow a lines first type of deployment. The parachute was deployed with the apex withdrawn inside the canopy by the centerline, which was prevented from burning the canopy by means of a protective rayon sleeve.

It was this configuration upon which initial testing commenced and which was subsequently modified in a number of steps so that at the outcome of these tests the following configuration defined as 80L-2 emerged. The manner of

achieving this design is discussed more fully in Section 3.2.1.

3.1.2 Configuration 80L-2 - (see foldout Figure 7)

The features of primary significance in this configuration were the replacement of the rearward opening circumferential slots in the front of the canopy with solid gores, and the removal of cloth from the leading (forward) surface skirt producing gores of varying length with up to a 40 inch reduction in length at the centermost gore.

A second vital modification was the inclusion of a 10 foot diameter ribless guide surface internal parachute, to assist in inflation. Among the less significant features were shortened rear risers, pocket bands on the forward skirt, longer suspension lines, and three forward facing slots in the front center gores near the skirt, intended to serve as pockets which would aid in inflating the front section of the canopy. In addition, a crown stabilization parachute was permenently attached in such a manner that a confluence point did not exist, allowing the parachute to collapse when the Para-Sail commenced to glide, thereby reducing drag on the front portion of the crown thru the attaching bridle.

3.1.3 Configuration 80L-3 - (see foldout Figure 8)

This configuration involved the addition of some slots in the upper crown section of the canopy and a change in rigging of the crown stabilization parachute. Rear risers were shortened as in the previous configuration, but provided with a 20 second delay for release to full length.

3.1.4 Configuration 80L-4 - (see foldout Figure 8)

The most significant change in this configuration was a change in location of the internal parachute so that the skirt position was actually outside the leading edge of the Para-Sail skirt. Reefing line length was shortened significantly and rear risers were foreshortened permanently with no provision for their extension.

3.1.5 Configuration 80A-1 (see foldout Figure 9.)

Possibly the most significant improvement in canopy inflation characteristics and reduction of opening loads occurred with this configuration through elimination of the center suspension line and inverted apex. To retain somewhat of the shallow profile exhibited by previous designs, canopy shape was modified from biconical to triconical. The upper conical crown portion was removed and replaced with a flat circular section. In actuality, an existing Para-Sail was modified in just this manner, splicing main seams and joining the old and new portions together at a cross seam. The new upper section was manufactured of lock seam, bias construction for maximum strength. A rather large vent of 68 inches in diameter was incorporated in the design to lessen opening shock. The previously used internal parachute was retained at the same location with respect to the Para-Sail skirt.

3.1.6 Configuration 80A-2 1/- (see foldout Figure 10).

The internal parachute was removed for this configuration, which was otherwise similar to 80A-1.

1/ References to this configuration in Volume 1, particularly page 15 should indicate Configuration 80L-2.

3.1.7 Configuration 80A-3 1/ - (see foldout Figure 9).

The geometry of this configuration was identical to that of 80A-1. Differences were of a construction nature, in which the canopy was fabricated throughout of bias cut, lock seam construction, with continuous circumferential reinforcing tapes. Bias construction was accomplished by cutting trapezoidal panels on a 45° bias utilizing wide goods. Considerable material is wasted in this manner, but added strength is theoretically gained in the seams.

3.1.8 Configuration 80A-4 - (see foldout Figure 11).

Canopy geometry and rigging were identical to the previous configuration. Two additional deployment aids were utilized however. These consisted of a nylon sleeve or boot which tied around each group of stabilizer panels, as shown in Figure 14a and a skirt hesitator bag, much like a personnel parachute quarter bag except that closure was accomplished by means of a butterfly loop on a suspension line and a locking loop on a main seam, in much the same manner as the military 64 foot diameter cargo parachute, the G-12C. This arrangement is shown in Figure 14b. It was necessary to increase strength of the line attaching to the "butterfly" in order to accommodate the anticipated stresses in opening the hesitator bag closure. This configuration also adopted the elastic vent hood often used on personnel parachutes. This hood is comprised of a cylinder of cloth of such size that one end could be attached to the upper lateral band of the canopy. The

1/ Reference to this configuration in Volume 1 particularly pp 15 should indicate Configuration 80L-3.

other end is fitted with an elastic cord which contracts to a diameter much smaller than of the normal vent but which will also enlarge under internal canopy pressure.

3.1.9 Configuration 80A-5 - (see foldout Figure 12).

This configuration represents the modification of 80A-1 Para-Sail by removal of the stabilizer panels. The internal parachute was retained along with the other features of this configuration.

3.1.10 Configuration 80A-6 - (see foldout Figure 13).

The geometry of this design was identical to 80A-4. The 8 foot diameter pilot/stabilizer parachute was changed to 6 feet. The hesitator bag of 80A-4 was eliminated but the nylon sleeve or boot retained. Stabilizer panel reefing was added by attaching reefing rings to the lower, inside edge of these panels, so that when folded, a 550 pound line could be passed through these rings and an adjacent reefing cutter and secured upon itself. In this manner two separate groups of reefed stabilizer panels were formed on each side of the canopy. Reefing was such as to permit stabilizer disreefing two seconds prior to skirt disreefing.

3.1.11 Configuration 80A-7 - (see foldout Figure 13).

This configuration is related to 80A-4 and 80A-6. The higher strength suspension line attaching to the "butterfly" of Configuration 80A-4 was replaced with a normal strength line. The stabilizer panel reefing and nylon boot were retained from 80A-6. The three forward facing slots in the center front gores near the skirt were reduced in area by attaching at the center to an adjacent cross seam and reinforcing with a tape. Reefing ring attachment at the skirt was strengthened.

3.1.12 Configuration 80A-8 - (see foldout Figure 13)

Only minor changes in construction and rigging occurred in this configuration. These changes consisted of an increase in diameter and strength of the elastic vent cord, the addition of a reinforcing band between panels 10 and 11 and an increase in the tensile strength of the reefing line.

The most notable change involved the manner of installing the reefing line. In this configuration, the line was passed directly through the rings on the gores adjacent to the stabilizer panels, the remainder of the line being evenly distributed among the gores fore and aft of the stabilizer panels.

Stabilizer panel reefing and boot were retained from the previous configuration. Figure 15 illustrates the manner in which rigging and deployment aids were employed to control opening.

3.1.13 Configuration 80A-9 (see foldout Figure 13)

This configuration is essentially the same as that of 80A-8 with the only modification being the change from nylon to cotton webbing of the stay line connecting apex of internal parachute to apex of Para-Sail.

This configuration was utilized in conducting turn tests and was additionally modified in the following manners:

1st Approach

a) An 8 foot diameter pilot chute was substituted for one of 6 foot diameter because of low drop speeds.

b) All turn slots on one side of the canopy were closed. In so doing a radial slit remained, but with fullness

being gathered and stitched to the main seam below the slot. In accomplishing this, loops attached to each slot panel were secured to the main seam. A total of twelve panels were closed in this manner.

2nd Approach

a) An 8 foot diameter pilot chute was substituted for one of 6 foot diameter because of low drop speeds.

b) For each of the two rows of slots on one side of the canopy, a nylon cord joined at the vent of the Para-Sail, was passed through the inside of the canopy, attaching to the connector links, its length being equal to the stretched out length of canopy and suspension lines. Stitched in the center of each turn slot panel was a tape, beginning at the leading edge and extending a short distance beyond the trailing edge, terminating in a small reefing ring. Each of the nylon cords mentioned above passed through these rings. Figure 16 illustrates the manner in which this system is arranged.

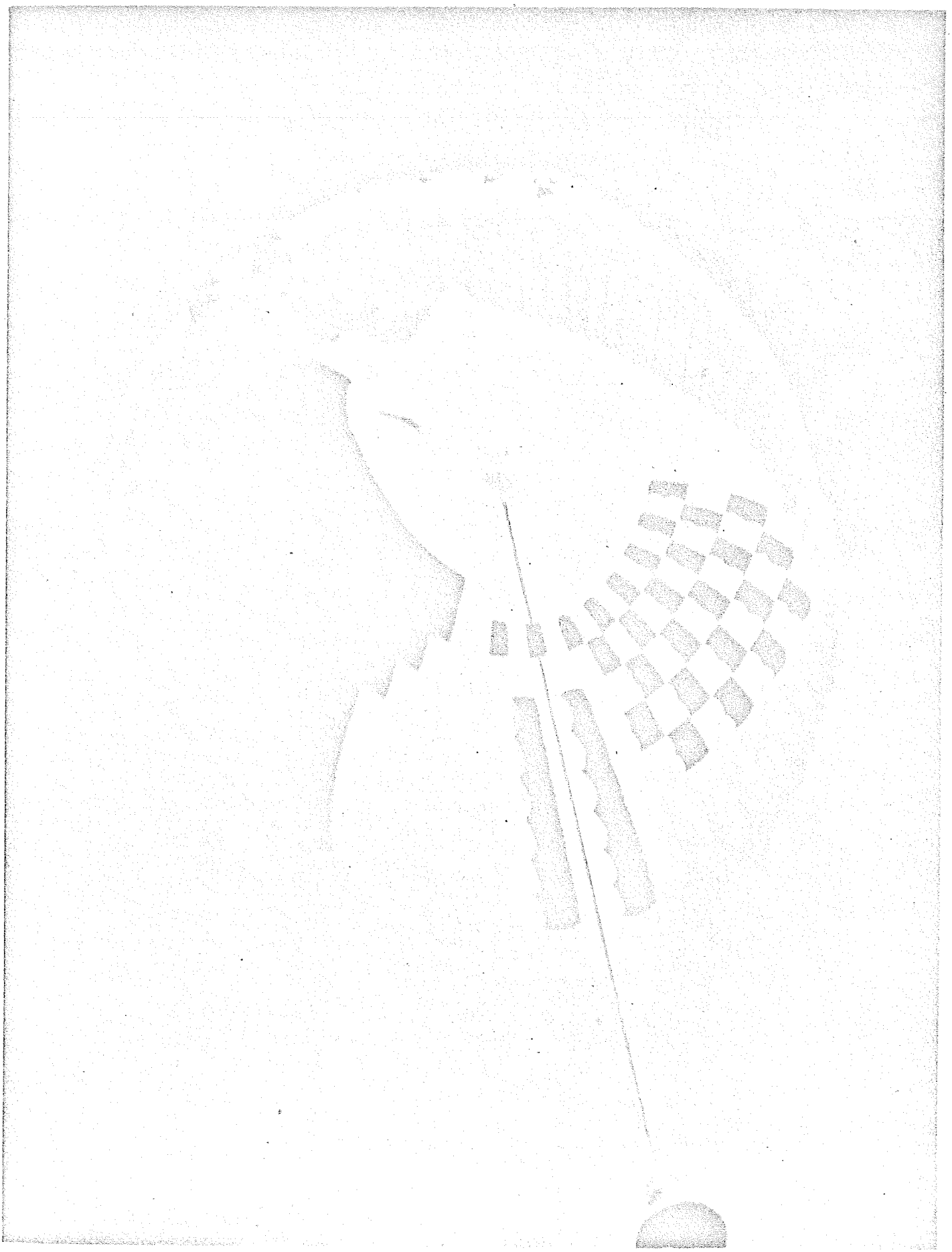

Para-Sail with Stabilizers and Centerline

Figure - 5 -

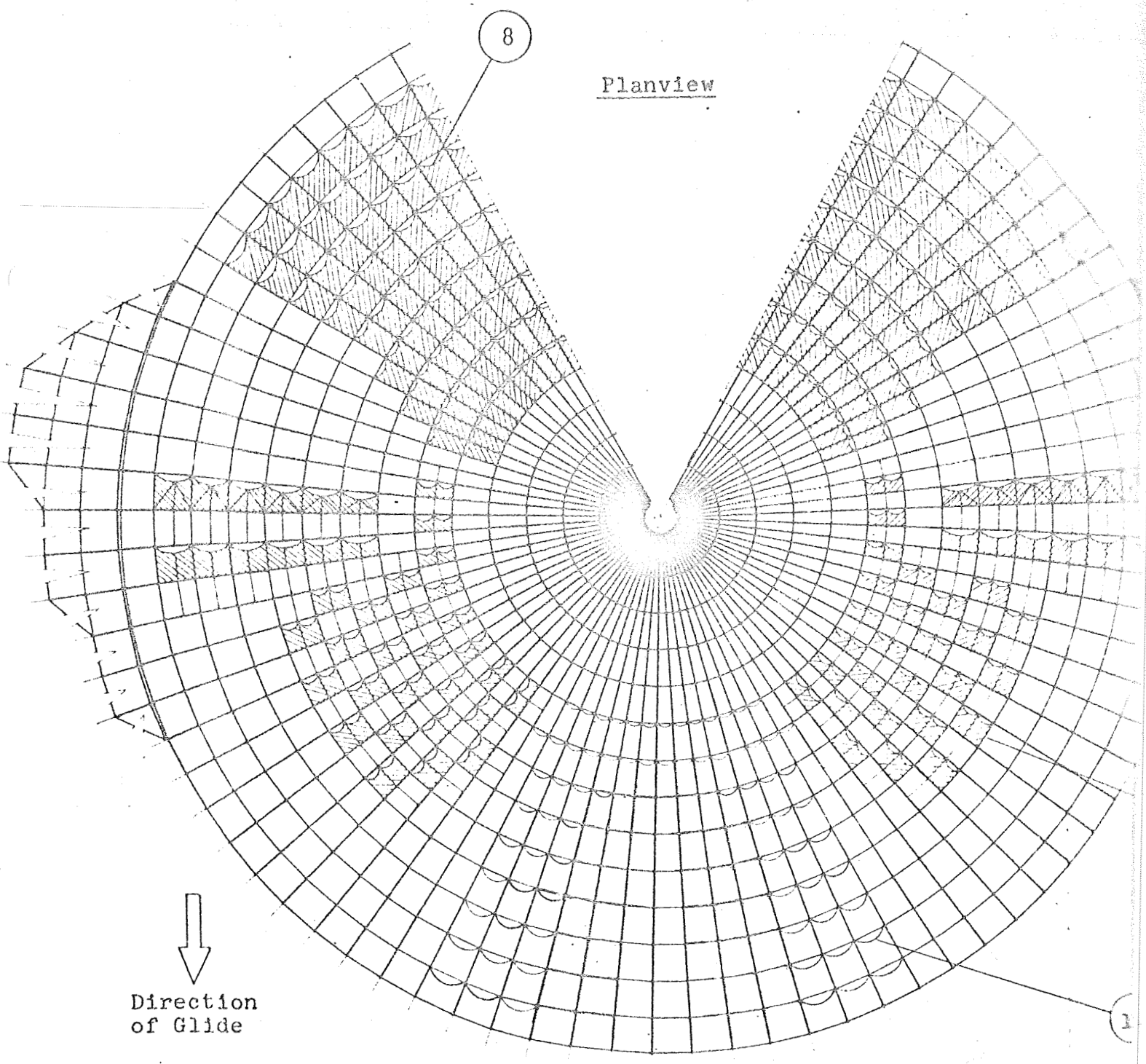

Significant Features:

1. 8 Ft. Dia. Ribless Guide Surface Pilot Chute.
2. Deployment Bag.
3. 80 Ft. Dia. Para-Sail.
4. Skirt Reefing (25' Line, 3 Sec. Delay).
5. Center Suspension Line, Apex Inverted.
6. Stabilizers.
7. Suspension System.
8. Circumferential S
9. Turn Slots.
10. Radial Slots.
11. Circumferential S

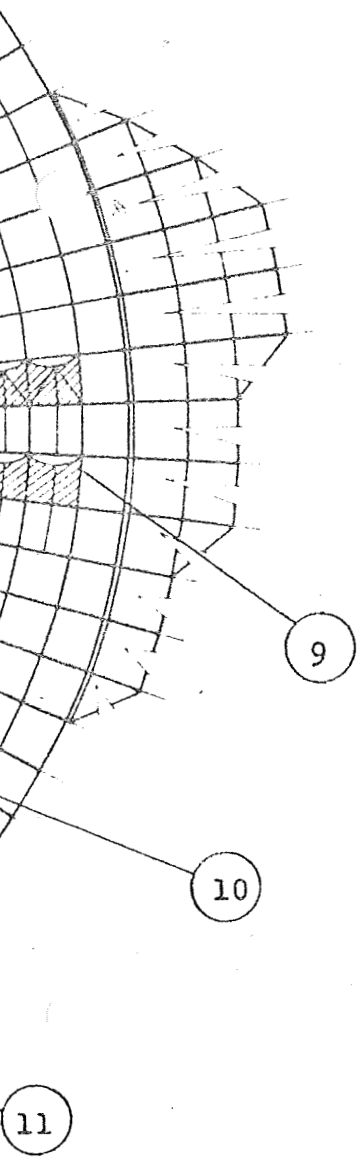

m, 67 Ft. Long.
Slots (Rear).

Slots (Front).

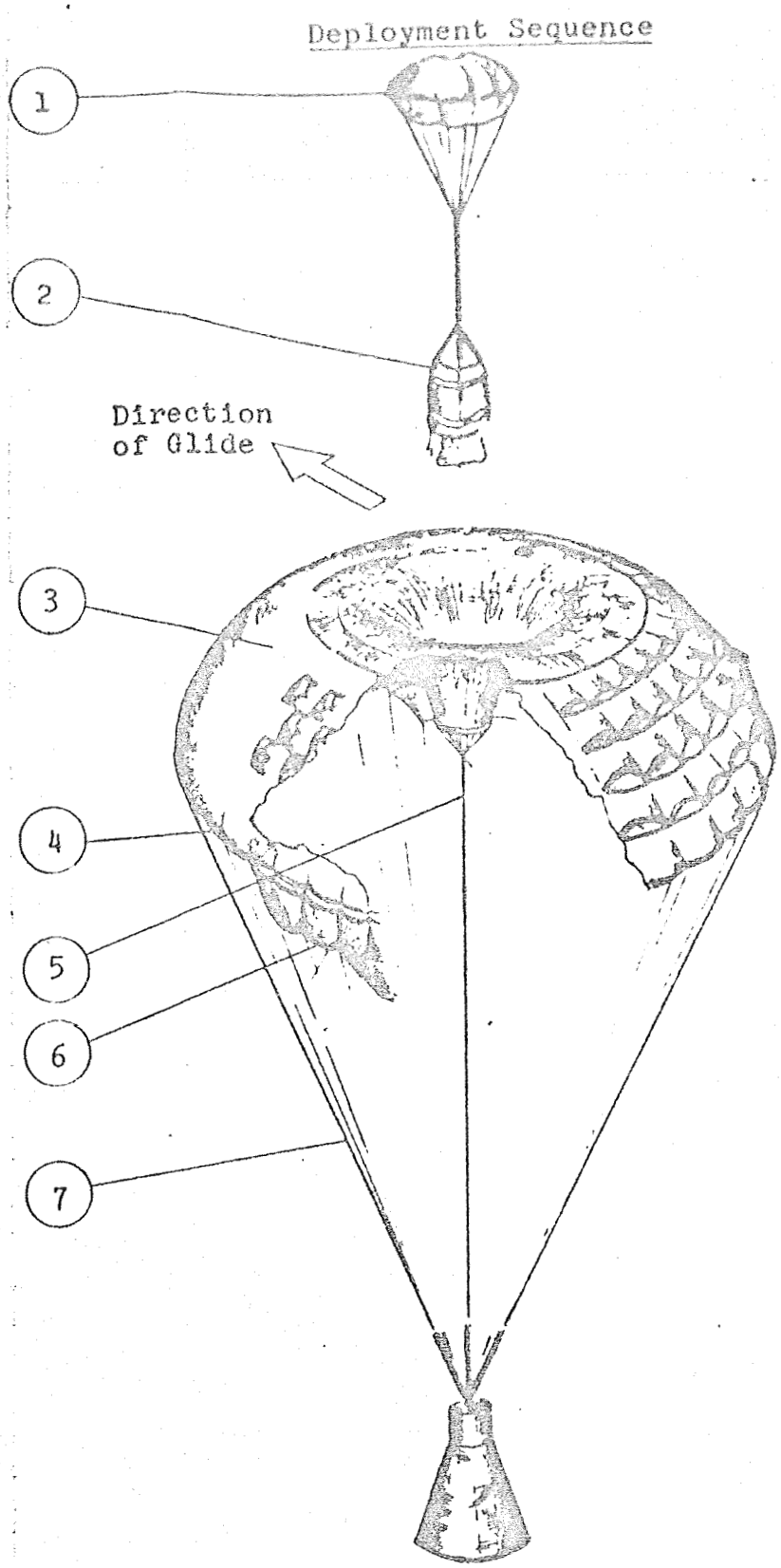

Configuration 80L-1

Figure - 6 -

Planview

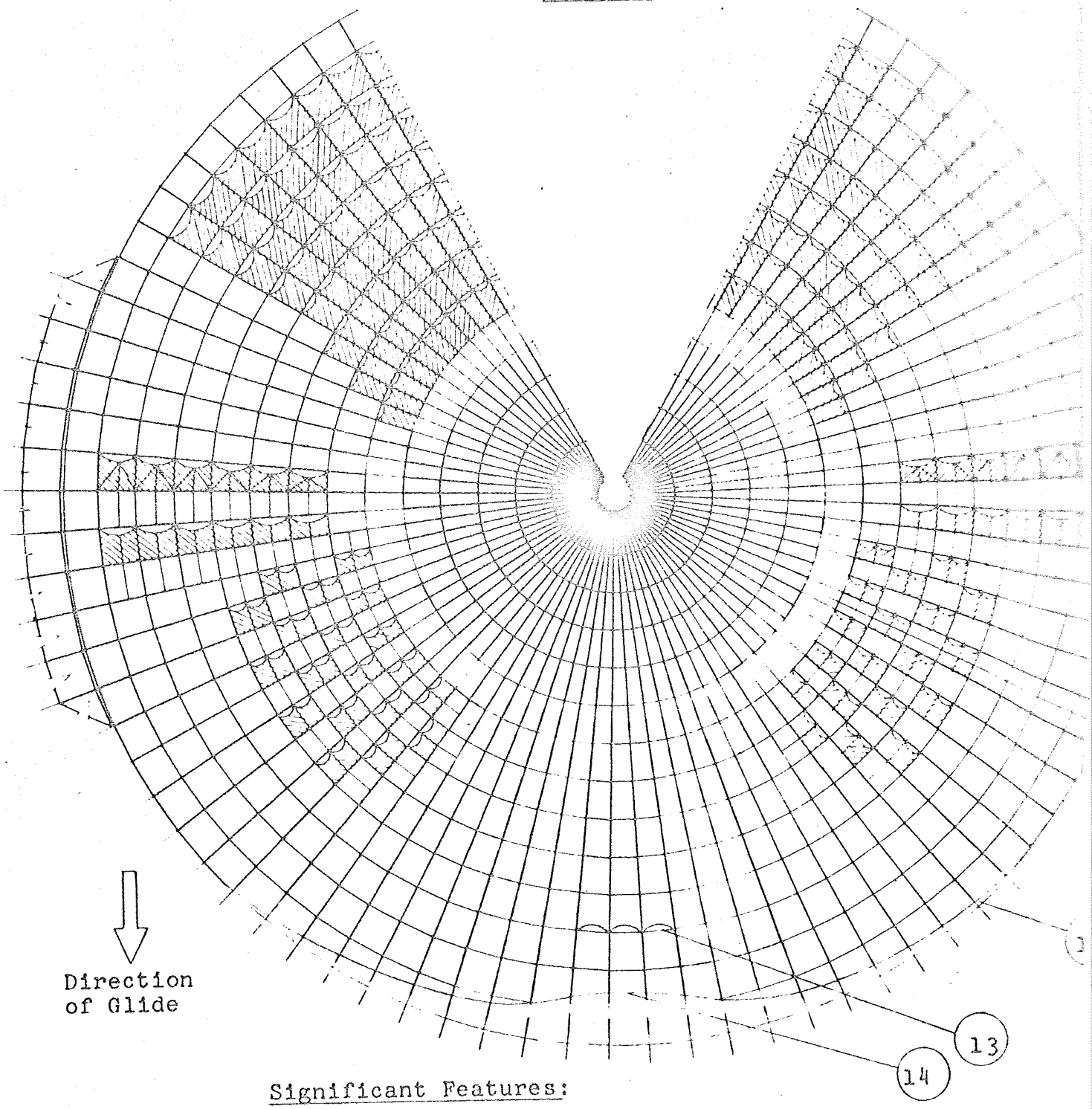

Significant Features:

1. 8 Ft. Dia. Guide Surface Pilot Chute.
2. Deployment Bag.
3. 6 Ft. Stabilization Parachute W/O Confluence.
4. 79.9 Ft. Dia. Para-Sail
5. 10 Ft. Dia. Guide Surface Internal Parachute.
6. Skirt Reefing.
7. Reduced Area Stabilizers.
8. Center Suspension Li
9. Suspension System, I
10. Rear Risers, Permane
11. Row of Radial Slots
12. Pocket Bands on 22 G
13. Forward Opening Slots
14. Height of Leading Ed Maximum.

Line, Apex Inverted.
Increased to 80 Ft.Lg.
ently Shortened 4' 3".
Closed.
Gores.
ts.
dge Gores Reduced 40 In.

Deployment System

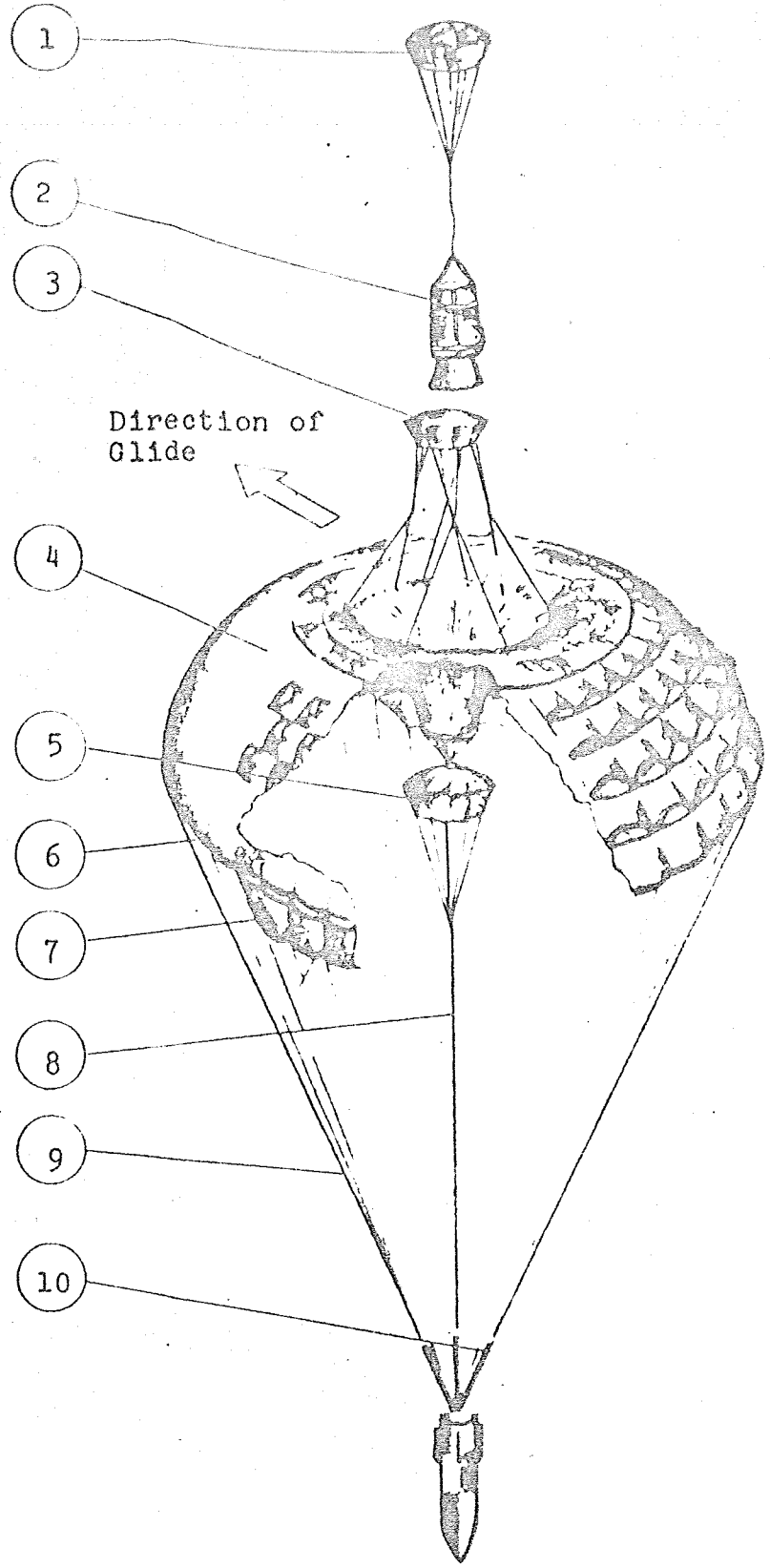

Configuration 80L-2

Figure - 7 -

Planview

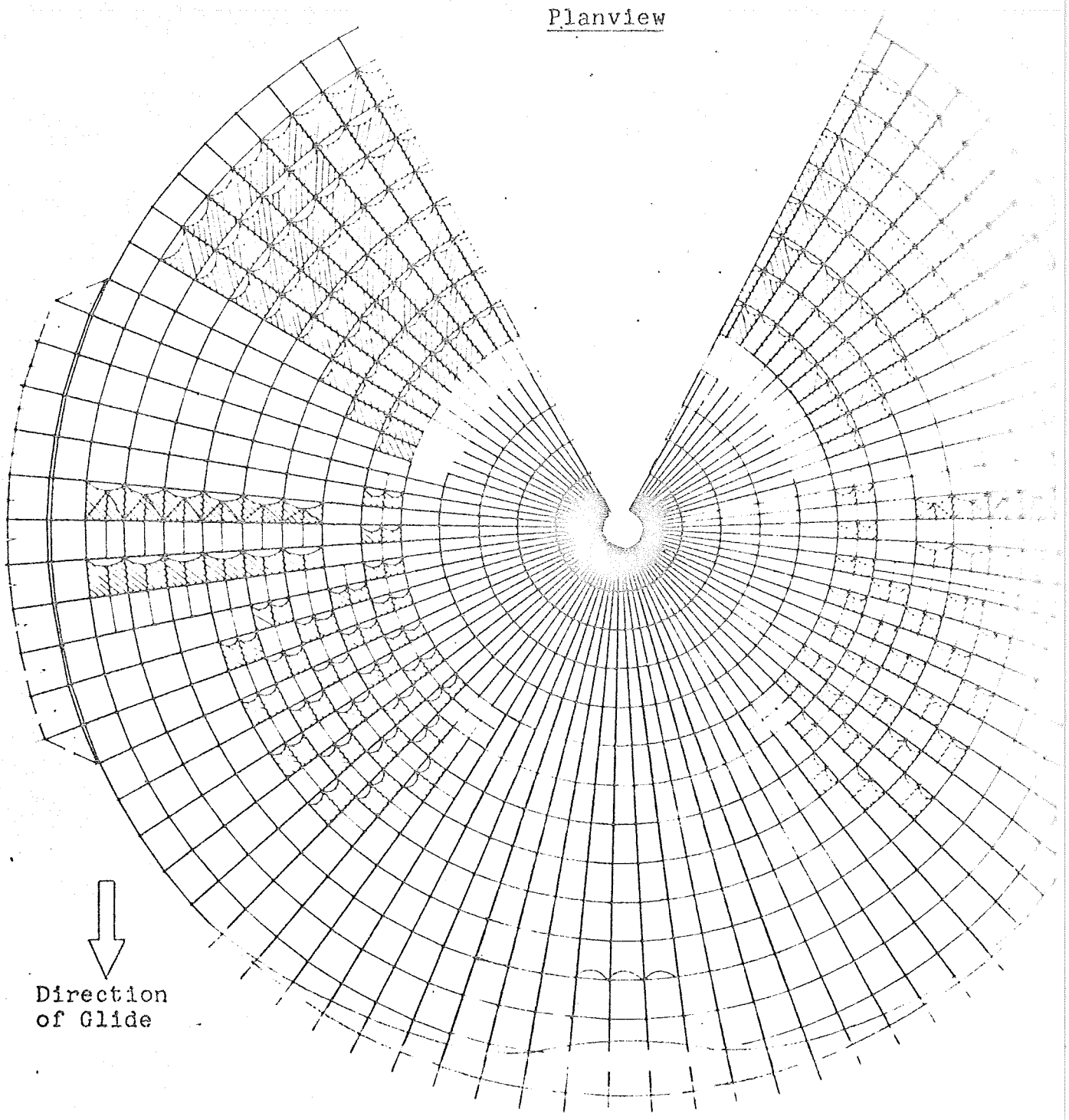

Significant Features, 80L-3:

1. 8 Ft. Dia. Guide Surface Pilot Chute.
2. Deployment Bag.
3. Multiple Crown Bridle.
4. 79.9 Ft. Dia. Para-Sail.
5. 10 Ft. Dia. Guide Surface Internal Chute.
6. Skirt Reefing.
7. Rear Risers Shortened 4' 3" Extended at 20 Sec.
8. Added Row of Radial S

Significant Features 8
(Ref. 80L-3):

9. Position of Internal Slightly.
10. Rear Riser Shortened Fabricated of 10,000 Strength Web.

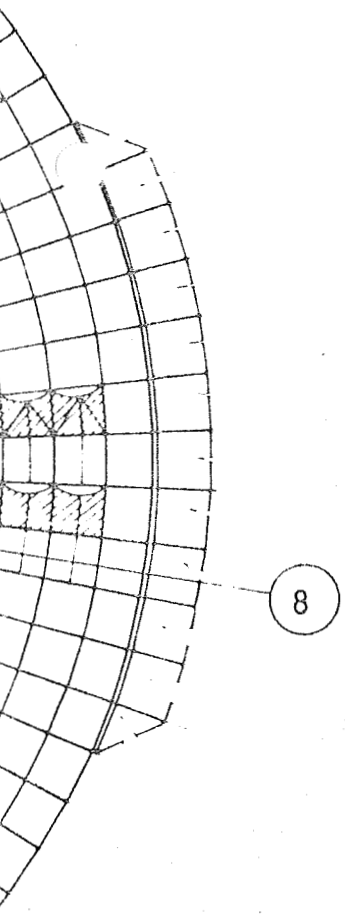

Deployment Sequence

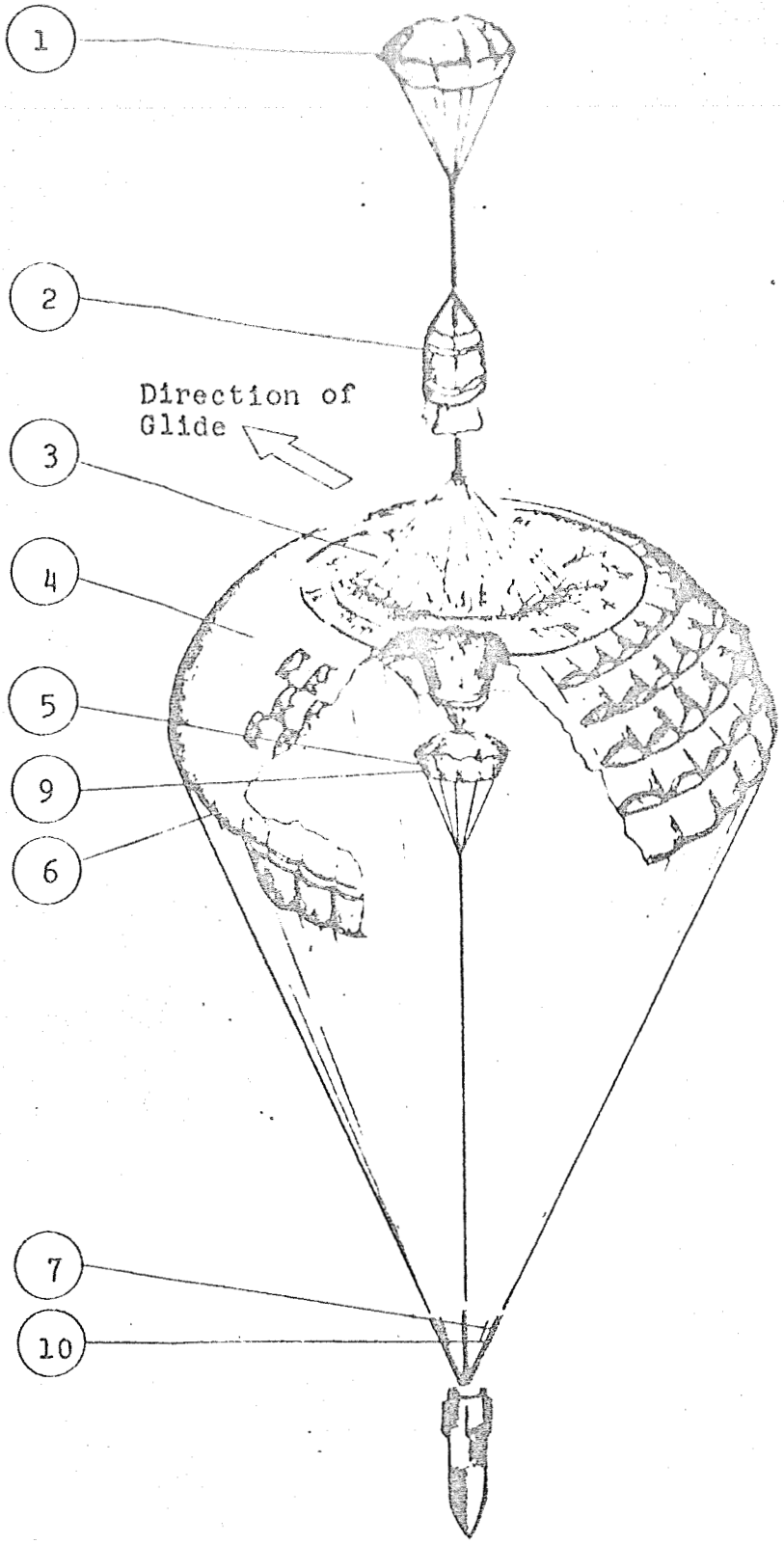

Configurations 80L-3, 80L-4

Figure - 8 -

ots.

-4

hute Lowered

'3" Permanently,
b. Tensile

Planview

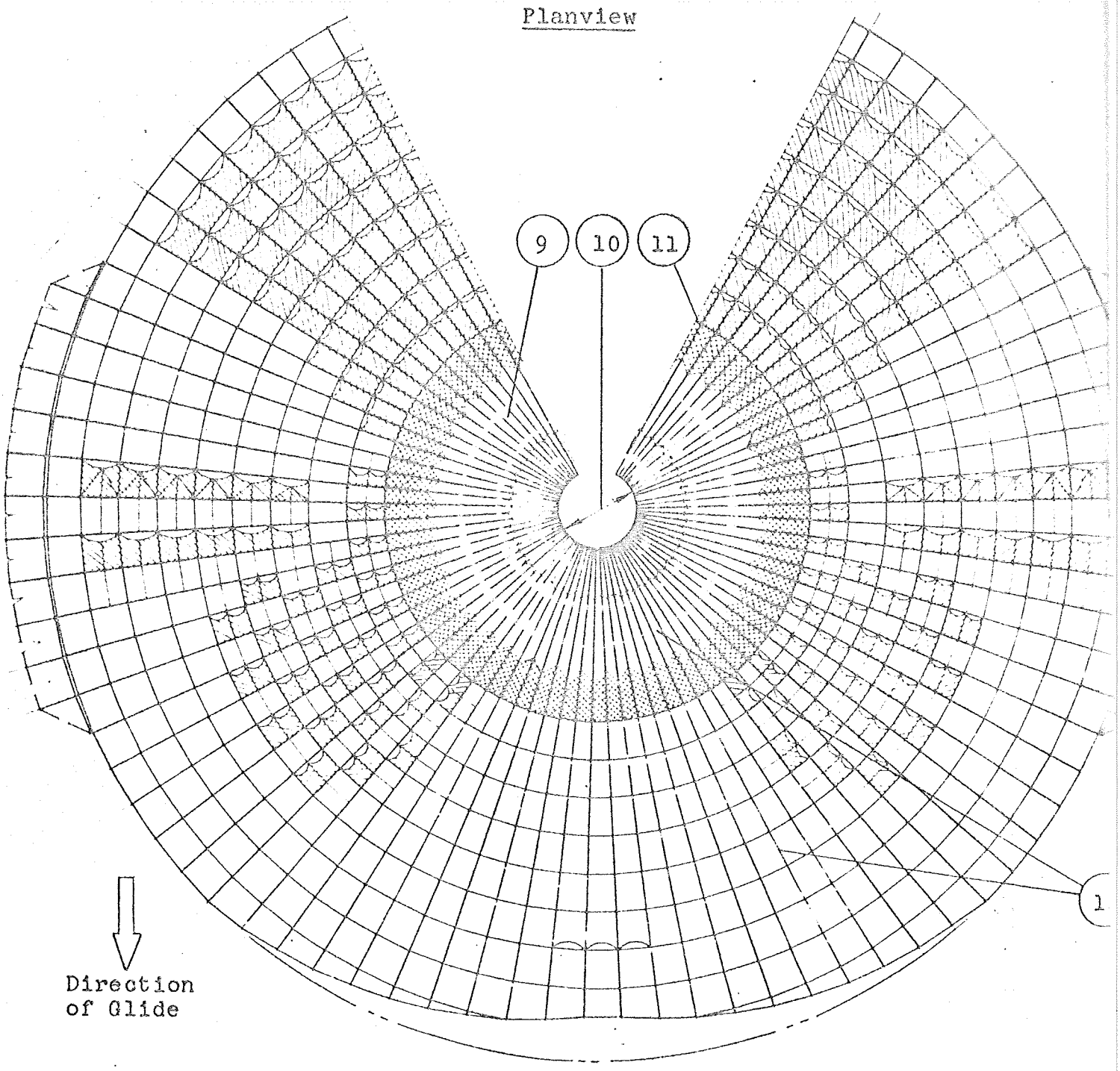

Significant Features, 80A-1:

1. 8 Ft. Dia. Guide Surface Pilot Chute.
2. Deployment Bag.
3. Conical Section Replaced With Flat Top.
4. 79.4 Ft. Diameter Para-Sail.
5. Internal Parachute Stay Line.
6. Skirt Reefing.
7. 10 Ft. Dia. Guide Surf
8. Internal Chute Center-
9. Lock Seam, Bias Constr Panels Only, Remainder
10. Vent Dia. Increased to
11. 1,000 Lb. Reinforcing

Significant Fea

12. Lock Seam, Bias Constr

e Surface Internal Chute.
enter-Line Riser.
Construction in Top (3)
ainder Butt Seam.
sed to 68 In.
rcing Band.

nt Features 80A-3:

Construction Throughout.

Deployment Sequence

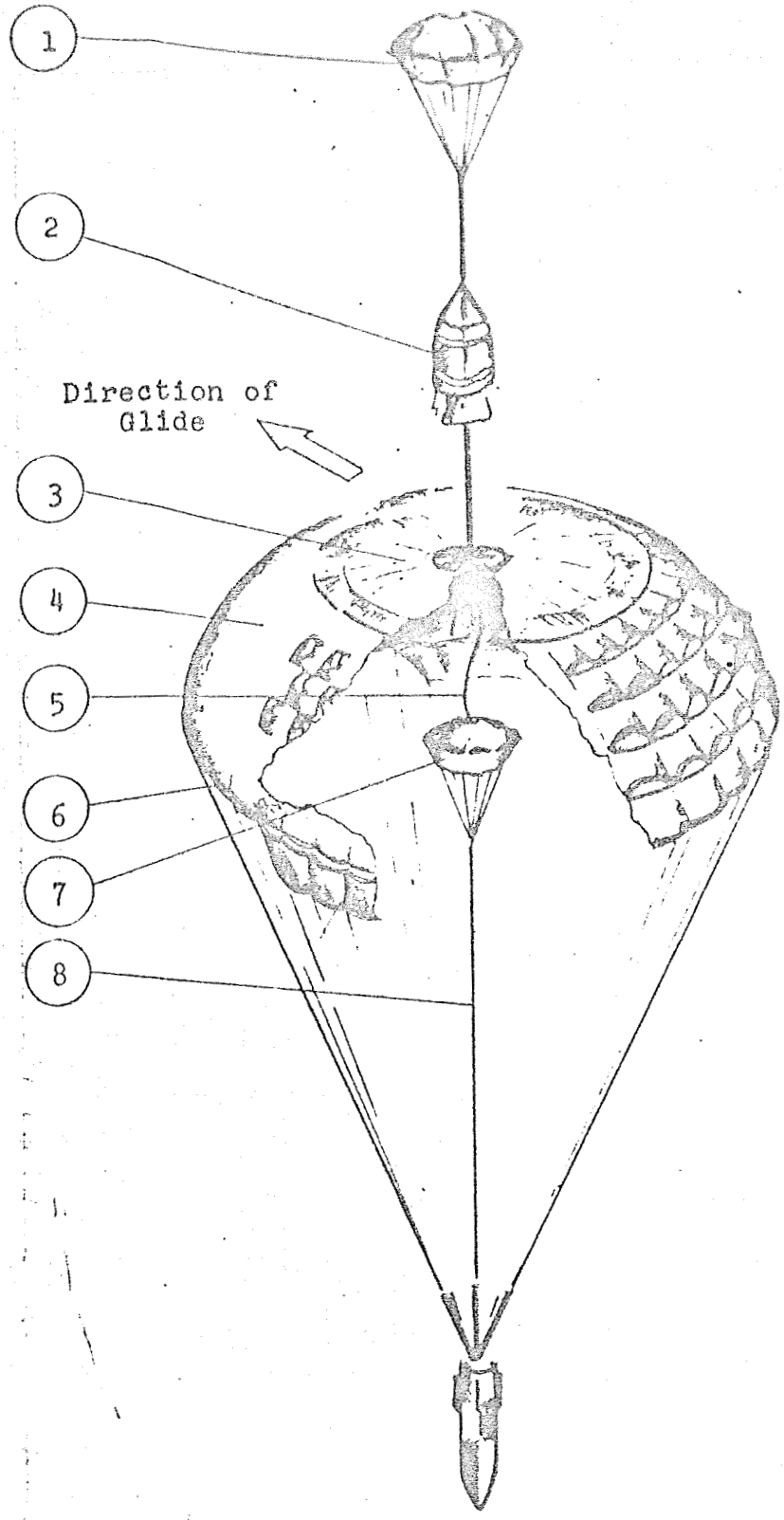

Configurations 80A-1, 80A-3

Figure - 9 -

Planview

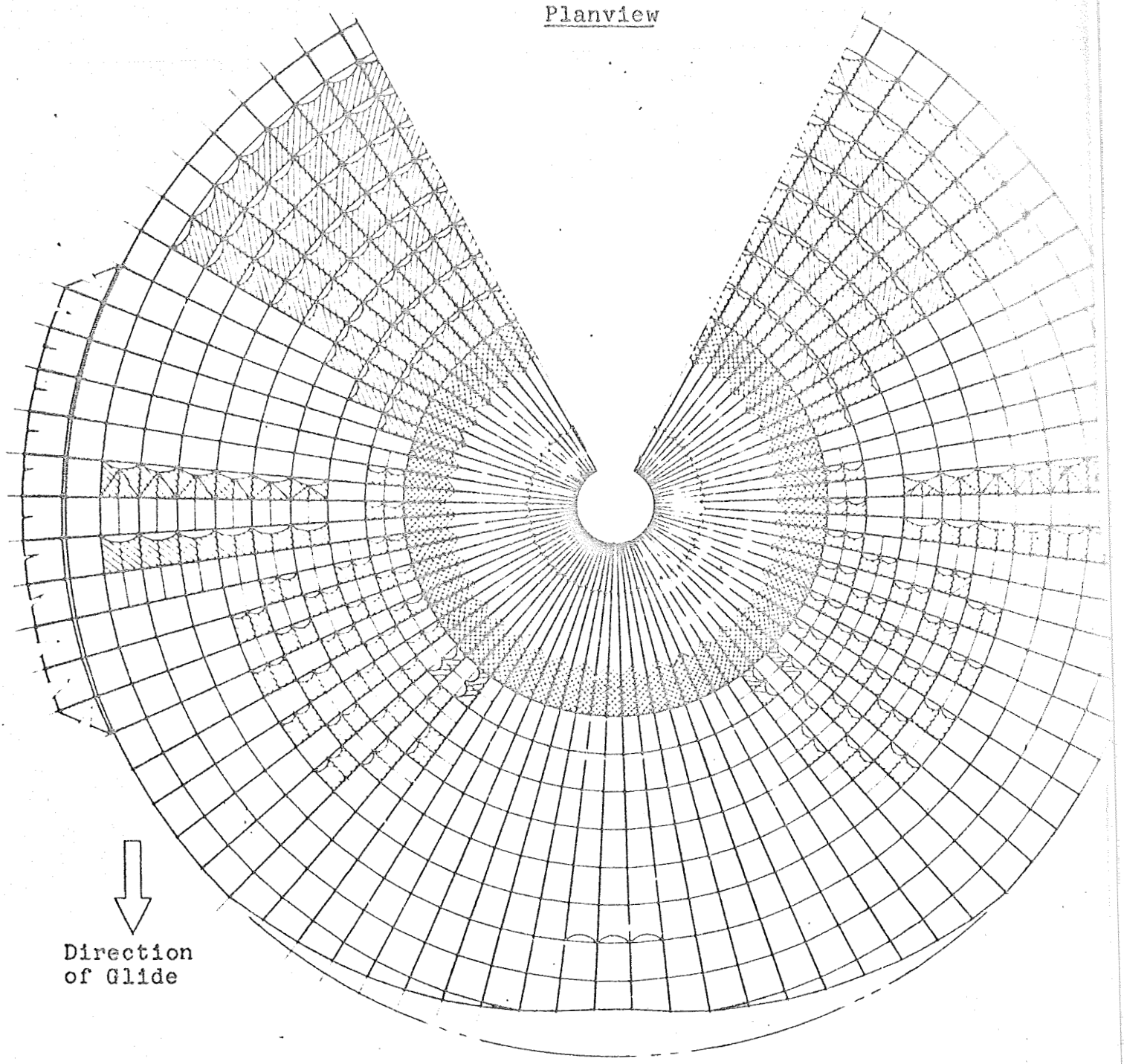

Significant Features 80A-2:

1. 8 Ft. Dia. Guide Surface Pilot Chute.
2. Deployment Bag.
3. 79.4 Ft. Dia. Para-Sail.
4. Internal Parachute Omitted.
5. Skirt Reefing.

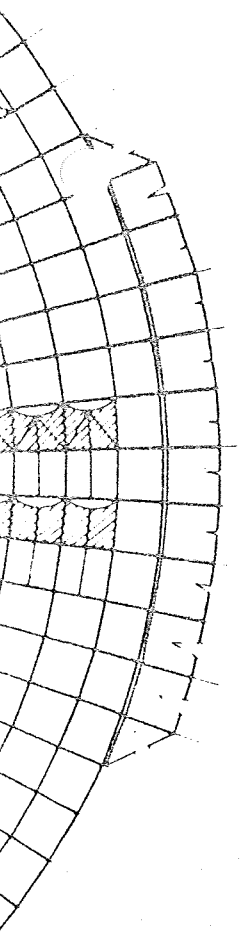

Deployment Sequence

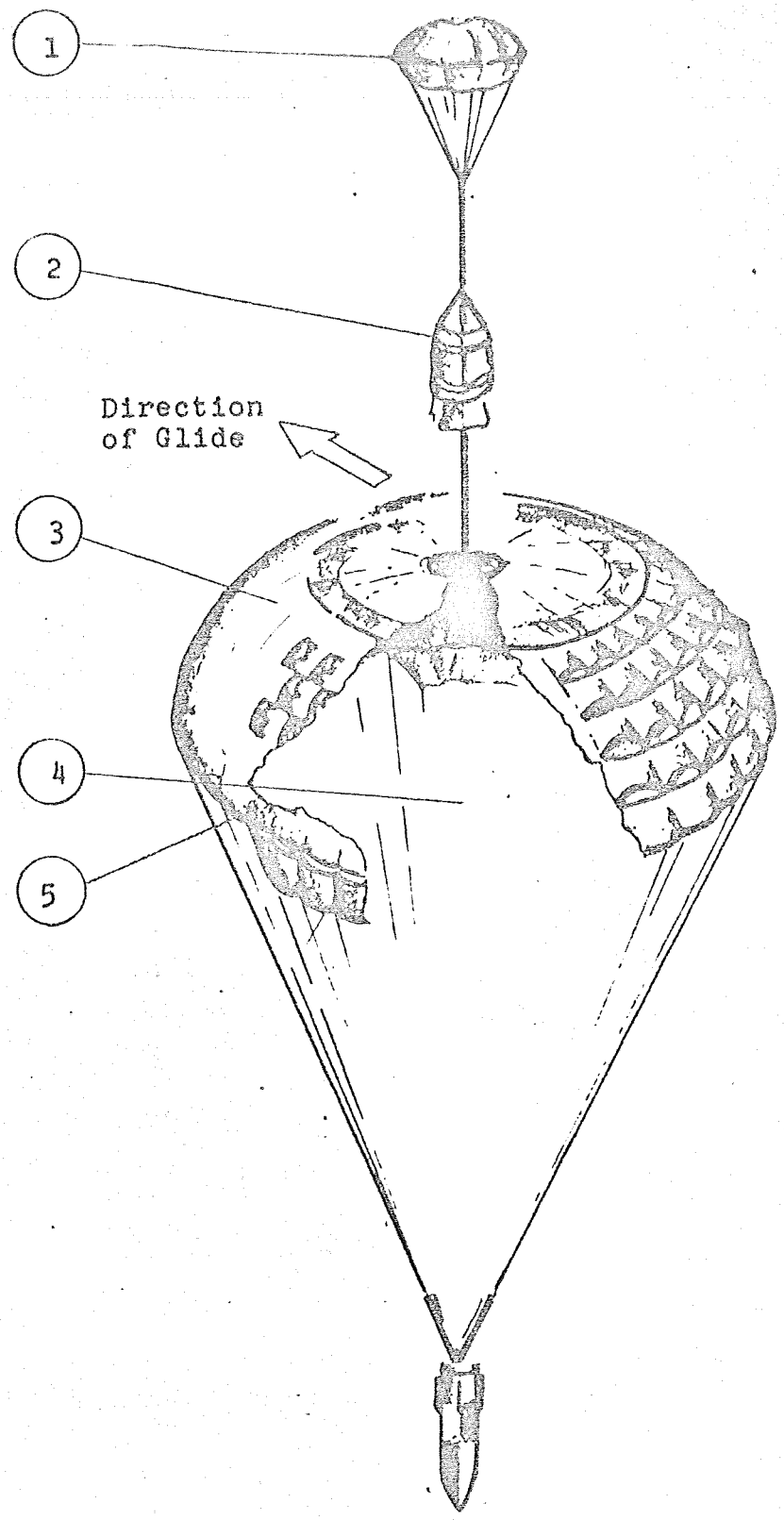

Configuration 80A-2

Figure - 10 -

Planview

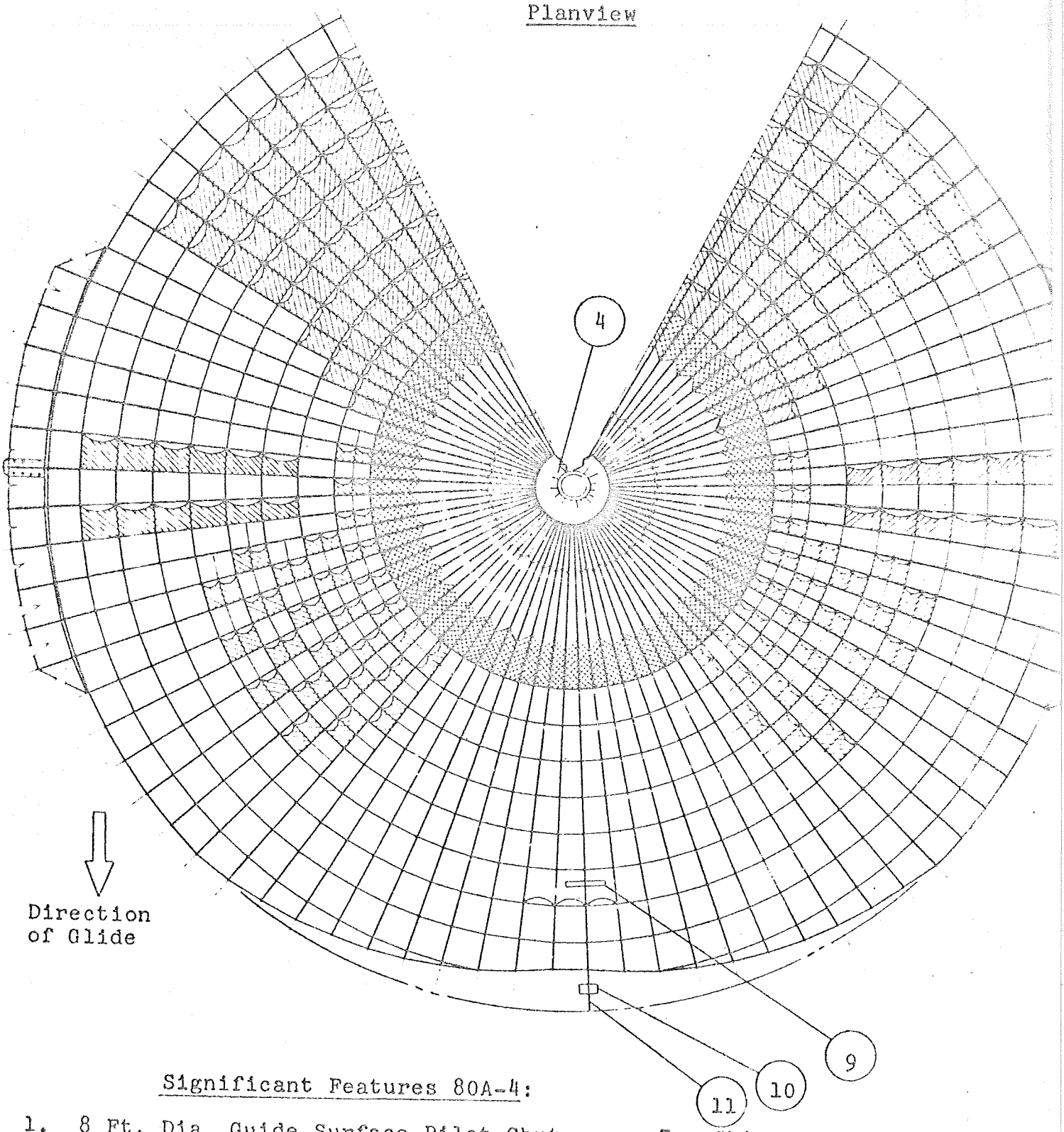

Significant Features 80A-4:

1. 8 Ft. Dia. Guide Surface Pilot Chute.
2. Deployment Bag.
3. Skirt Hesitator Bag.
4. Elastic Vent Hood.
5. 79.4 Ft. Dia. Para-Sail.
6. 10 Ft. Dia. Guide Surface Internal Chute.
7. Skirt Reefing.
8. Stabilizer Sleeve.
9. Hesitator Loop (Closure).
10. Butterfly Loop (Closure).
11. 1,000 Lb. Suspension Line

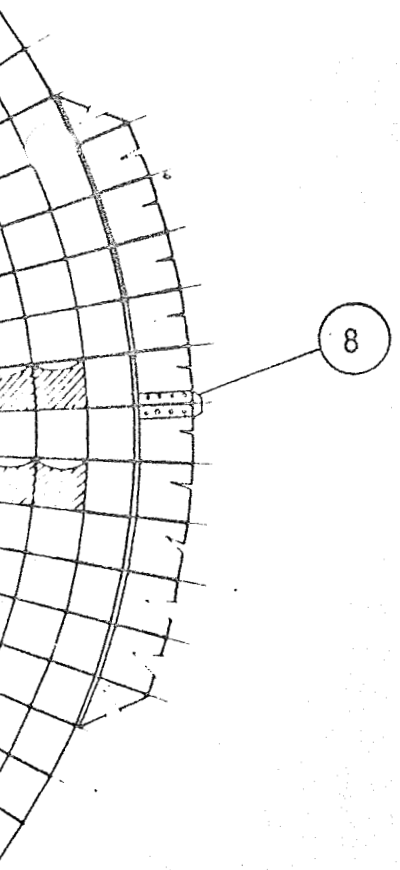

sure).
sure).
Line.

Deployment Sequence

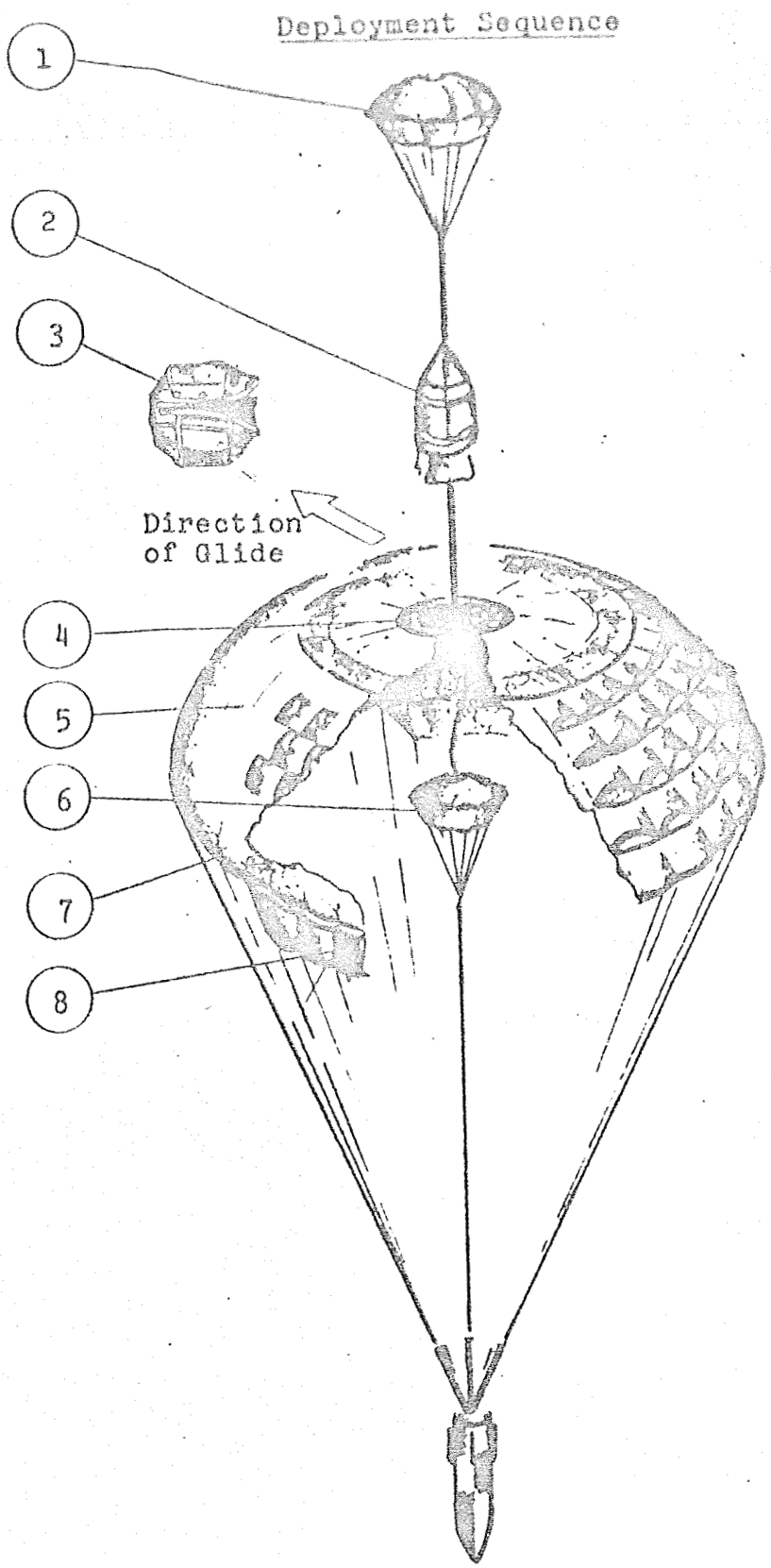

Configuration 80A-4

Figure - 11 -

Planview

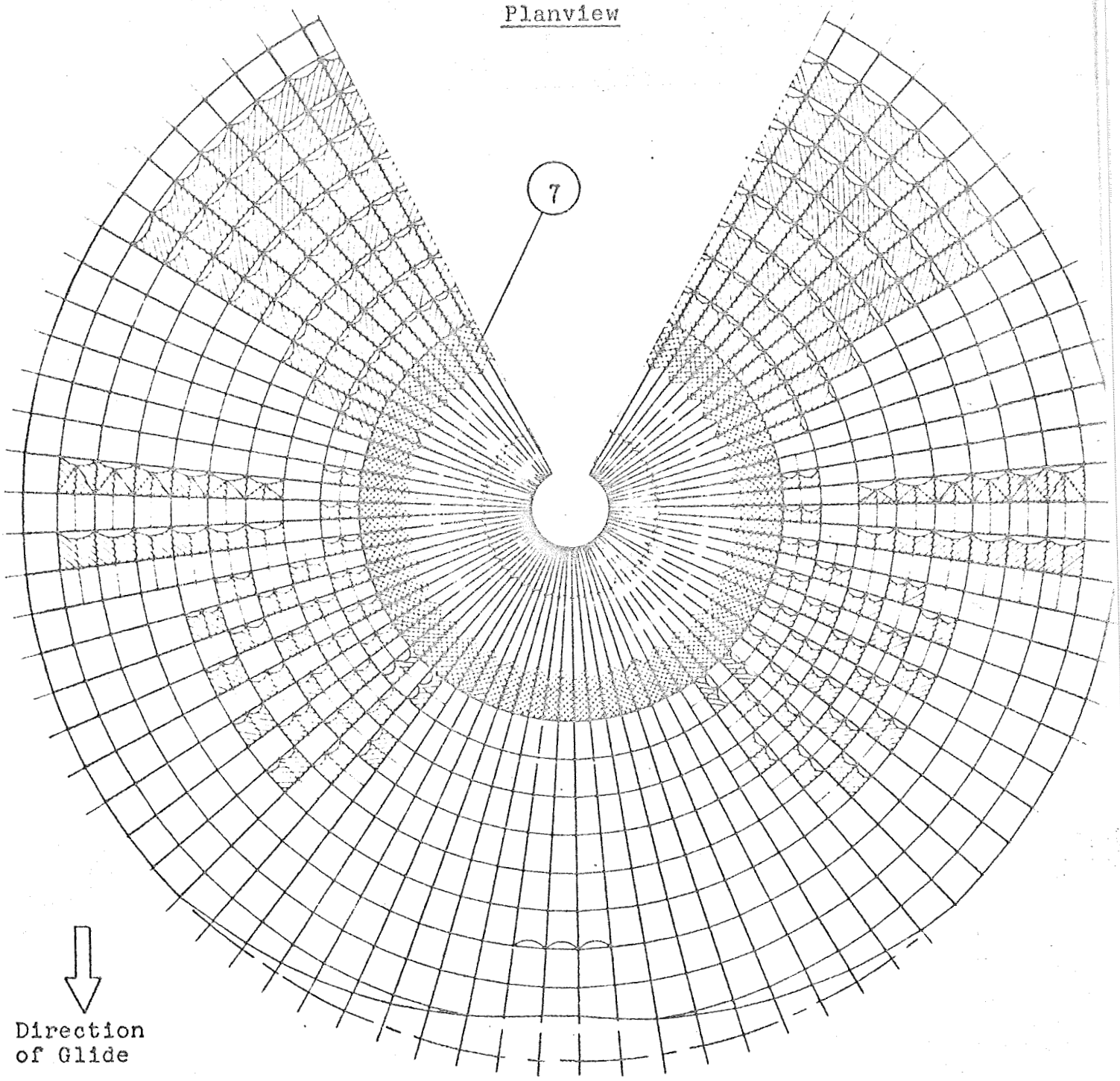

Significant Features 80A-5:

1. 8 Ft. Dia. Guide Surface Pilot Chute.
2. Deployment Bag.
3. 77.6 Ft. Dia. Para-Sail.
4. 10 Ft. Dia. Guide Surface Internal Parachute.
5. Skirt Reefing.
6. Stabilizers Removed.
7. Bias Construction Lock Seam in Upper Three Sections Only - Remainder Butt Seam.

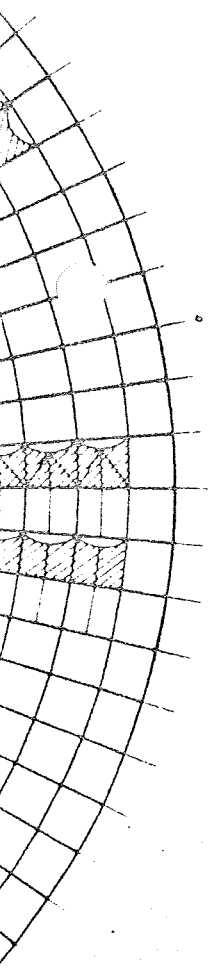

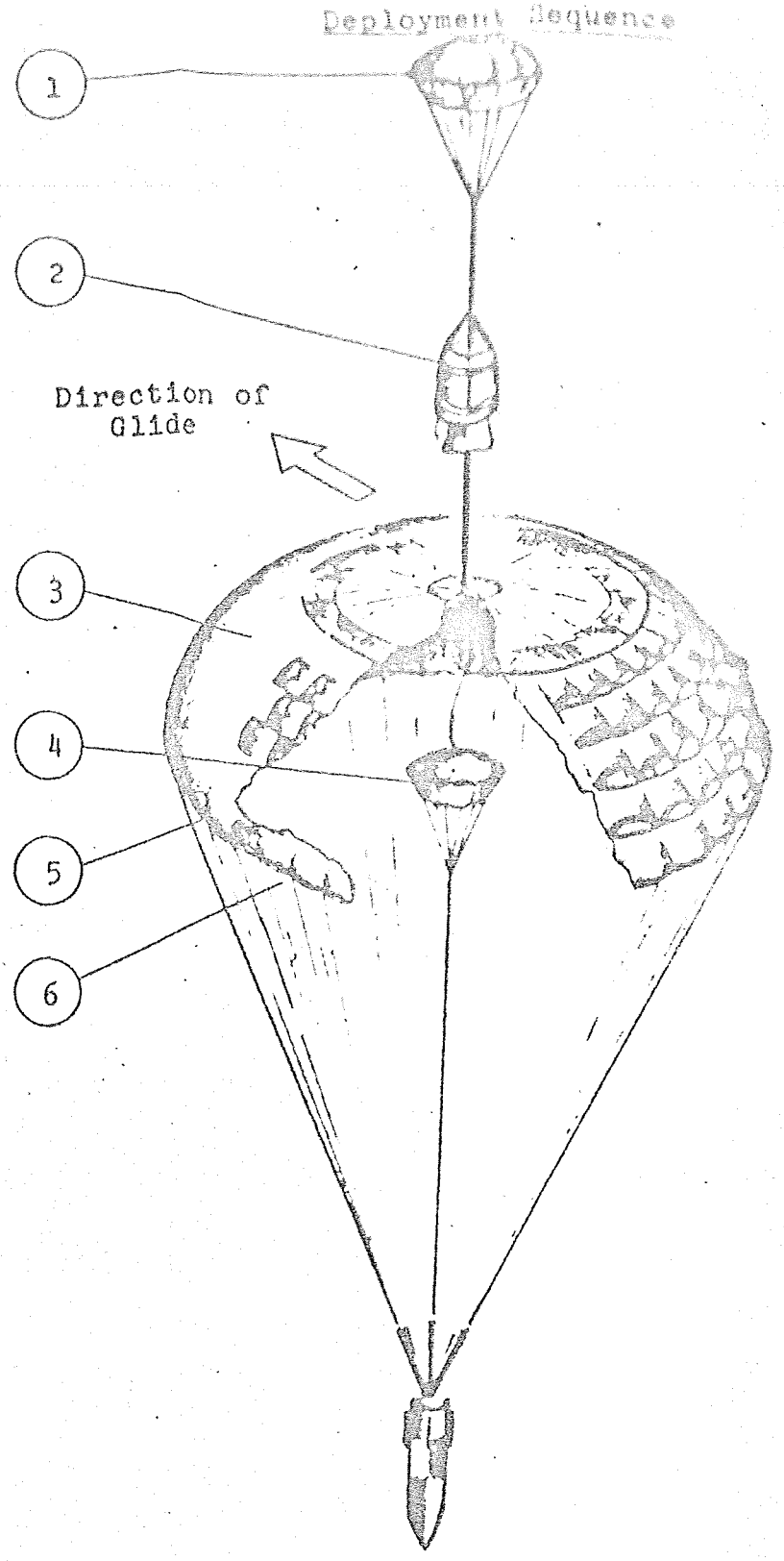

Configuration 80A-5

Figure - 12 -

Planview

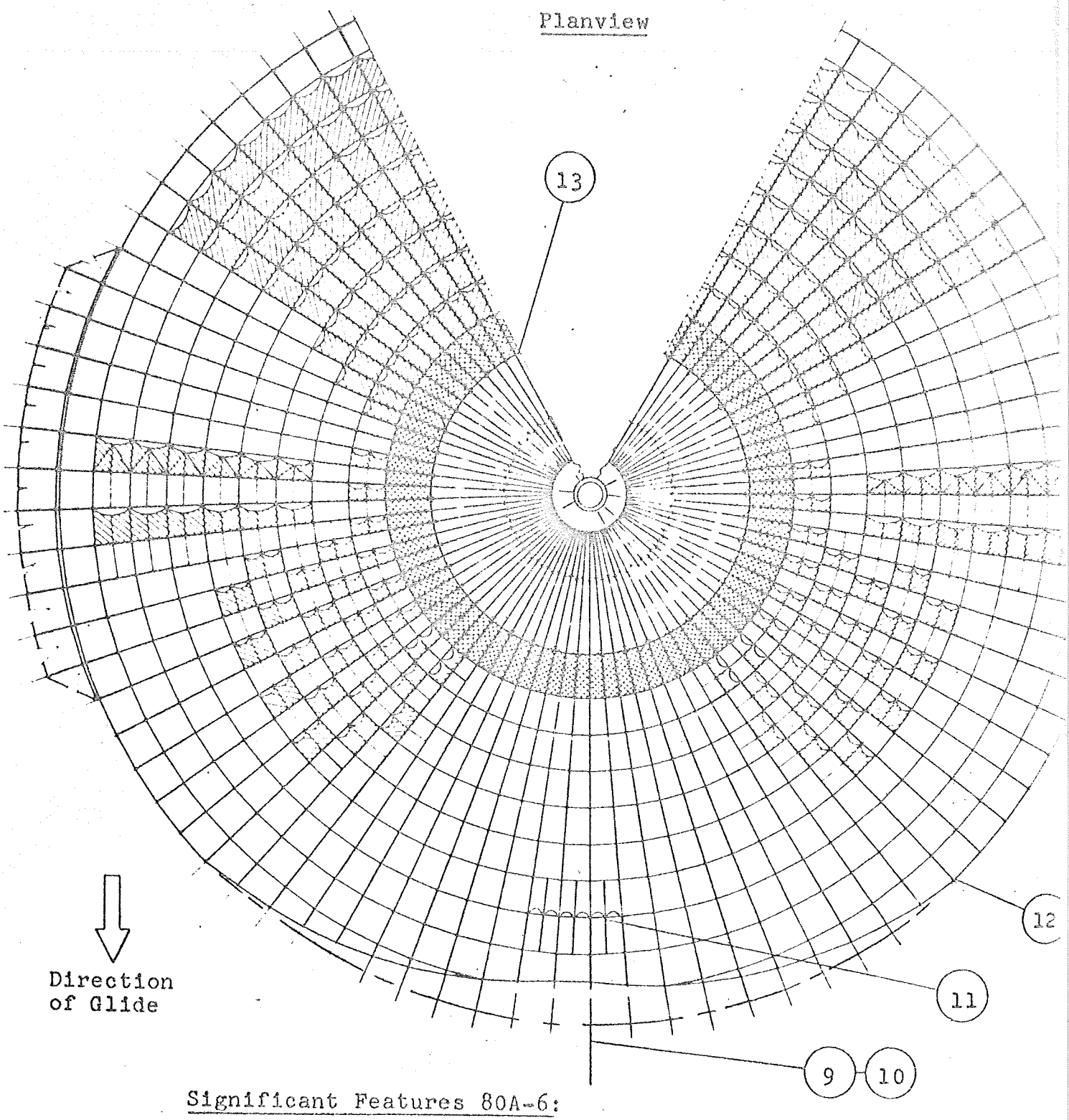

Significant Features 80A-6:

1. 6 Ft. Dia. Guide Surface Pilot Chute (High Speed Tests).
2. Deployment Bag.
3. Elastic Vent Hood.
4. 79.4 Ft. Dia. Para-Sail.
5. 10 Ft. Dia. Guide Surface Internal Chute.
6. Skirt Reefing.
7. Stabilizer Sleeve.
8. Reefing on Stabilizers.
9. 1,000 Lb. Line Retained

Significant Features 80A-

10. 1,000 Lb. Line Removed a with 550 Lb. Line.
11. Center of Each Front Slo Center of Adjacent Cross
12. Reefing Ring Attachment Increased

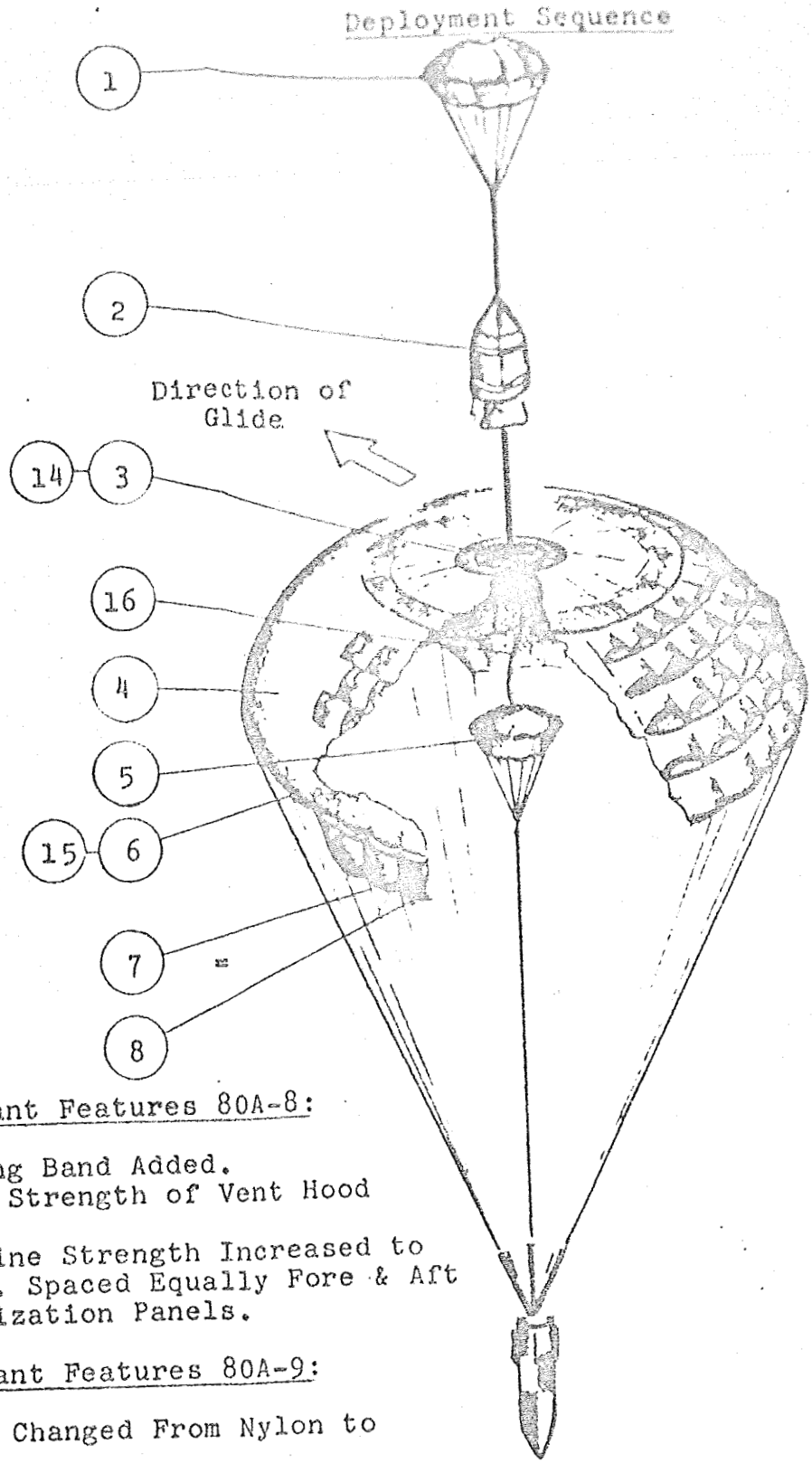

Significant Features 80A-8:

13. Reinforcing Band Added.
14. Increased Strength of Vent Hood Elastic.
15. Reefing Line Strength Increased to 1,500 Lbs. Spaced Equally Fore & Aft of Stabilization Panels.

Significant Features 80A-9:

16. Stay Line Changed From Nylon to Cotton.

Configurations 80A-6, 80A-7, 80A-8, 80A-9

Figure - 13 -

ers.
ined From 80A-4.

80A-7:

ved and Replaced

t Slot Attach to
Cross Seam.
ment Strength

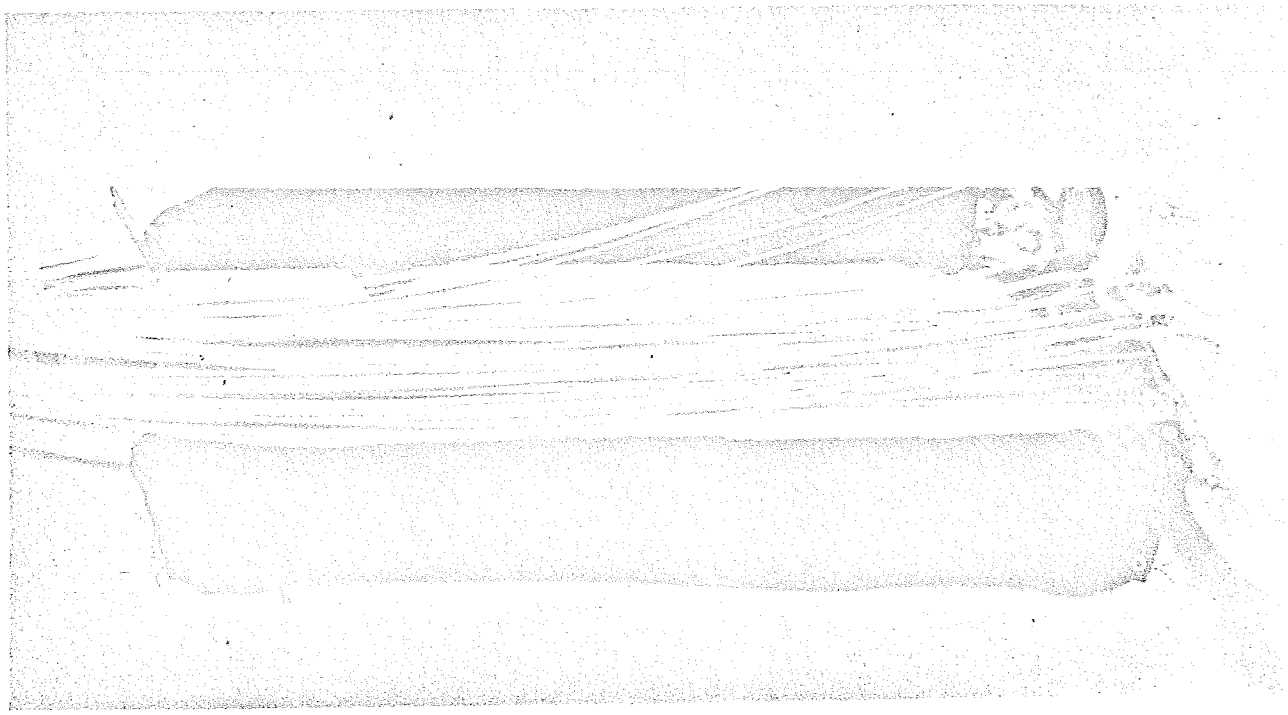

Figure - 14a -

Stabilizer Sleeves - Configuration 80A-4

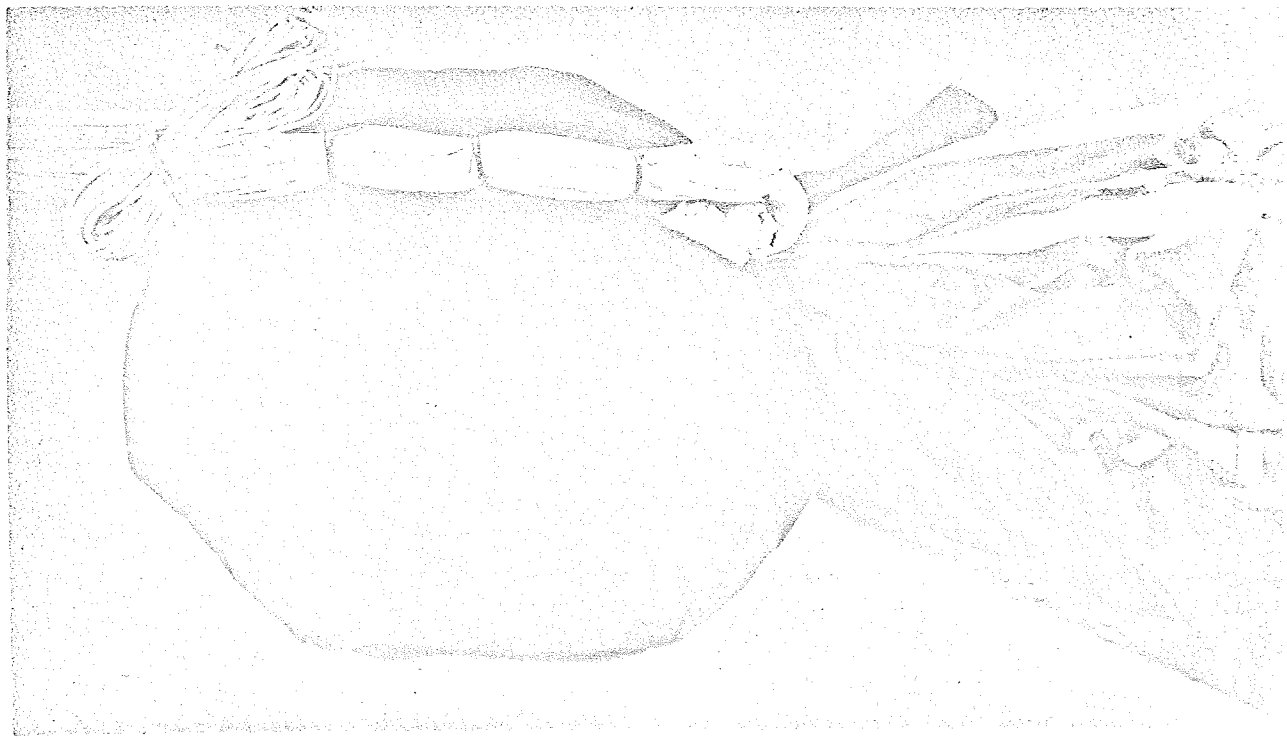

Figure - 14b -

Hesitator Bag - Configuration 80A-4

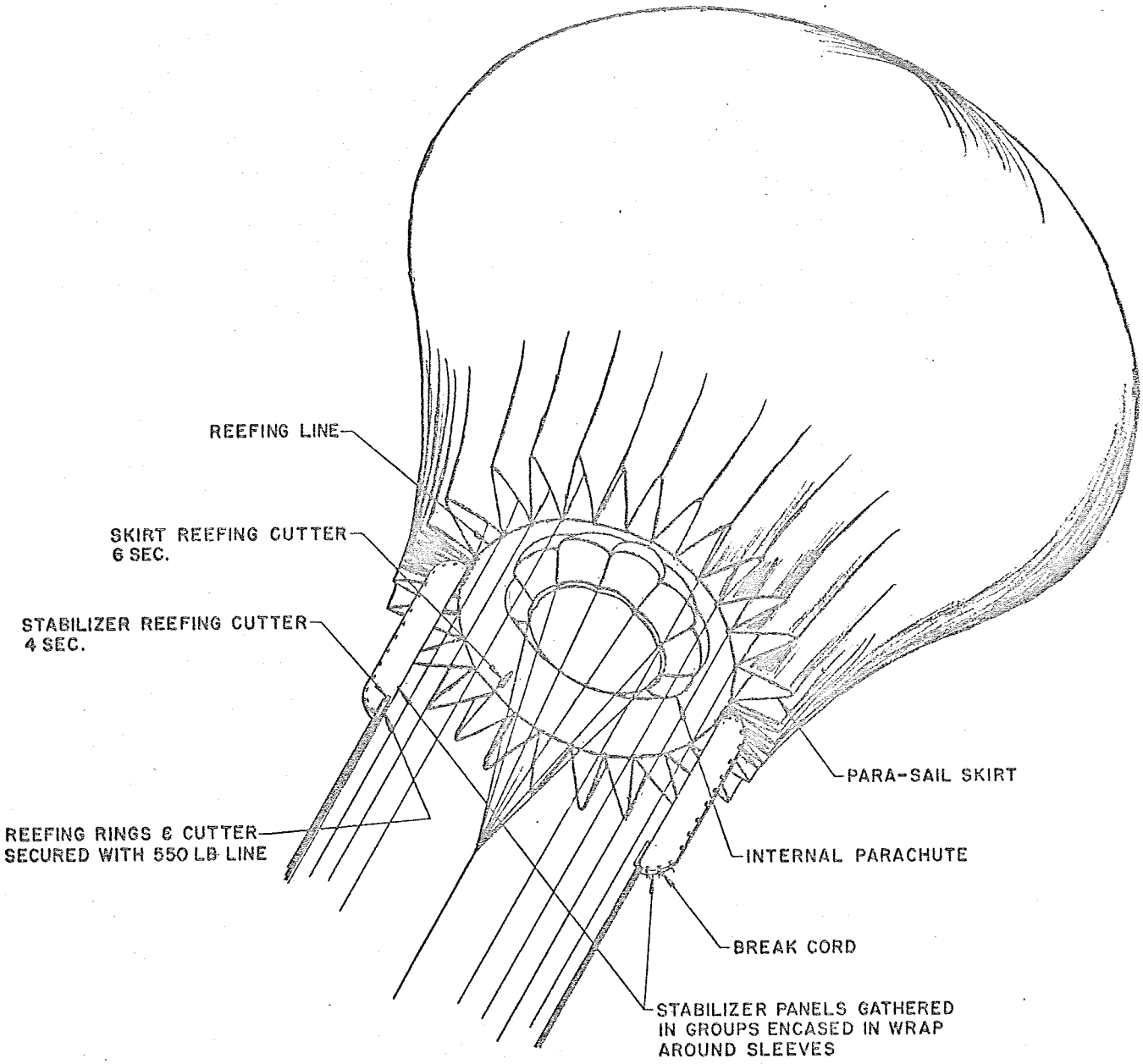

FIGURE - 15 -
SCHEMATIC ARRANGEMENT
OF DEPLOYMENT AIDS ON
REEFED PARA-SAIL

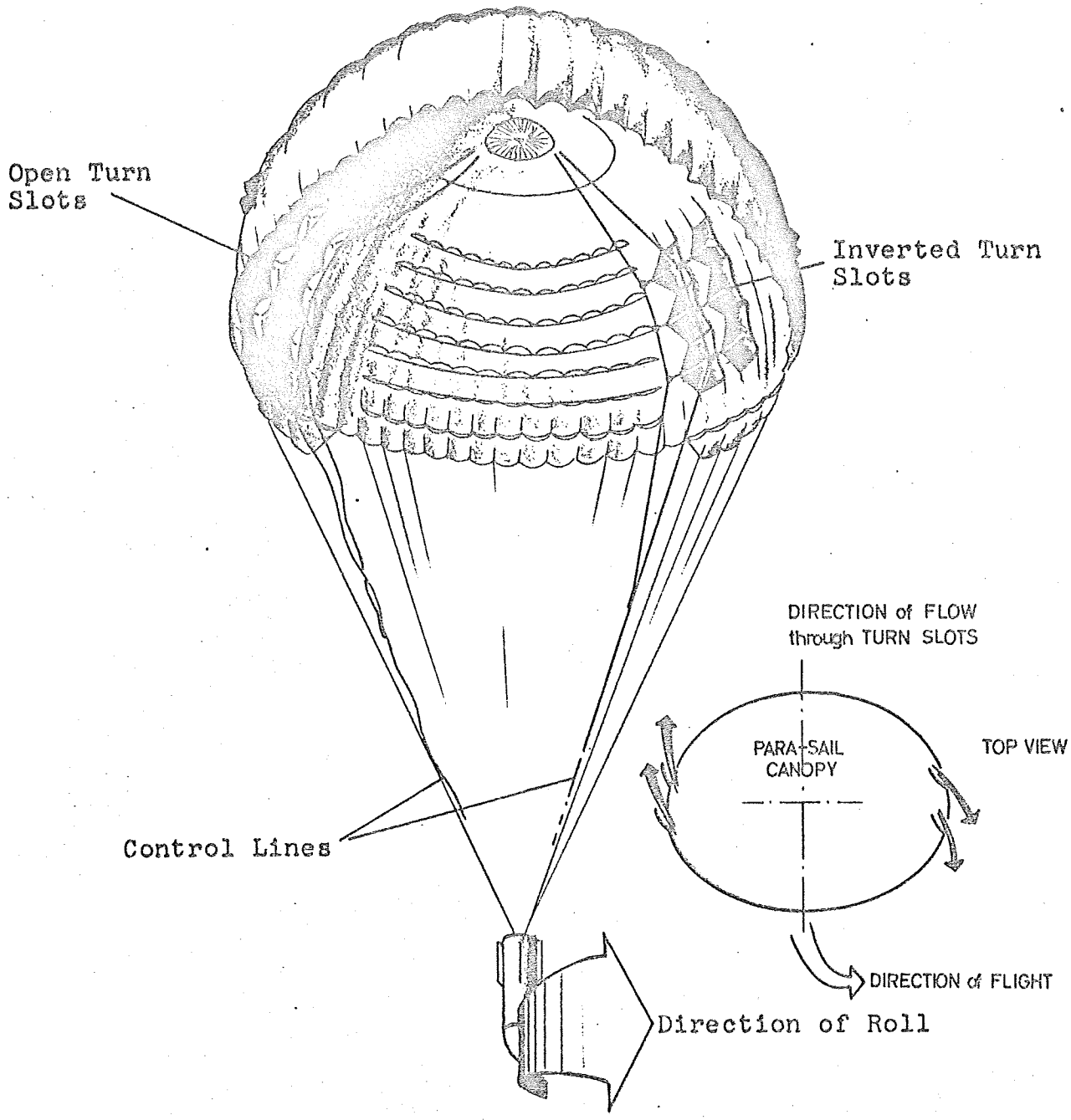

Figure - 16 -

W.R.M.
4 Nov. 1964

Method of Inducing Canopy Roll Moments About a Vertical Axis

3.2 Description of Test Programs

In the course of development of the Para-Sail parachute a number of investigative drop test programs were performed in addition to the primary program at the Joint Parachute Test Facility. These included a series of preliminary functional tests performed by the Contracting Agency in Houston, Texas and supplemental drop tests with small Para-Sails, by both the Manned Space Craft Center and the contractor, as an aid in the solution to deployment problems. All of the respective programs are discussed in the following with emphasis on the primary testing at the Joint Parachute Test Facility. References 2 and 3 contain additional information related to these test programs and other associated tests.

3.2.1 Preliminary Functional Tests

These tests were performed with a full size 80 foot diameter Para-Sail by the National Aeronautics and Space Administration, Manned Space Craft Center, at Galveston Bay and San Marcus, Texas test sites. The purpose of these tests was originally of a functional nature, being only a portion of an in-house program by the Contracting Agency. However, as deployment and inflation difficulties were encountered the objectives became developmental in kind. Eleven such tests were conducted before sufficiently satisfactory inflation characteristics were exhibited to indicate that safe recovery of a test vehicle could be anticipated. At such time the primary test program was then commenced at the Joint Parachute Test Facility by the contractor.

The first drop test of this preliminary series with Para-Sail 80L-1 was successful. Deployment speed and vehicle

weight were low. Opening was somewhat erratic but nevertheless satisfactory. However, it was on subsequent tests that difficulties were encountered. These problems were centered around the unsymmetrical inflation characteristics of the Para-Sail, i.e. the tendency of the leading surface of the canopy to be blown, or sucked, back against the slotted trailing surface of the parachute. In some instances this condition was so severe that cloth entanglement with the center suspension line would result. A typical malfunction of this nature is shown in Figure 17.

A number of modifications to the initial design, 80L-1 followed in an attempt to remedy the difficulties. Slots in the leading surface were closed, in an effort to retain air pressure in the front section of the canopy and induce an outward motion.

The leading edge of the canopy was trimmed back (i.e. cloth removed) to a maximum of 40 inches above the lower lateral band. Wind tunnel experiments performed prior to this contract had shown these modifications to increase angle of attack, as reported in Volume I. It was also theorized that reduced frontal skirt drag area would decrease the forces tending to prevent its outward motion. There was some indication of the correctness of this theory when the modification was incorporated into much smaller Para-Sails, however, little improvement could be noted with the full size Para-Sail.

A crown stabilization parachute was added which contributed to a more orderly deployment but did not improve inflation characteristics appreciably.

Attempts were made to reef the rear, slotted surface of the canopy, to reduce its effectiveness in producing glide during inflation, and to retain pressure, but these steps also were unsuccessful.

The most notable improvement in canopy inflation resulted from the introduction of an internal parachute into the inlet or mouth of the Para-Sail canopy. Reference 4 and other unpublished sources indicated that the internal parachute had a very marked effect in reducing opening time with little or no increase in opening shock. This was also substantiated in wind tunnel tests of model Para-Sails (see Volume I). In previous tests wherein full inflation had been achieved, opening times were in the order of 18 - 20 seconds. Inclusion of the internal parachute reduced opening time to 10 - 12 seconds and produced a more orderly inflation, although a great need for improvement was still indicated.

In conjunction with this modification, conventional pocket opening bands were added to the gores of the forward surface and suspension line length increased to approximately one D_o. The effect of these modifications on opening could not be ascertained since in all probability the influence of the internal parachute was much greater. However, the overall effect produced results which were desirable, even though the approach may not have been systematic.

It had been noted from drop test films that during the reefed state the slotted rear surface of the canopy would inflate and thereby raise the lower lateral band in that section above the remainder of the skirt in the less inflated portions.

It was theorized that by foreshortening the rear risers the proper amount, the canopy skirt could be kept more or less even and that glide would be reduced, thereby effecting improved inflation of the front section. A release was provided to extend these risers to full length after inflation was achieved. The results of this modification were not conclusive.

In view of the undesirable effects normally associated with an uneven parachute skirt, the size of stabilizer panels was reduced drastically in an attempt to improve this situation. The results of this change could not be ascertained adequately, but it is likely that a higher degree of reliability was produced with the particular configuration.

Of the modifications discussed, all but the reefing of the rear section were adopted. Conventional skirt reefing was also incorporated.

Sufficient reliability at low speed and less than maximum payload weight was demonstrated in three tests prior to beginning the Primary Test Program at the Joint Parachute Test Facility. It was with the configuration 80L-2, evolved through the efforts of the Preliminary Program, that this work commenced.

3.2.2 Primary Developmental Tests

In August of 1963 test work was initiated at the Joint Parachute Test Facility through the 6511th Test Group under local project LIC 9211. Originally a test program in accordance with Reference 5 was anticipated, with a total of 18 tests, including cluster deployments. However, with actual test experience of the Para-Sail came the realization that the scope of such

a program was beyond physical capability of the parachute within the foreseeable future of the program. And also since space craft requirements had changed, a revised program in accordance with Amendment 3 of Reference 1 was issued by the Contracting Agency.

In total, 20 drop tests summarized in Table I, were performed under this contract. This number of tests includes failures and side line investigations pertaining to the effect of internal parachute and stabilizer panels.

This section shall present the objectives and observations of each of the twenty tests. These observations might normally be included with results, but because of their influence on following tests they are presented with the objectives for the purpose of continuity.

3.2.2.1 Test Number: 1

Configuration 80L-2

Objectives: To study deployment and inflation characteristics and to evaluate steady state performance.

Test Conditions: Weight - 3,782 Pounds

Speed - 119 KIAS

Altitude - 4,950 Feet

Observations: The test was successful. The canopy exhibited a slow left turn. Minor burn damage was noted in several panels. Satisfactory disreefed opening was observed. The pilot chute collapsed after reefed opening as was intended by the omission of a single confluence point. (See Figure 7). The purpose of this rigging was to prevent the pilot chute from retarding inflation of the forward surface during glide while in the reefed state, however,

a tuck was still noted in the forward surface of the crown.

3.2.2.2 Test Number: 2

Configuration: 80L-3

Objectives: To further study deployment and inflation characteristics and to evaluate steady state performance.

Test Conditions: Weight - 3,740 Pounds

Speed - 120 KIAS

Altitude - 5,020 Feet

Observations: The test was successful. A tuck was noted in the forward surface of the crown of the reefed canopy. Rear risers were released at 20 seconds thereby extending to full length. Stitching on the pilot chute bridle failed at the bag connection; the pilot chute was retained however. The strain link failed and force data was not available.

3.2.2.3 Test Number: 3

Configuration: 80L-3

Objectives: To further study deployment and inflation characteristics and to evaluate steady state performance.

Test Conditions: Weight - 4,998 Pounds

Speed - 120 KIAS

Altitude - 5,000 Feet

Observations: The test was unsuccessful. The rear risers failed at reefed opening, at the point of attachment to the release device. The rear riser was hurled past the canopy and entangled with the pilot chute. The reefing line then failed.

The rear of the canopy was severely damaged. Measured opening loads were excessive, being 17,600 pounds.

3.2.2.4 Test Number: 4

Configuration: 80L-4

Objectives: Repeat of Test Number 3.

Test Conditions: Weight - 4,998 Pounds

Speed - 120 KIAS

Altitude - 5,000 Feet

Observations: The test was unsuccessful. After system stretch stitching failed in pilot chute bridle at the attachment to the deployment bag, resulting in a bridle failure and allowing the multiple crown bridle to rebound into the canopy apex. Vent lines then failed, permitting the crown to fully deploy, since it was no longer retained by the center suspension line. At this instant split gores developed and suspension lines began to separate until the canopy was free from the vehicle and suspension system.

3.2.2.5 Test Number: 5

Configuration: 80A-1

Objectives: To study deployment and inflation characteristics and evaluate steady state performance of a Para-Sail without a center suspension line.

Test Conditions: Weight - 2,785 Pounds

Speed - 120 KIAS

Altitude - 5,000 Feet

Observations: The test was successful. However, the formation of an inflated apex was slow. The tendency of the stabilizer panels to inflate in the reefed state was noted. They attempted to pull the skirt outward, but were restrained by the reefing line.

3.2.2.6 Test Number: 6

Configuration: 80A-1

Objectives: To study deployment and inflation characteristics and to evaluate steady state performance. In particular it was desired to ascertain the effect of a change in reefing line length.

Test Conditions: Weight - 2,785 Pounds
Speed - 120 KIAS
Altitude - 5,035 Feet

Observations: The test was successful. Better reefed inflation characteristics were noted due to an increased reefing circle diameter; however, the need for improvement was indicated. Disreefing was more erratic than previously noted.

3.2.2.7 Test Number: 7

Configuration: 80A-2

Objectives: To study deployment and inflation characteristics of the "A" type of Para-Sail without internal parachute.

Test Conditions: Weight - 2,775 Pounds
Speed - 120 KIAS
Altitude - 4,930 Feet

Observations: The test was successful. The canopy filled quickly in the reefed state, but appeared very unstable and

fluttered violently. The skirt was very disorderly. The general appearance was not as good as with the internal chute. Disreefed opening time was increased very significantly.

3.2.2.8 Test Number: 8

Configuration: 80A-1

Objectives: To study deployment and inflation characteristics and evaluate steady state performance. A specific objective was to learn the effect on opening of an increase in deployment altitude.

Test Conditions: Weight - 2,785 Pounds
Speed - 120 KIAS
Altitude - 10,600 Feet

Observations: The test was successful. The reefed inflation shape was attained quickly and smoothly, possibly accounting in part for a higher reefed opening force. The canopy and skirt shape were good.

3.2.2.9 Test Number: 9

Configuration: 80A-1

Objectives: To study deployment and inflation characteristics, evaluate steady state performance, and to ascertain the effect on these by an increase in payload weight.

Test Conditions: Weight - 3,880 Pounds
Speed - 119 KIAS
Altitude - 10,590 Feet

Observations: The test was unsuccessful. Prior to reefed inflation, a group of stabilizer panels passed under the skirt of the

canopy on the opposite side from where attached, and inflated in this position, drawing more of the canopy through and forming an inflated lobe. This was essentially a partial inversion type of malfunction. Upon disreefing suspension line failures occurred and the canopy was destroyed.

3.2.2.10 Test Number: 10

Configuration: 80A-3

Objectives: To study deployment and inflation characteristics and evaluate steady state performance and to ascertain the effect of an increase in payload weight. In addition it was desired to learn if revised packing, achieved by spacing and tacking the reefing line at each ring, and by applying light break ties around the folded stabilizers, would control the deployment problems associated with the last test.

Test Conditions: Weight - 3,860 Pounds
Speed - 119 KIAS
Altitude - 10,600 Feet

Observations: The test was successful. The deployment and inflation appeared normal. Stabilizers were not observed to pre-inflate. A slight tucking in the front of the canopy was noted in the reefed state. Forces were higher than test number 8, as expected.

3.2.2.11 Test Number: 11

Configuration: 80A-3

Objectives: To analyze deployment and inflation characteristics and evaluate steady state performance. It was intended also to

study the effect on these properties of an increase in payload weight and a slight reduction in reefing line length. The strength of ties around the stabilizer panels was increased to provide a more positive retention and the effectiveness of this procedure was to be evaluated.

Test Conditions: Weight - 4,750 Pounds

Speed - 120 KIAS

Altitude - 10,600 Feet

Observations: The test was unsuccessful. A canopy malfunction occurred. As in Test Number 9, a group of stabilizer panels appeared to pass under the opposite side canopy skirt and inflate, prior to the canopy being completely withdrawn from the deployment bag. Again, this malfunction appeared to be the start of a partial inversion, a small lobe being formed by the stabilizer panels and a portion of the adjacent skirt. At disreefing, suspension lines failed and several split gores developed along with numerous other rips. The canopy did retain sufficient inflation for the vehicle to be recovered at a high rate of descent. These results indicate that stabilizer control and restraint were ineffective.

3.2.2.12 Test Number: 12

Configuration: 80A-4

Objectives: To analyze deployment and inflation characteristics and evaluate steady state performance under increased payload weight. A specific objective was to study the effectiveness of controlling the stabilizer panels during inflation by the use of special deployment aids consisting of a skirt hesitator bag and a

sleeve encasing each of the folded stabilizers.

Test Conditions: Weight - 4,755 Pounds

Speed - 120 KIAS

Altitude - 10,600 Feet

Observations: The test was successful. Normal inflation was noted. The hesitator bag came free at skirt emergence from bag, rather than at system stretch as intended, due to unanticipated high acceleration forces at skirt emergence from the deployment bag. The canopy had acquired partial reefed inflation when the stabilizer panels emerged from the encasing sleeve. However, stabilizers did not inflate while the canopy was in the reefed condition. Although the test was successful, the method of stabilizer control did not function as proposed and needed additional development.

3.2.2.13 Test Number: 13

Configuration: 80A-5

Objectives: To analyze deployment and inflation characteristics and evaluate steady state performance of a Para-Sail without stabilizer panels. This experiment was considered worthwhile in view of the deployment difficulties relating to these panels.

Test Conditions: Weight - 2,820 Pounds

Speed - 120 KIAS

Altitude - 10,600 Feet

Observations: The test was successful. Deployment and inflation were good. The canopy had a satisfactory shape. The fully inflated canopy was very stable and exhibited a slow right turn. An unusual phenomenon was observed during the steady state descent

in that a radial tuck or fold was noted in the leading surface of the canopy near the skirt, as shown in Figure 18. Examination of the test item disclosed no deficiencies in line lengths or any indication of actual fouling of the reefing line. A possible cause of this occurrence is discussed further in Section 4.3.1.

3.2.2.14 Test Number: 14

Configuration: 80A-6

Objectives: To analyze deployment and inflation characteristics and evaluate steady state performance. Additionally, it was intended to appraise another method of stabilizer retention by means of reefing (see sub-section 3.1.10), since the hesitator bag and sleeves had not provided sufficiently positive control in Test Number 12.

Test Conditions:

Weight	-	4,750 Pounds
Speed	-	140 KIAS
Altitude	-	10,600 Feet

Observations: The test was unsuccessful. The canopy deployed and opened but with heavy damage. Test films revealed that reefing rings on gores 27 through 46 were pulled free from the canopy skirt prior to full reefed opening. Main seam number 36 and line number 38 were broken. Two gores were split from crown reinforcing band to vent.

Break cords retaining sleeves over stabilizer panels broke after disreefing and allowed stabilizers to inflate properly. The necessity for additional investigation of reefing methods is indicated. A possible cause of failure considered was line number 36 which was fabricated of 1,000 pound cord, in lieu of

550 pound cord as were adjacent lines. This cord had been retained from Configuration 80A-4 in which the strength was necessary to open the closure tie on the hesitator bag. It was felt that variations in line stretch might have created high local stress which in turn precipitated a progressive type of failure, although as will be seen from the following test, some unusually high forces appeared to exist in the reefing line.

3.2.2.15 Test Number: 15

Configuration: 80A-7

Objectives: To analyze deployment and inflation characteristics and evaluate steady state performance as well as to determine if proper corrective action had been taken to prevent recurrence of the Test 14 malfunction. This action consisted of replacing the 1,000 pound line No. 36 with 550 pound line and strengthening the reefing ring attachment.

Test Conditions:	Weight	-	4,750 Pounds
	Speed	-	140 KIAS
	Altitude	-	10,600 Feet

Observations: The test was unsuccessful. The canopy inflated fully in the reefed state. At this point the reefing line failed and inflation continued. Next a tear developed in gore 1 from panel 10 toward the vent. One group of stabilizers opened, followed by another. The canopy then fully inflated. All reefing cutters had actuated, only one containing nylon from the line. The reefing line was recovered in two lengths which matched the original length. All reefing rings remained attached. A photograph of the inflated damaged canopy is shown in Figure 19.

3.2.2.16 Test Number: 16

Configuration: 80A-8

Objectives: To analyze deployment and inflation characteristics and evaluate steady state performance as well as to determine if proper corrective action had been taken to prevent recurrence of the Test No. 15 malfunction. This action consisted of increasing reefing line strength from 1,000 pounds to 1,500 pounds and by spacing the reefing line so that all slack was spaced equally fore and aft of the stabilizer sections. (See Section 3.1.12).

Test Conditions: Weight - 4,750 Pounds

Speed - 140 KIAS

Altitude - 10,600 Feet

Observations: The test was successful, although medium damage was encountered. The canopy did not fill evenly, a crease forming initially in the forward section during the reefed phase, although complete inflation did occur before disreef. Stabilizer panels unfurled as the skirt disreefed. Two panels were blown in Section 10 and some burning was noted from the internal parachute stay line.

3.2.2.17 Test Number: 17

Configuration: 80A-9

Objectives: To study the effect of increased launching speeds on deployment and inflation and to evaluate steady state performance. It was also intended to ascertain the effect of a slight reduction in reefing line length. The internal chute stay line was changed to cotton.

Test Conditions: Weight - 4,750 Pounds

Speed - 154 KIAS

Altitude - 10,600 Feet

Observations: The test was successful, although medium canopy damage was encountered, in the nature of four (4) blown panels in the upper sections. Normal inflation was noted. Force data was not available for comparison. No burn damage from the cotton stay line was observed.

3.2.2.18 Test Number: 18

Configuration: 80A-9

Objectives: To study the potential turn characteristics with a specific method of fixed turn incorporated in the canopy rigging. This was achieved by closing the turn slots on one side of the canopy, as described in Section 3.1.13.

Test Conditions: Weight - 4,750 Pounds

Speed - 105 KIAS

Altitude - 10,600 Feet

Observations: The test was successful. Little or no damage was noted. Turn rates of approximately 9 degrees per second were observed which did not fulfill requirements.

3.2.2.19 Test Number: 19

Configuration: 80A-9

Objectives: To study deployment and inflation characteristics and evaluate steady state performance. An additional objective was to ascertain damage for comparison with Test No. 17.

Test Conditions: Weight - 4,750 Pounds

Speed - 154 KIAS

Altitude - 10,600 Feet

Observations: The test was successful, although damage was medium. One panel in the crown section was destroyed. The pilot chute bridle failed at system stretch and the internal parachute failed and collapsed before disreefing occurred. The skirt was unsymmetrical after loss of the internal chute.

3.2.2.20 Test Number: 20

Configuration: 80A-9

Objectives: To study the potential turn characteristics with an alternate method of inducing fixed turns incorporated in the rigging and compare results with those of Test Number 18. This was achieved by inverting the turn slots on one side of the canopy, as discussed in Section 3.1.13.

Test Conditions:	Weight	-	4,750 Pounds
	Speed	-	154 KIAS
	Altitude	-	10,600 Feet

Observations: The test was successful. Little or no damage was noted. The scoops inverted very well. Turn rates of approximately 18 degrees per second were observed.

3.2.3 Supplemental Drop Tests With Small Para-Sails

In an effort to achieve a method of controlling stabilizer panels during the opening process both the Manned Space Craft Center and the contractor embarked on simultaneous drop test programs with smaller, personnel sized Para-Sails of approximately 24 feet in diameter. These canopies were of a configuration similar to the full sized canopy, without centerline. Both programs had the same objectives, but sought the solution by different means. The approach selected by the Contracting Agency utilized a system of reefing on the lower edge of the stabilizer panels, in conjunction with break cords tied around the folded panels. Various combinations of stabilizer and skirt reefing times were tried. The optimum configuration appeared to be a four (4) second delay on stabilizers in conjunction with six (6) second delay on the skirt. With this sytem stabilizers would remain tied in groups until skirt disreefing (even through the stabilizer reefing had been activated) at which time the opening force of the skirt would break the tie cords.

Although this manner of controlling stabilizers worked well, it did introduce a potential reliability problem in that three (3) independent reefing systems must function in order for the Para-Sail to perform its mission satisfactorily. The details of these tests are discussed more fully in Reference 6.

Meanwhile the contractor had also performed a limited number of tests of a similar nature. The approach was one of attempting to achieve control of the stabilizers by means of proper strength break cords retaining the stabilizers in folded groups.

Unfavorable results were achieved in the initial test of this method. In packing, a strip of light airplane cloth, its length equal to the width of the stabilizer panels, was folded around the pleated panels and secured with a number of break ties. At skirt disreefing, one group of panels failed to unfurl and inflate, although the test vehicle was recovered at a low rate of descent. The airplane cloth had bunched, and the tie cords had failed to break.

In the second test, each group of panels was fitted with a sleeve or legging, which was permanently attached to the center panel. This sleeve was fitted with rows of grommets through which light break cords could be passed, permitting the sleeve to be secured around the pleated panels. (See Figure 14a for example). An additional safeguard was also provided by adapting a personnel parachute quarter deployment bag, commonly termed a quarter bag, to contain the skirt and stabilizer panels, sleeve encased. Closure was accomplished by means of a locking thong attached to the canopy main seam and a butterfly loop on a suspension line. In essence this was an adaptation of the conventional skirt hesitator used with cargo parachutes. This arrangement was such that the quarter bag was retained by the break cord closure tie. The object of this method was to contain the stabilizers in the quarter bag until system stretch, preventing air blast from opening the sleeves or inducing a malfunction before tension had been applied to the suspension system. The sleeves should then restrain the stabilizers until skirt disreefing, whereupon sufficient force would be available to break the securing ties on the sleeve.

This approach was tested, and inasmuch as the photographic

evidence available could indicate, was successful. Sequence photographs of the deployment, inflation and disreefing are presented in Figure 20. These photographs show that the deployment sequence functioned as intended, and this approach was, therefore, adopted for application to the larger Para-Sail and testing at El Centro. (Reference Sections 3.1.8 and 3.2.2.12). This method offered the advantage of not requiring additional reefing, but did present a problem in choosing suitable strength break ties, since the forces available to break these cords, either prematurely or at the correct instant were not known on the large Para-Sail and could not be determined without experiment. Even then the predictability of such forces under the same or other deployment conditions would be questionable.

As a parallel to Test Number 13 of the primary test program, both the Manned Spacecraft Center and the contractor performed drop tests of the small Para-Sails without the stabilizer panels. No attempt was made to measure L/D, however, rate of descent measurements showed an increase of as much as 15 percent. Photographs indicated greater height or depth profile than for Para-Sails with stabilizers.

3.3 Data Acquisition

The determination of steady state performance, deployment and inflation forces, and times was of paramount importance in this program. Only in this manner could the characteristics of the Para-Sail parachute be determined and its suitability for spacecraft recovery evaluated. The required performance data may be listed as follows:

a) Opening forces and times (individual riser as well as total).

b) Steady State forces (individual riser as well as total).

c) Lift/Drag measurements.

d) Rate of descent measurements.

e) Turn rate measurements.

f) Photographic coverage of steady state and non steady state phases.

These items are discussed in the following sections.

3.3.1 Opening Forces and Times

The initial instrumentation concepts proposed the use of telemetry in conjunction with an on board recording oscillograph for purposes of redundancy. The telemetry and associated strain links were to be supplied by the testing agency and the oscillograph was to be furnished and maintained by the contractor. Accordingly a Consolidated Electrodynamics Type 5-118A Oscillograph was procured. However, latter improvements in telemetry reliability made the use of this item unnecessary and it was consequently not utilized in the program.

Prior to the primary development tests at El Centro, force data on the large Para-Sail was non existent. Initial attempts at obtaining this information were unsuccessful due to strain link failures and deployment problems. However, structural failures were indicative of one fact. Specifically, opening forces were not equally distributed throughout the suspension system as was evidenced by the rear riser failures and the incidence of damage in the canopy rear sections.

It was, therefore, directed by the Contracting Agency that force measurements be obtained on individual risers and

centerline as well as in total. This system of instrumentation was instituted with drop test number 5.

However, satisfactory individual riser force measurements were not immediately available. Considerable difficulty was encountered in achieving reliable transmission of these signals, and instrumentation personnel at the test agency were not able to determine the causes directly. In time, the difficulties were eliminated when a change in test vehicles was instituted. The transmission problem was ultimately related to the compatability of drop aircraft and test vehicle. The test vehicle is normally determined by the type of aircraft which is in turn determined by the weight, speed and altitude requirements. In this instance speed was comparatively low, 120 KIAS for many of the tests. Therefore, the use of a comparatively low flying cargo aircraft such as the C-130 was required. This necessitated the use of a weight bomb type of vehicle as shown in Figure 21 which could be extracted over roller conveyors in the floor of the aircraft.

However, previous experience with multi-channel telemetry had involved the use of a different type of drop weight, termed a cylindrical vehicle which is shown in Figure 22. This item is normally dropped from higher speed aircraft such as the B-66, which utilizes a different delivery system from the bomb bay. It was finally determined that transmission problems were associated with a flexible antenna required for use with the weight bomb and that the frequencies necessary for some of the individual riser forces were affected by movement of this antenna. Correction of this difficulty

merely necessitated use of the cylindrical vehicle which was not affected by this problem. However, one difficulty remained regarding the manner of extracting the cylindrical vehicle from the aircraft. Fortunately, a method had been previously devised for project Apollo by test agency personnel to provide a means of extraction over the roller conveyors. This system uses a sled for support of the vehicle, which is extracted and then separates from the vehicle, at the same time deploying the test item pilot parachute. Recovery of the sled is then also effected. For a more complete description of this method see Reference 7.

The use of the cylindrical vehicle eliminated data transmission problems and adequate force information was recorded for the remainder of the tests. In all, eight (8) channels of telemetry were utilized satisfactorily.

3.3.2 Steady State Forces

It was also desirable to establish steady state forces on the individual risers in order to determine center of pressure and to analyze the effect of loading on canopy profile. The manner of achieving these measurements was to continue telemetry transmission during steady state descent. Again, the ability to accomplish this reliably depended upon the change in drop test vehicles discussed in the previous section. When this was accomplished very satisfactory data was received, which has been tabulated in the results section.

3.3.3 Determination of Lift/Drag Ratio

The manner of determination of this parameter was through the use of standard photo-theodolity equipment. In order to calculate L/D, tangent plane velocity and rate of climb must be determined.

$$L/D = \frac{V_{TP}}{V_V} \qquad (1)$$

All wind vectors are assumed parallel to the tangent plane. Hence rate of climb is not wind corrected, although tangent plane velocity must be.

Therefore, in order to calculate reliable glide ratios, it becomes necessary to accurately determine the wind profile of the atmosphere through which the parachute descends at the time of the drop.

Atmospheric profiles at the test site are normally determined by RAWIN balloon. Such information as pressure, density, and temperature are transmitted back to a test site receiving and tracking station by the balloon as it ascends through the atmosphere. Wind velocities are determined by radar tracking of this balloon. This method provides accurate data on wind conditions above 2,000 feet. However, considerable difficulties occur when attempting to coordinate release of the balloon with time of drop and differences in time of up to an hour are not unusual. Needless to say, wind profiles may change considerably in the course of an hour.

In an attempt to provide better data, a non-gliding wind drift parachute was utilized on many of the tests. The advantage of its use was one of coordination, in that the drift

chute could be dropped shortly after the test item, on either a second pass of the drop plane, or by an auxilliary aircraft, and then tracked by photo-theodolite. Comparisons of drift chute and Rawin L/D data may be seen in Table II, and for the tests examined show very good correlation.

It was felt, however, that Lift/Drag ratios computed on the basis of wind drift chute data were more reliable due to the proximity to drop time.

3.3.4 Determination of Vertical Velocity

Determination of vertical velocity (rate of climb) was accomplished by photo-theodolite as per standard procedures. No wind corrections were necessary to this data which was utilized as tabulated.

3.3.5 Measurement of Turn Ratio

In the planning stage of this program it was anticipated that accurate measurement of turn rates and responses would necessitate the use of an on board turn rate gyroscope. A Humphrey 12-28 Series rate gyro was procured for this purpose, but was not utilized because of other factors. First, the only turn rates to measure were produced by fixed turns of the canopy caused by modifications to the rigging. The parachute was deployed in this manner and would then begin turns immediately upon inflation, making measurements of response and angular accelerations of little value. Secondly, the connection of parachute to vehicle was accomplished through a single point attachment, permitting a degree of swiveling in the riser. Hence an on board gyroscope would have determined the roll characteristics of the vehicle but not those of the Para-Sail. The

The relationship of vehicle to canopy response becomes in this case a function of the type of connection between vehicle and canopy and the moment of inertia of the particular vehicle.

Consequently, canopy roll rates were determined from phototheodolite (Askania) and Contraves film data. Both films indicated good agreement and differd only slightly due to viewing angle and station position. Results are presented in Section 4 and are sufficiently accurate for the type of testing performed.

3.3.6 Photography

During the course of this program photography proved an invaluable tool in studying the opening characteristics and ascertaining the causes of deployment problems. High speed motion picture coverage (200 FPS) was provided of each test from every possible vantage point, from the drop and chase aircraft, on board the vehicle, and from a number of ground stations through high powered telephoto cameras.

Many times the solution to a particular problem resulted from a careful analysis of drop test films. In addition to their use in analyzing inflation characteristics, these films also proved useful in determining canopy profiles and gore curvatures in the steady state conditions, as discussed in Section 5.9.

3.4 Data Evaluation

Altogether a considerable amount of valuable performance data (steady state and non steady state) was made available from the tests under this program. In order to become meaningful, much of this information must be examined and

compared with similar data under other conditions. In accomplishing this analysis, the results of which are submitted in Section 4, particular methods were utilized which are discussed in the following sub-sections.

3.4.1 Lift/Drag Ratios

If lift/drag histories presented in Appendix G are examined, it will be noted that large fluctuations occur during descent. The extent and rate of these variations is such that a visual mean value cannot be accurately determined. Consequently it has proven necessary to arithmetically average the lift/drag ratios for each test, using a time basis. The range over which this data is averaged has generally been chosen as beginning at 20 seconds after drop (to allow the Para-Sail parachute to open and stabilize) to a 2,000 foot altitude. This was chosen as the cut-off point since data below this altitude is reported as unreliable in some instances. Values are taken at one second increments within this range, and then averaged. The values so obtained were then used for the comparative data plots of Section 4.

3.4.2 True Drag Area

True drag area, which is based upon total velocity, as distinguished from effective drag area, which is based on vertical velocity, is determined by the equation,

$$C_D S = \frac{M}{q} \left(\frac{dV_T}{dt} - g \sin \theta \right) \qquad (2)$$

and finds general use in data reduction of the Joint Parachute Test Facility. Consequently the derivation is not included.

When so requested, tabulation sheets with this information are supplied by the test agency.

Again, for comparative purposes it becomes necessary to establish average values of $C_D S$ from which C_D can then be determined. This is accomplished in the same manner as with L/D using equal time increments of one second and from 20 seconds after drop to a 2,000 foot altitude. This approach was utilized in arriving at the values for C_D presented in Section 4.

In addition, the drag area determined by the above equation is useful in establishing shock factors during inflation since time correlated force data is also available.

3.4.3 Effective Drag Area

Effective drag area is possibly one of the more important indications of Para-Sail performance. Although significant lift/drag ratios may be evidenced, vertical velocity is probably the most critical component to be considered in the safe recovery of payloads. Percise determination of this velocity requires accurate calculations of effective drag area.

Hence it was proven necessary to establish an equation for the determination of instantaneous effective drag area. This equation is as follows:

$$C_{D_{eff}} S = \frac{2W}{\rho\left(\frac{dh}{dt}\right)^2}\left[1 - \frac{1}{g}\left(\frac{d^2h}{dt^2}\right)\right] \qquad (3)$$

For completeness the derivation of this equation is presented in Appendix A.

Equation 3 was programmed for computer solution and presented to the contractor in tabulated and plotted form after each drop test.

As with other data, fluctuations occurred making visual averaging difficult. Consequently, it became necessary to determine arithmetical average values for each drop in the same manner as for L/D and $C_D S$.

When this must be done by desk calculator or adding machine, it becomes quite time consuming. Consequently, another method was applied for expedient results, although the arithmetical approach was performed for comparative purposes.

The more expedient method is based on an average with respect to density, providing results quickly, and is accurate to the extent that density varies linearly with altitude. This equation for average effective drag area is presented as follows:

$$C_{D_{eff}} S_{avg} = \left(\frac{tb-ta}{ha-hb}\right)^2 \cdot 8W \left(\frac{\sqrt{\rho b} - \sqrt{\rho a}}{\rho b - \rho a}\right)^2 \qquad (4)$$

The derivation of this equation is presented in Appendix A and is arrived at through integration over a density range.

Table III presents the results of both the arithmetical and integration methods and shows reasonably good agreement between the two.

Table I

TEST PROGRAM PLAN

EL CENTRO PROJECT L1C-9221

Test Condition	Canopy Configuration	No. Tests	Total Weight Lbs.	Launch Altitude Ft.	Deployment q/KEAS	Purpose
1	80L-2,-3	2	3,700	5,000	49/120	Study Deployment and steady state characteristics.
2	80L-3,-4	2	4,800	5,000	49/120	" " "
3	80A-1,-2	3	2,800	5,000	49/120	Study deployment and steady state characteristics, effect of internal chute and variation of reefing line length.
4	80A-1	1	2,800	10,600	49/120	Study deployment and steady state characteristics.
5	80A-1,-3	2	3,900	10,600	49/120	" " "
6	80A-3,-4	2	4,750	10,600	49/120	" " "
7	80A-5	1	2,800	10,600	49/120	Study effect of removal of stabilizer panels.
8	80A-6,-7,-8	3	4,750	10,600	66/140	Study deployment and steady state characteristics.
9	80A-9	2	4,750	10,600	80/154	" " "
10	80A-9	2	4,750	10,600	37/105	Study fixed turn characteristics and methods.

Table II

COMPARISON OF LIFT/DRAG RATIOS

COMPUTED FROM RAWIN BALLOON AND

DRIFT CHUTE DATA

Test No.	L/D Rawin	L/D Drift Chute
10	1.07	1.00
12	1.05	1.02
13	1.02	1.07
14	1.10	1.08
15	1.11	1.13

Based on arithmetical average.

Table III

COMPARISON OF AVERAGE EFFECTIVE

DRAG AREAS AND COEFFICIENTS

BASED ON DENSITY AND TIME

Drop Test Number	Average Effective Drag Area, Ft.^{2}		Average Effective Drag Coefficient		Percent Variation
	Based on Time*	Based on Density**	Based on Time*	Based on Density**	
5	10,256.4	10,287.3	2.07	2.08	.5
6	8,702.5	8,902.4	1.76	1.80	2.2
7	9,528.0	9,941.1	1.93	2.01	4.0
8	9,710.0	9,397.0	1.96	1.90	3.1
10	7,995.3	8,012.2	1.62	1.62	0
12	7,025.3	6,924.1	1.42	1.40	1.4
13	7,016.9	6,924.1	1.42	1.40	1.4
14	7,626.8	7,715.4	1.54	1.56	1.3
15	7,351.6	7,220.9	1.49	1.46	1.4
16	7,229.0	7,072.5	1.46	1.43	2.1
17	8,268.8	8,061.7	1.67	1.63	2.42
18	8,161.0	7,913.3	1.65	1.60	3.1
19	7,056.9	6,825.2	1.42	1.38	2.9
20	6,529.7	6,231.7	1.32	1.26	4.6
				Average Percent Variation	= 2.2

* Determined from arithmetical average of tabulated data.

** Determined from equation:

$$C_D S = \left(\frac{\Delta t}{\Delta h}\right)^2 \cdot 8W \left(\frac{\sqrt{\rho b} - \sqrt{\rho a}}{\rho b - \rho a}\right)^2$$

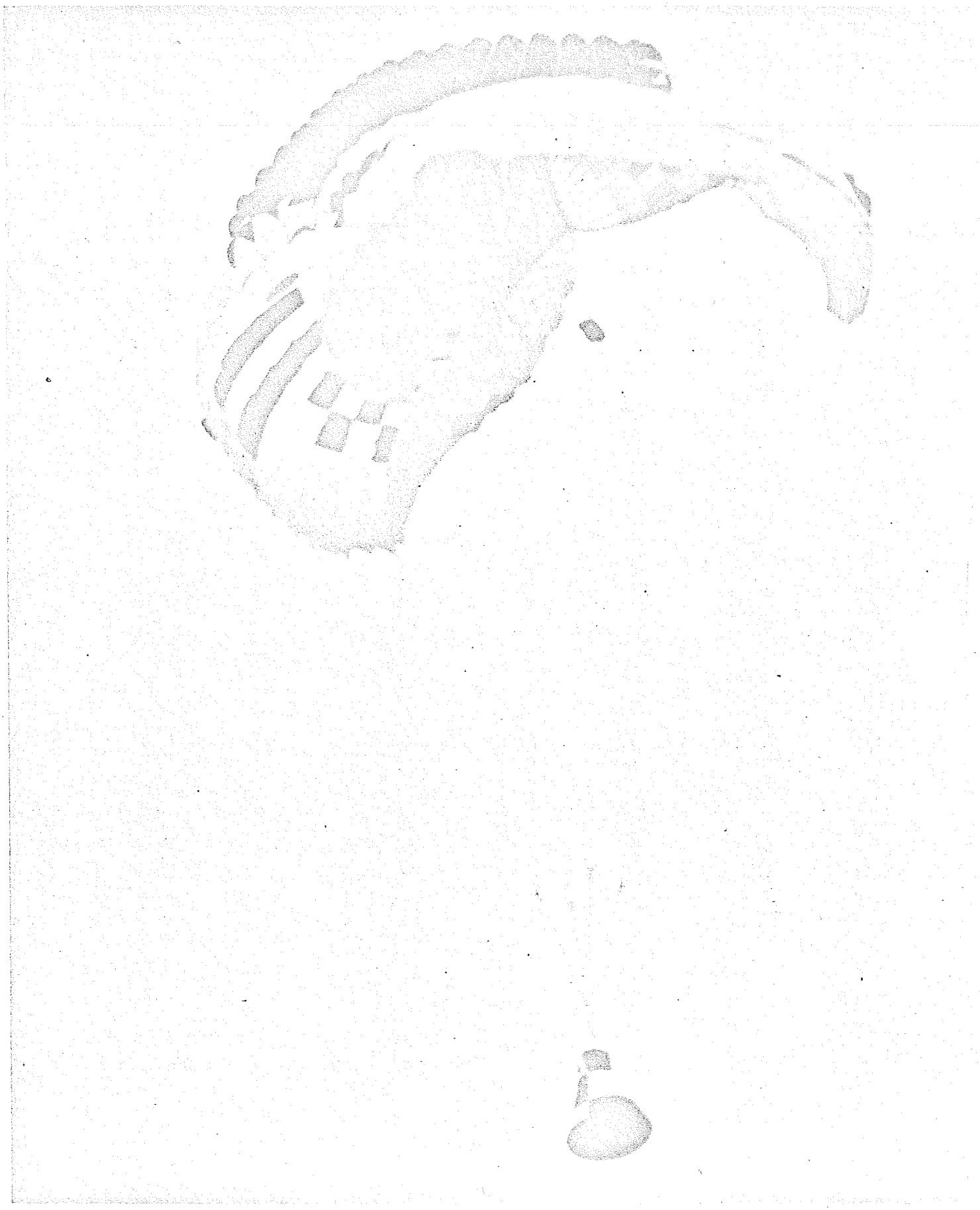

Figure - 17 -

Malfunction of Para-Sail Configuration 80L-1
During Preliminary Functional Tests

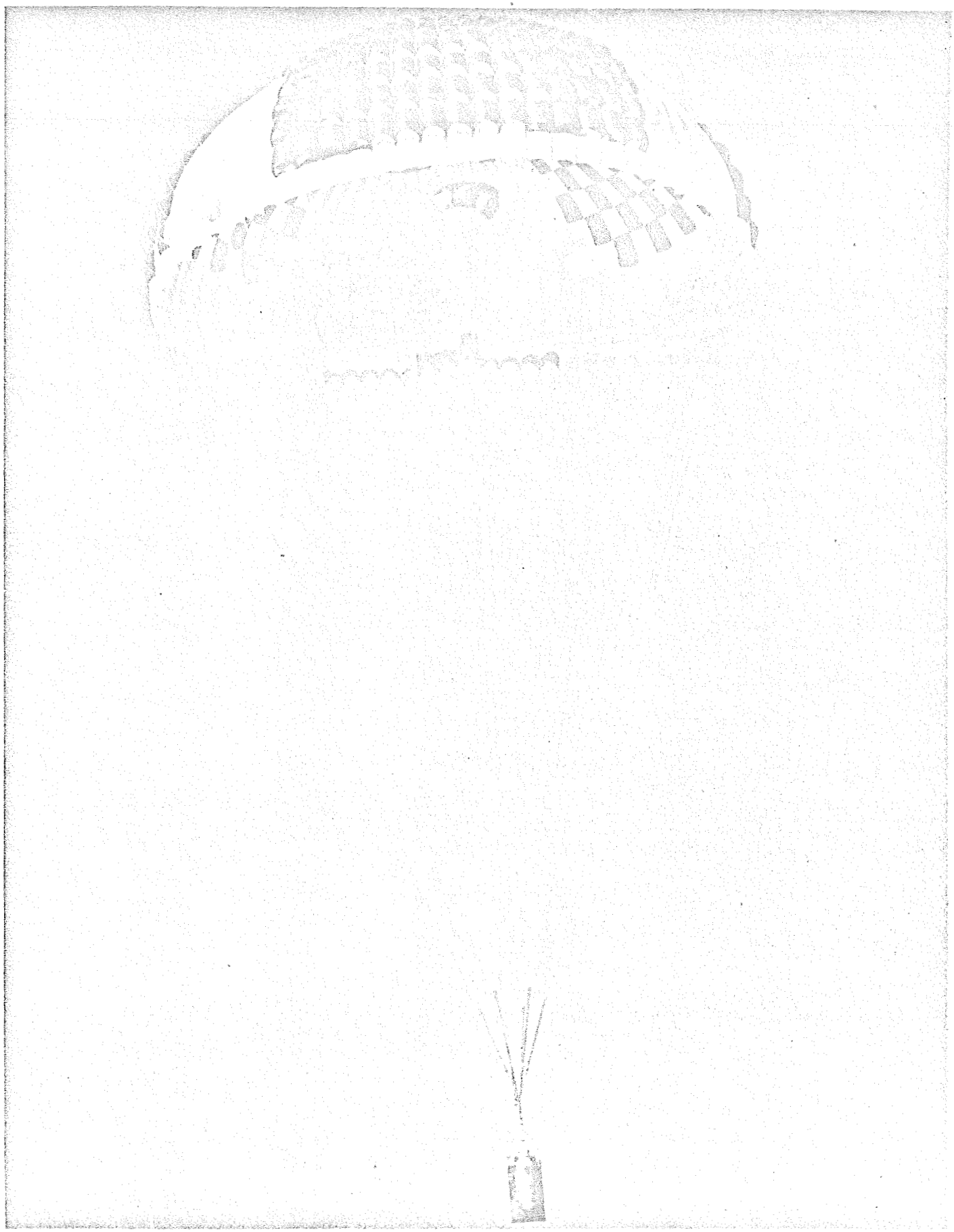

Figure - 18 -

Para-Sail Without Stabilizers - Test No. 13

Figure - 19 -

Para-Sail as Damaged in Test No. 15

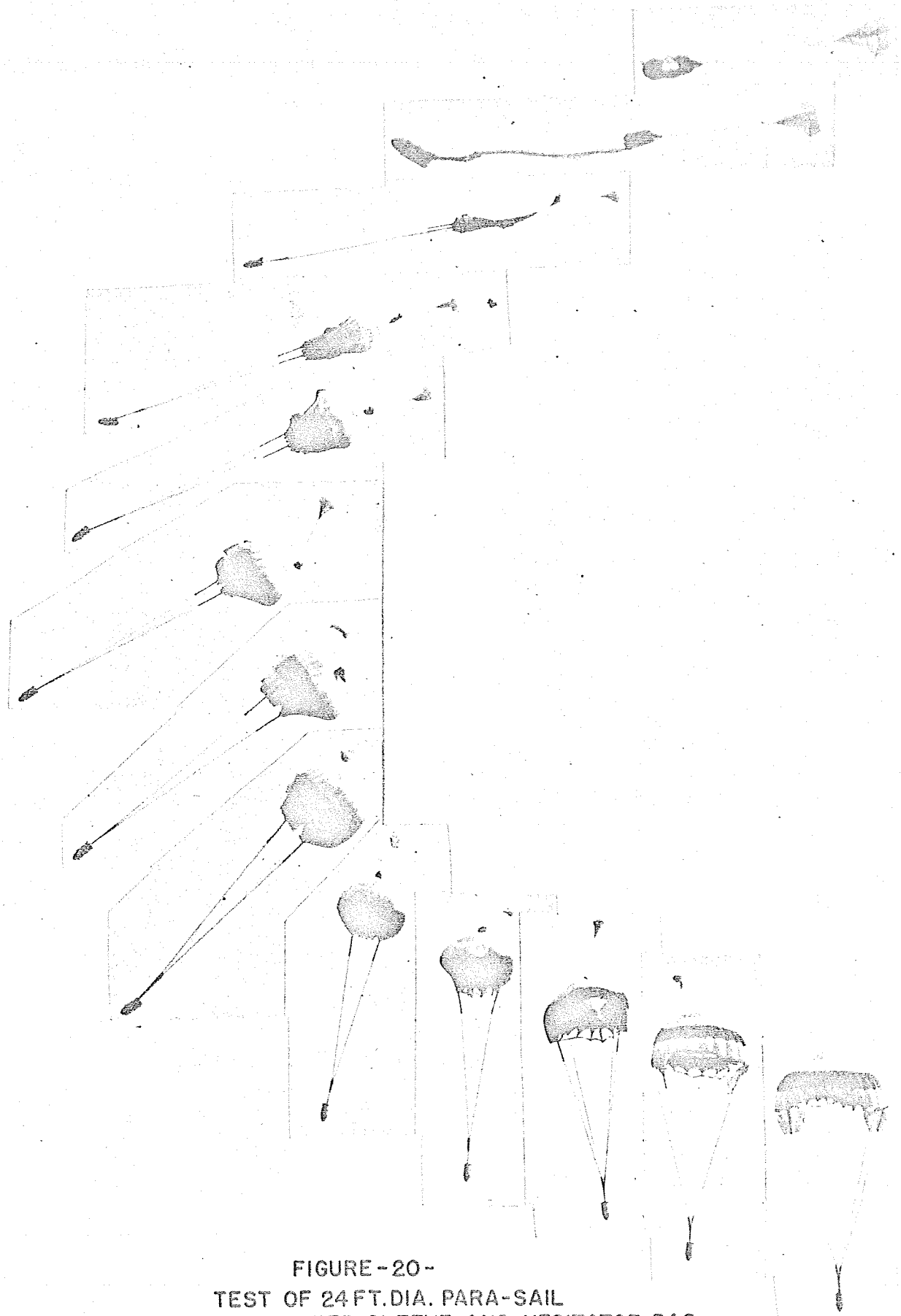

FIGURE-20-
TEST OF 24 FT. DIA. PARA-SAIL
WITH STABILIZER SLEEVE AND HESITATOR BAG

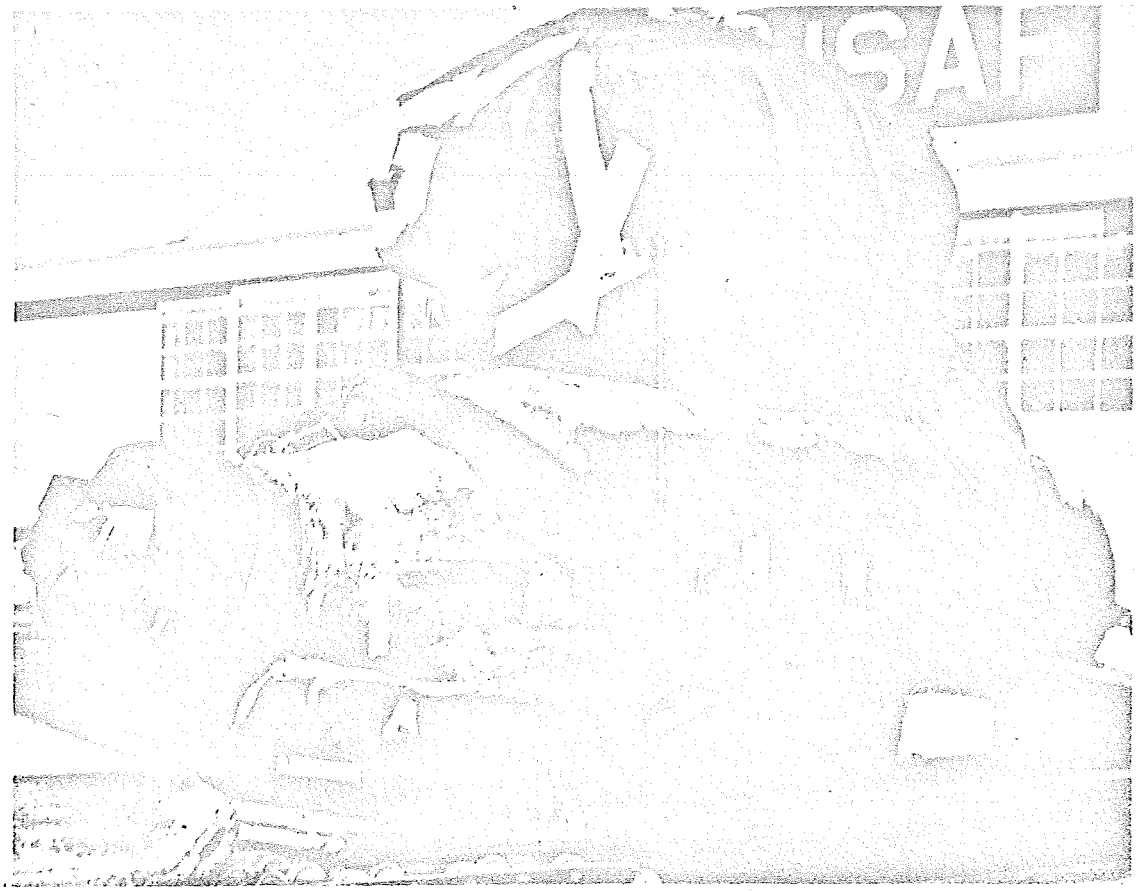

Figure - 21 -

Weight Bomb Vehicle With Para-Sail Attached

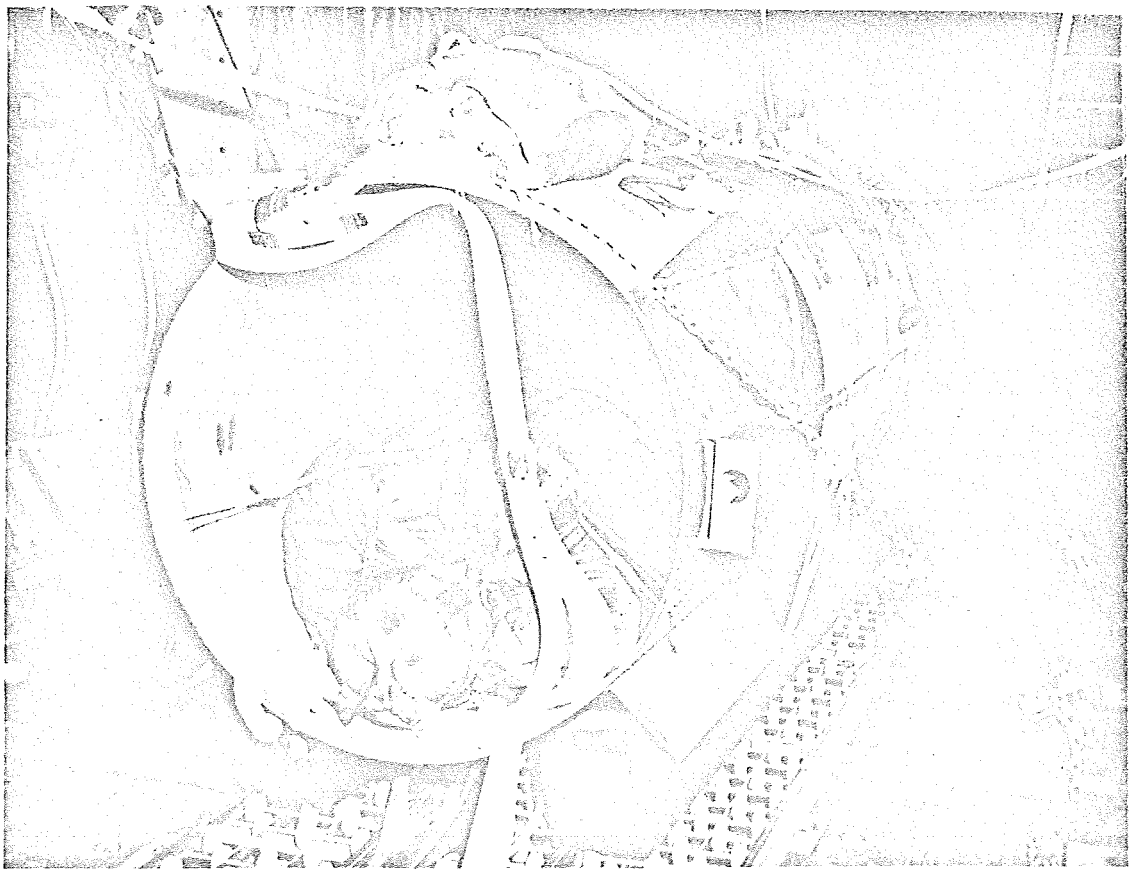

Figure - 22 -

Cylindrical Vehicle on Extraction Sled

4.0 TEST RESULTS AND DISCUSSION OF DATA

This section presents a tabulation and summation of test results on all configurations of the test item. Representative data in support of this section is included in Appendixes E, F, and G. A summary data sheet for all tests is provided as Table VII of this section.

4.1 Steady State Performance

4.1.1 Effective Drag Coefficient

Figures 23 and 24 present effective drag areas for the various configurations tested at El Centro. The values shown are averages, for each drop, and are computed with respect to density. Both curves indicate a decided effect of canopy loading (and vertical velocity) with a decrease in coefficient for an increase in these parameters. At a canopy loading of .56 lbs./ft.^{2}, the effective drag coefficient was approximately 1.95, and at a loading of .96 lbs./ft.^{2} this value decreased to 1.45.

Also worth noting in these figures is the effect of certain variables in the configuration geometry. For an 80L-3 configuration in drop No. 2, with center suspension line, a coefficient of 2.58 was calculated at a canopy loading of .75, which is indicative of a vastly more efficient canopy than those without centerline. In drop No. 13, the stabilizers were removed, and effective drag coefficient was reduced significantly.

In drop numbers 18 and 20 the Para-Sail was deployed with a turn incorporated in the rigging. In drop No. 18, which had a turn rate in the order of 9 deg./sec., the coefficient seemed little effected in contrast to test number 20, with a turn rate of 18 deg./sec., which showed a very noticeable decrease.

As will be seen in later discussions, the decrease in coefficient for drop 13, 18 and 20 is related to a reduction in lift force. It appears that the noticeably greater value for test number 2 is the result of greater canopy efficiency.

4.1.2 Lift/Drag Ratio

Figures 25 and 26 present the lift/drag ratios averaged for each drop versus canopy loading and vertical velocity. A slight decrease in lift/drag takes place with increased canopy loading. At canopy loading values of .56 an average L/D of approximately 1.16 exists, decreasing to 1.13 at a loading of .96 lbs./ft.^{2}. Drop number 13 (without stabilizers) exhibits lower values of L/D as does the turn test of drop number 20. These points tend to substantiate the trends in effective drag coefficient shown in Figures 23 and 24. It is worth noting that the value of L/D determined for test number 2, with center suspension line, was in the same order of magnitude as for the configurations without centerline. This is as was predicted by wind tunnel experiments. (See Volume I).

4.1.3 Drag Coefficient

Figure 27 presents the average drag coefficient. This is the true drag coefficient, based on equation 2. Again it will be noted that this value decreases with respect to increased canopy loading. The drag efficiency of the centerline configuration, test number 2, was very high, while the efficiency of the canopies in a turn exercise, tests 18 and 19, was not effected, notwithstanding the large amplitude of swing out noted in these tests, and the tilting of the canopy which resulted.

4.1.4 Lift Coefficient

The averaged values for lift coefficient are shown in Figure 28. Again the dependency upon canopy loading is shown. Drop number 2 with centerline also indicates a high lift efficiency, as well as high drag efficiency, even though L/D is not greater than configurations without centerline. The reduction of C_L shown in the turn test, number 20, is as would be expected from experience with air foils in a banking turn, wherein lift force is decreased toward the inside of the turn.

Figure 29 correlates both lift and drag coefficients together, showing the effect of canopy loading and configuration geometry.

4.1.5 Turn Rates

The results of the turn tests described in Section 3.2.2 (sub-sections 18 and 20) are plotted in Figure 30, showing the effectiveness of the two methods. The turn rate achieved by completely inverting the slots on one side was twice that obtained by merely closing them. These turn rates correlate roughly with the sum of exhaust areas normal to the direction of rotation, these areas being approximately doubled by inverting the slots on one side.

4.1.6 Riser Forces

The forces acting on individual risers are listed in Table IV for various drops. Figure 31 shows the riser geometry. It will be seen that the distribution of these forces is not symmetrical. The risers and suspension lines attaching to the front (leading surface) carry approximately 28% of the suspended load. The side risers carry 44% (22% each side) of this load

and the rear risers sustain 40% of the load. The internal parachute centerline carries no load during steady state descent. This data is utilized in Section 5.9.3 in determining the center of pressure of the Para-Sail.

4.2 Opening Characteristics

4.2.1 Individual Riser Forces

Table V summarizes the available data on individual riser forces for both reefed and disreefed cases (1st and 2nd peaks). An analysis of the presented values indicates a high degree of asymmetrical loading during inflation. The highest loads were experienced primarily on the rear risers, although side risers were subjected to some higher forces. The average deviation from the mean was determined to be 26.6 percent. This indicates that a member of the suspension system could be subjected on an average to a load 26.6 percent higher than would be expected under symmetrical loading. A more accurate value could be obtained by averaging results under design conditions, however, force data from only one such test was available. This one value does correlate closely with the average determined from all test conditions.

4.2.2 Typical Force and Trajectory Curves

The force trace from drop number 19 which might be considered a typical test under design conditions, is shown in Figure 32. However, it must be noted that the internal parachute was destroyed after opening and this force trace becomes zero sooner than normal. Trajectory data for the same test is presented in Figure 33, which may be considered as representative for the design conditions.

4.2.3 Inflation Parameters

An interesting trend was noted in the study of canopy reefed drag area. The pecularity of this information is in the apparent relationship of reefed drag area to canopy loading, which was quite unexpected. It will be noted from Figure 34 that drag area increases with increase in canopy loading, i.e. increase in vehicle weight. Drag area is plotted as proportionate to the ratio of nominal diameter to reefed diameter, although the result is the same if actual drag area is used. It may be theorized that this effect is due to higher internal pressure which forces the canopy to assume a broader projected diameter. It has been observed from drop test films that the Para-Sail normally assumes a very spherical reefed shape, rather than the so-called "light bulb shape" normally associated with conventional canopies. However, it is also worth noting that conventional solid canopies will also form a more spherical reefed shape under higher canopy loading.

As an aid in analyzing the opening process, filling times have been graphed against what appears to be the influencing parameters of velocity, diameter, weight and density ratio as shown in Figures 35 and 36 for the reefed and disreefed cases respectively.

In a similar manner, opening force is shown versus the momentum of the system at the time of line stretch, or more simply, the product of vehicle weight and speed. This was done for reefed and disreefed cases as presented in Figures 37 and 38.

This information serves as the basis for additional analysis in Section 5.10 in attempting to arrive at empirical data curves for opening shock relations.

4.2.4 Internal Parachute Performance

A separate study was made of the inflation characteristics of the internal parachute, a 10 foot diameter Ribless Guide Surface. The information was obtained from force traces and trajectory history of the drop tests. This data is summarized in Table VI. The relationship of filling time to velocity is shown in Figure 39a. Two shock (xK) factors are included in Figures 39b and c. One is based on velocity at skirt emergence from the bag and the other on velocity at inflation. Of the two, the former is probably the more useful and shows a nearly constant shock factor of .8 over the range of data. These are all at a primary canopy loading of .96. Unfortunately the effect of the canopy loading variable cannot be determined.

4.3 Observed Results

4.3.1 Radial Fold of Drop Number 13

More recent experience under other contracts may provide a clue to causes of the radial tuck exhibited in drop test number 13 as shown in Figure 18. Tests have shown that the addition of excessive fullness to the gore width will crease a radial fold in the leading surface. The stabilizers normally exert a force tending to distort the canopy into an elliptical planform. This force also appears to influence canopy profile as well. Hence it may be theorized that the absence of these stabilizers permitted an excess of cloth to form on the leading surface which could not be supported by internal pressure and therefore formed a radial fold.

4.3.2 Reefing Forces

Drops 14 and 15 which were unsuccessful, exhibited certain problems related to reefing. To recapitulate, in test number 14, the reefing rings were ripped from the forward skirt of the canopy, which was at that time attributed to an over strength suspension line retained from a previous test. This situation was remedied and the reefing ring attachment strengthened. In the next test under identical conditions the reefing line failed. Both tests indicate that unusually high forces were produced in the reefing line. Whether or not these forces are normal with Para-Sail inflation is not known. On a subsequent test, reefing line strength was increased from 1,000 to 1,500 pounds and the manner of spacing the line described in Section 3.1.12 adopted. Further difficulties did not insue after this action.

4.3.3 Damage Reports

Planview damage charts are included in Appendix D. Unfortunately accurate records were not always kept of the damage, since many times a canopy was so completely destroyed that the task of charting became enormous and to some extent the information of little value. However, among damage charts of successful tests a certain pattern of damage is indicated. This pattern shows the highest incidence of damage to be in the 10th panel from the skirt and primarily in the rear, but extending to the side areas. This is substantiated by the results of Table V, showing the rear risers to sustain a higher opening load.

Table IV

STEADY STATE FORCES ON INDIVIDUAL RISERS

Drop Test No.	Riser 1-12 Rear	% Susp. Wgt.	Riser 61-72 Rear	% Susp. Wgt.	Riser 13-24 Side	% Susp. Wgt.	Riser 49-60 Side	% Susp. Wgt.	Riser 25-36 Front	% Susp. Wgt.	Riser 37-48 Front	% Susp. Wgt.	Susp. Weight
12	1,000	21.9	1,000	21.9	1,000	21.9	1,000	21.9	600	13.1	625	13.6	4,590
14	900	19.6	875	19.1	1,000	21.8	1,200	26.2	425	9.3	1,100	24.0	4,585
15	925	20.2	900	19.6	1,000	21.9	1,025	22.4	600	13.1	655	14.3	4,586
16	1,000	21.9	880	19.2	900	19.6	1,025	22.4	400	8.7	700	15.3	4,586
18*	925	20.2	975	21.3	975	21.3	1,050	22.9	900	19.6	550	12.0	4,589
19	900	19.6	800	17.4	950	20.7	1,100	24.0	600	13.1	600	13.1	4,588
20*	800	17.5	900	19.6	800	17.5	940	20.5	555	12.1	550	12.1	4,586

* Turn Tests

Average Percent Suspended Load

Rear Riser - 19.9

Side Riser - 21.9

Front Riser - 13.8

Table V

OPENING FORCES ON INDIVIDUAL RISERS

Drop Test No.	Force	Total Weight	Rear 1-12	Rear 61-72	Side 13-24	Side 49-60	Front 25-36	Front 37-48	Avg.	Max. Dev.	% Max. Dev.	Total Recorded Force
12	1st Peak	2820	2400	2050	1900	1600	1900	1800	1942	458	23.6%	14,100
12	2nd Peak	2820	3000	3100	2500	1850	2625	1500	2429	671	27.6%	13,800
14	1st Peak	4750	2650	2860	2700	2800	2100	2875	2664	211	7.9%	15,900
14	2nd Peak	4750	2775	3300	2200	2400	2200	2175	2508	791	31.5%	12,600
15	1st Peak	4750	3500	2900	3000	3310	2250	2550	2860	632	22.0%	16,100
15	2nd Peak	4750	4700	3900	2950	2800	2800	2700	3308	1392	42.0%	16,450
16	1st Peak	4750	2680	3000	2290	2700	1300	1900	2312	688	29.8%	15,000
16	2nd Peak	4750	2750	2520	2550	2500	1400	1700	2236	514	23.0%	11,000
18*	1st Peak	4750	2025	2100	1625	1790	1800	1600	1823	267	14.6%	11,560
18	2nd Peak	4750	3675	3100	1575	1700	2000	3415	2578	1097	42.6%	13,700
19	1st Peak	4750	3100	2500	2900	1700	2300	2100	2433	667	27.4%	14,800
19	2nd Peak	4750	3000	2900	2300	2700	2000	1800	2450	550	22.4%	12,600
20*	1st Peak	4750	1900	1950	1650	2100	1500	1650	1792	308	17.2%	12,000
20	2nd Peak	4750	3525	3200	1700	2000	2100	2500	2504	1021	40.8%	14,750

* Turn Test

Avg. % Max. Dev. = 26.6%

M.T.G.
5 Nov. 64

Table VI

INFLATION CHARACTERISTICS OF A 10 FT. DIA.

RIBLESS GUIDE SURFACE INTERNAL PARACHUTE

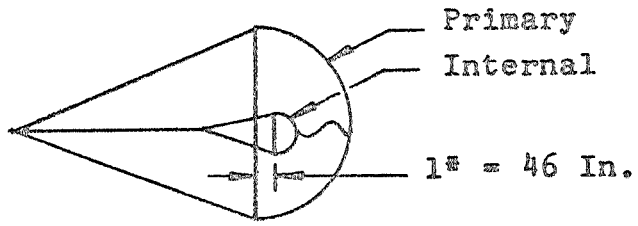

Test No.	Altitude Ft.	Launch Velocity Ft./Sec.	Main Canopy Skirt Emergence Velocity Ft./Sec.	Main Canopy Skirt Emergence Pressure PSF	Internal Canopy Inflation Velocity Ft./Sec.	Internal Canopy Inflation Pressure PSF	Opening Force F_I Lbs.	Filling Time t_f** Sec.
12	10,600	230	235	46	210	38	2,200	1.1
14	10,600	285	290	73	280	64	3,800	0.6
15	10,600	280	285	68	262	57	3,100	0.8
16	10,600	280	272	62	225	45	2,700	1.1
18	10,600	185	200	35	200	35	2,000	1.1
19	10,600	300	300	77	255	60	4,000	0.9
20	10,600	195	200	34	200	34	1,400	1.5

* Determined for deflated condition - from skirt of internal to skirt of Para-Sail farthest from apex.

** Determined from main canopy skirt emergence until peak force on internal parachute.

TABLE

PARA-SAIL TEST DA

	GENERAL DATA						AIRCRAFT DATA			PILOT CHUTE		PARACHUTE DATA						WEIGHT DATA										
TEST NUMBER	VEHICLE DROP NR	DROP DATE	TEMP F	BARO PRESS INCHES HG	REL HUMIDITY PER CENT	GROUND WIND KNOTS	TYPE	IAS/EAS KNOTS	PRESS ALT FEET	DIA-KIND DEPLOYMENT	DIA-KIND PERM ATTACH	DIAMETER	PARACHUTE SERIAL NR	CONF NR	REEFING LINE LENGTH, FT	REEFING DELAY STAR PANELS	REEFING DELAY SKIRT SECS	VEHICLE WT LBS	PARACHUTE WT, LBS	ACCESSORY WT, LBS	TOTAL WT, LBS	REEFED OPEN TIME, SEC	FULL OPEN TIME, SEC	OPENING TIME SEC	[illegible]	[illegible]	[illegible]	[illegible]
1	1103 F63	1 AUG. 63	97	29.91	69	5	C-130	119	4950	8' RGS	6' RGS	79.9	PS 6399	80L-2	37'		6	3600	177		3782		10.8	21[illegible]				
2	1210 F63	12 AUG. 63	107	29.82	60	6	C-130	120	5020		8' RGS	79.9	PS 6399	80L-3	37'		6		177		3738		9.2	255.4	[illegible]	[illegible]	[illegible]	[illegible]
3	1230 F63	15 AUG. 63	96	29.91	75	8	C-130	120	5000		8' RGS	79.9	PS 6399	80L-3	37'		5	4821	177		4998			25.[illegible]				
4	1326 F63	27 AUG. 63	83	29.96	75	6	C-130	120	5000		8' RGS	79.9	PS 6400	80L-4	37'		10	4821	177		4998			23.4				
5	1433 F63	25 SEPT. 63	86	29.90	49	6	C-130	120	5000		8' RGS	79.4	PS 6339	80A-1	29'		6		177		2785	3.3	11.3	259.9	14.3	1.25	1.33	
6	1510 F63	2 OCT. 63	88	29.92	65	2	C-130	120	5035		8' RGS	79.4	PS 6339	80A-1	33'		6		177		2785	6.7	12.5	254.4	16.6	1.53	1.10	
7	1550 F63	8 OCT. 63	96	29.87	51	5	C-130	120	4930		8' RGS	79.4	PS 6339	80A-2	33'		6		177		2775	4.37	19.9	201.6	16.5	2.01	.96	
8	1782 F63	22 OCT. 63	83	29.99	49	0	C-130	120	10,600		8' RGS	79.4	PS 6339	80A-1	33'		6		177		2785	6.3	11.3	600.6	16.1	1.[illegible]	1.17	
9	1805 F63	29 OCT. 63	88	29.95	33	5	C-130	119	10,590		8' RGS	79.4	PS 6339	80A-1	33'		6		177		3880			86.5				
10	1832 F63	6 NOV. 63	78	29.87	35	0	C-130	119	10,600		8' RGS	79.4	PS 63109	80A-3	33'		6		165		3860	5.8	9.8	466.4	21.6	1.53	1.00	
11	1893 F63	27 NOV. 63	72	30.09	21	5	C-130	120	10,600		8' RGS	79.4	PS 63109	80A-3	31.5'		6	4585	165		4750			183.2				
12	1996 F63	18 DEC. 63	47.3	30.12	36	4	C-130	120	10,600		8' RGS	79.4	PS 63114	80A-4	31.5'		6	4590	165		4755	4.3	13.5	393.3	23.97	1.[illegible]	1.02	
13	2018 F63	19 DEC. 63	51.3	30.07	41	0	C-130	120	10,600		8' RGS	77.6	PS 6398	80A-5	31.5'		6	2620	176		2820	4.36	10.47	5[illegible]	18.13	1.[illegible]	1.02	
14	2045 F63	13 JAN. 64	59	30.24	13	8	B-66	140	10,600		6' RGS	79.4	PS 63114	80A-6	31.5'	4	6	4585	165		4750	3.8	10.5	401	24.2	1.35	1.11	
15	3 F64	29 JAN. 64	62	30.21	31	0	B-66	140	10,600		6' RGS	79.4	PS 63114	80A-7	31.5'	4	6	4586	164		4750	3.7	4.6	423.8	21.7	1.46	1.13	
16	0117 F64	13 FEB. 64	45	29.97		0	B-66	140	10,600		6' RGS	79.4	PS 63114	80A-8	31.5'	4	6	4586	164		4750	4.34	15.4	402.7	24.15	1.43	1.17	
17	0172 F64	4 MAR. 64	64	30.14	17	2	B-66	155	10,595		6' RGS	79.4	PS 64130	80A-9	31'	2	6	4589	161		4750	3.35	9.54	435.5	24.3	1.65	1.09	
18	0225 F64	9 MAR. 64	53	30.18	21	0	C-130	105	10,600		8' RGS	79.4	PS 63114	80A-9	31'	4	6	4589	161		4750	5.0	11.2	422.8	22.5	1.50	1.15	
19	0302 F64	13 MAR. 64	68	29.97	29	4	B-66	155	10,600		6' RGS	79.4	PS 64130	80A-9	31'	4	6	4588	162		4750	3.4	10.5	397.8	23.9	1.33	1.16	
20	0332 F64	18 MAR. 64	67	29.74	19	2	C-130	105	10,600		8' RGS	79.4	PS 63114	80A-9	31'	4	6	4586	164		4750	4.9	11.1	365.5	24.6	1.25	.96	

TABLE VII
TEST DATA SUMMARY

TEST DATA						DAMAGE					REMARKS
CD EFF AVERAGE	L/D AVG.	OSCILLATION DEG.	SNATCH FORCE, LBS	REEFED OPEN FORCE, LBS	FULL OPEN FORCE, LBS	LIGHT	MEDIUM	HEAVY	TEST SUCCESSFUL		
		0	N/A	N/A	N/A	✓			YES	SMALL BURNS AND TEARS.	FUNCTIONAL TEST - TUCK IN CROWN OF REEFED INFLATED CANOPY. 1,000 POUND TENSILE STRENGTH REEFING LINE. REAR RISERS PULLED DOWN PERMANENTLY. NO T.M. OR PHOTO THIS SHOTS.
2.58	1.18	0	N/A	N/A	N/A	✓			YES	STITCHING ON PILOT CHUTE TO BAG BRIDLE FAILED. ONE MAIN SEAM TAPE SPLIT. SMALL BURNS AND TEARS.	REAR RISERS EXTENDED AFTER 20 SECONDS. TUCK IN CROWN OF REEFED INFLATED CANOPY. STRAIN LINK FAILED, NO T.M. 2,000 POUND TENSILE STRENGTH REEFING LINE. REAR RISER BRIDLE TIED IN PACKING.
				17600				✓	NO	REAR RISER FAILED. CANOPY DAMAGED BEYOND REPAIR. FRONT OF CANOPY ONLY MINOR DAMAGE.	IMPACT VELOCITY 60 - 70 FPS. T.M. AND CAMERA UNDAMAGED. 2,000 POUND TENSILE STRENGTH REEFING LINE. REAR RISERS WERE CONTRACTED AS TEST NO. 2.
				10900				✓	NO	PILOT CHUTE BRIDLE FAILED. VENT LINES RIPPED FREE. SUSPENSION LINES RIPPED FREE. CANOPY DAMAGED BEYOND REPAIR.	APEX WAS ALLOWED TO DEPLOY FULLY WHEN VENT LINES SEPARATED, THEN SPLIT GORES DEVELOPED. CAMERA DEPLOYED ON IMPACT. 2,000 POUND REEFING LINE.
2.08	1.37	0	3250	4050	9300	✓			YES	SMALL BURN HOLES IN UPPER CANOPY. ONE (1) VENT LINE DAMAGED. SOME LIGHT DAMAGE TO DEPLOYMENT BAG FLAPS.	FULL INFLATION OF APEX WAS SLOW. A TENDENCY OF STABILIZED PANELS TO INFLATE DURING REEFED PHASE WAS NOTED. 2,000 POUND REEFING LINE.
1.80	1.10	0	3600	6500	7450	✓			YES	SMALL BURN HOLES IN UPPER CANOPY. REAR CIRCUMFERENTIAL SLOT PANEL RIPPED. CASINGS ON VENT LINES DAMAGED. MINOR BAG DAMAGE.	BETTER INFLATION OF APEX THAN TEST NO. 5, HOWEVER, THERE IS ROOM FOR IMPROVEMENT. DISREEFING WAS NOT AS SMOOTH AS IN PREVIOUS TESTS. 2,000 POUND REEFING LINE. NO INTERNAL PARACHUTE.
2.01	.96	0	3200	5380	6790	✓			YES	ONE (1) BROKEN SUSPENSION LINE. FOUR (4) TEARS IN REAR PANELS. RIPPING NOTED ADJACENT TO CIRCUMFERENTIAL TAPES.	CANOPY FILLED QUICKLY, BUT APPEARED UNSTABLE AND FLUTTERED VIOLENTLY. SKIRT WAS DISORDERLY IN REEFED AND DISREEFED STATE. 2,000 POUND REEFING LINE. NO INTERNAL CHUTE.
.90	1.17	0	3950	7800	5680	✓			YES	ONE (1) 1/2 INCH DIAMETER HOLE AND ONE (1) RIP.	GOOD INFLATION OF APEX. CANOPY AND SKIRT SHAPE WERE GOOD. 1,000 POUND REEFING LINE (MIL-W-5625).
			5620	7330				✓	NO	CANOPY DAMAGED BEYOND REPAIR. LINES 5 - 30, 47 - 57 FAILED AT SKIRT ATTACHMENT.	STABILIZERS PRE-INFLATED AND PASSED UNDER SKIRT ON OPPOSITE SIDE, A PARTIAL INVERSION RESULTING. CANOPY FAILED AFTER DISREEF. 1,000 POUND REEFING LINE (MIL-W-5625).
.62	1.00	0	4100	10580	8650	✓			YES	VERY LIGHT. TWO (2) 1 INCH TEARS AS THE RESULT OF GROUND HANDLING.	DEPLOYMENT AND INFLATION NORMAL. SLIGHT TUCKING OF THE CROWN DURING THE REEFED STATE. 1,000 POUND REEFING LINE TACKED AT EACH RING. STABILIZERS FOLDED AND TIED WITH SAFETY THREAD.
			5000	13400				✓	NO	CANOPY DAMAGED BEYOND REPAIR.	CANOPY MALFUNCTIONED AS WITH TEST NO. 9 DUE TO PRE-INFLATION OF STABILIZERS, WHICH WERE FOLDED AND TIED 3 PLACES WITH 5 CORD. 1,000 POUND REEFING LINE. (PARTIAL INVERSION).
.40	1.02	0	3600	14100	13800		✓		YES	TWO (2) BLOWN NO. 9 PANELS IN REAR.	STABILIZER "BOOTS" AND HESITATOR BAG USED. HESITATOR BAG CAME FREE AT SKIRT EMERGENCE FROM BAG. STABILIZER BOOTS OPENED DURING REEFED PHASE, BUT PANELS DID NOT INFLATE.
.40	1.02		4100	8675	6500				YES	NONE.	NO STABILIZER PANELS. GOOD DEPLOYMENT AND INFLATION. CANOPY HAD SLOW RIGHT TURN. RADIAL CREASE NOTED IN FRONT OF CANOPY DURING STEADY STATE. 1,000 POUND REEFING LINE.
.56	1.11	0		15900	12600			✓	NO	REEFING RINGS 27 - 45 (EXCEPT 35 AND 37) RIPPED FROM CANOPY. NUMBER 36 MAIN SEAM FAILED, NUMBER 38 SUSPENSION LINE FAILED. TWO GORES SPLIT IN CROWN ONLY.	HESITATOR BAG OMITTED AND STABILIZER REEFING ADDED. 1,000 POUND REEFING LINE. STABILIZERS DID NOT OPEN UNTIL DISREEF.
.46	1.	0	4900	16100	16400			✓	NO	REEFING LINE FAILED. GORE NUMBER 1 DEVELOPED SPLIT FROM PANEL 10 TO VENT.	REEFING RING ATTACHMENT STRENGTH INCREASED. REEFED SHAPE FORMED QUICKLY AND THEN 1,000 POUND TENSILE STRENGTH REEFING LINE FAILED.
.43	1.17	0	4360	15000	11000		✓		YES	BURNING IN UPPER SECTION FROM INTERNAL CHUTE STAY LINE. TWO (2) BLOWN PANELS IN SECTION 10.	REEFING LINE STRENGTH INCREASED TO 1,500 POUND TENSILE STRENGTH (MIL-W-5625). LINE WAS SPACED EVENLY FORE AND AFT OF STABILIZER PANEL GROUPING. NORMAL FILLING.
.63	1.09	0	N/A	N/A	N/A		✓		YES	BLOWN NUMBER 10 PANELS IN GORES 13, 67 AND 6. BLOWN NUMBER 7 PANEL IN GORE 7. OTHER DAMAGE LIGHT. BAG SLIGHTLY DAMAGED.	NORMAL FILLING. REEFING LINE SPACING RETAINED.
.60	1.15	0	4000	11560	13700	✓			YES	VERY LIGHT.	TURN TEST. CANOPY DEPLOYED WITH ALL TURN SLOTS CLOSED ON ONE SIDE. TURN RATE ABOUT 9 DEG./SEC.
.38	1.16	0	6000	14400	12600		✓		YES	PANEL NUMBER 10 IN GORE 50 BLOWN. NUMEROUS SMALL BURNS AND TEARS. BLOWN GORE IN INTERNAL PARACHUTE. PILOT CHUTE BRIDLE FAILED.	LOST PILOT CHUTE. INTERNAL PARACHUTE INFLATED AND THEN BEGAN TO OSCILLATE BEFORE BLOWING A GORE AND COLLAPSING. SKIRT UNSYMMETRICAL AFTER LOSS OF INTERNAL CHUTE.
.26	.96	0	4400	12000	14750	✓			YES	VERY LIGHT.	TURN TEST. CANOPY WAS DEPLOYED WITH ALL TURN SLOTS ON ONE SIDE INVERTED BY A LINE FROM VENT TO CONNECTOR LINKS. TURN RATE ABOUT 19 DEG./SEC.

K+E 10 X 10 TO 1/2 INCH 46 1323
KEUFFEL & ESSER CO.

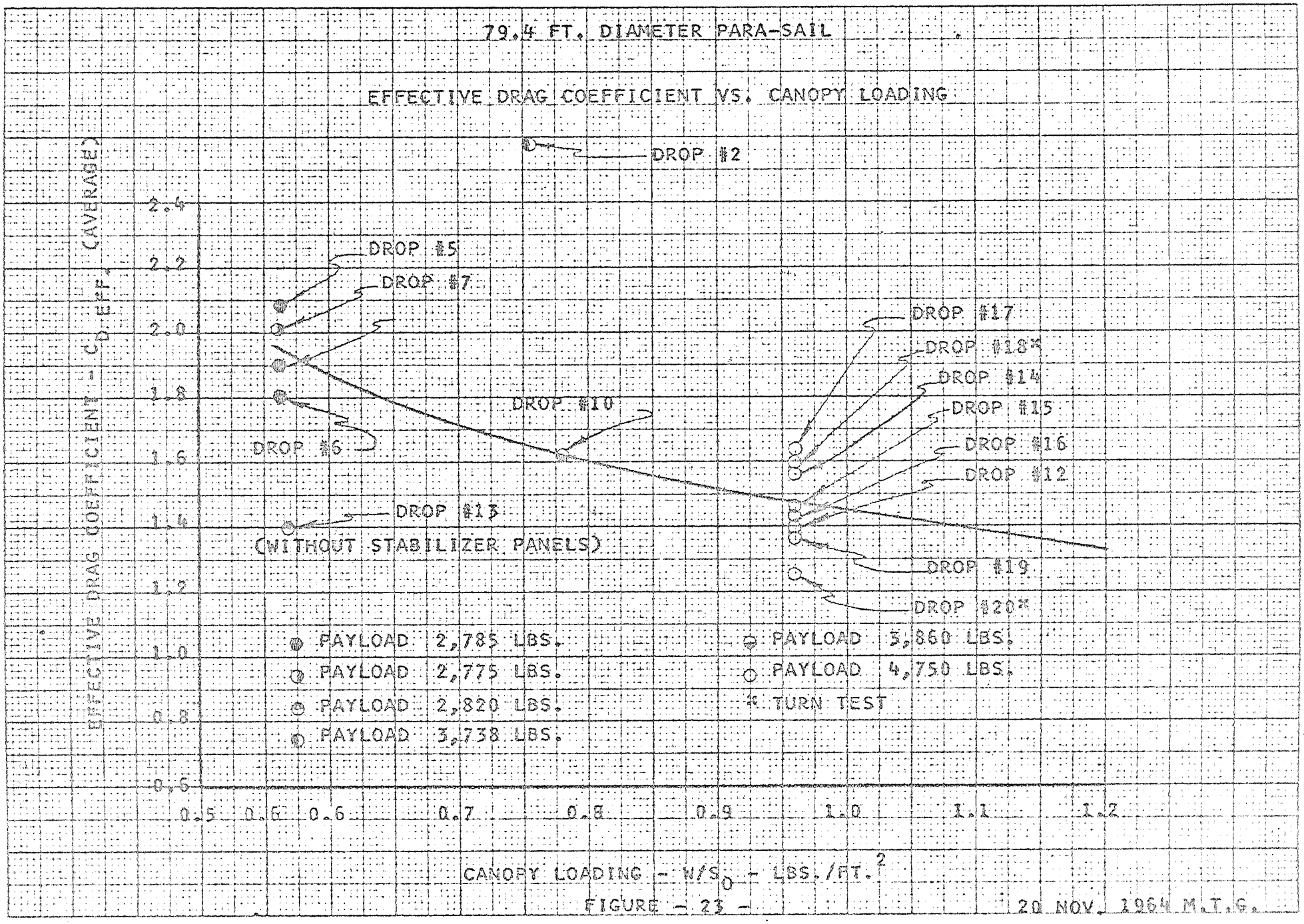

FIGURE - 23 -

20 NOV. 1964 M.T.G.

K+E 10 X 10 TO ½ INCH 46 1323
7 X 10 IN. HELD MADE IN U.S.A.
KEUFFEL & ESSER CO.

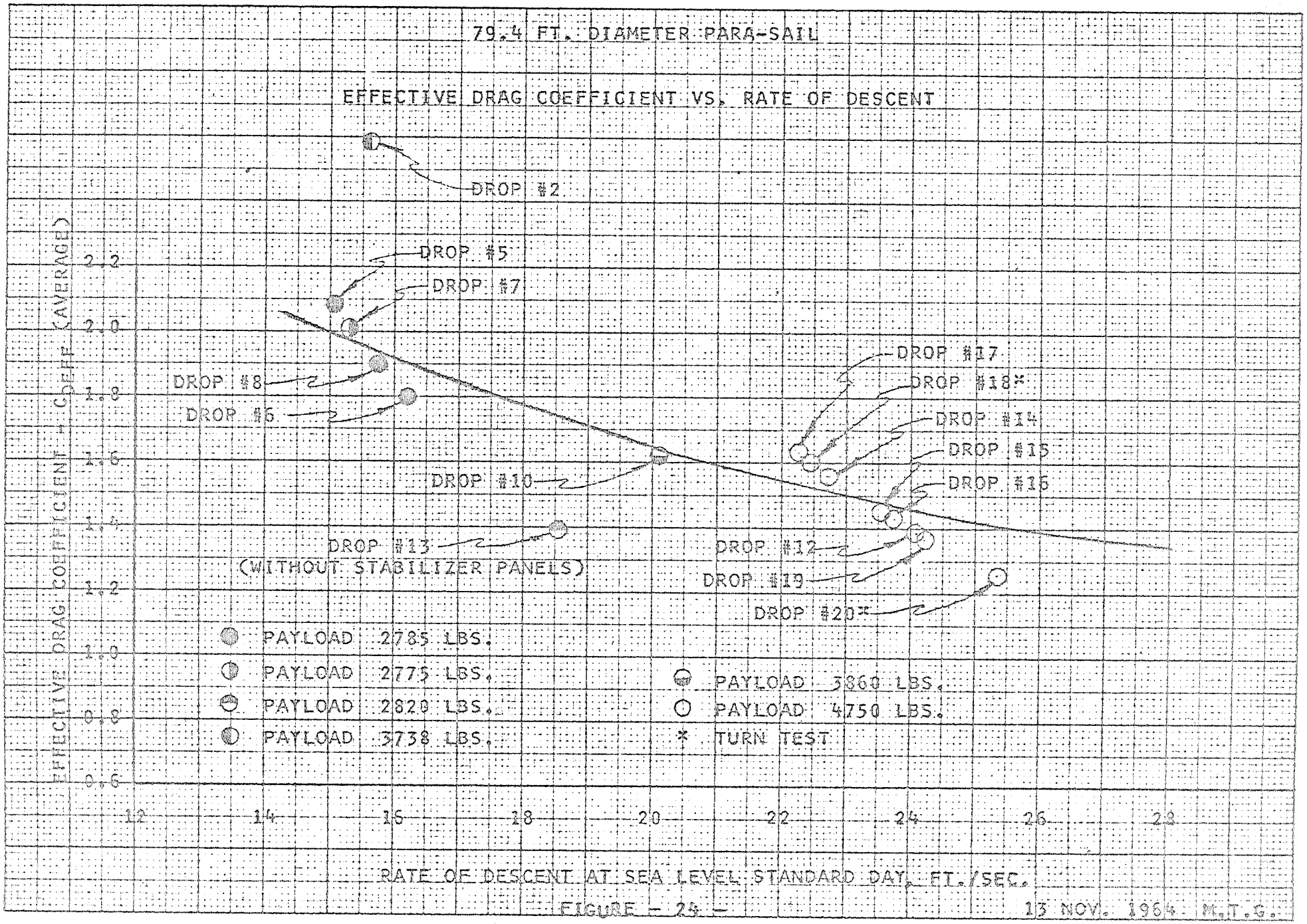

FIGURE - 24 -

13 NOV. 1964 M.T.G.

K+E 10 X 10 TO ½ INCH 46 1323
7 X 10 INCHES MADE IN U.S.A.
KEUFFEL & ESSER CO.

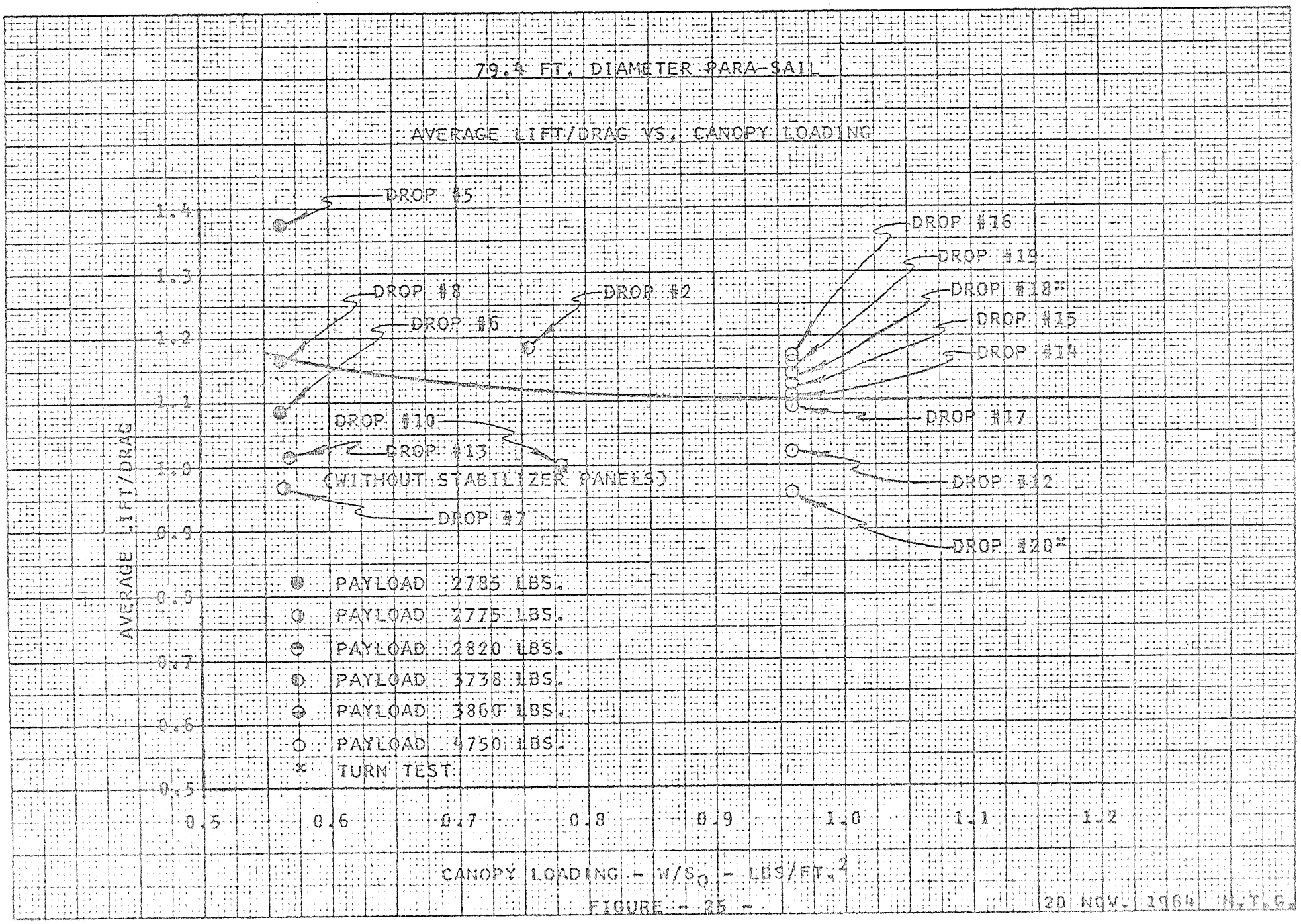

FIGURE - 25 -

20 NOV. 1964 N.T.G.

K+E 10 X 10 TO ½ INCH 46 1323
7 X 10 INCHES MADE IN U.S.A.
KEUFFEL & ESSER CO.

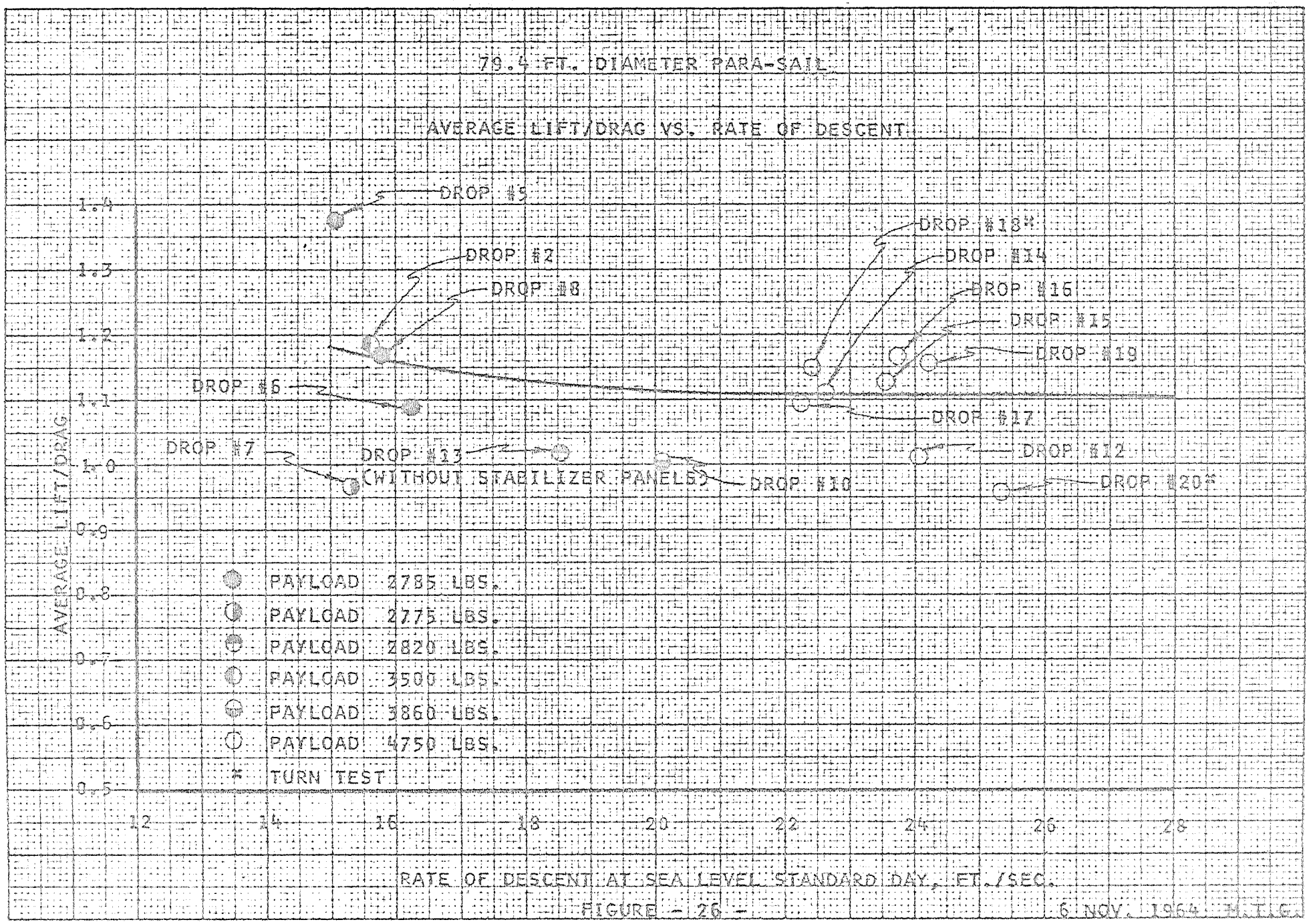

FIGURE - 26 -

6 NOV. 1964 M.T.G.

K+E 10 X 10 TO ½ INCH 46 1323
7 X 10 INCHES MADE IN U.S.A.
KEUFFEL & ESSER CO.

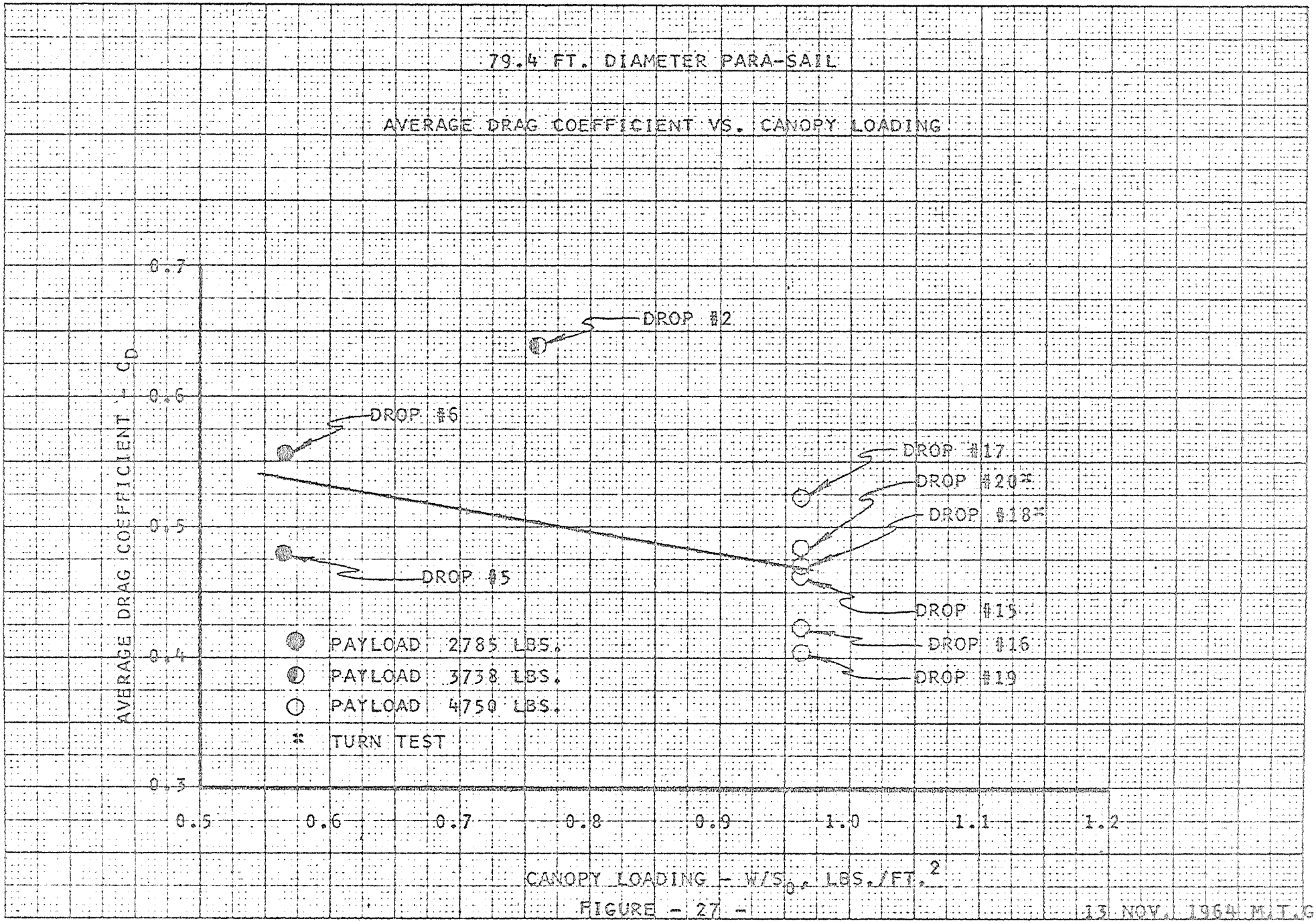

FIGURE - 27 -

13 NOV. 1964 M.T.G.

K+E 10 X 10 TO ½ INCH 46 1323
7 X 10 INCHES MADE IN U.S.A.
KEUFFEL & ESSER CO.

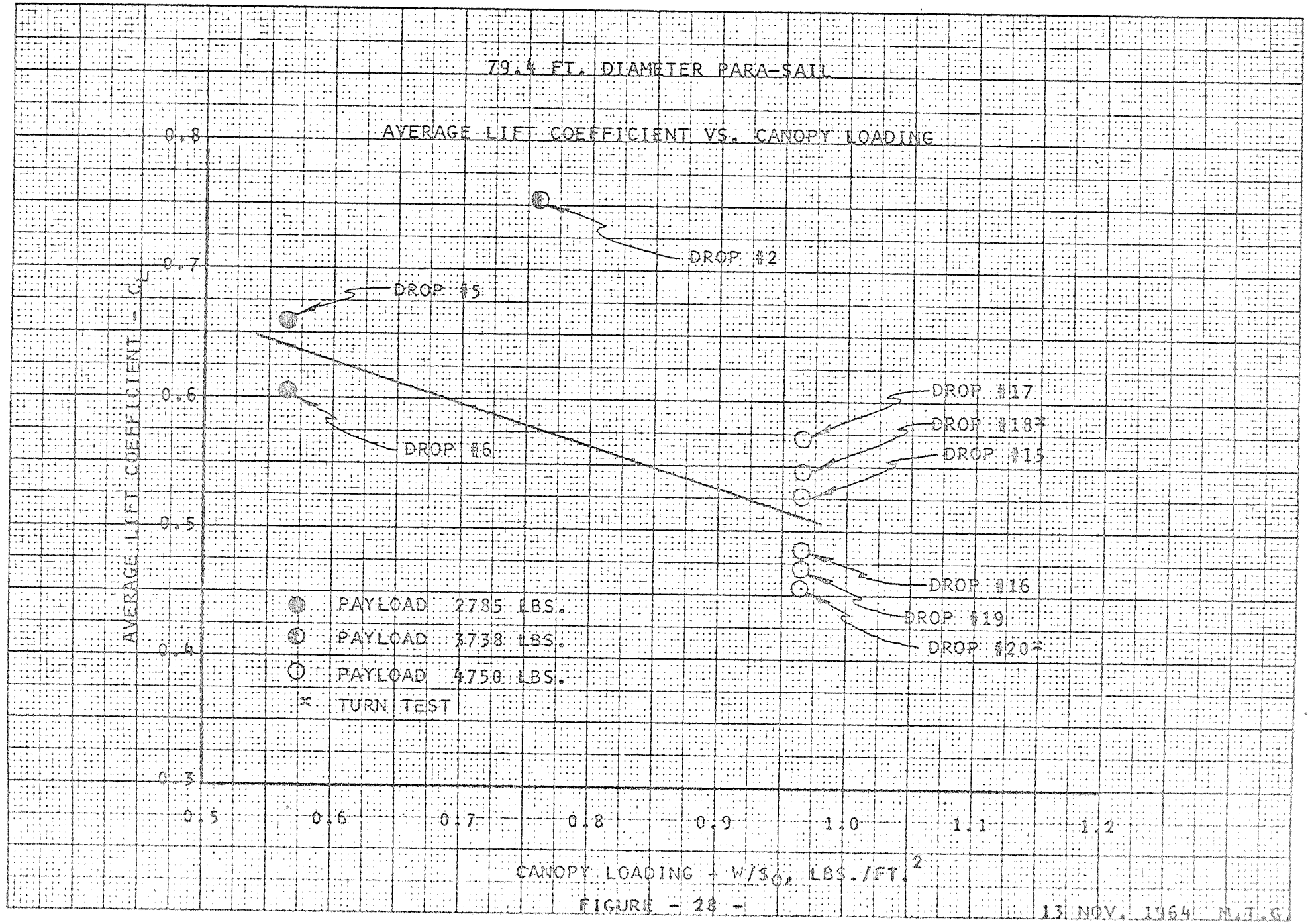

FIGURE - 28 -

13 NOV. 1964 N.T.G.

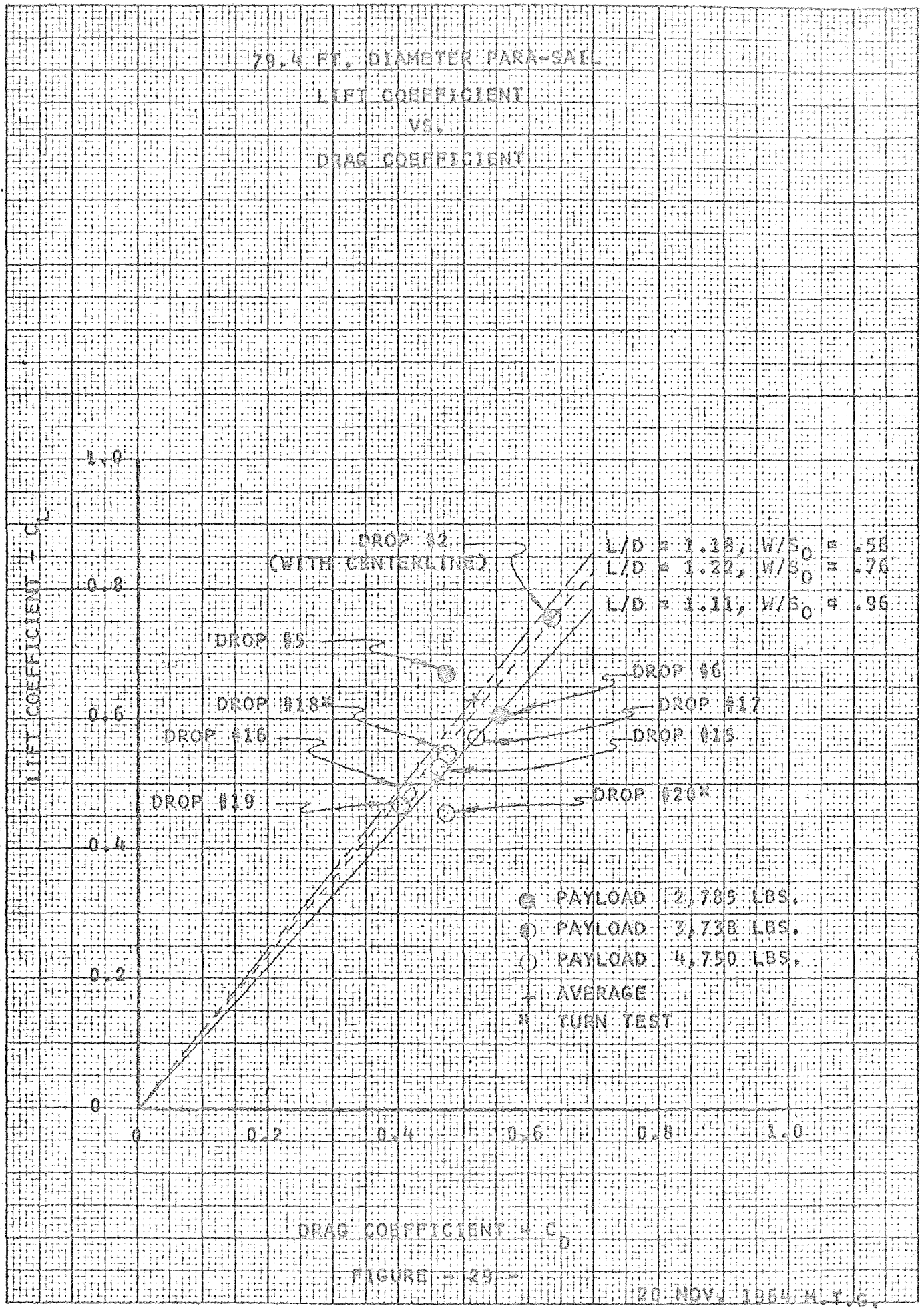

FIGURE - 29 -

20 NOV. 1964 M.T.G.

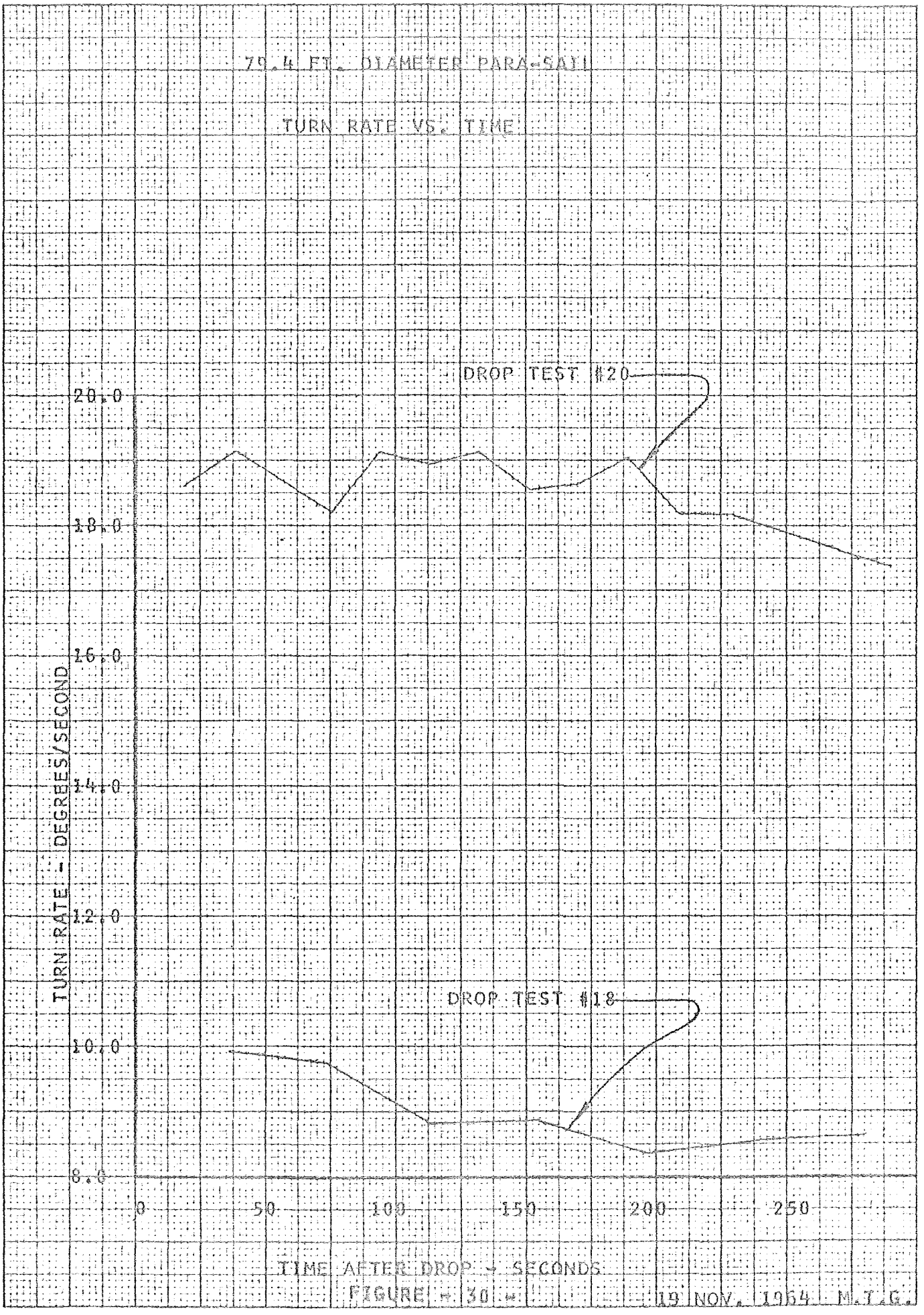

K&E 10 X 10 TO ½ INCH 46 1323
7 X 10 INCHES MADE IN U.S.A.
KEUFFEL & ESSER CO.

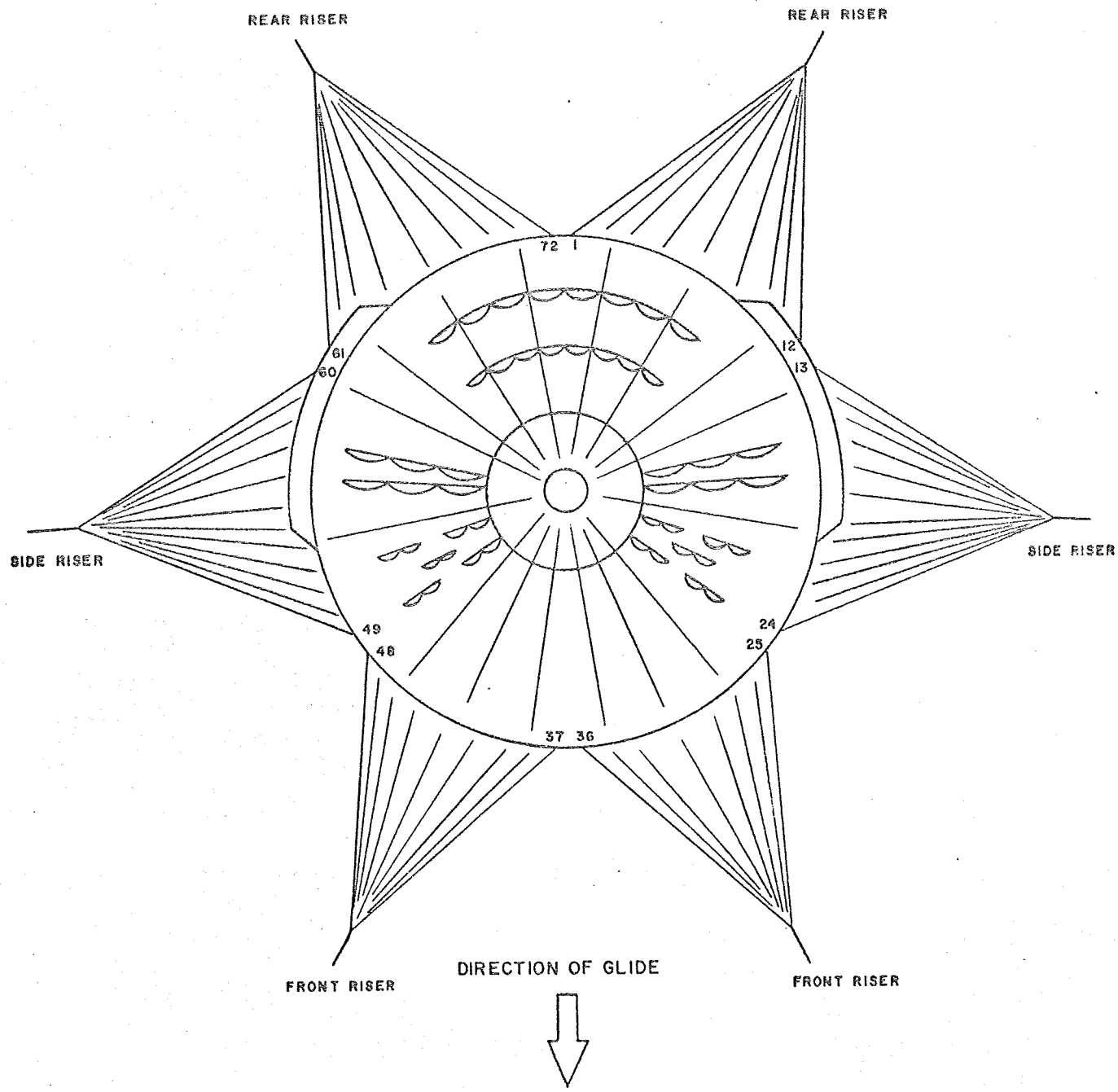

FIG. - 31 -
SCHEMATIC CORDING DIAGRAM
FOR 79.4 FT. DIA. PARA-SAIL

TYPICAL FORCE VS. TIME HISTORY

79.4 FT. DIAMETER PARA-SAIL

DROP SPEED 154 KIAS, WEIGHT 4750 LBS.

ALTITUDE 10,600 FT., TEST #19

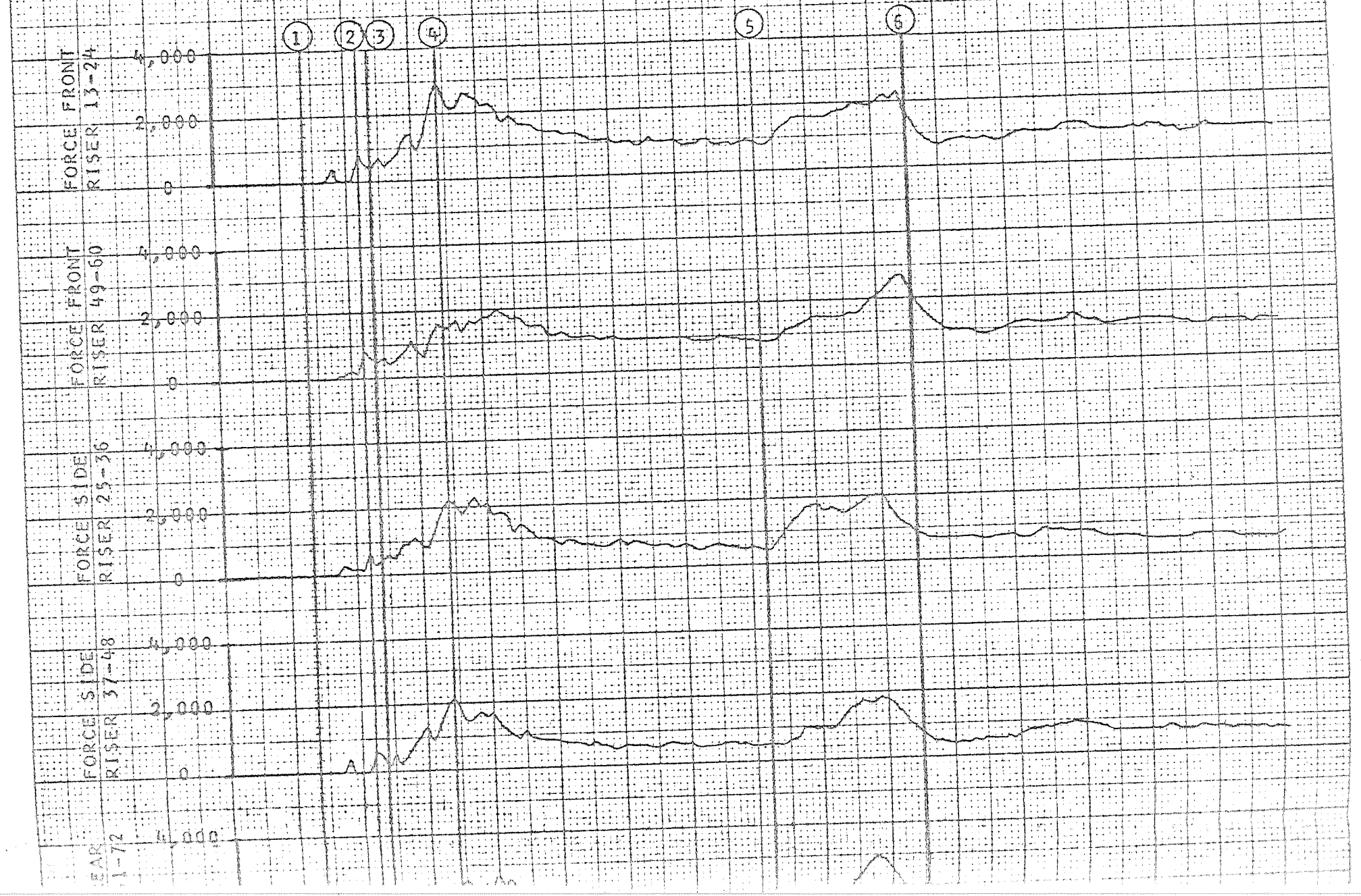

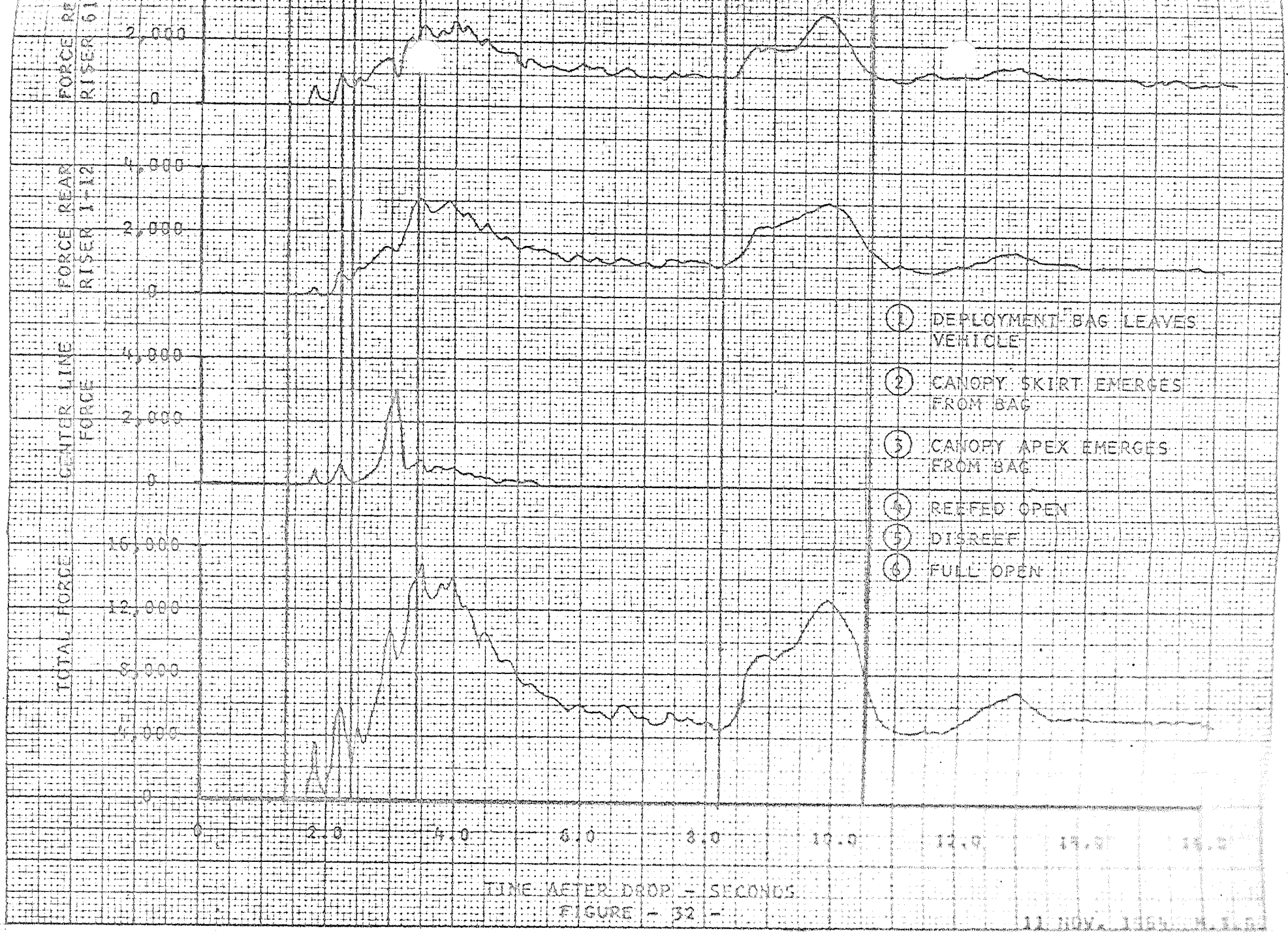
FORCE RE
RISER 61
2,000
0
FORCE REAR
RISER 1-12
4,000
2,000
0
CENTER LINE
FORCE
4,000
2,000
0
TOTAL FORCE
16,000
12,000
8,000
4,000
0
0
2.0
4.0
6.0
8.0
10.0
12.0
14.0
16.0
TIME AFTER DROP - SECONDS
1 DEPLOYMENT BAG LEAVES VEHICLE
2 CANOPY SKIRT EMERGES FROM BAG
3 CANOPY APEX EMERGES FROM BAG
4 REEFED OPEN
5 DISREEF
6 FULL OPEN
11 NOV. 1964

- 32 -

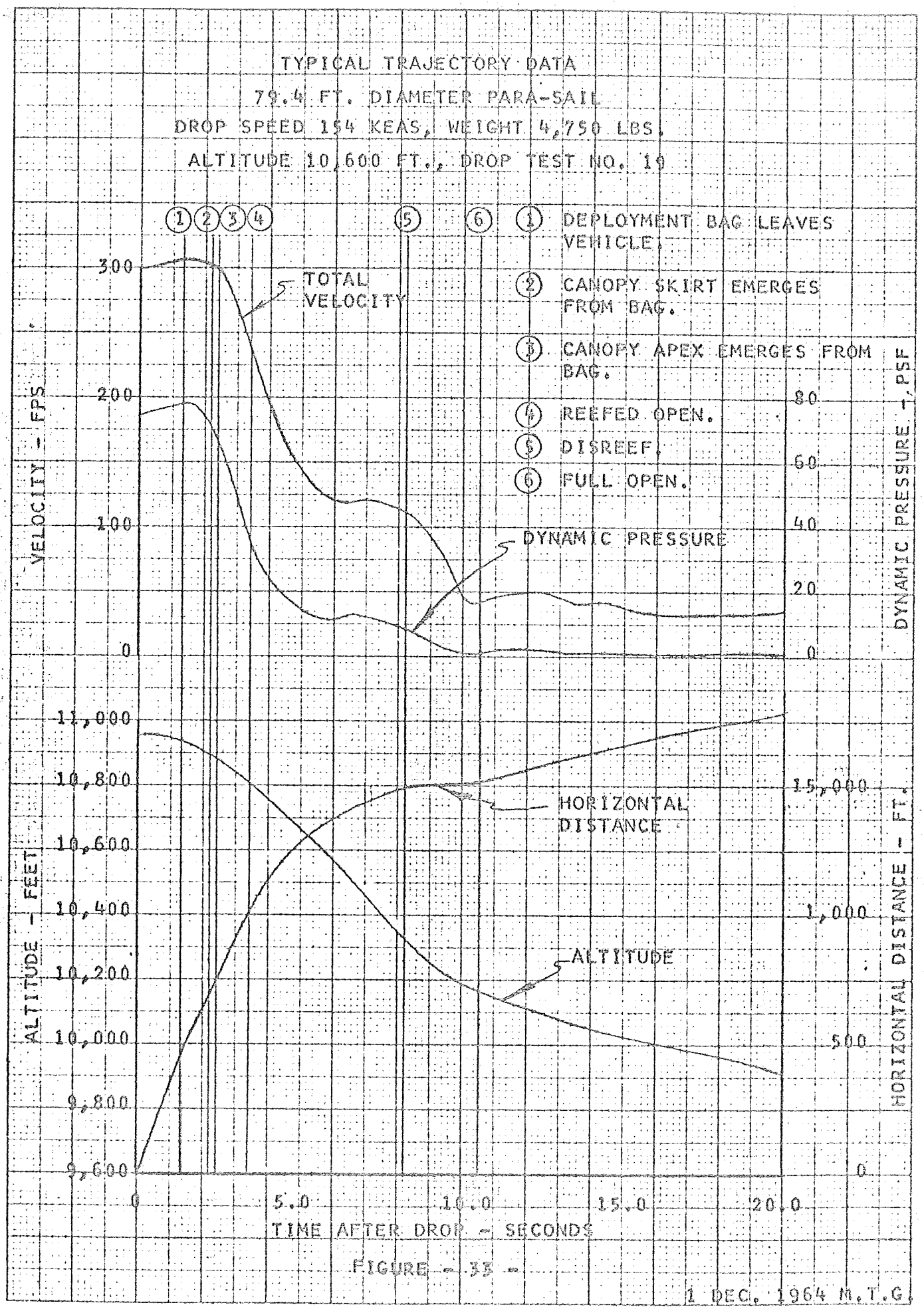

FIGURE - 33 -

1 DEC. 1964 M.T.G.

K+E 10 X 10 TO ½ INCH 46 1323

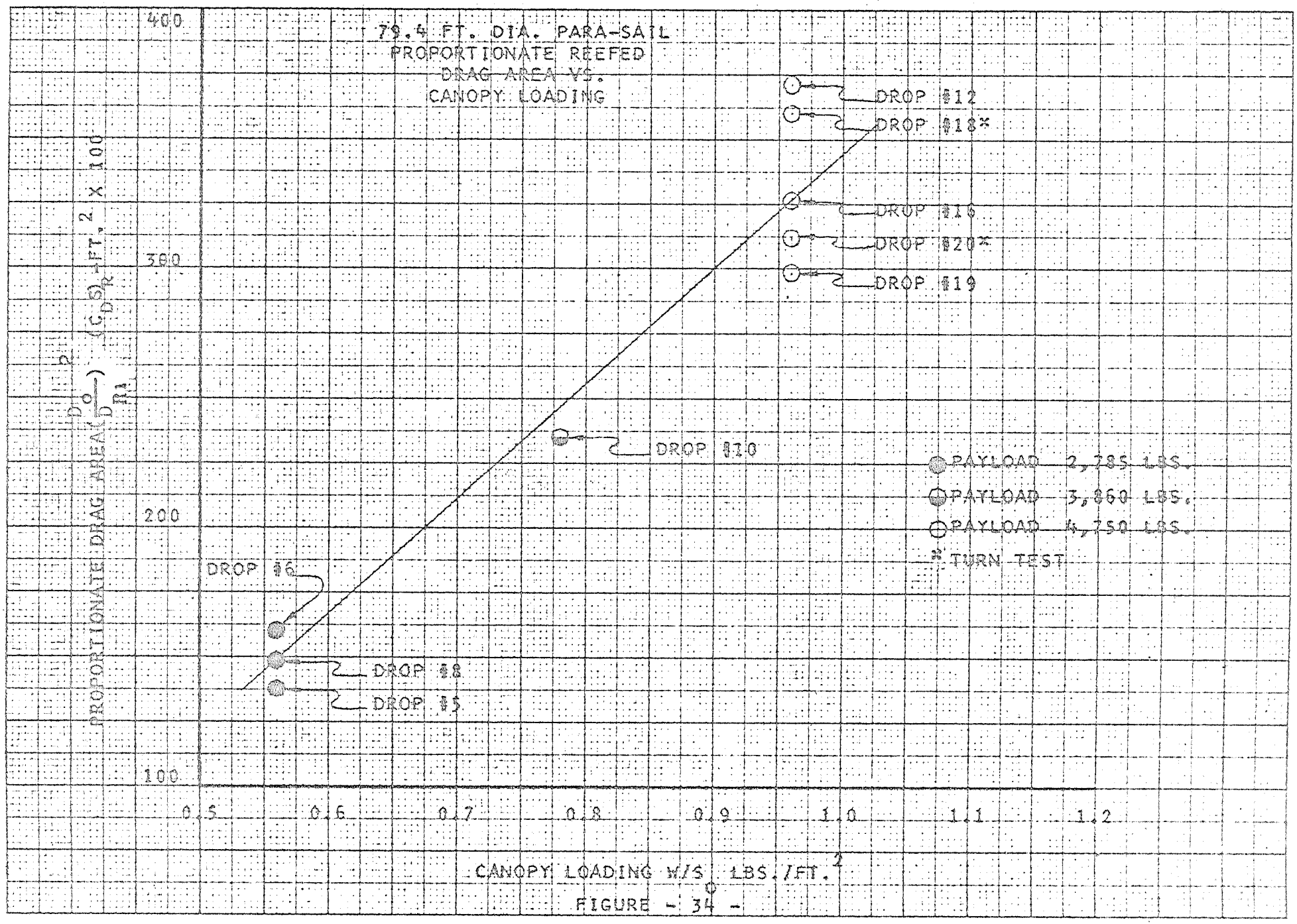

FIGURE - 34 -

K+E 10 X 10 TO ½ INCH 46 1323
7 X 10 INCHES MADE IN U.S.A.
KEUFFEL & ESSER CO.

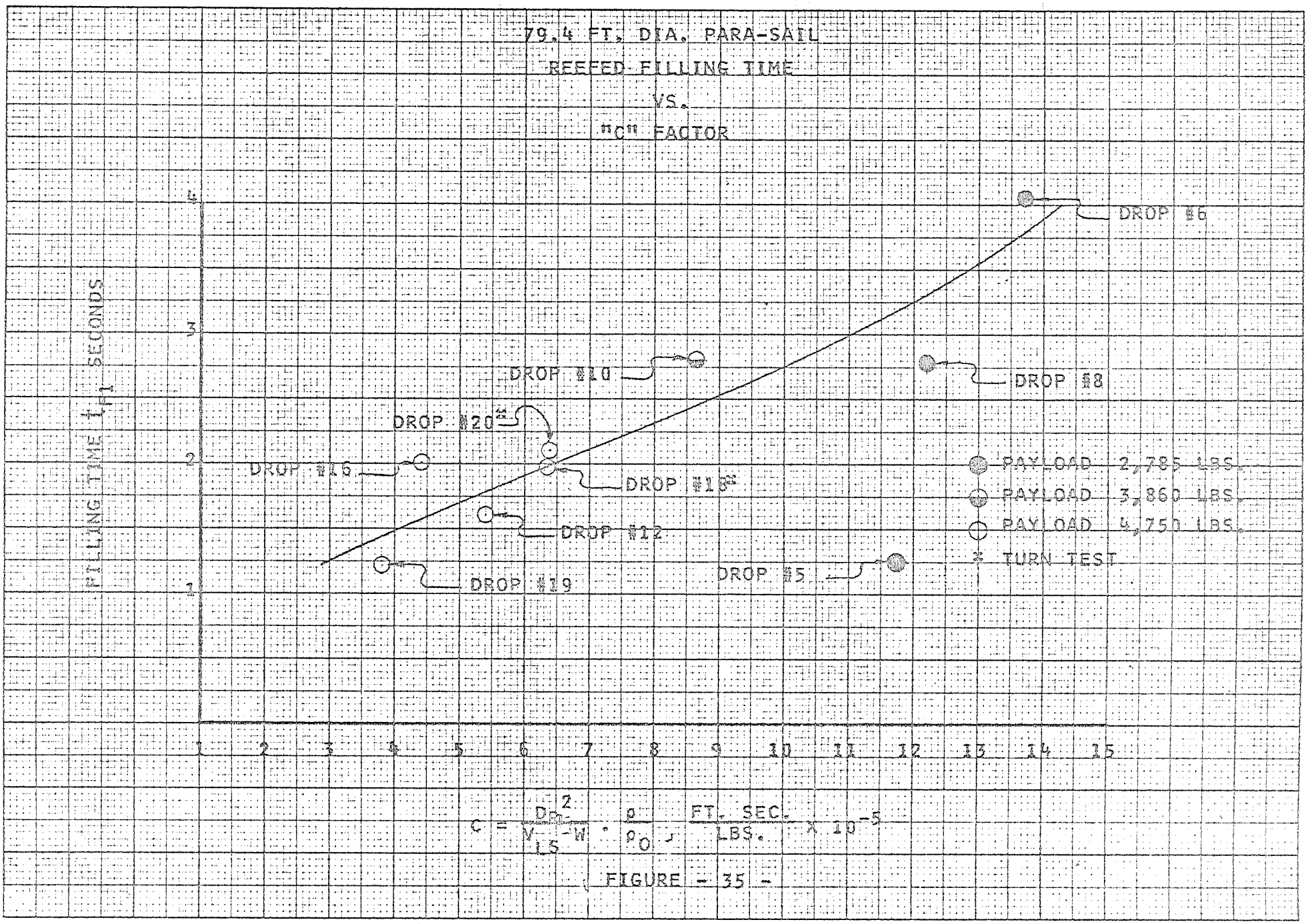

FIGURE - 35 -

K+E 10 X 10 TO ½ INCH 46 1323
7 X 10 INCHES MADE IN U.S.A.
KEUFFEL & ESSER CO.

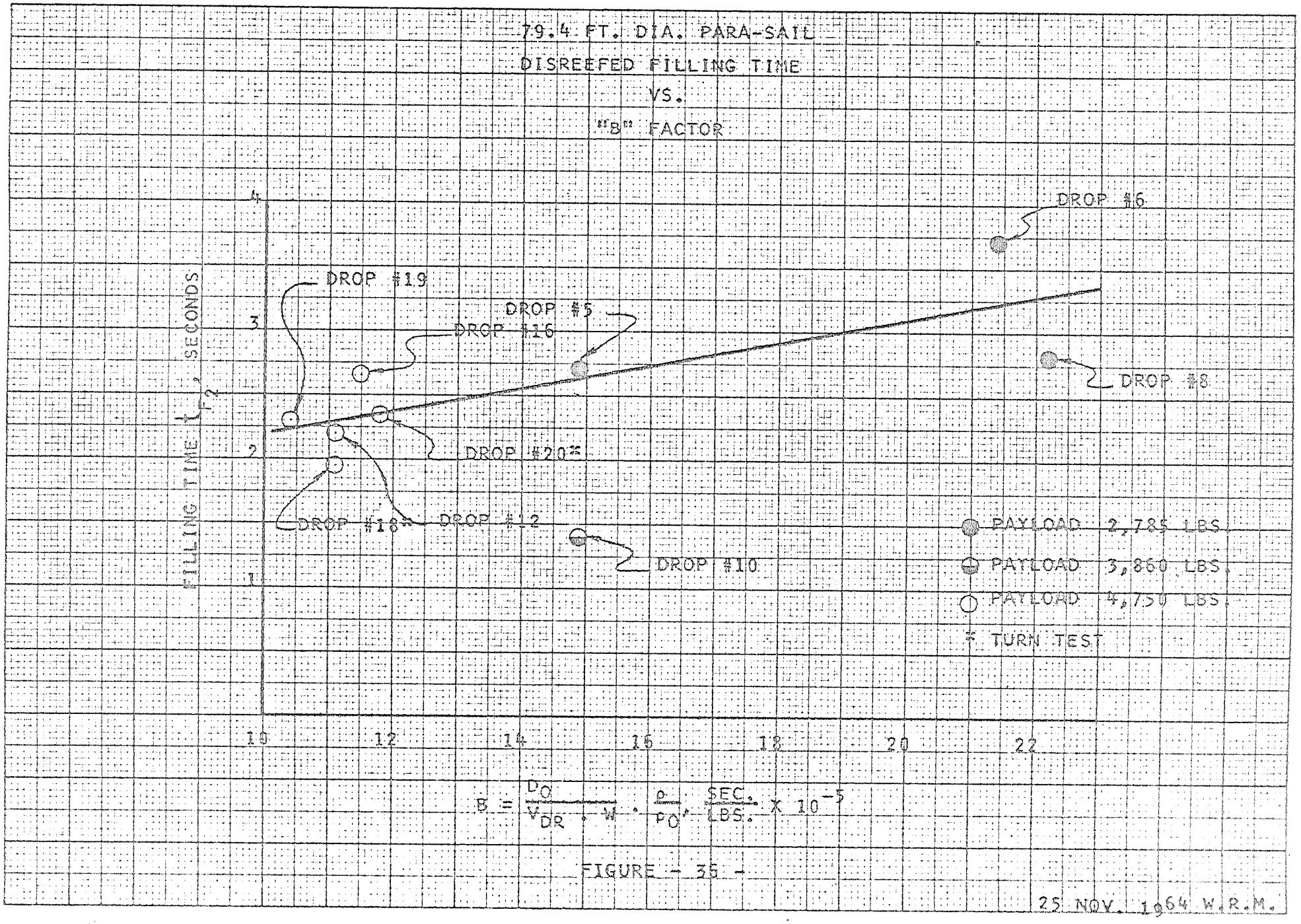

FIGURE - 35 -

25 NOV. 1964 W.R.M.

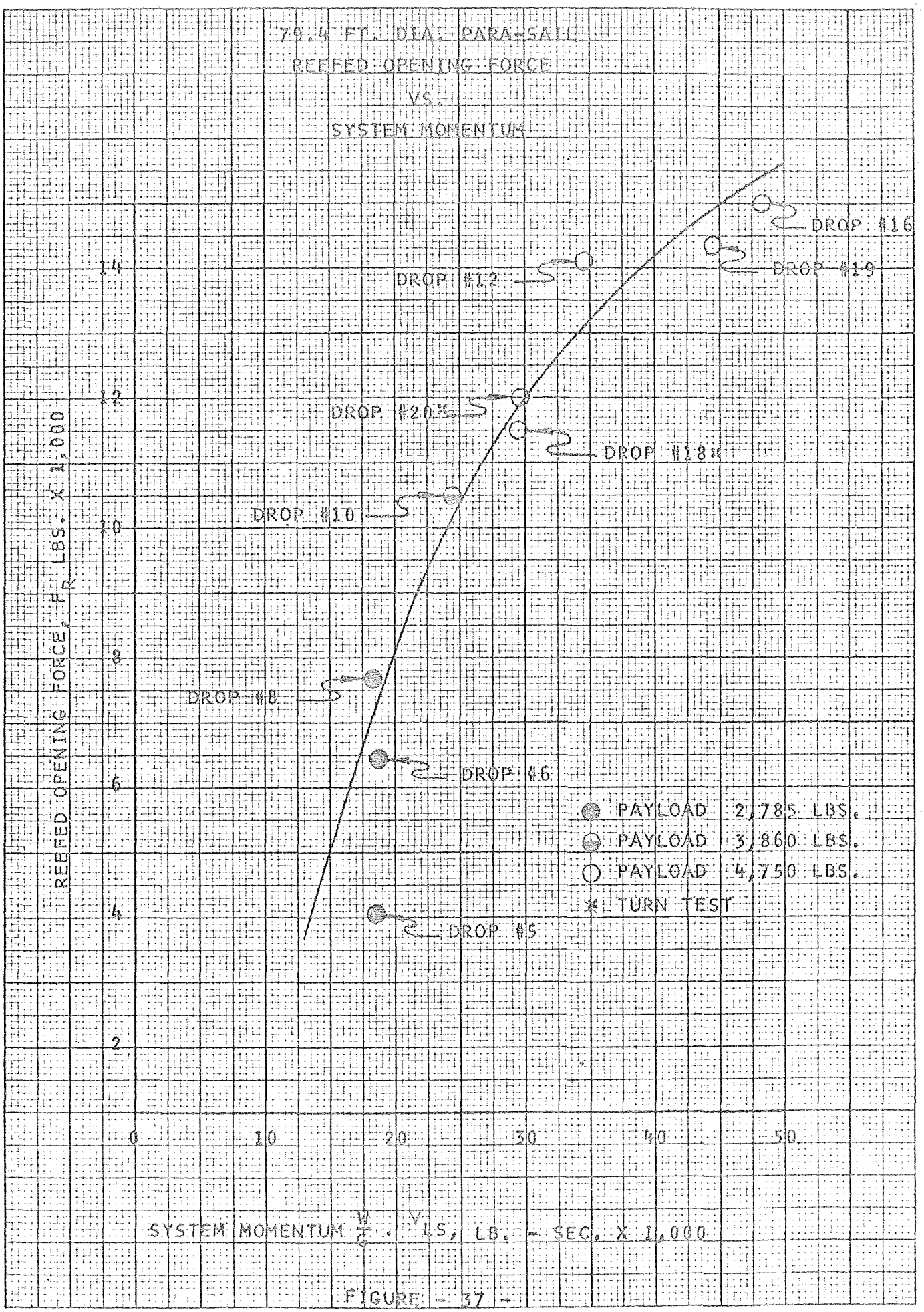
79.4 FT. DIA. PARA-SAIL
REEFED OPENING FORCE
VS.
SYSTEM MOMENTUM
DROP #16
DROP #19
DROP #12
DROP #20
DROP #18
DROP #10
DROP #8
DROP #6
DROP #5
PAYLOAD 2,785 LBS.
PAYLOAD 3,860 LBS.
PAYLOAD 4,750 LBS.
TURN TEST
REEFED OPENING FORCE, F_R LBS. X 1,000
SYSTEM MOMENTUM $\frac{W}{g} \cdot V_{LS}$, LB. - SEC. X 1,000
0
10
20
30
40
50
2
4
6
8
10
12
14

FIGURE - 37 -

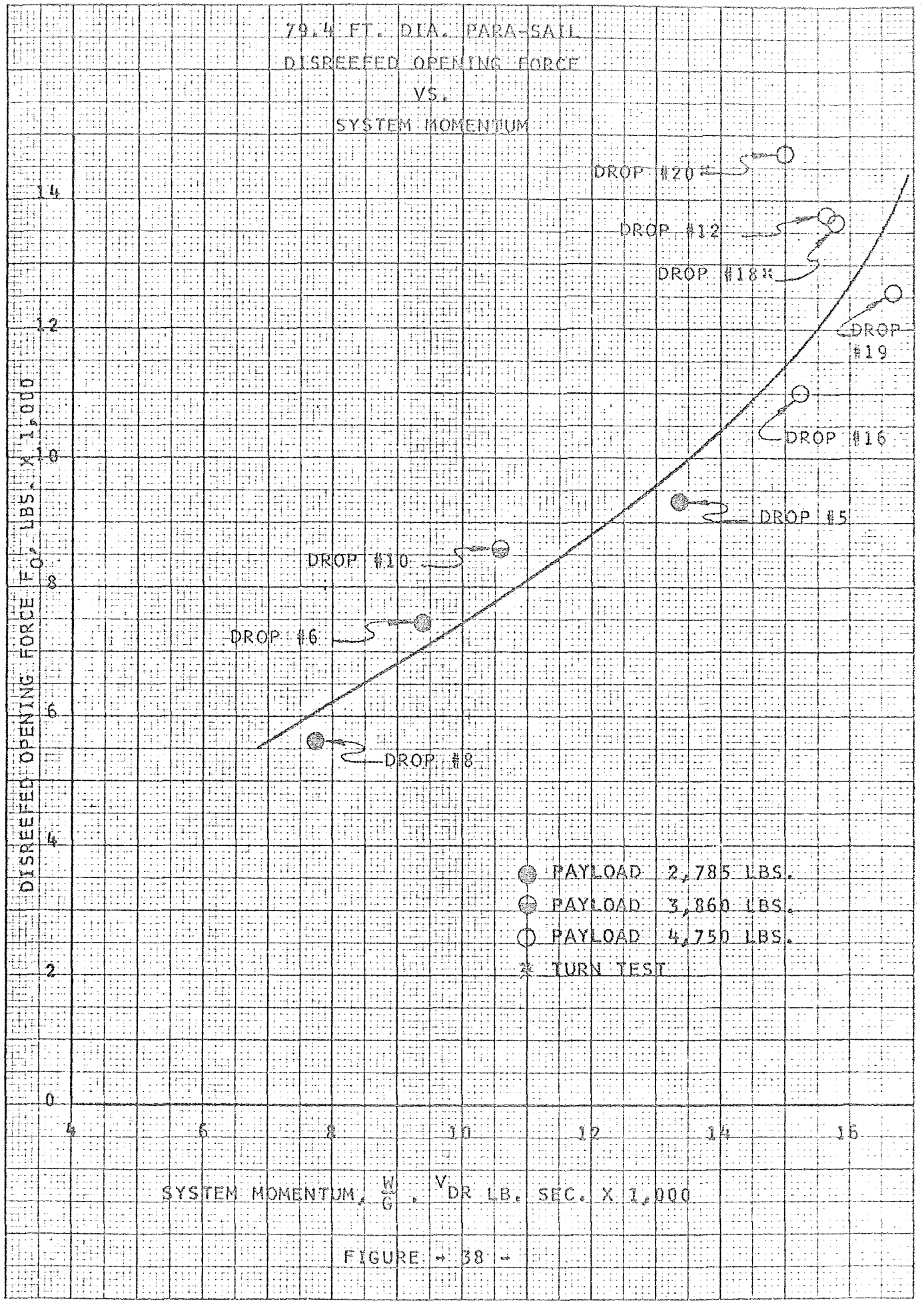

FIGURE - 38 -

K&E 10 X 10 TO ½ INCH 46 1323
7 X 10 INCHES MADE IN U.S.A.
KEUFFEL & ESSER CO.

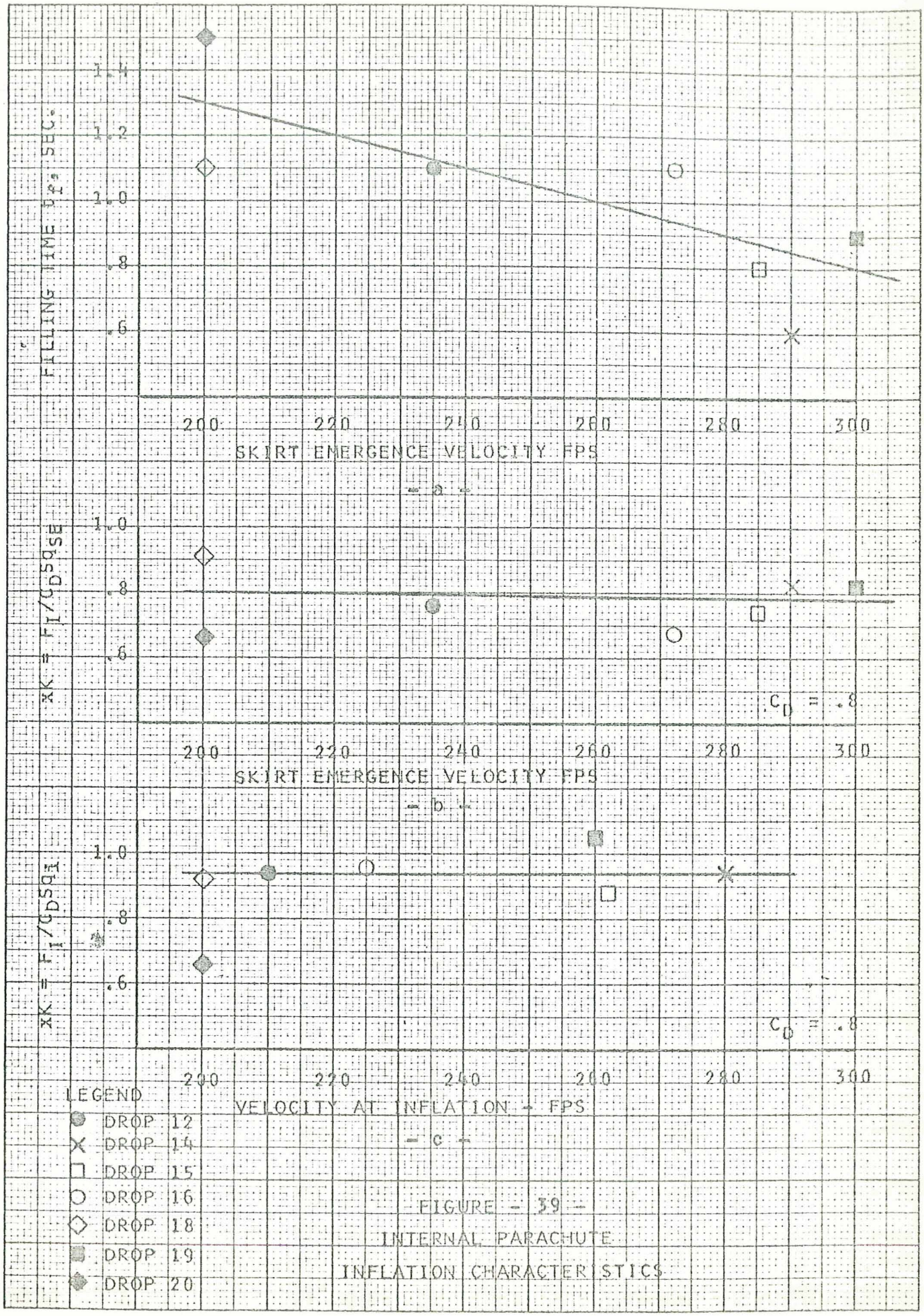

FIGURE - 39 -
INTERNAL PARACHUTE
INFLATION CHARACTERISTICS

K&E 10 X 10 TO ½ INCH 46 1323
7 X 10 INCHES MADE IN U.S.A.
KEUFFEL & ESSER CO.

5.0 DESIGN ANALYSIS OF THE FINAL CONFIGURATION

At the outcome of this program, a large Para-Sail emerged which although it had not achieved all of the desired characteristics anticipated for it, had nevertheless attained a level of development which makes worthwhile some analysis of the important design characteristics. The results of this analysis may serve as a reference point in future development efforts. In the following sub-sections such items as the basic canopy shape, area distribution, geometry, structural and stress analysis, and profile and planform details will be considered.

5.1 Basic Canopy Shape

The Para-Sail parachute of this program began its existance as what might be termed a biconical design. This configuration was well suited to the inverted apex and center suspension line features of 80L-1. However, as can be seen from Table VII of Section 4, these features produced immense deployment problems with excessive loads, and consequently the shape was modified to a triconical design by removing the upper conical apex or crown section and replacing with a flat circular cap, deleting the center suspension line also.

Figure 40 presents the basic canopy shape derived from this program. This shape is comprised of a flat circular plate capping the small diameter of a truncated right circular cone which has an included half angle of 65° 08' 45". This cone in turn has its large diameter joined to the small diameter of another right circular cone with a half angle of 02° 02' 58".

This design has demonstrated that the lift/drag ratio was unaffected by removal of the centerline, although the loss of drag was significant.

The representative gore is shown shaded in Figure 40 and is established as the segment between suspension lines from the canopy defined above. The gore so derived from this shape for the test item of this program is shown in detail in Figure 41. It will be noted that the final gore represented by Frame 1 includes a significant amount of additional cloth between suspension lines in certain areas. This cloth is termed "fullness" and was added to provide more curvature to the gore circumferentially and thereby reduce stress.

5.2 Determination of Nominal Diameter

A number of methods are available for the calculation of nominal diameter. It is possible to determine actual cloth area of the parachute by summing the individual panels (of which there are 49 in the configuration under study) and expressing this total area by means of diameter. It might be argued that the open areas of the many slots should be added to this value since the area of the open spaces in ribbon and ring slot canopies is included in total area. However, neither of these methods of expressing size has been selected. By their complexity and detail they become too cumbersome to be of use. The procedure utilized is based upon the area of the representative gore shown in Figure 40 and Frame 2 of Figure 41, plus the area of stabilizer panels. This area includes that of the vent but not of the slots. The effect of gores of varying length is not included. The area is therefore determined by the area of the representative gore multiplied by the total number of gores plus the area of the stabilizer panels. This figure is then expressed thru the term "nominal diameter".

For comparative purposes the three areas discussed above are shown below, computed for the test item 80A-9.

1. Total panel area = 5,154.0 ft.^{2} or 81.0 ft. dia.
2. Total panel area + slot area = 5,545.6 ft.^{2} or 84.8 ft. dia.
3. Area based on representative gore = 4,916.3 or 79.4 ft. dia.

It will be noted from these figures that diameter does not vary significantly by any of the methods. For the sake of convenience and for the wide range of application the latter method appears to be the most sound.

5.3 Porosity and Area Distribution

The areas and porosities for the final configuration have been calculated and are presented in Table VIII. In this tabulation the reduction in vent size created by the elastic hood has been neglected and the constructed vent area is used.

Determination of slot areas is accomplished by assuming the slot shape in the inflated canopy to be bounded by an arc (leading edge of panel) and a cord (trailing edge of adjacent panel). Actually such a method is not entirely correct, since in an inflated canopy the trailing edge of a slot panel also forms an arc. The curvature of the two arcs bounding the slot can be determined if the inflated profile of the canopy is known. The effect will be one of reduction in area compared to the arc cord method. However, for general design purposes the simpler method suffices.

Porosity is also based upon the area of the canopy without including the area of stabilizer panels. Although

stabilizers are included in the determination of canopy size, they cannot be considered a contributing part of canopy drag area. There is, however, a distinct probability that the presence of stabilizers may influence canopy planform and effect the lift coefficient.

Although the Para-Sail parachute is fabricated primarily of a nearly zero permeability cloth, it will be noted from Table VIII that total porosity is in the order of 8.84%. This value may be converted to an equivalent permeability for the entire canopy by multiplying by the factor $\frac{27.4 \text{ Ft.}^3/\text{Ft.}^2/\text{Min. (Perm.)}}{1\% \text{ (Porosity)}}$, which produces a value of 242 $\text{Ft.}^3/\text{Ft.}^2/\text{Min.}$ under 1/2 inch of water pressure. This permeability is unusually high for a parachute of this application, at least when compared to conventional type solid canopies. The permeability range for such parachutes is in the range of 80 to 150. Even among the more permeable Mil-Spec fabrics for parachutes this value does not exceed 200 cu. ft./sq. ft./min.

Consequently, it is not surprising in view of this aspect, that Para-Sail openings were slow and erratic and that introduction of the internal parachute proved a valuable inflation aid.

5.4 Basic Engineering Geometry

Figures 41 thru 43 present schematically the basic geometry of the derived 80A-9. This data combined with the porosity information of Table VIII comprises the essential design information for this configuration and should be utilized as a guide in future designs. The basic gore of Figure 41 has been determined

in accordance with the basic canopy shape shown in Figure 40. Fullness, or additional cloth, is indicated in Frame 1 of Figure 41.

5.5 Fabrication and Materials Studies

5.5.1 Materials Investigations

Structural failures in the Para-Sail canopy fabric presented evidence indicating the necessity for improvement in three areas: fabrication techniques, (seam efficiencies) design geometry, (fullness, gore shape) and improved materials. In regard to this latter area a limited effort investigation was instituted to locate more suitable materials. Prior to fabrication of the first Para-Sail for sport use a reasonably thorough search for low porosity materials of adequate strength had been made of the various cloth suppliers and finishers. The most promising of the materials appeared to be a close weave nylon taffeta calendered to a porosity of less than 10 cu. ft./sq. ft./min. It was this material which has since been used in Para-Sail fabrication. Prior to this time additional experience had been gained in the search for low porosity materials for utilization in the Vortex Ring Parachute, a rotating parachute which gained lift thru autorotation of the panels. For this application various Nylon and Dacron sail fabrics as well as coated fabrics were investigated in a very extensive program. In general these results produced evidence that fabrics of low porosity and suitable weight often exhibited adequate tensile strengths, but lacked sufficient tear strength and produced conventional parachute seams of comparatively low efficiency.

With this background of experience, renewed efforts were initiated to locate more suitable materials. Although the two previous investigations had been quite extensive it was possible that new developments had arisen in the field of low porosity fabrics. In the most current investigation the only notable cloths were the family of coated fabrics presented in Table IX. The information presented represents test results and is supported by data in Appendix B. The maximum permeability values in this table indicate the effect of "man handling" the material as would perhaps occur in a parachute inflation.

It will be noted from Table IX that some of the investigated materials exhibited mechanical properties seemingly superior to the taffeta material of present usage. However, a complete picture is not obtained until fabrication techniques have been studied for a particular fabric.

For this analysis, identical seams were fabricated from the applicable new materials, as well as the previously used taffeta, so that seam strengths and efficiencies could be determined and compared. The results of these tests are shown in the last column of Table IX and indicate that although a material may exhibit very desirable mechanical properties, actual fabrication may produce less than the desired results.

This fact is evidenced by the comparatively poor seam efficiencies generated by some of the materials which otherwise exhibited somewhat superior tensile and tear properties. This is generally attributed to the fact that these were coated fabrics, the coating reducing the extensibility of the fibers and their ability to realign to reduce stress. The outcome of this in-

vestigation was the conclusion that the taffeta material was superior to any of the other materials studied for this application and its use in the canopy was continued.

5.5.2 Fabrication Studies

In an effort to improve structural integrity, a study was made of possible improvements in seam construction as has been stated previously. Because of former satisfactory experience with the butted radial seam type of construction in the smaller Para-Sails, this method was adopted in the larger version. However, deficiencies became apparent as drop testing progressed. These deficiencies necessitated a reevaluation of the type of radial seam construction, requiring one of a higher efficiency. The results of these studies are presented in Table X with reference to Figure 44 for construction information. Tests were performed in accordance with the methods outlined in Reference 8. From this table, test group number 7 is representative of the original radial seam construction. Of the seams and materials investigated, test group number 3 appeared to be the most promising and was selected for application in a redesigned Para-Sail. This new design also utilized bias construction which, it should be noted from the above table, affords added strength. These results were also utilized in establishing the sewing efficiencies presented in Table IX.

Actual fabrication of a Para-Sail with the selected lock seam produced a canopy of lighter weight (by approximately 10 pounds) and of higher strength than the original butt seam construction. This change in construction contributed very greatly toward achievement of the deployment and strength capability which was demonstrated.

5.6 Para-Sail Component Strength

Considerable knowledge regarding actual opening forces was acquired during this program. Prior to the initial design of Configuration 80A-1 only very rudimentary information for 25 foot diameter Para-Sails had been obtained, (see Reference 5). This data did not indicate significantly higher opening shocks when compared to a conventional flat circular canopy. However, it is not feasible to extrapolate this data for the larger parachute. As a result it was necessary to perform the initial design without any knowledge of opening forces or canopy stresses. Because of the introduction of a centerline in the original configuration, an extremely unusual canopy shape resulted both during and after inflation. Such a shape precluded the application of conventional stress analysis, including simple hoop stress. Actual force data was not available until instrumented tests had been accomplished at El Centro. Although there were no attempts made to measure individual riser loads during the early stages of testing, actual structural failure on the canopy as well as photographic evidence indicated an asymmetric loading of the canopy suspension system. The rear portion of the canopy always appeared to inflate first and produce higher loadings. As a result some attempts were made to reinforce these sections of the canopy. Since canopy construction varied somewhat throughout the program, only the results of investigative destructive tests which apply to the final configuration are presented.

These results are summarized in the fold-out pictorial view of Figure 45. The test reports in support of these results are included in Appendix C. For additional details regarding con-

struction, the following Pioneer Parachute Company, Inc., drawings are referenced:

Assembly - 19.1481

79.4 Ft. Dia. Para-Sail - 1.149

Deployment Bag - 13.3212

Riser - 3.7426

72 In. Dia. G. S. Canopy - 1.9234

120 In. Dia. G. S. Canopy - 1.9915

Bridle - 13.6252

Bridle - 13.6253

Deployment Bag - 13.2064

5.7 Determination of Stress

As the result of data acquired under this program, an empirical form of stress analysis becomes applicable.

Utilizing the information contained in Section 4.0 regarding non-steady state characteristics, an attempt has been made in determining the stress in the canopy cloth, in the suspension system, reefing line and rings, and in deployment aids such as the internal parachute and pilot parachute. These calculations are then related to the actual structural evidence in Section 5.6.

5.7.1 Cloth Stress

A simplified form of stress analysis is presented herein, which is based on the method presented in Reference 9, Page 203. This technique equates internal pressure to opening force, but does not consider gore buldge or high local radii of curvature, and is based on the assumption that the drag producing surface may be represented as a thin walled hemisphere.

The equation developed for cloth stress is as follows:

$$L_S = \frac{F}{\pi D_p 12} \qquad (5)$$

where the units of L_S are lbs./in.

After full reefed opening, the force on the parachute decays until disreef occurs. At such time the force again increases until a maximum is reached, which if proper reefing line length and time delay are combined, will be slightly less than the reefed opening force. Hence, it can be seen from Equation 5 that at a maximum F will be no greater disreefed than reefed, whereas D_p (the diameter projected at a particular instant) will continue to increase very significantly. Therefore, from the mathematics, the maximum cloth stress, L_S, in the disreefed phase must be significantly less than for the reefed opening stage.

Experience under this program tends to support this theory, since it has been shown in drop tests that major canopy damage occurred during the reefed portion of inflation and it is only for this phase that cloth stress is calculated.

With motion picture data, force time history and sequence of events history, all from drop tests under this program, it was possible to establish two dimensionless curves, one for force (Figure 45) and one for projected reefed diameter (Figure 46). Also from the motion picture film it was possible to establish some fairly precise dimensional relationships for the reefed Para-Sail. From

these films a maximum projected diameter of 27.3 ft. was determined. It will be noted that two heavy curves for force are indicated in Figure 46, one determining the maximum force encountered and the other an average. Likewise, two such curves are indicated for projected diameter in Figure 47, one of these representing a minimum value and the other an average. By selecting simultaneous values from each of these curves, equation (5) can be solved for cloth stress at that particular degree of inflation. The combination of maximum force and minimum diameter yields the case of maximum stress, which is presented in Table XI, Case I. Combining average values indicates somewhat lower stresses which are also included in the above table as Case II. This manner of presentation is intended to show a possible range of stresses which could be encountered during reefed inflation. If these values are compared with the seam strengths indicated in Figure 45, (Tests 12, 13, 14, and 15) which are the minimum strengths expected, it would appear that very ample safety factors exist, in the order of 3. This would not account for the damage encountered in actual drop testing. It is conceivable however, that this damage may have resulted from causes other than internal pressure, such as high local accelerations of cloth, or as the result of minor damage inflicted during deployment.

5.7.2 Stress in the Suspension System

The maximum opening force encountered during a successful test was in the order of 16,000 lbs. for the

this is the number of lines per link, thus requiring a tested strength of 3,096 lbs. It can be seen from Test Number 1 that this value is surpassed.

5.7.3 Reefing Ring Attachment

Actual reefing line forces are not available. The only information providing any indication whatsoever of the magnitude of these forces has been provided by the failure of a 1,000 lb. tensile strength reefing line in Test Number 15 and a similar failure reported by the contracting agency during in-house testing. Packing procedures with the final configuration utilized a 1,500 lb. tensile strength line and an unorthodox spacing of the line, equally fore and aft of the stabilizers with no spacing adjacent to the stabilizers. No failures were encountered with this method.

Based on the assumption that a force of approximately 1,000 lbs. exists in the reefing line and that symmetry exists, the applied load on the reefing ring may be calculated.

$$F_{RR} = 2\ F_{RL}\ \text{Sin}\ \frac{360}{2n} = 2(1{,}000)(\text{Sin}\ \frac{360}{2 \cdot 48}) = 131\ \text{Lbs.} \qquad (8)$$

Where n is the number of reefing line spaces. Because of the unusual packing procedure, this number is reduced to 48, rather than 72 as with conventional packing.

It will be noted from test number 9 of Figure 45, that the strength of the reefing ring attachment greatly exceeds this value.

5.7.4 Internal Parachute Loading

A considerable amount of data was collected through centerline force measurements during the drop test program. Based on this information which is presented in Table VI and

Figure 39 of Section 4.2.4 it is possible to make a reasonable determination of internal parachute forces within the range of data. It will be noted from Figure 39 that an xK factor of less than unity is present. If the velocity at skirt emergence from the deployment bag is used as a criterion, this factor is in the order of .82. Therefore, the force under launch conditions of 154 KIAS for a 10 foot diameter Ribless Guide Surface chute would be determined as follows:

$$F = C_D Sq\ (xK) = 3{,}960 \text{ Lbs.} \tag{9}$$

Applying the factors of Reference 9, Page 370 would yield the following suspension line strength for a 10 gore internal canopy.

$$F_{SL} = \frac{F}{N}\left(\frac{j \times c}{u.o.e.k}\right) = 915 \text{ Lbs.} \tag{10}$$

Deducting sewing losses accounted for in the above factors the suspension system should be capable of withstanding an applied load of 7,320 pounds.

It will be noted from Figure 45, test 20, that adequate safety factors do not exist in the suspension system of the internal chute. In addition, damage resulting to the internal parachute of Test 19 indicate that canopy fabric strength (MIL-C-7020, Ty. II) was also inadequate.

5.7.5 Pilot Parachute Loading

Test information is unavailable in this instance to calculate or relate actual forces to loading. However, a simple drag calculation for a 6 foot diameter Ribless Guide Surface pilot parachute, assuming a shock factor of 1.4, yields a load of 2,500 pounds. Applying proper factors as before, but not including the effect of sewing indicates that the pilot parachute and connections

to the canopy should produce a minimum test strength of 4,650 pounds. Examination of Figure 45 shows this value is exceeded in tests 18 and 19.

5.8 Weight and Volume of the Para-Sail

The actual weight and volume of the Para-Sail 80A-9 are presented in Table XII. Volumes indicated are under hand packed pressure and in a container of rectangular cross section.

This results in a packed density of 24.8 Lb./Ft.^{3}, which is comparatively high when compared to standard parachutes under similar conditions. In tests performed by the Contracting Agency, it became necessary to package the unit in a compartment with a volume of 4.64 Ft.^{3}, with a resulting density of 35.1 Lbs./Ft.^{3}, without the use of significant pressure packing techniques. This fact is somewhat surprising since this density is normally acquired by medium pressure packing. (See Reference 9, Pages 372 - 374).

A significant reduction in canopy weight accompanied the change from butt to lock seam construction. Assembly weight was reduced from 176 to 163 pounds. The weight saving was achieved thru the use of lighter radial seam tapes with the lock seam fabrication.

Table XIII presents a comparison between the specific drag areas of the Para-Sail and examples of efficient conventional parachutes. The drag areas utilized are those normal to the vertical axis of the parachute (effective drag area) and are computed for a vertical velocity of 25 FPS. It may be seen that the Para-Sail compares favorably with these other types, in spite of the fact that only limited efforts were made during development to optimize weight.

A diagram for determining weight and volume for various sized Para-Sails is presented in Figure 48. This information should only serve as a general guide since future efforts in improving design will undoubtedly affect these values.

5.9 Planform and Profile

Utilizing enlargements from 16mm drop test motion picture film, an analysis was made of canopy planform, profile, and aerodynamic center of pressure.

5.9.1 Canopy Planform

This study was made possible thru the use of motion picture film taken from aboard the test vehicle during steady state descent. In particular this study was directed toward determining the effect of canopy loading. As may be noted in Figure 49, canopy planform is elliptical in shape, the degree of ellipticity appearing to increase slightly with increase in canopy loading. This tendency is substantiated in Figure 50 which shows that planform is not a true ellipse, but rather a combination of two ellipses with equal semi-major axis, but unequal semi-minor axis. Apparently the elliptical planform is influenced by the presence of the stabilizer panels. The variation in minor axis and increased ellipticity are probable the result of increased forward motion pressure at higher canopy loading, tending to force the leading surface of the canopy toward the rear.

From the aerodynamic view point, this planform is desirable because of the increased aspect ratio which produces

greater lift in airfoils. Of the test configuration without stabilizers, no effect on planform is noted by the lack of their presence, although it was indicated in Section 4.1 that the aerodynamic coefficients were decreased. The planform of the configuration with centerline does not show an influence on variation in semi-minor axes by increased canopy loading and dynamic pressure.

5.9.2 Canopy Profile and Gore Curvature

Utilizing drop test motion picture film from chase aircraft, an analysis was made of the inflated shape of the final configuration during steady state descent. This profile in front and side views is shown in Figure 51. The distortion from the conventional circular parachute shape will be noted. With the information of the above figure, and dimensional details of the actual gores, it was possible to compute the curvature of the cloth between suspension lines for the length of the gore. This is presented in Figure 52 as the ratio of gore curvature (arc) to the cord between suspension lines. It should be borne in mind that a ratio of 1.57 is equivalent to a semi-circle or an included angle of 180 degrees.

5.9.3 Center of Pressure

Utilizing average values from steady state individual riser forces and drop test motion picture enlargements, it was possible to compute the aerodynamic centerline of the parachute, as had been accomplished with wind tunnel models, see Volume I. The result of this calculation indicated an aerodynamic centerline 2.4° aft of the parachute centerline as shown

in Figure 53. This is in good agreement with the models for which this value was determined to be from 1 to 2 degrees depending upon configuration.

5.10 Opening Shock Factor

With the available data, an attempt has been made to derive an empirical relationship between opening shock factor and the variables of weight, speed, diameter, density and filling time. This was done in the manner presented in Reference 12, Page 4-2-4, by relating a decreasing shock factor, xK, to an A factor which is comprised of the above variables. This was performed for both the disreefed and reefed cases as shown in Figures 54 and 55 respectively.

In an initial attempt at deriving a significant relationship, applicable drop tests were selected and the variables appearing in equations 11 thru 14 below were tabulated for both reefed and disreefed cases.

$$xK = \frac{F_o}{C_D S_o \, q_{DR}} \quad \text{(disreefed)} \tag{11}$$

$$xK = \frac{F_R}{C_D S_R \, q_{LS}} \quad \text{(reefed)} \tag{12}$$

$$A = \frac{2W}{C_D S_o \, \rho_{DR} \, t_{f2q} V_{DR}} \quad \text{(disreefed)} \tag{13}$$

$$A = \frac{2W}{C_D S_R \, \rho_{LS} \, t_{f1} \, q V_{LS}} \quad \text{(reefed)} \tag{14}$$

Actual values from test records for each test appear in Table XIII for reference. From these variables, values for xK and A factors were calculated and plotted. However,

because of normal scatter in the data, and variations in interpretation, these graphics did not disclose any type of pattern or curve.

Consequently, it was necessary to establish "smoothed" values for certain of these variables and to recalculate xK and A factors with theoretical rather than actual data. The so called "smoothed" values were obtained from Section 4.2 wherein these variables were plotted versus the influencing parameters of weight, velocity, diameter and density. The variables and sources are indicated as follows:

Reefed Drag Area, $(C_D S)_R$, - Figure 34

Full Open Drag Area, $(C_D S)_o$ - Figure 23

Reefed Filling Time t_{f1} - Figure 35

Disreefed Filling Time t_{f2} - Figure 36

Reefed Opening Force, F_R - Figure 37

Disreefed Opening Force, F_o - Figure 38

It was therefore possible to establish the meaningful relationships for disreefed and reefed opening shock factors as shown in Figures 54 and 55.

The apparent influence of canopy loading on shock factor will be noted in Figure 55, which was somewhat unexpected as was the dependence of drag area on canopy loading discussed in Section 4.2.3. This effect is also noted in Figure 56, which

would require a family of curves of various canopy loadings to establish drag area ratios from known reefing line lengths.

It must be understood that in this first attempt, sufficient data did not exist to provide a wide range of coverage and that some intuition was required in establishing the curves.

As additional data becomes available these relationships may be modified and expanded to provide more accurate values covering a broader scope.

Table VIII

AREA AND POROSITY DISTRIBUTION

IN PARA-SAIL 80A-9

Areas - Ft.^{2}			**Porosities - Percent		
*Turn Slots	-	61	Turn Slots	-	1.29
*Radial Slots	-	62.5	Radial Slots	-	1.32
*Circumferential Slots	-	242	Circumferential Slots	-	5.12
Vent	-	25.2	Vent	-	.53
Canopy Area (W/O Stabilizers)	-	4,729.9	Total Geometric	-	8.26
Stabilizer Area	-	186.4	Mechanical	-	.56
Total Canopy Area	-	4,916.3	Total	-	8.84

* Slot area determined as bounded by arc and chord.

** Based on canopy area w/o stabilizers.

Table IX

CHARACTERISTICS OF MATERIALS INVESTIGATED

FOR APPLICATION IN THE PARA-SAIL PARACHUTE

Trade Name or Specification	Wgt. Oz/Yd^2	Tensile Strength Lbs./In. Warp	Tensile Strength Lbs./In. Fill	Tear Resistance Lbs. Warp	Tear Resistance Lbs. Fill	Permeability $Ft^3/Ft^2/Min.$ Nominal	Permeability $Ft^3/Ft^2/Min.$ After Mechanical Handling	Sewing* Efficiency Warp	Sewing* Efficiency Fill
Zephrylite Ripstop	1.0	47	42	3.2	3.3	4.9	31.5		
Dynalite Ripstop	1.25	57.5	73	4.8	4.4	4.0	4.19	58.6	55.6
Spinnaker Ripstop	2.0	113	85	5.8	5.75	1.38	1.64	50.6	53.9
Taffeta MIL-M-10747D	2.0	85.8	70.5	5.9	5.95	6.75	13.0	71.4	80.4
K Kote Ripstop	2.4	35	38.8	5.5	6	0	Specimen Tore Under Handling		
Force 9 Ripstop	2.9	127.5	99.5	8.3	9.3	2.75	2.89	51.0	52.0

* For comparative purposes a 3/4 inch 4 needle lock seam with attached radial tape was utilized.

Table X

SUMMARY OF SEAM TEST

INVESTIGATIONS*

Test Group Number	Material	Seam Type	Results Lbs./In. (Average 3 Tests) Warp	Fill	Bias**	Construction Figure No.
1	Taffeta	Modified Lap	51.7			44-a
2	Taffeta	Modified Lap	50.5		84	44-b
3	Taffeta	Lock	61.2	56.7	87	44-c
4	Taffeta	Butt	41.0			44-d
5	Taffeta	Butt	41.2			44-e
6	Taffeta	Butt	39.7			44-f
7	Taffeta	Butt	43.0			44-i
8	Spinnaker Ripstop	Modified Lap	57.5	40.0	96.7	44-b
9	Spinnaker Ripstop	Lock	57.2	45.8	77.3	44-c
10	Dynalite Ripstop	Modified Lap	32.0	34.3	54.3	44-b
11	Dynalite Ripstop	Lock	32.7	37.8		44-c
12	Dynalite Ripstop	Lock	34.7	43.5	52.3	44-c
13	Dynalite Ripstop	Modified Lap	38.7	42.7		44-g
14	Dynalite Ripstop	Lap	36.0	43.2		44-h
15	Force 9	Lock	65.0	51.8	135.0	44-c

* Testing methods in accordance with Reference

** For bias seams the strength per inch is determined by dividing the force by (W-D) where W = width of sample and D = jaw separation.

Table XI

CALCULATION OF CANOPY CLOTH STRESS

EQUATION FOR STRESS $L_S = \frac{F_o}{\pi D_p 12}$

Per Cent Inflation Time	Case I Maximum Stress			Case II Average Stress		
	F_R, Opening Force, Lbs. (From Fig. 46)	D_p Projected Diameter Ft. (From Fig. 47)	L_S Stress Lbs./In.	F_R, Opening Force, Lbs. (From Fig. 46)	D_p Projected Diameter Ft. (From Fig. 47)	L_S Stress Lbs./In.
0	3,895	3.28	31.7	2,993	6.0	13.2
5	4,560	6.82	17.7	4,085	7.9	13.7
10	4,987	7.92	16.7	4,750	10.1	12.5
20	5,035	9.01	14.8	4,180	14.7	7.5
30	6,365	13.10	12.9	5,225	17.5	7.9
40	8,360	17.47	12.7	6,887	21.0	8.7
50	10,355	20.48	13.4	8,313	23.2	9.5
60	9,500	22.39	11.3	8,217	24.6	8.9
70	11,734	22.93	13.6	10,213	25.4	10.7
80	13,395	23.21	15.3	12,065	25.4	12.6
90	14,583	24.57	15.8	13,585	26.2	13.8
100	12,825	27.3	12.5	12,160	27.3	11.8

Table XII

PARA-SAIL WEIGHT AND VOLUME

	Weight (Lbs.)	Volume (In.^{3}) @ 1 Lb./In.^{2}
	of Para-Sail Config. 80A-9	
Canopy, Lines, and 10 Ft. Internal G. S. Chute	148.5	10,262.0
Pilot Chute Canopy	4.3	313.5
Bridle		
- - - 6 Ft.	0.7	114.8
- - - 20 Ft.	1.7	57.4
Main Canopy Deployment Bag	7.0	535.2
Pilot Chute Deployment Bag	0.8	74.3
Total	163.0	11,357.2

Table XIII

COMPARISON OF SPECIFIC DRAG AREAS

FOR LARGE PARACHUTES

Parachute	Application	Drag Area $C_{D\ eff}S$, Ft.^{2} @ 25 FPS	Weight of Parachute Lbs.	Specific Drag Area $C_{D\ eff}S/W$ Ft.^{2}/Lb.
79.4 Ft. Dia. Para-Sail (Config. 80A-9)	Space Craft	7,050	155.9	45.3
100 Ft. Dia.[1] 108 Gore Triconical	Missile	6,440	168	38.3
100 Ft. Dia. 88 Gore Triconical (Light Weight)	Ryan 147 Series Drone	6,440	105	61.2
63.1 Ft. Dia.[2] Ring Sail	Mercury Capsule	2,410	57.2	42.2

1. See Reference 10

2. See Reference 11

Table XIV

SUMMARY OF OPENING SHOCK VARIABLES

Test No.	Total Weight, W Lbs.	Drag Area Reefed $C_D S_R$ Ft.^{2}	Density @ Line Stretch ρ_{DR}, Slugs/Ft.^{3}	Reefed Filling Time t_{f_1} Sec.	Velocity @ Line Stretch V_{LS} Ft./Sec.	Dynamic Pres. @ Line Stretch q_{LS} Lb./Ft.^{2}	Reefed Open Force F_R, Lbs.	Drag Area Full Open $C_D S_O$ Ft.^{2}	Density @ Disreef ρ_{DR}, Slugs/Ft.^{3}	Disreefed Filling Time t_{f_2} Sec.	Velocity @ Disreef V_{DR} Ft./Sec.	Dynamic Pres. @ Disreef q_{DR} Lb./Ft.^{2}	Disreefed Open Force F_O, Lbs.
5	2,785	176	1.92×10^{-3}	1.25	212.8	43.4	4,050	10,256	1.95×10^{-3}	2.7	154.5	23.3	9,300
6	2,785	285	1.93	4.1	218.6	46.1	6,500	8,702	1.97	3.7	108.6	11.6	7,450
8	2,785	261	1.67	2.77	209.7	36.7	7,800	9,710	1.70	2.8	90.0	7.0	5,680
10	3,860	412	1.66	2.80	206.5	35.6	10,580	7,995	1.70	1.4	96.4	7.9	8,650
12	4,755	590	1.69	1.62	234.0	46.2	14,100	7,229	1.72	2.2	106.3	9.7	13,800
16	4,750	520	1.69	2.01	276.1	64.8	15,000	7,229	1.73	2.65	103.3	9.3	11,000
18	4,750	556	1.70	1.93	202.0	34.3	11,560	8,160	1.74	1.95	107.2	10.0	13,700
19	4,750	465	1.68	1.21	304.9	78.1	14,400	7,057	1.71	2.30	113.3	11.0	12,600
20	4,750	485	1.71	2.11	200.1	34.3	12,000	6,530	1.74	2.35	101.6	9.0	14,750

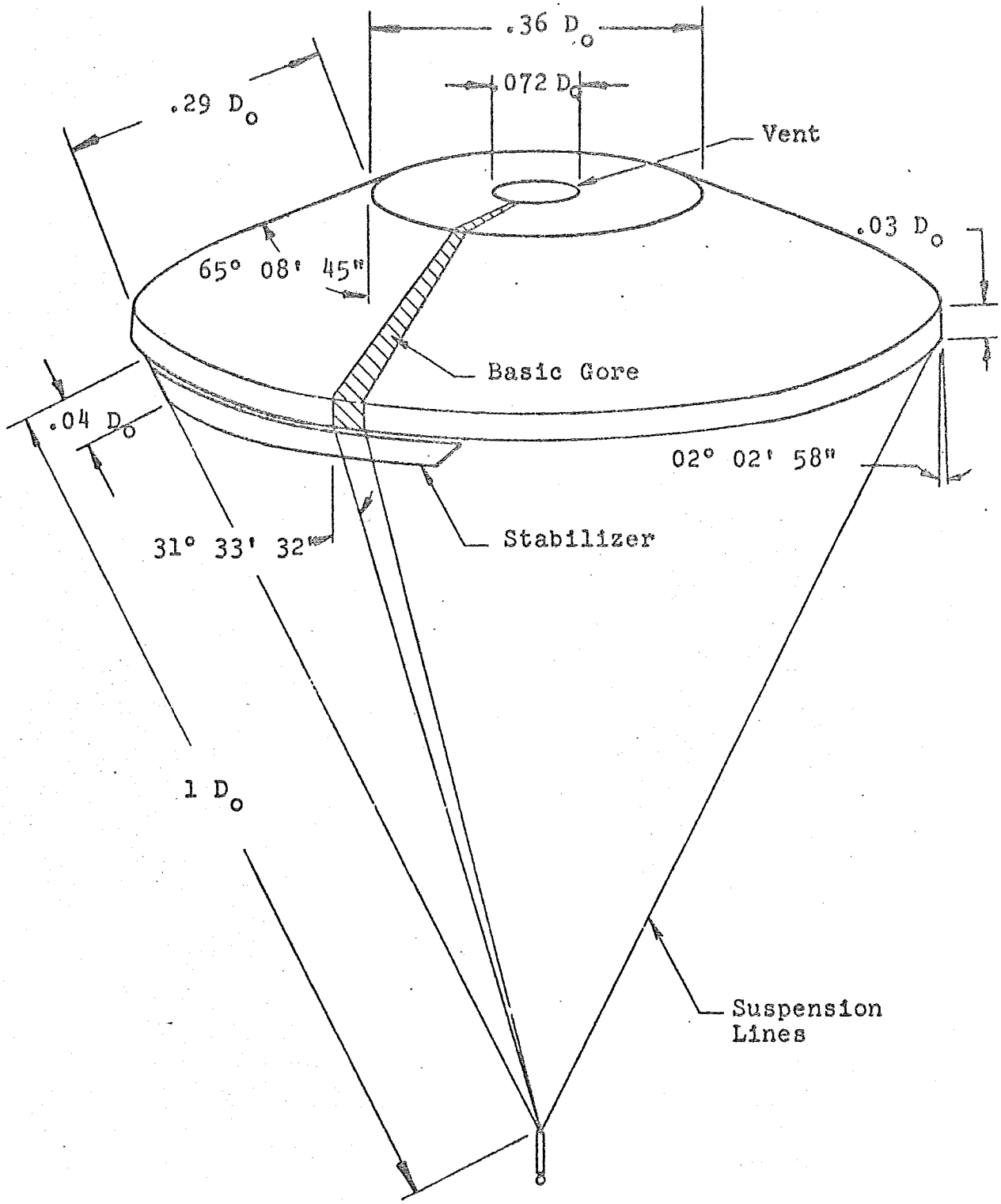

Figure - 40 -

Basic Canopy Shape for a Large Para-Sail

TYPICAL GORE PATTERN FOR 79.4 FT D_o PARA-SAIL, IDENT. NO. 80A-9
72 GORES

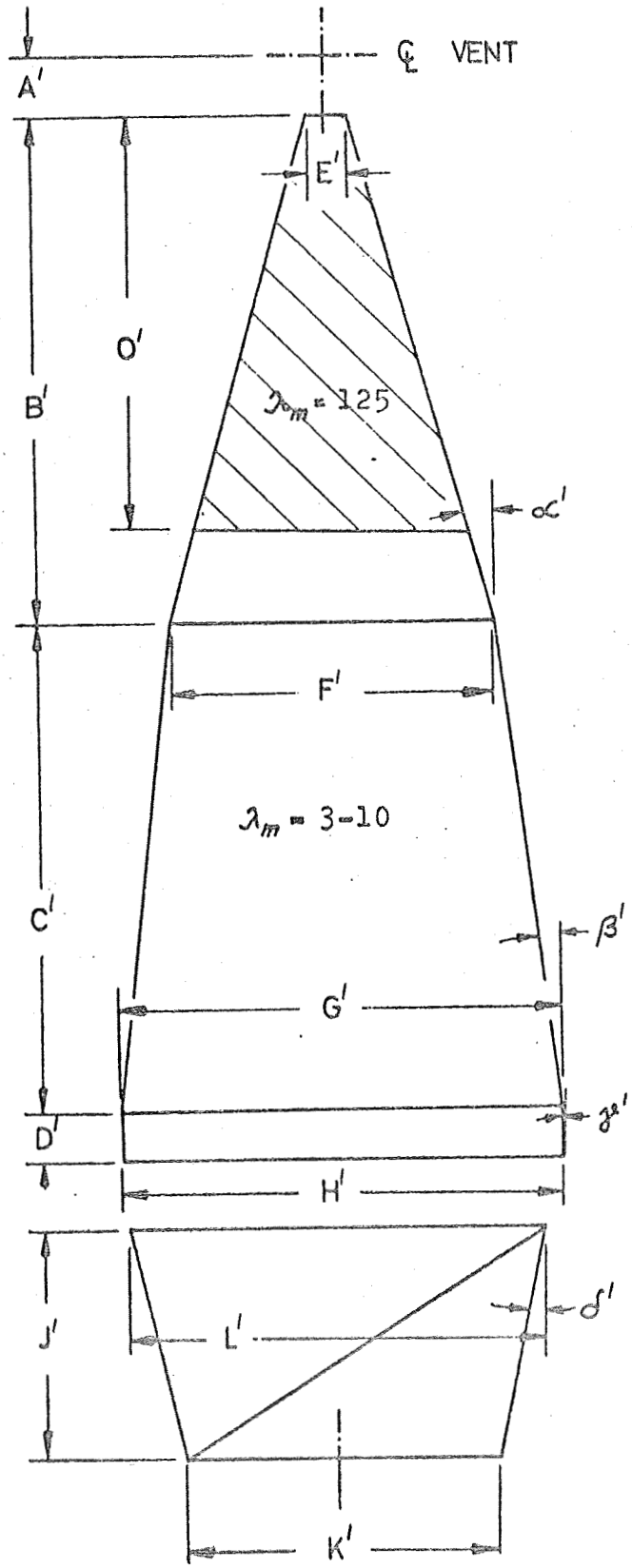

	FRAME 1 incl. fullness	FRAME 2 no fullness
	INCHES	
A' =	34.00	34.00
B' =	135.88	135.88
C' =	274.00	274.00
D' =	31.88	31.88
E' =	5.25	2.97
F' =	15.00	14.82
G' =	36.53	36.53
H' =	36.63	36.63
J' =	34.25	34.25
K' =	34.84	34.84
L' =	36.41	36.41
O' =	95.50	95.50
α' =	02°03'16"	02°29'48"
β' =	02°14'58"	02°16'06"
γ' =	00°05'22"	00°05'22"
δ' =	01°18'45"	01°18'45"

Figure - 41 -

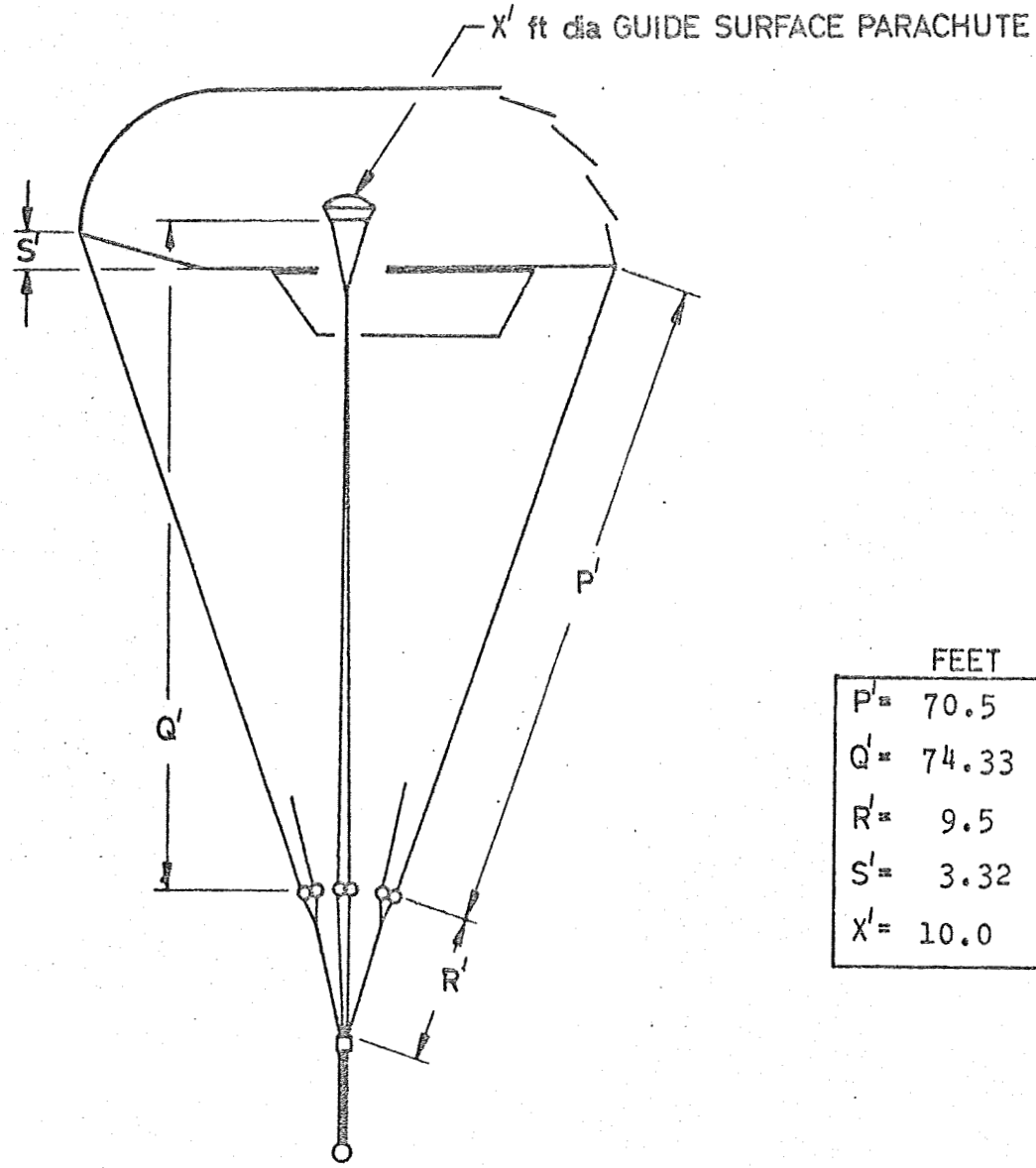

	FEET	INCHES
P'=	70.5	846.0
Q'=	74.33	892.0
R'=	9.5	114.0
S'=	3.32	39.88
X'=	10.0	120.00

Figure - 42 -
GENERAL GEOMETRY 79.4 FT D_o PARA-SAIL (deflated condition)
IDENT. NO. 80A-9 72 GORES

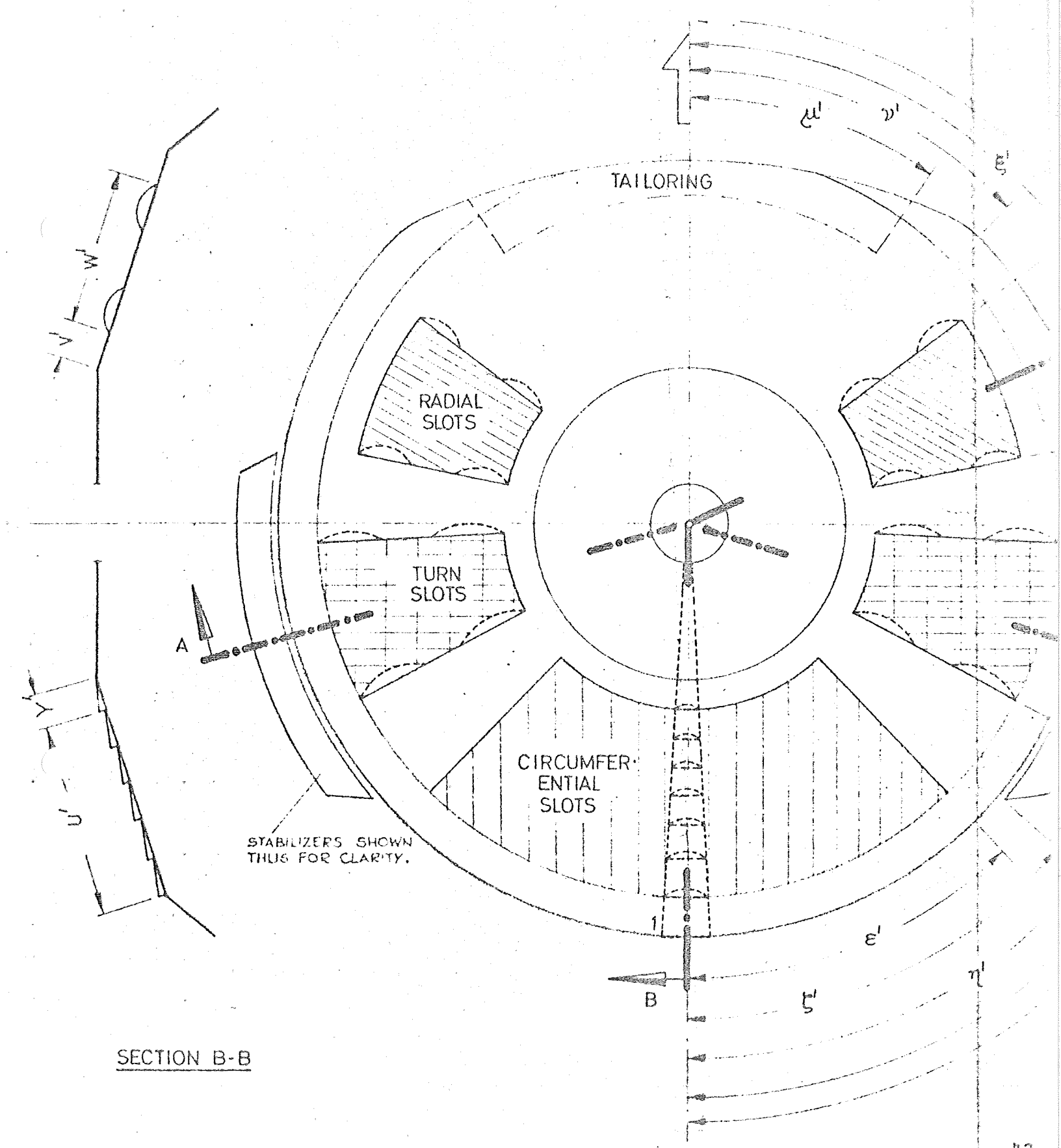

Figure - 43
PARA-SAIL 79.4FT D_o ENGINEERING PLAN
IDENT. NO 80A-5

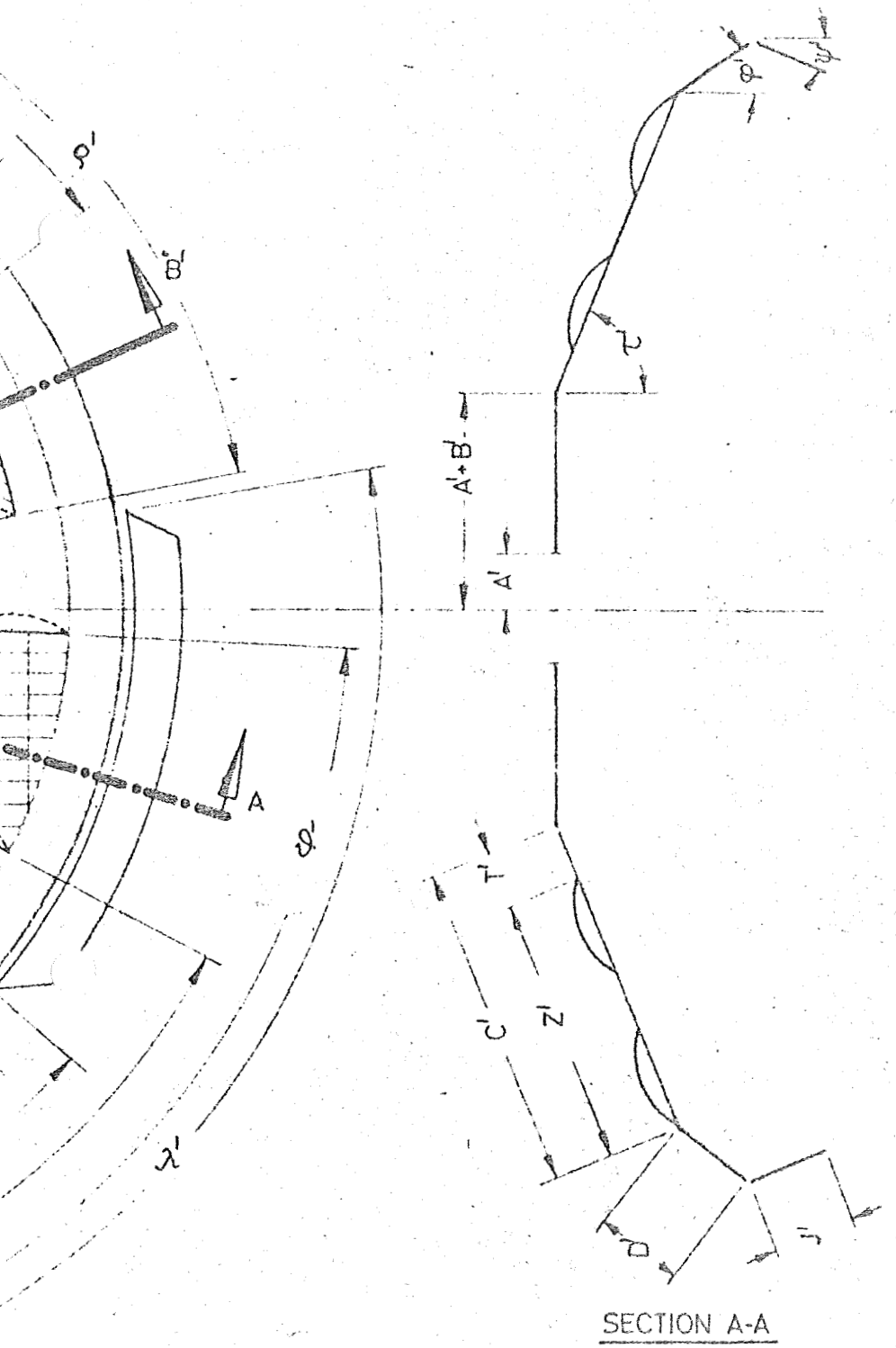

	FEET	INCHES
A'=	2.83	34.00
B'=	11.32	135.88
C'=	22.83	274.00
D'=	2.66	31.88
J'=	2.85	34.25
T'=	5.71	68.50
U'=	19.98	239.75
V'=	0	0
W'=	14.27	171.25
Y'=	2.85	34.25
Z'=	17.13	205.50

	DEGREES	GORES
ε'=	41.25	8.25
ζ'=	42.50	8.5
η'=	67.50	13.5
ϑ'=	77.50	15.5
λ'=	102.50	20.5
μ'=	0	0
ν'=	52.50	10.5
ξ'=	49.15	9.83
ρ'=	97.50	19.5
τ'=	65° 08' 45"	
φ'=	02° 02' 58"	
ψ'=		

$\frac{360}{72}$ = 5°/Gore

43 -
LANVIEW (Frame 1 disconsidered in FIG 41)
DA-9 72 GORES

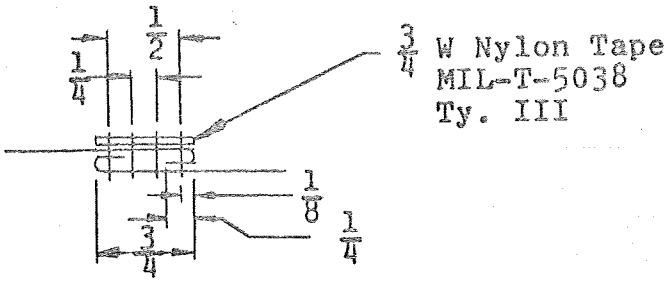

- A -

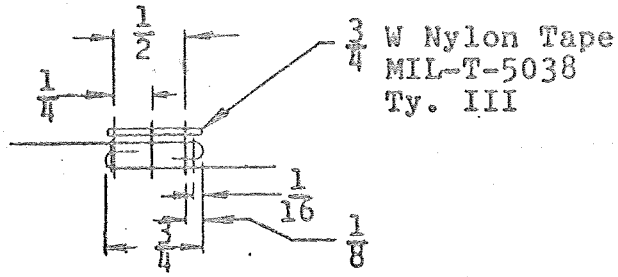

- B -

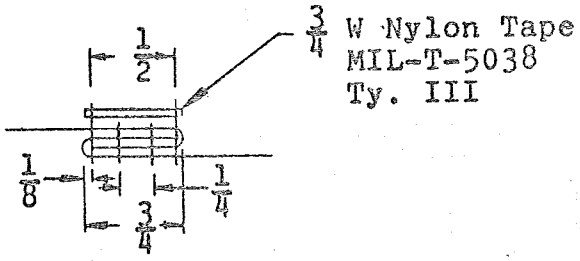

- C -

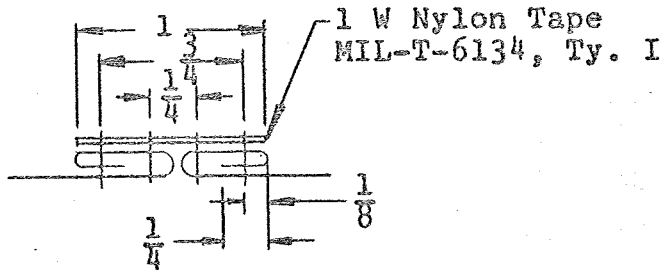

- D -

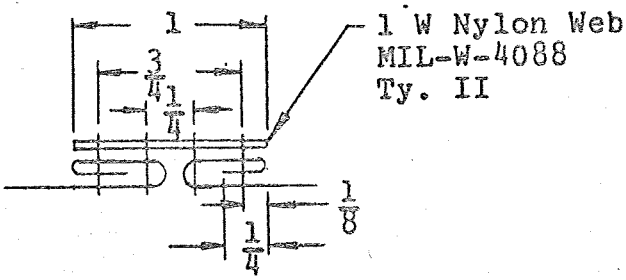

- E -

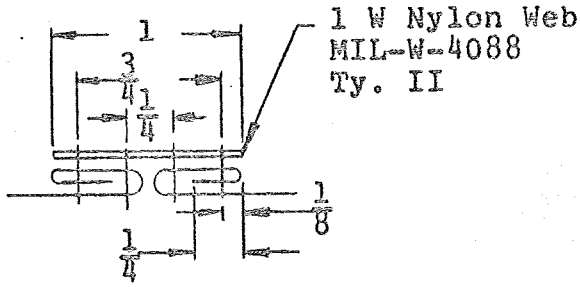

- F -

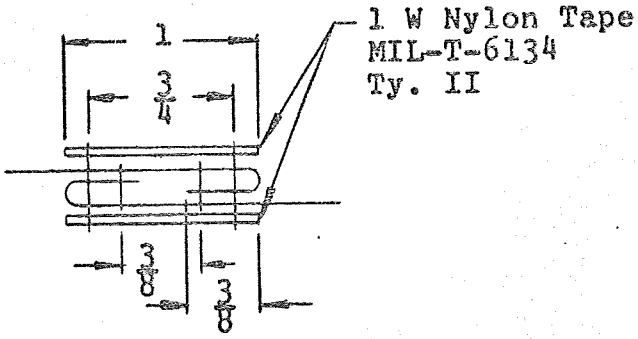

- G -

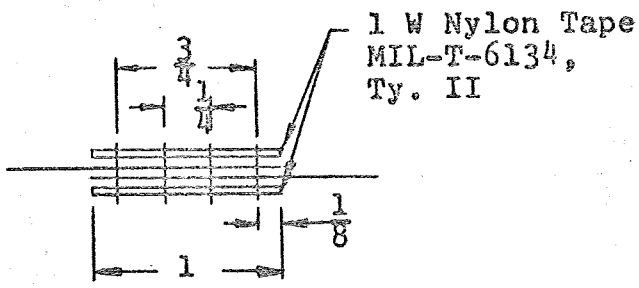

- H -

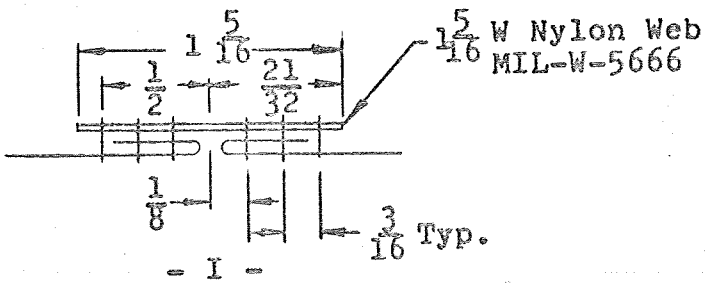

- I -

FIGURE - 44 -
CROSS SECTIONAL VIEWS OF
SEAM CONSTRUCTIONS STUDIED

M. Knor
20 Nov. 64

Test No.

See Appendix C for Test Reports

1. Connector Link Riser
   Avg. T.S. = 9,566 Lbs.

2. Suspension Lines 1-11 & 62-72 to Connector Links
   Avt. T.S. = 754 Lbs.

3. Suspension Lines 12-61 to Connector Links
   Avg. T.S. = 582.6 Lbs.

4. Suspension Lines 22-51 Attached With Skirt
   Avg. T.S. = 489 Lbs.

5. Stabilizer Panel Attachment With Skirt
   Avg. T.S. = 510 Lbs.

6. Skirt Band Joint
   Avg. T.S. = 1,246.7 Lbs.

7. Suspension Lines 1-8 & 65-72 Attached With Skirt
   Avg. T.S. = 621.7 Lbs.

8. Radial Seam at Turn Scoop Edge
   Avg. T.S. = 622 Lbs.

9. Reefing Ring Attachment
   Avg. T.S. = 826.6 Lbs.

10. Radial Seam Single Ply
    Avg. T.S. = 722 Lbs.

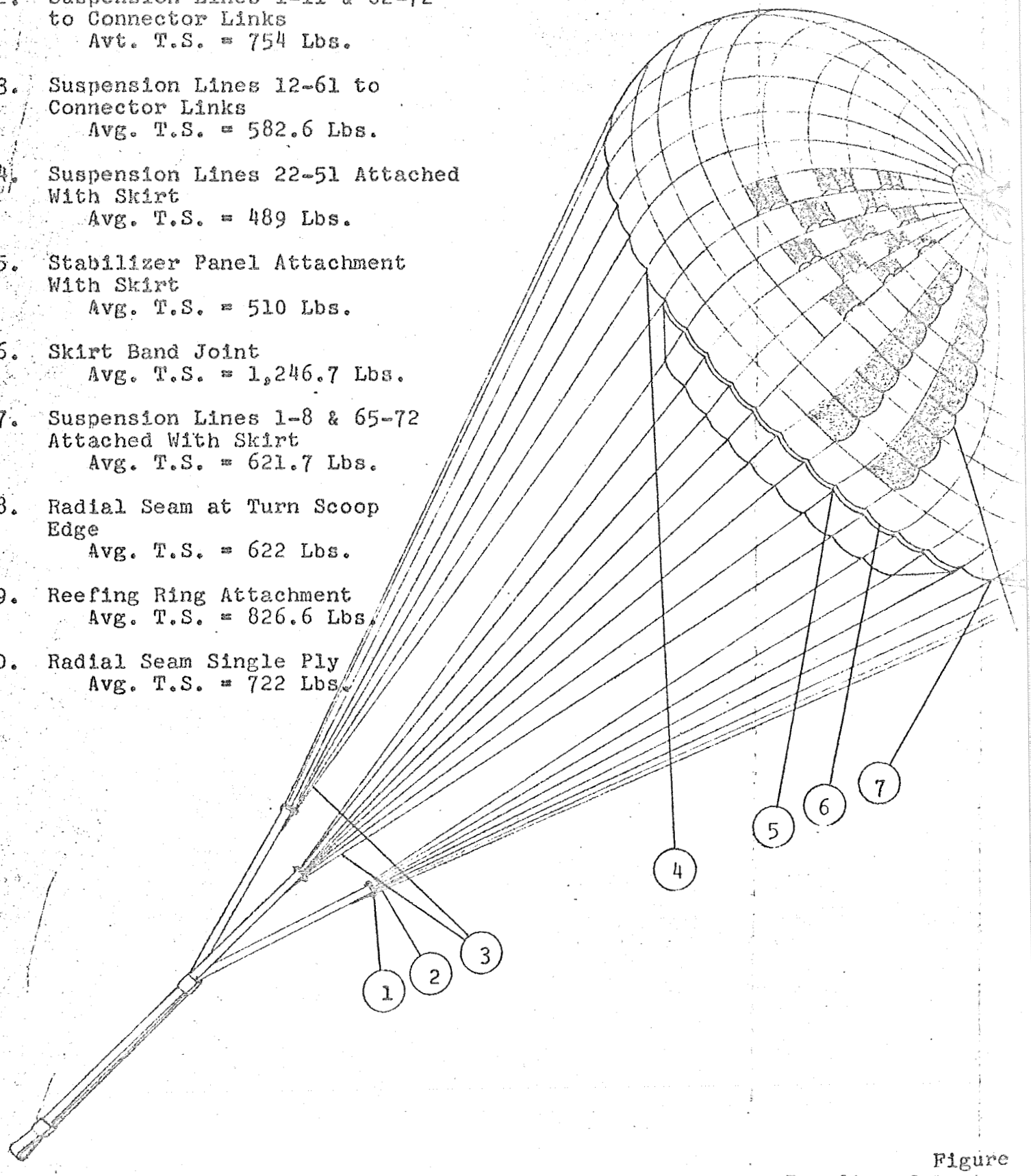

Figure
Results of Destruc
of Para-Sail

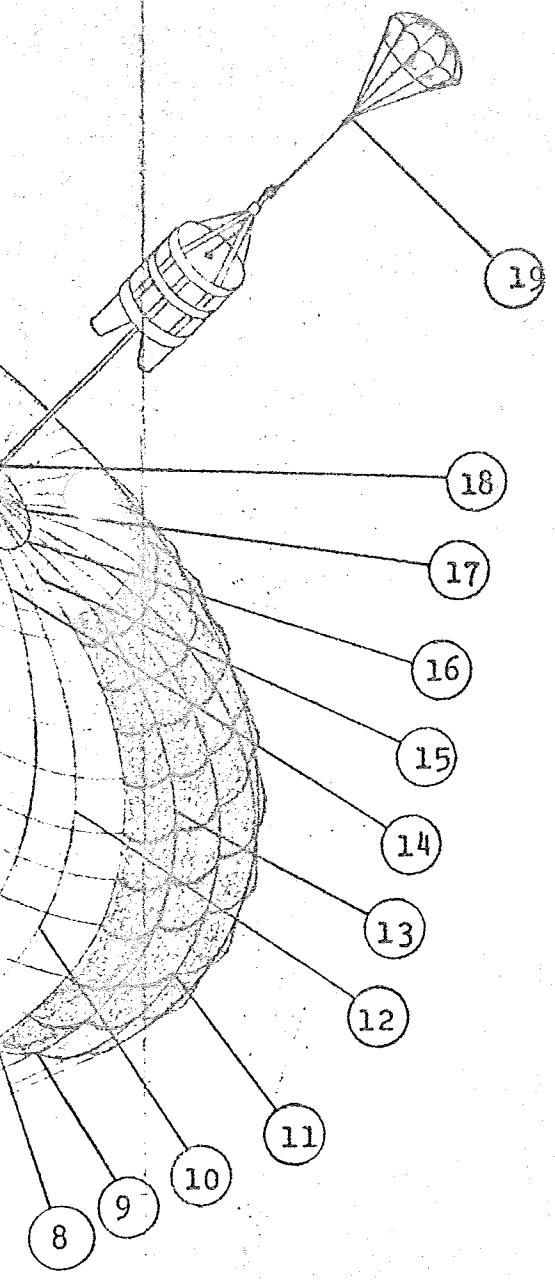

11. Main Seam Longitudinal
    Avg. T.S. = 971 Lbs.

12. Main Seam, Taffeta, Single Ply
    Warp - 71.3 Lbs./In.
    Fill - 57.3 Lbs./In.

13. Main Seam, Taffeta, Double Ply
    Warp - 64.3 Lbs./In.
    Fill - 55.3 Lbs./In.

14. Main Seam MIL-C-7350, Type I, Single Ply
    Warp - 83 Lbs./In.
    Fill - 71.3 Lbs./In.

15. Main Seam MIL-C-7350, Type I, Double Ply
    Warp - 77 Lbs./In.
    Fill - 73 Lbs./In.

16. Vent Line Attachment
    Avg. T.S. = 558 Lbs.

17. Vent Band Joint
    Avg. T.S. = 3,933 Lbs.

18. Bridle/Bridle Loop/Vent Line
    Avg. T.S. = 7,443 Lbs.

19. Stab./Pilot Chute Confluence
    Avg. T.S. = 7,753 Lbs.

20. Internal Parachute Confluence (Not Shown)
    Avg. T.S. = 6,013 Lbs.

e - 45 -
uctive Static Tests
il Components

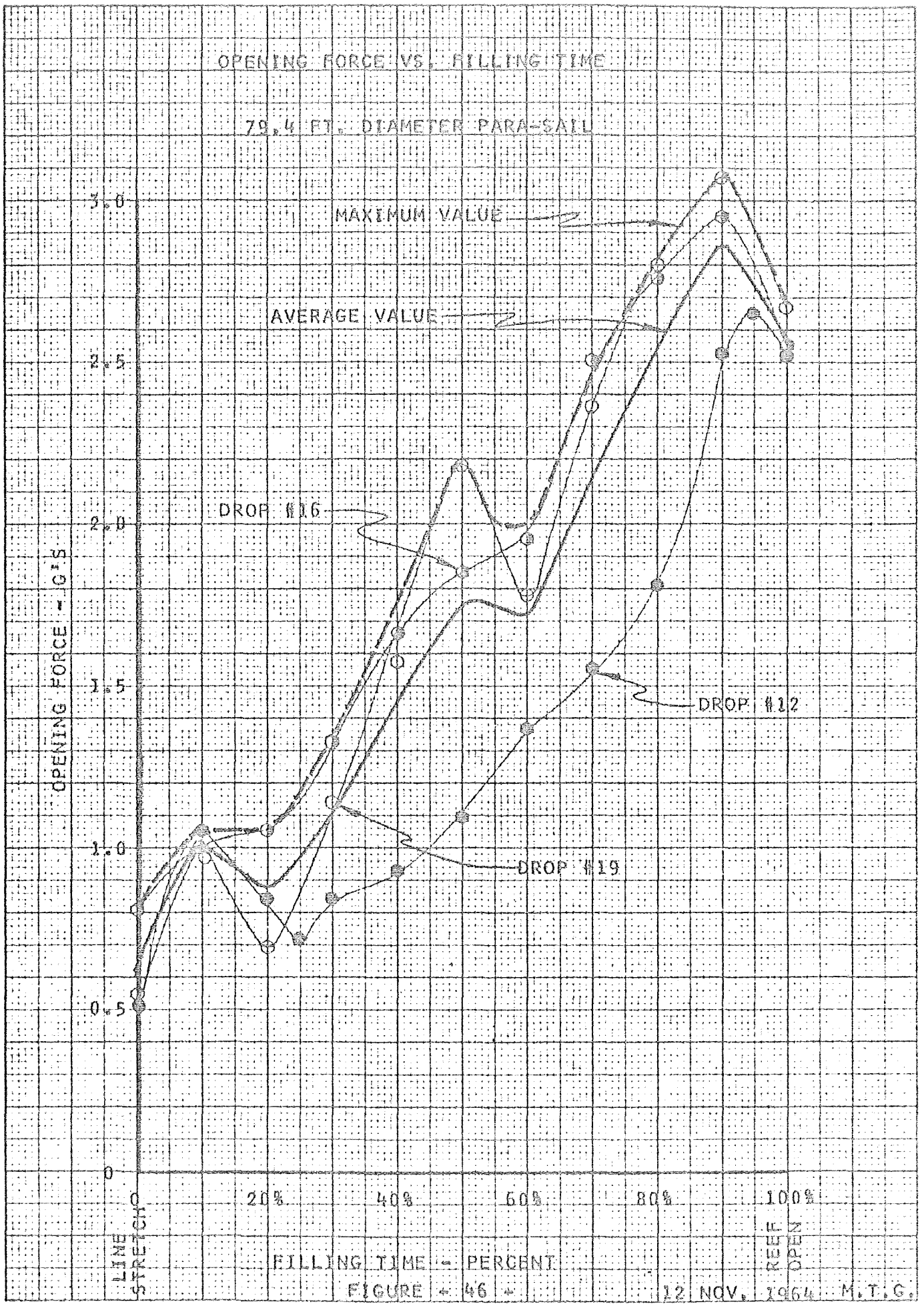

FIGURE - 46 - 12 NOV. 1964 M.T.G.

K+E 10 X 10 TO ½ INCH 46 1323
7 X 10 INCHES MADE IN U.S.A.
KEUFFEL & ESSER CO.

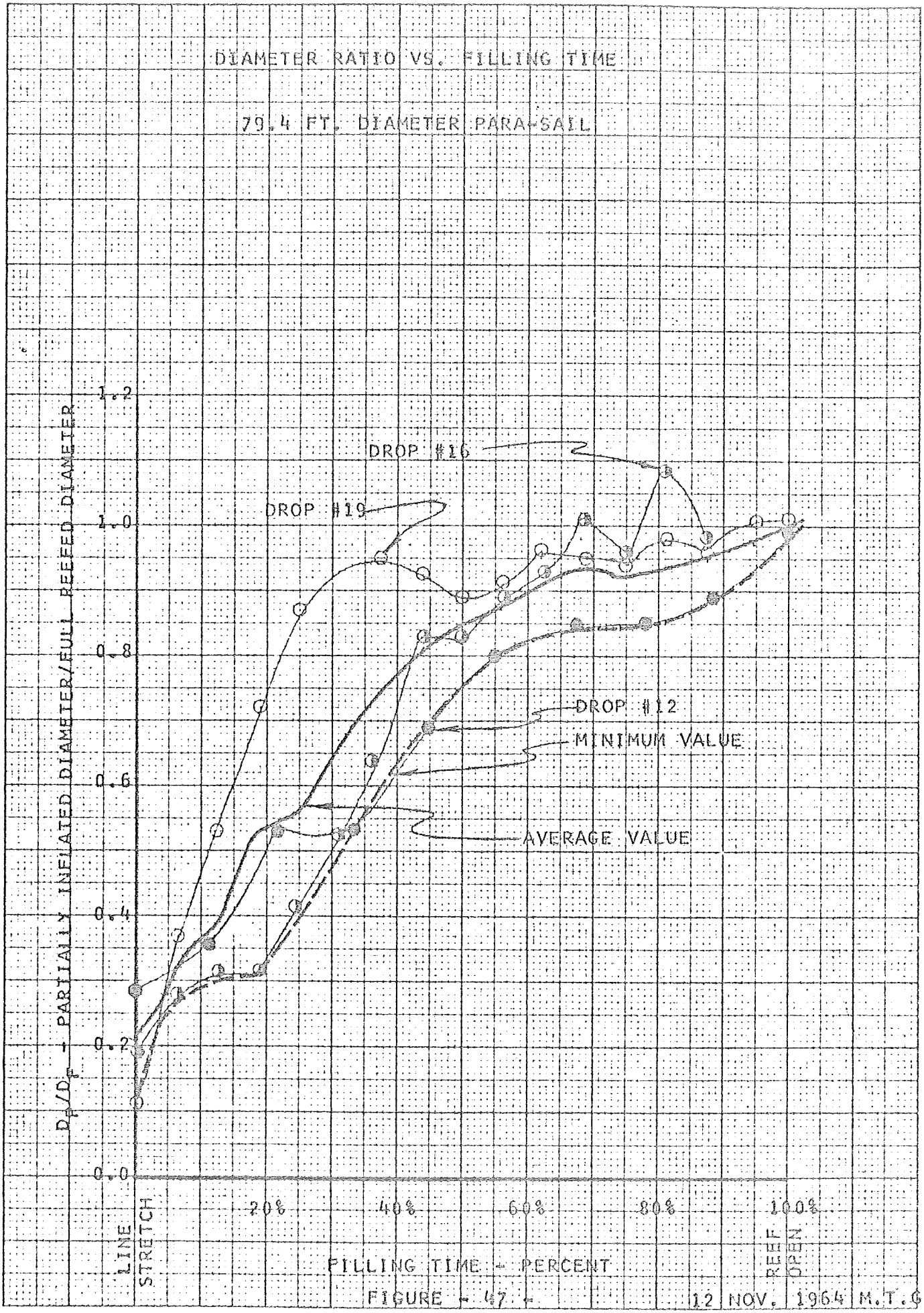

FIGURE - 47 -

12 NOV. 1964 M.T.G.

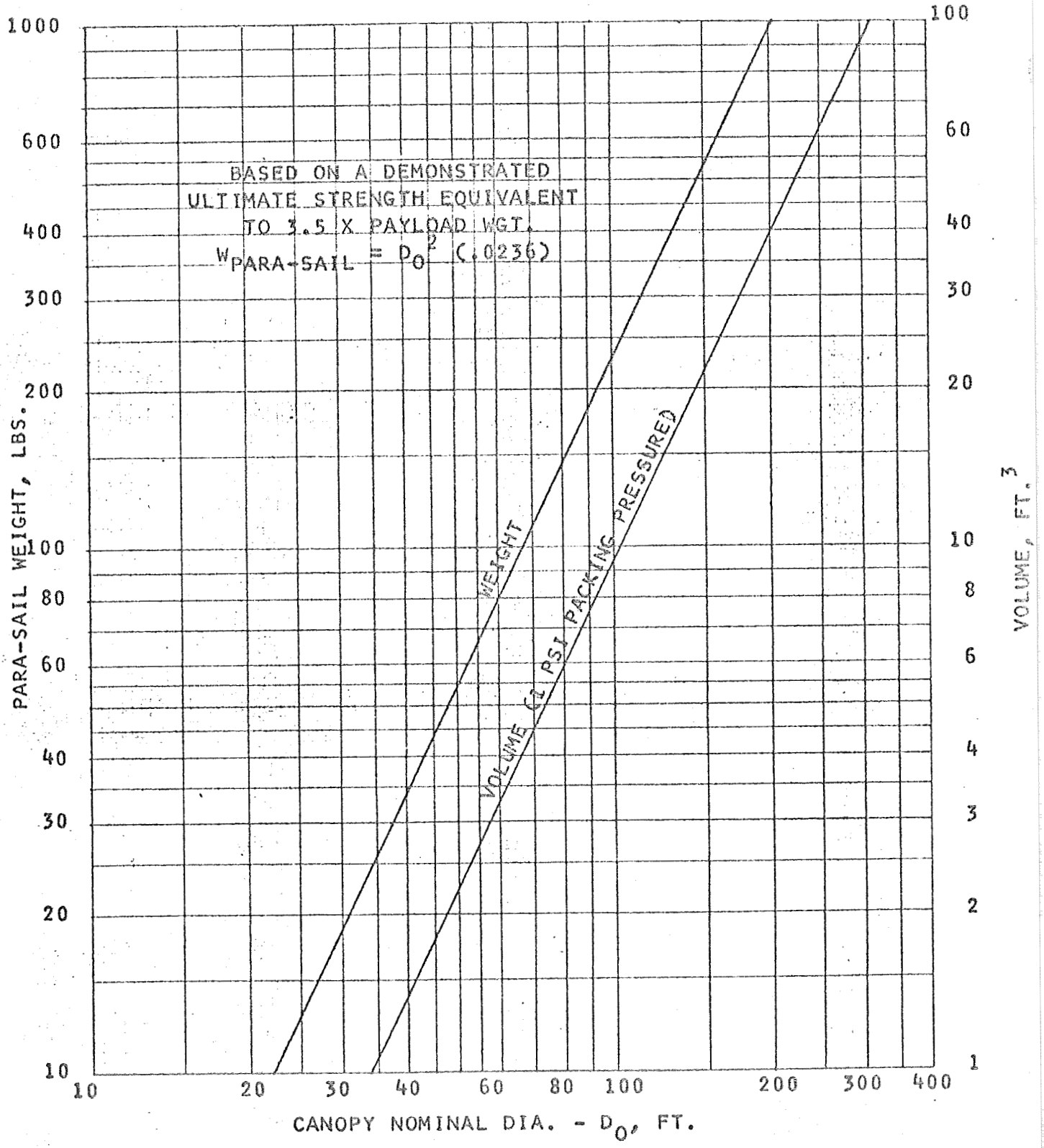

FIGURE - 48 -

CALCULATED WEIGHT & VOLUME FOR
PARA-SAIL RECOVERY PARACHUTES

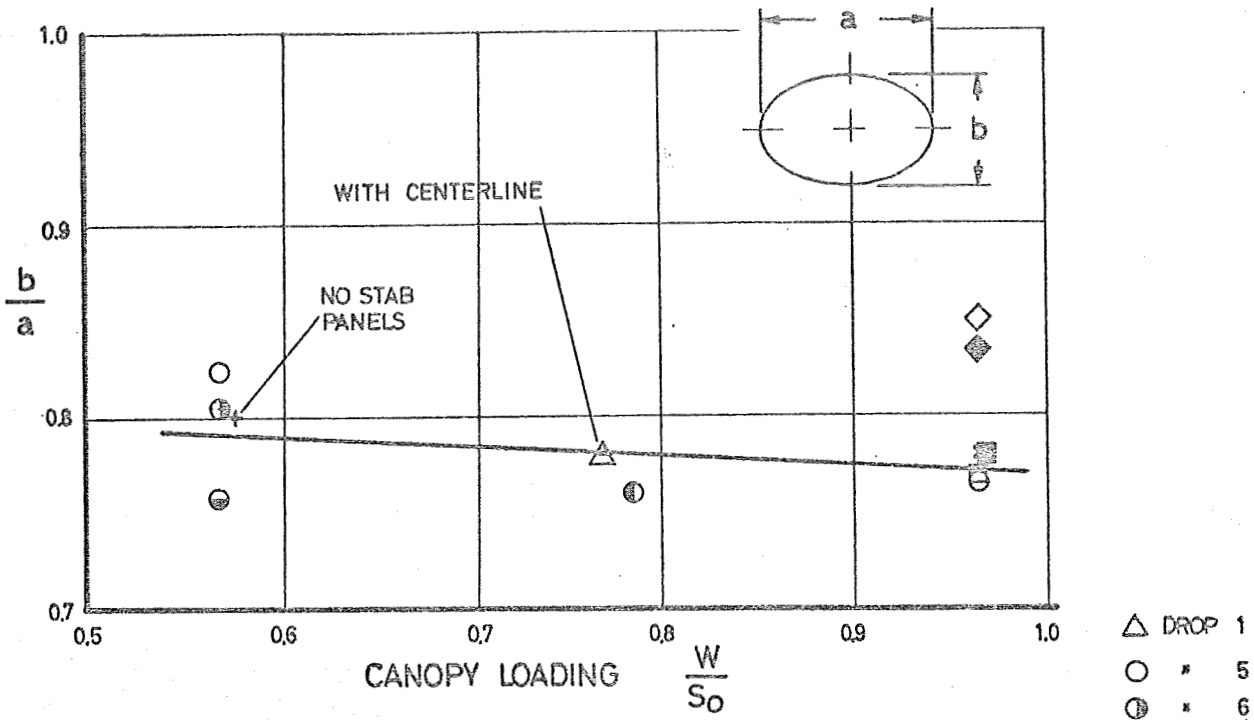

FIGURE - 49 -

THE EFFECT OF CANOPY LOADING
ON MAJOR & MINOR AXES OF
PARA-SAIL PLANFORM

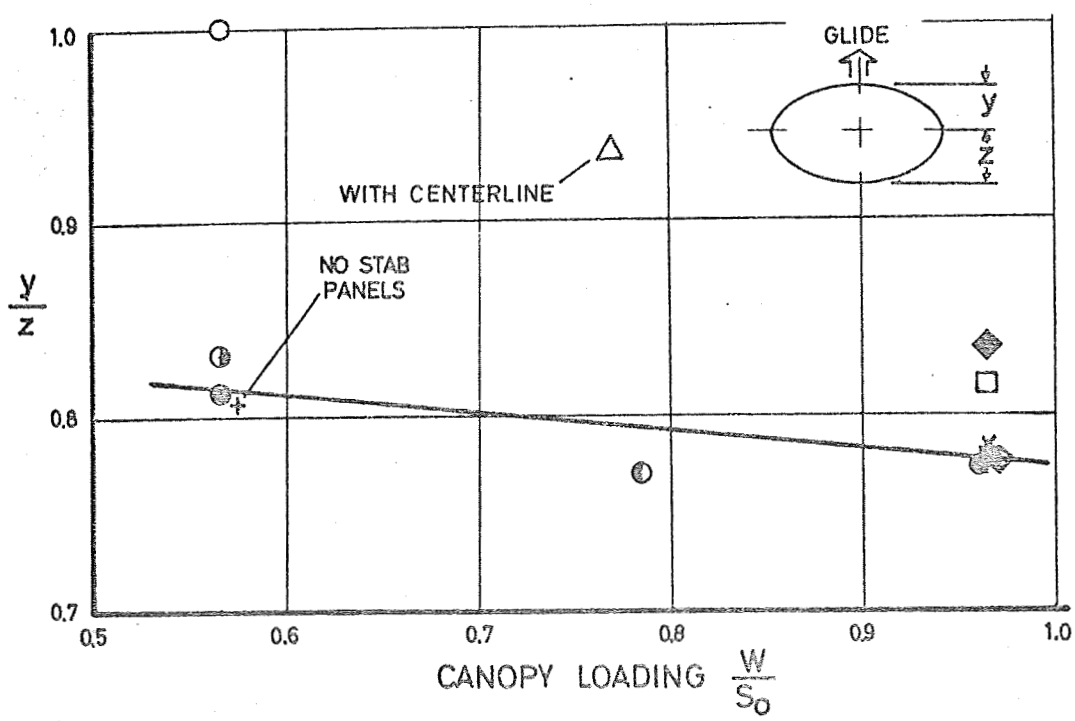

FIGURE - 50 -

THE EFFECT OF CANOPY LOADING
ON SEMI-MINOR AXES OF
PARA-SAIL PLANFORM

INFLATED PROFILE
OF 79.4 FT. DIAMETER
PARA-SAIL

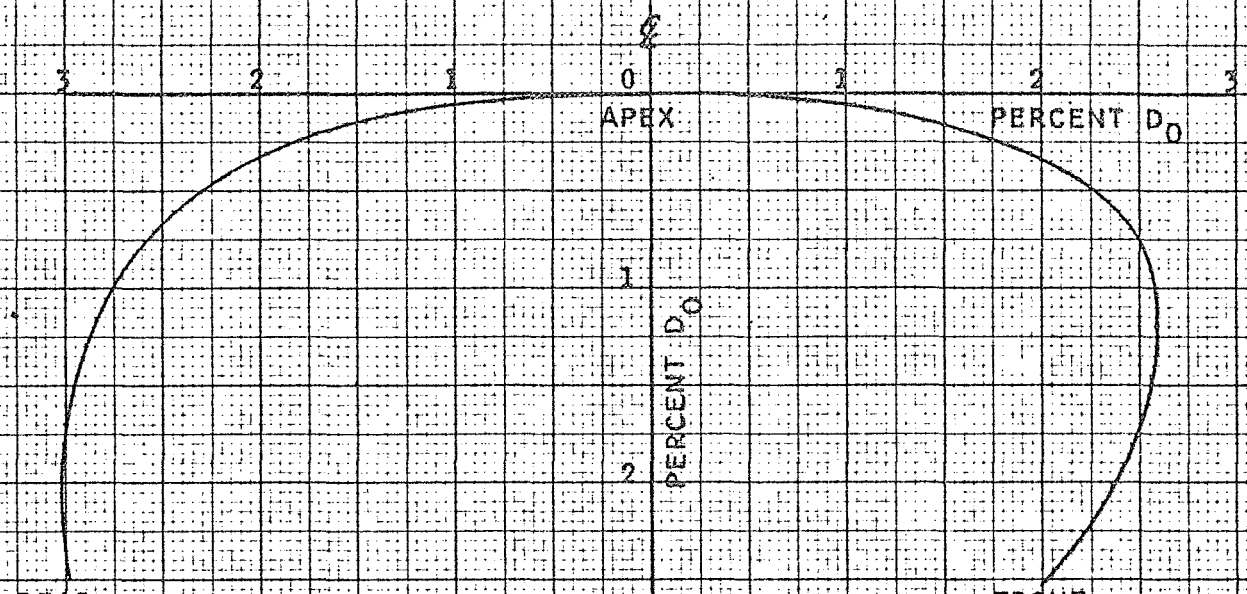

SIDE PROFILE

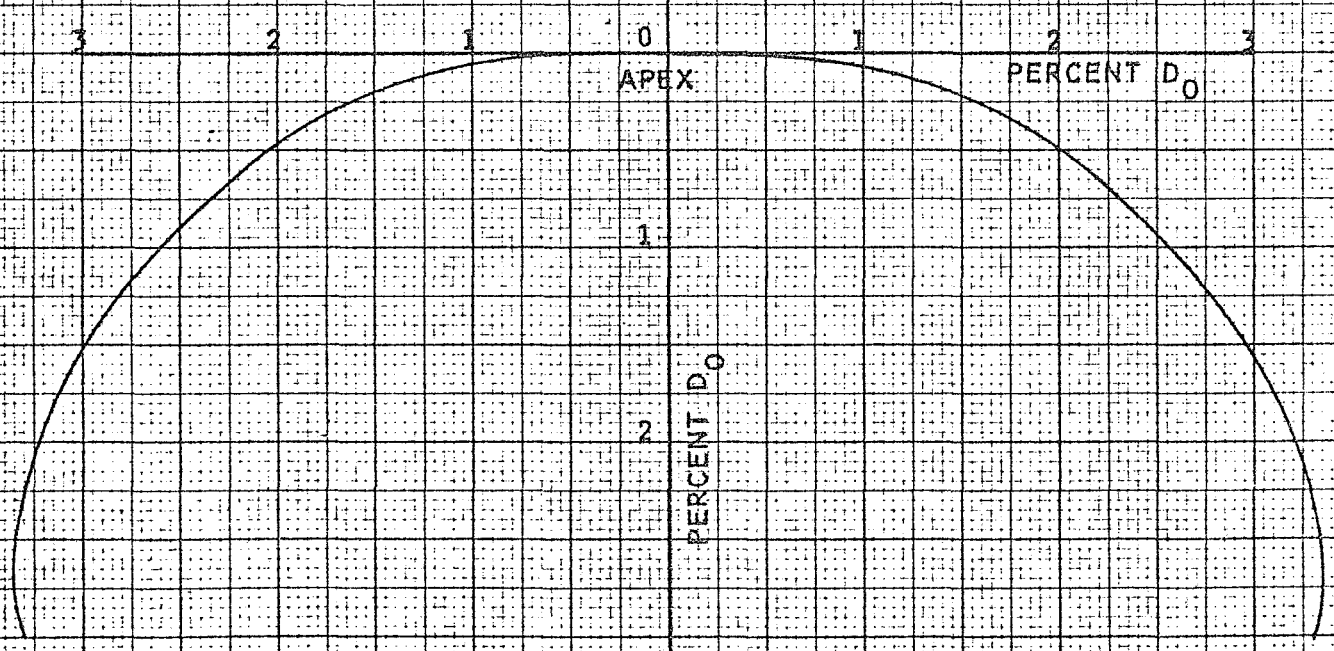

FRONT PROFILE
(STABILIZERS NOT INCLUDED)

FIGURE - 51 -

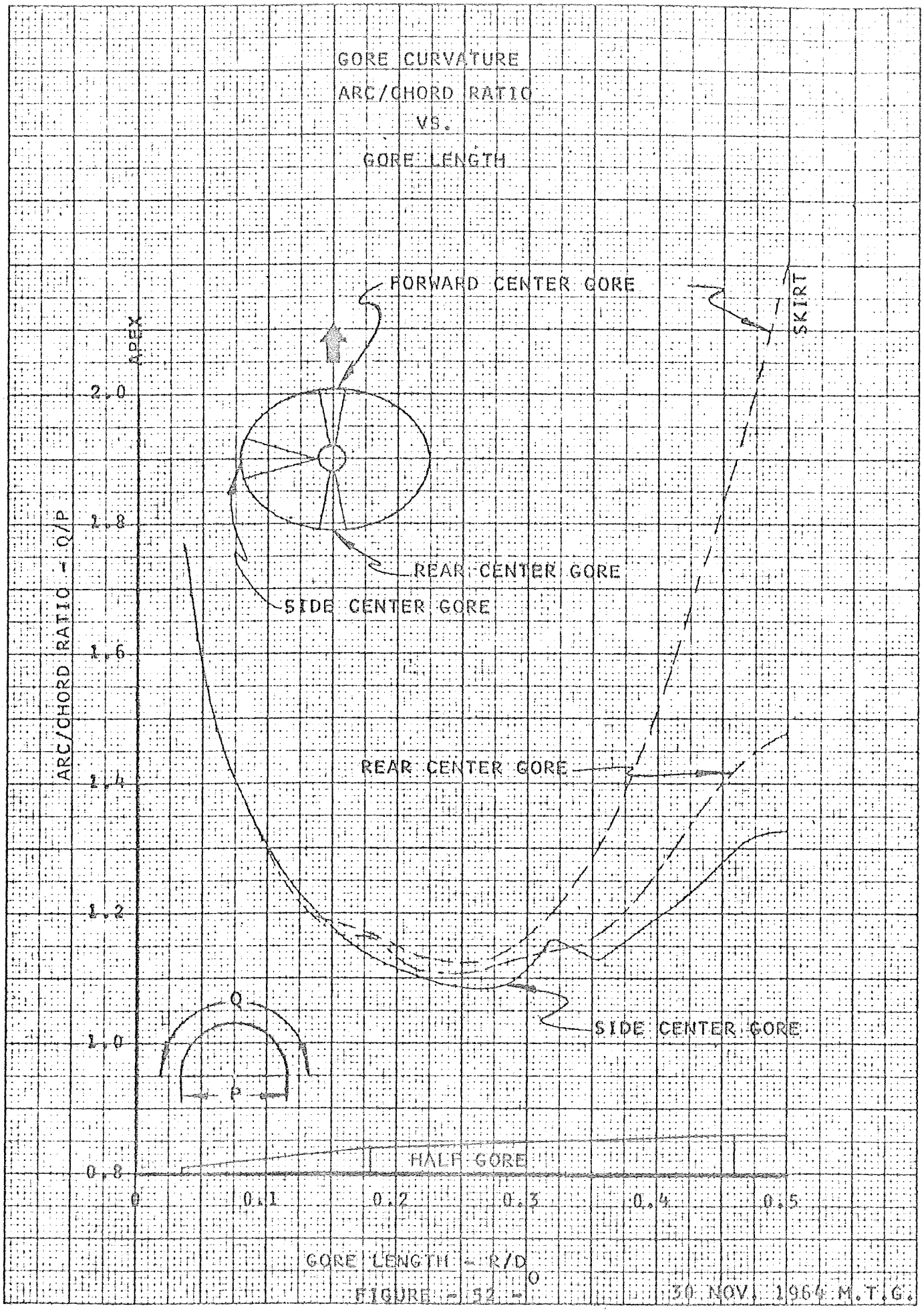
GORE CURVATURE
ARC/CHORD RATIO
VS.
GORE LENGTH
FORWARD CENTER GORE
SKIRT
APEX
REAR CENTER GORE
SIDE CENTER GORE
REAR CENTER GORE
SIDE CENTER GORE
ARC/CHORD RATIO - Q/P
2.0
1.8
1.6
1.4
1.2
1.0
0.8
Q
P
HALF GORE
0
0.1
0.2
0.3
0.4
0.5
GORE LENGTH - R/D
30 NOV. 1964 M.T.G.

FIGURE - 52 -

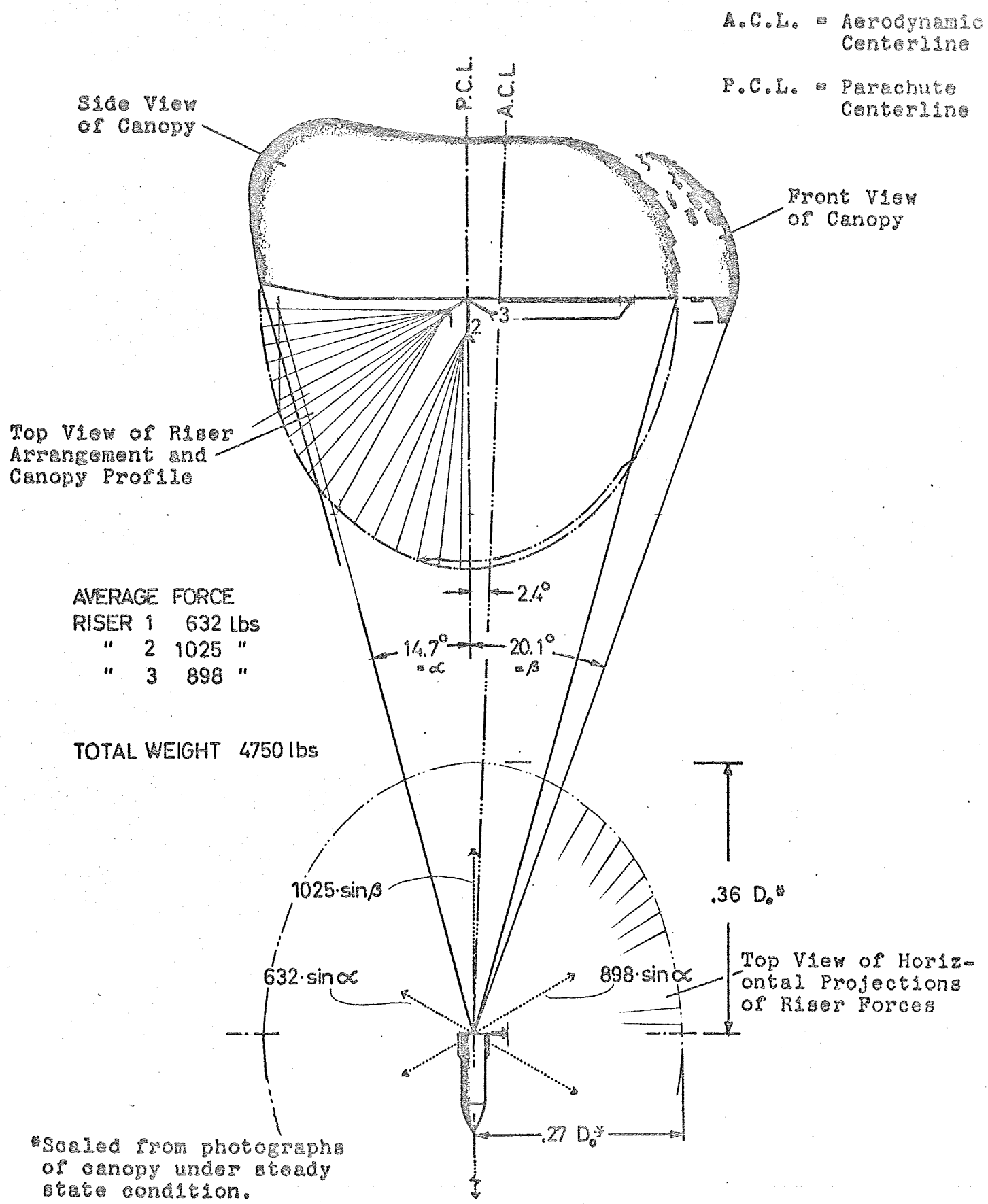

*Scaled from photographs of canopy under steady state condition.

Figure - 53 -
Center of Pressure, Para-Sail 80A-9

W.R.M.
4 Nov. 1964

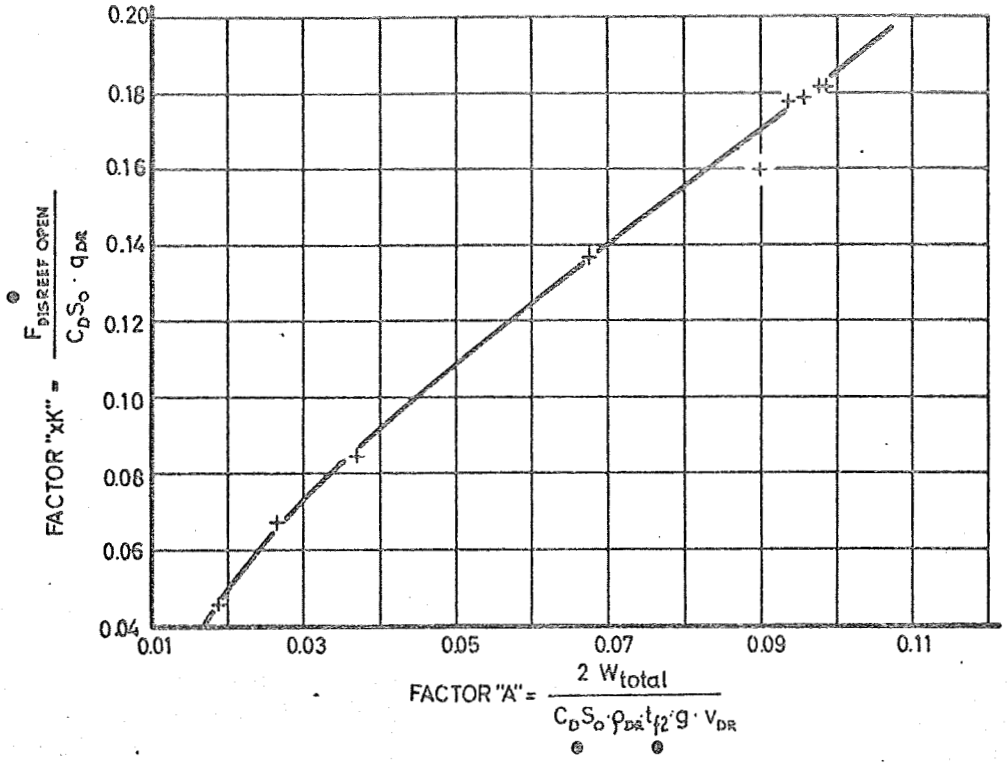

FIGURE - 54 -

DISREEFED OPENING SHOCK FACTOR

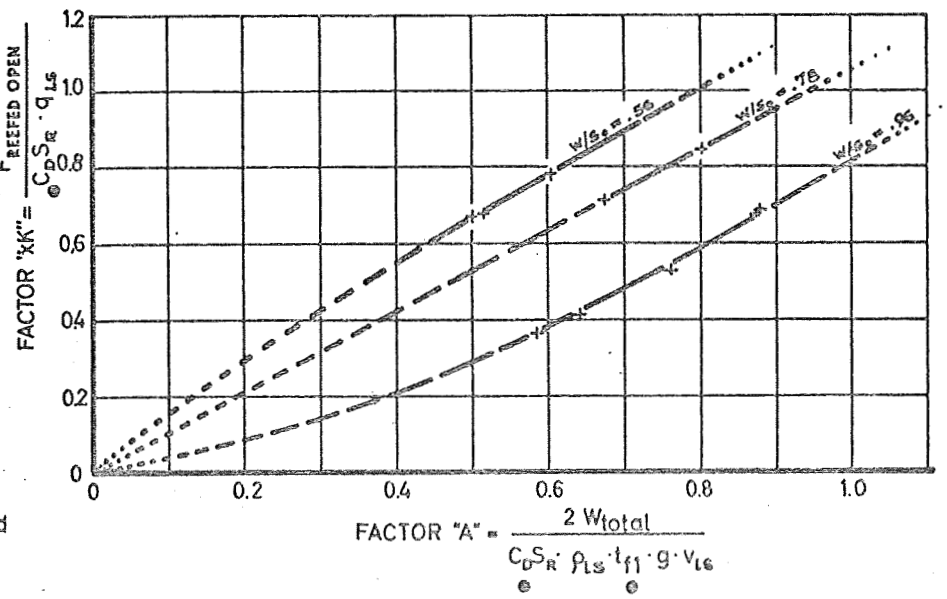

● smoothed values

FIGURE - 55 -

REEFED OPENING SHOCK FACTOR

W.R.M.
25 NOV. 1964

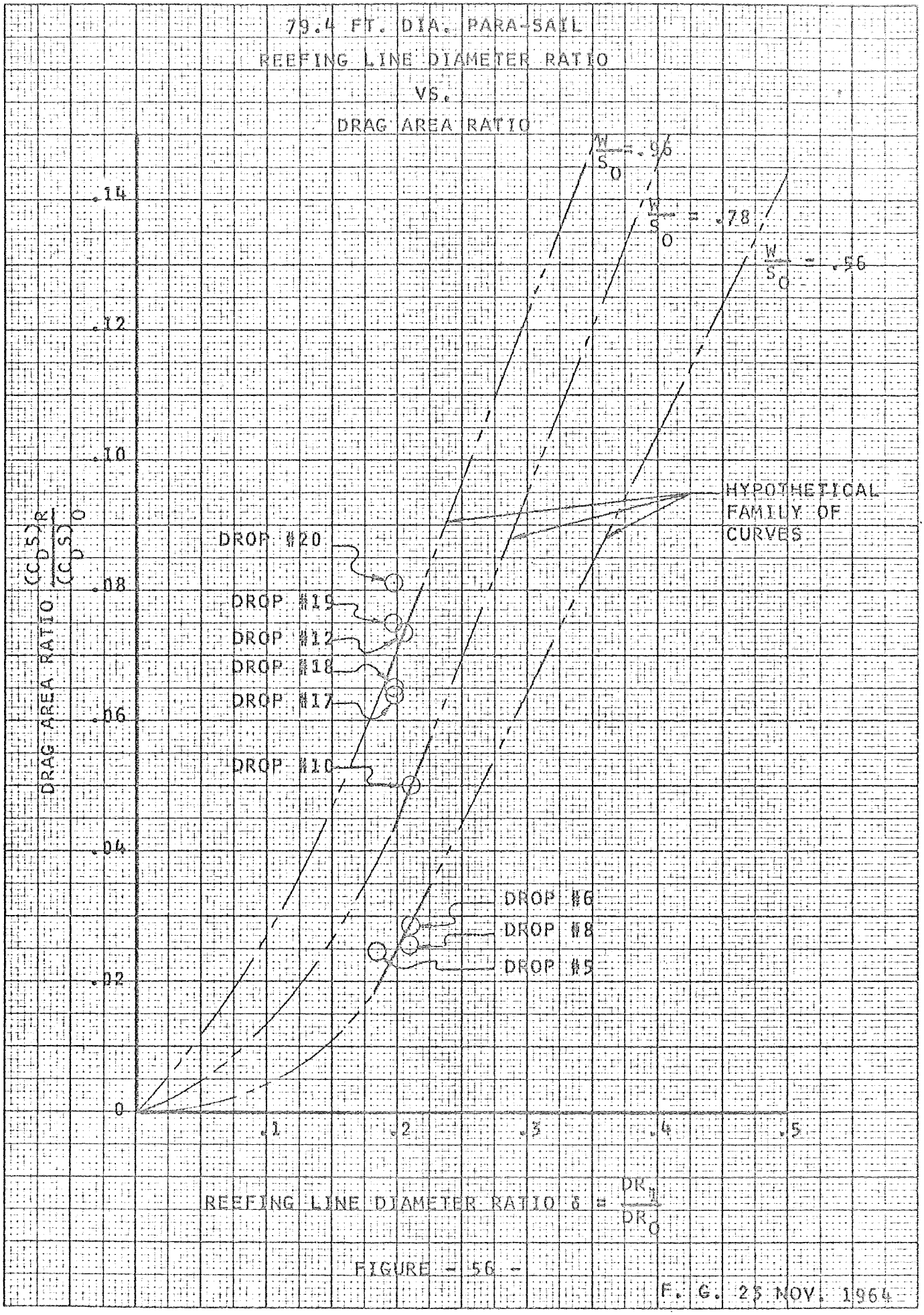

FIGURE - 56 -

F. G. 25 NOV. 1964

6.0 CONCLUSIONS AND RECOMMENDATIONS

All evidence indicates the successful attainment of program goals as shown by the following comparisions:

		Required	Demonstrated
Payload Weight	-	4,750 Pounds	4,750 Pounds
Deployment Speed	-	154 KEAS	154*KEAS
Lift/Drag Ratio	-	1.0	1.13
Canopy Turn Rate	-	10 Deg./Sec.	18.5 Deg./Sec.
Rate of Descent	-	30 FPS Maximum	24 FPS
Deployment Altitude	-	10,600 Feet	10,600 Feet

The lift/drag ratio indicated above, which corresponds to an angle of attack of 48.5 degrees was produced at a canopy loading of .96 lbs./ft.^{2}. Test data shows a slight increase in the angle of attack with decrease in canopy loading.

On the basis of vertical velocity, an effective drag coefficient of 1.47 was established at the above canopy loading.

Peak opening forces were in the order of 15,000 pounds. Damage was encountered under the conditions producing these loads and there is indication of structural weakness in some components.

The efficiency of the canopy regarding drag area per unit weight is comparable to highly efficient conventional canopies although this factor could nc doubt be improved through additional materials and construction studies.

The performance of the full size canopy correlated well with wind tunnel results of models, (Volume I) making these latter studies extremely worthwhile in a development program of this nature.

*Medium damage encountered at this speed.

It is felt that additional aerodynamic studies, both free drop and wind tunnel, should be performed to investigate the following areas:

1. Internal parachute size and placement.
2. Optimum degree of geometric porosity and distribution.
3. Effect of the stabilizers.
4. Optimum line length.
5. Improved lift/drag ratio.
6. Reefing line forces.

A complete study should be made of the available low porosity materials and if necessary development work initiated with a cloth producer or finisher for a suitable fabric. This fabric should have high tensile and tear strength combined with good fabrication efficiency and low weight. More than one weight of cloth may be advisable. Construction methods should be reviewed and strength optimized.

Additional analytical work on canopy stresses would be benificial in future design efforts combined with a study of canopy planform and gore profile. Gore shape should be reviewed with respect to reduction of cloth stresses.

Deployment techniques should be studied to insure maximum reliability and minimum damage.

It should be concluded from this report that very significant advances in the state of development of the Para-Sail parachute took place under this program. A parachute evolved which has shown very high performance, making it most desirable for application in the recovery of manned space craft.

However, it is also evident that additional development work should be initiated to overcome current limitations on deployment speed due to stress problems.

If the recommendations presented herein are initiated through additional efforts, the development of a reliable, high performance gliding decelerator is insured.

REFERENCES

1. National Aeronautics And Space Administration Contract NAS9-1157 and following amendments, January 1963
2. Norman, Leland, C., West, Robert, B., Brown, David, L., Development of the Para-Sail Parachute as a Landing System for Manned Spacecraft, NASA Manned Space Craft Center, Presented to the Symposium on Parachute Technology and Evaluation, El-Centro California, April 1964
3. Norman, Leland, C., Para-Sail Evaluation Phase II Drop Test Program, NASA Program Apollo Working Paper No. 1118, May 1964
4. Heinrich, Helmut, G. and Niccum, Ronald, J., A Method To Reduce Parachute Inflation Time with a Minor Increase of Opening Force, WADD TR 60-761, August 1960
5. Technical Proposal for Para-Sail Evaluation and Development, for NASA Manned Space Craft Center, Houston 1, Texas, RFP Number MSC - 63- 239P, Pioneer Project E-2038, November 1962
6. Watts, James, H., Project Quickie Investigation of Para-Sail Stabilization Panel Reefing Characterists, National Aeronautics and Space Administration, Manned Space Craft Center

7. Weintraub, Phillip, L., Design and Test of a Sled, Sled Extraction System and Sled Recovery System Used With the Gemini Full Scale Boiler Plate Test Vehicle, Presented to the Symposium on Parachute Technology and Evaluation, El-Centro, California, April 1964

8. Coplan, M. J., Bloch, M. G., A Study of Parachute Strength of Nylon and Rayon Cloth Seams, WADC Technical Report 56-313, June 1956

9. Performance of and Design Criteria for Deployable Aerodynamic Decelerators, Technical Report No. A5D-TR-61-579, December 1963

10. Gimalouski, Edward, A., Development of a Final Stage Recovery System for a 10,000 Pound Weight., WADC Technical Report 59-109, December 1958

11. Ewing, E. G., Ring Sail Parachute Characteristics, Radioplane Report No. PTM-323-A, January 1961

12. United States Airforce Parachute Handbook, WADC Technical Report 55-265, December 1956

APPENDIX A

Derivation of Equations

1. Derivation of Effective Drag Area

For many applications it is necessary to determine the vertical descent rate of a parachute, including gliding parachutes such as the Para-Sail. Hence it is desirable to establish through testing, the effective drag area, $C_{D_{eff}} S$ which is normal to the vertical axis of the Para-Sail. Actually, drag area is possibly poor terminology, since the retarding force produced on this surface is the result of both lift and drag forces. The free body diagram of Figure 1 shows the various forces, acting through the center of gravity of the system.

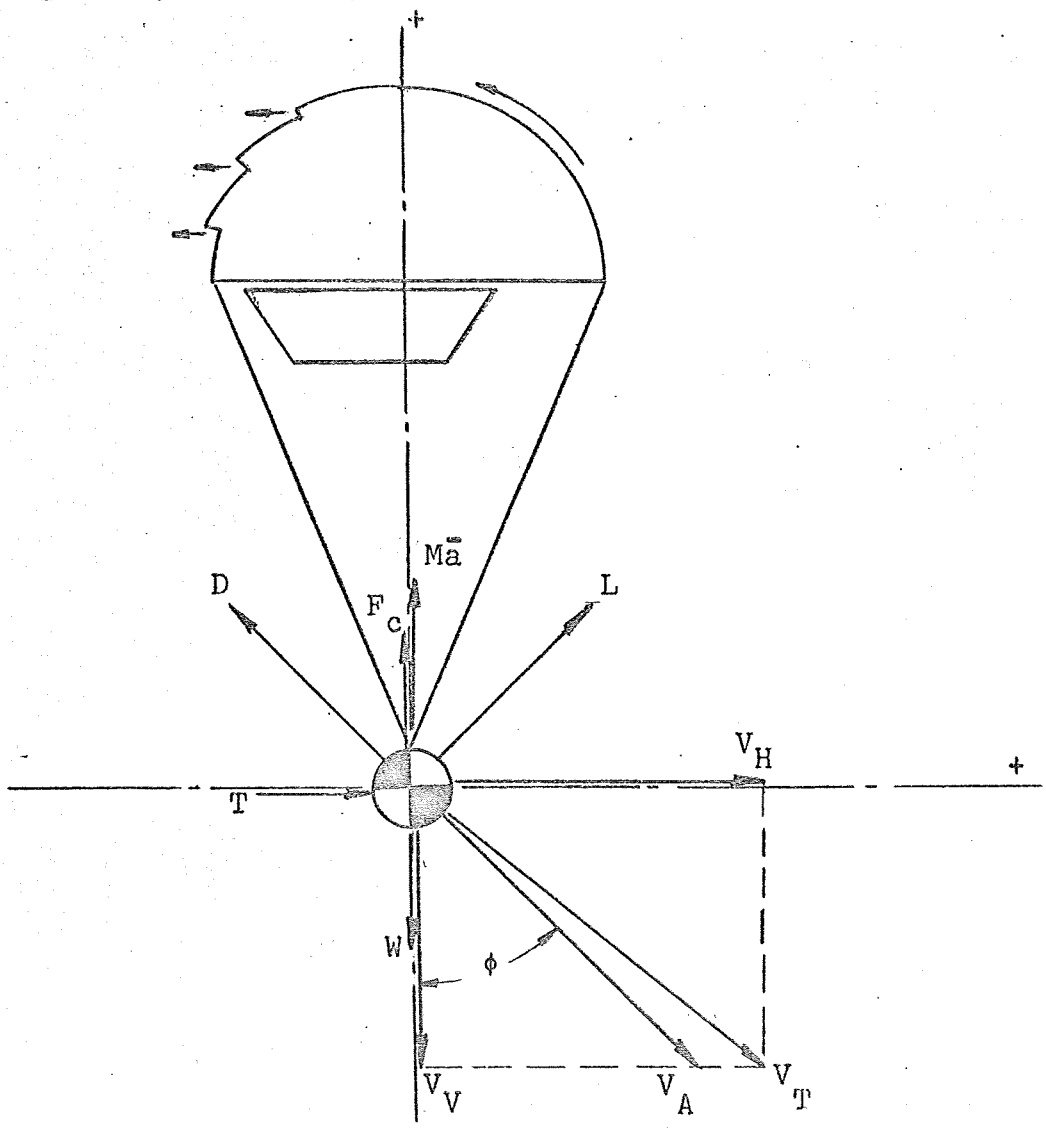

Figure - 1 -

Since the drag area normal to the vertical axis is desired, only vertical components of forces and velocities need be considered.

Assume F_c to be negligible, since the earth radius is large and the velocities are small.

$$\text{Let } R = D \cos \phi + L \sin \phi = \frac{C_{D_{eff}} S \rho V_V^2}{2} \tag{1}$$

Summing forces in the vertical direction we obtain:

$$(R) + (-W) + \left(\frac{-W}{-g} \frac{dV_V}{dt}\right) = 0 \tag{2}$$

or:

$$C_{D_{eff}} \frac{S \rho V_V^2}{2} - W + \frac{W}{g} \frac{dV_V}{dt} = 0 \tag{3}$$

Solving equation 3 for $C_{D_{eff}} S$:

$$C_{D_{eff}} S = \frac{2W}{\rho V_V^2} \left(1 - \frac{dV_V}{g dt}\right), \tag{4}$$

when $\frac{dV_V}{dt}$ is in the positive direction.

The sign will become positive for $\frac{dV_V}{dt}$ in the negative direction.

In the terminology of the Test Agency, V_V = rate of climb = $\frac{dh}{dt}$.

$$\text{Hence, } C_{D_{eff}} S = \frac{2W}{\rho \left(\frac{dh}{dt}\right)^2} \left[1 - \frac{1}{g} \left(\frac{d^2h}{dt^2}\right)\right] \tag{5}$$

2. Simplified Method for Determination of Average Effective Drag Area (Based on Density)

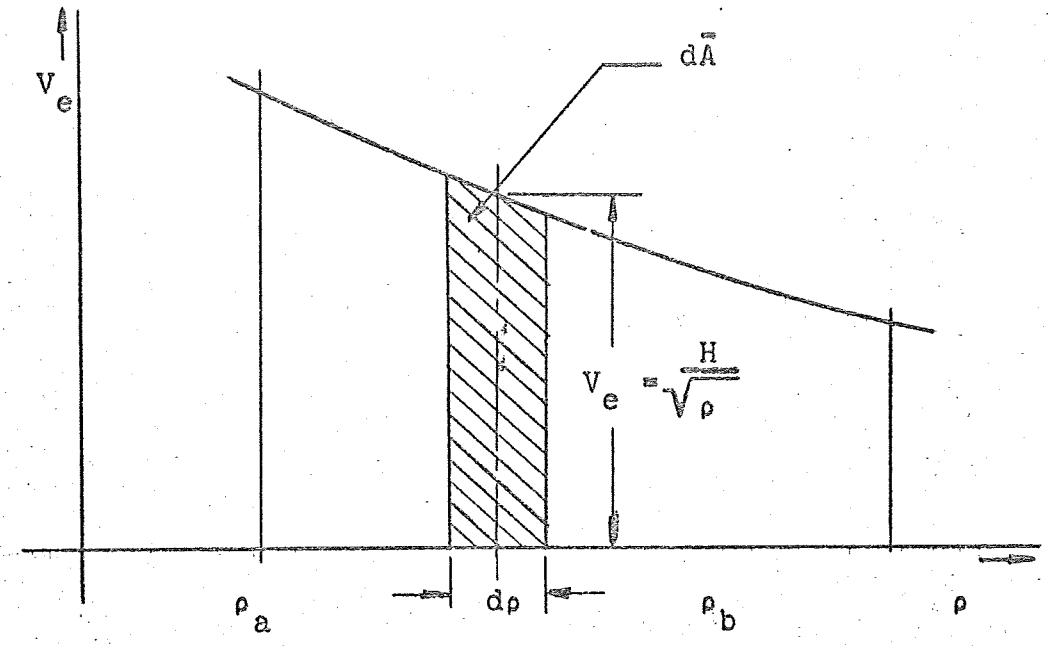

Figure - 2 -

Assumptions: Density is a continuous linear function of altitude over the interval examined.

It is known that the instantaneous equilibrium velocity,

$$V_e = \sqrt{\frac{2W}{(C_{D_{eff}} S)\rho}} = \frac{H}{\sqrt{\rho}} \tag{6}$$

$$\text{where } H = \sqrt{\frac{2W}{C_{D_{eff}} S}} \tag{7}$$

If the area under the curve from a to b can be calculated, it would be possible to determine $\overline{V_e}$, the average velocity, by dividing this area by the interval length.

It can be seen from Figure 2 that the incremental area,

$$d\bar{A} = \frac{H}{\sqrt{\rho}}\, d\rho \tag{8}$$

Integrating over the interval,

$$\int d\bar{A} = \bar{A} = H \int_a^b \frac{d\rho}{\rho^{\frac{1}{2}}} = 2H \left[\rho_b^{\frac{1}{2}} - \rho_a^{\frac{1}{2}}\right] \tag{9}$$

then,

$$\overline{V_e} = \frac{\bar{A}}{(\rho_b - \rho_a)} = 2H \left[\frac{\rho_b^{\frac{1}{2}} - \rho_a^{\frac{1}{2}}}{\rho_b - \rho_a} \right] \tag{10}$$

It is also known that

$$\overline{V_e} = \frac{h_a - h_b}{t_b - t_a} = \frac{\Delta h}{\Delta t} \tag{11}$$

Equating (10) and (11), drag area may be solved for as follows:

$$C_D S = \left(\frac{\Delta t}{\Delta h}\right)^2 \cdot 8W \left[\frac{\sqrt{\rho_b} - \sqrt{\rho_a}}{\rho_b - \rho_a} \right]^2 \tag{12}$$

Limitations: Because density does not truly vary linearly with altitude, certain inaccuracies may be introduced if the interval chosen is too great. Experimental evidence in drop tests of from 40,000 feet to sea level has shown good agreement with calculated values for V_e in equation (10). For greater altitudes more accurate methods are advised.

APPENDIX B

Materials Investigations

SCOTT MODEL J-3

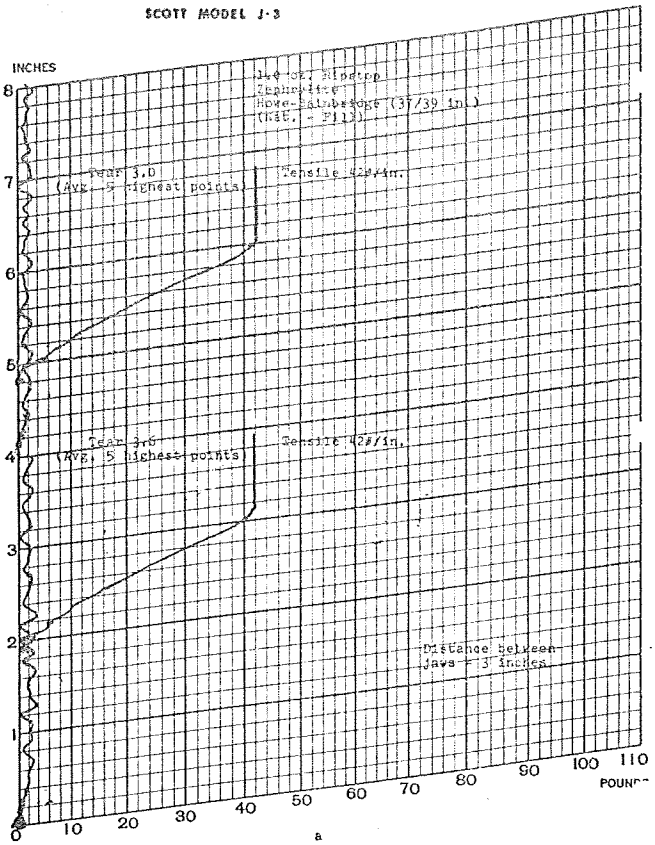

a

SCOTT MODEL J-3

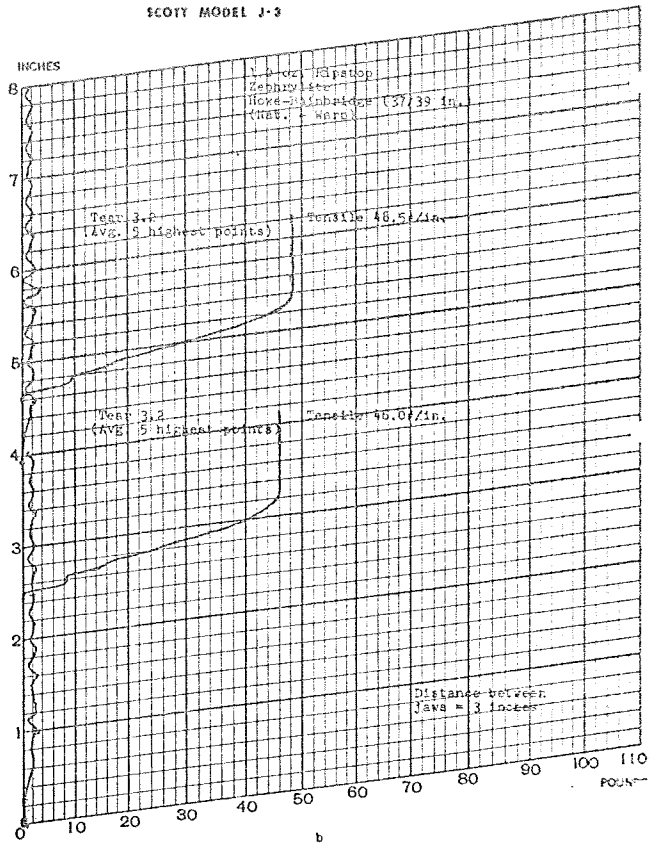

b

SCOTT MODEL J-3

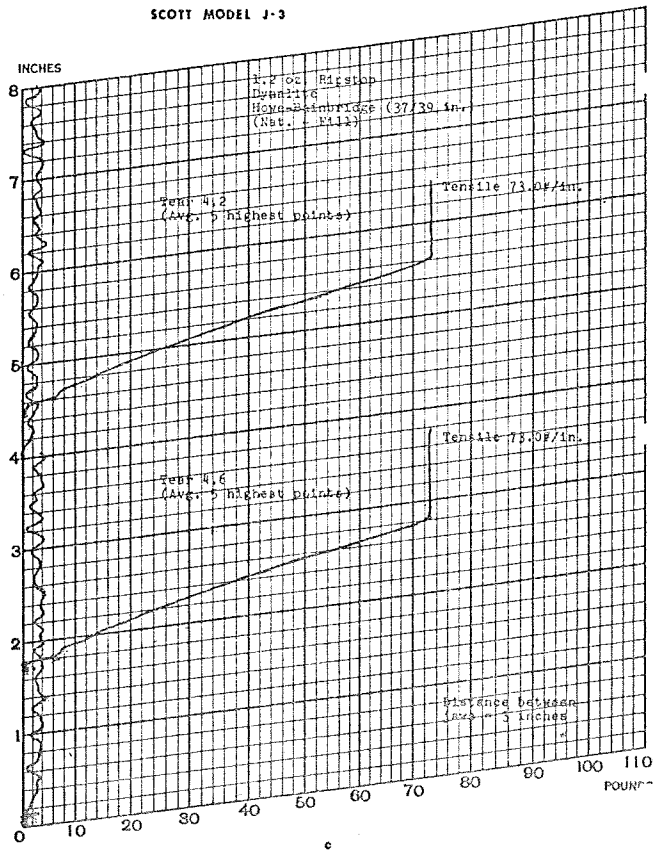

c

SCOTT MODEL J-3

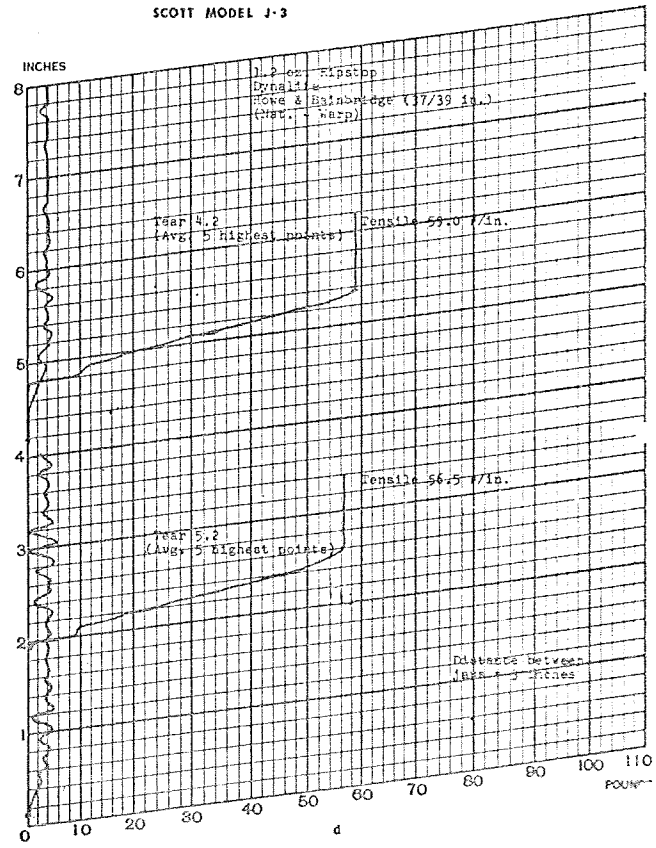

d

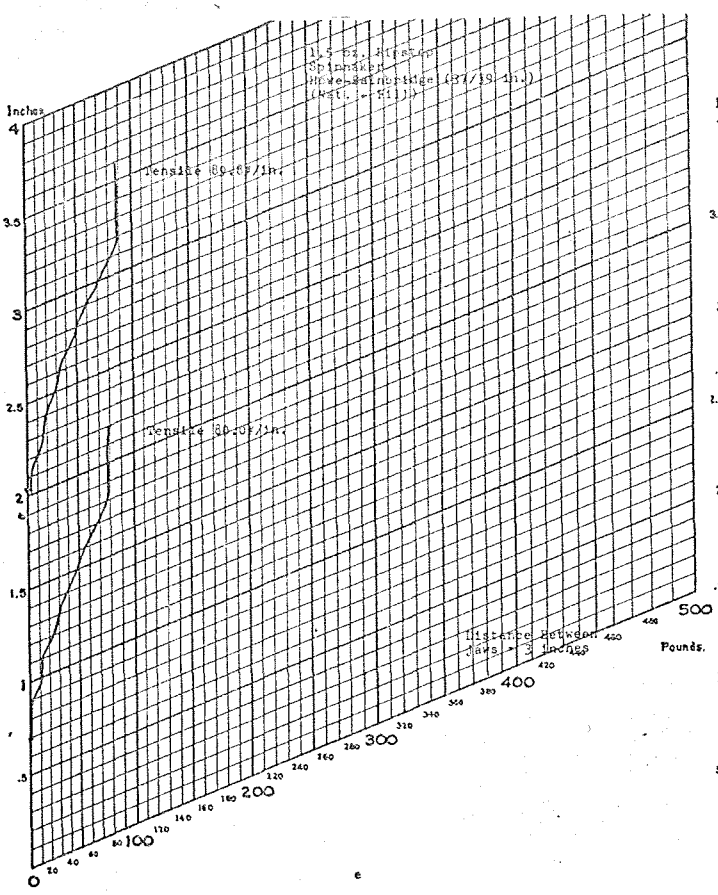

e

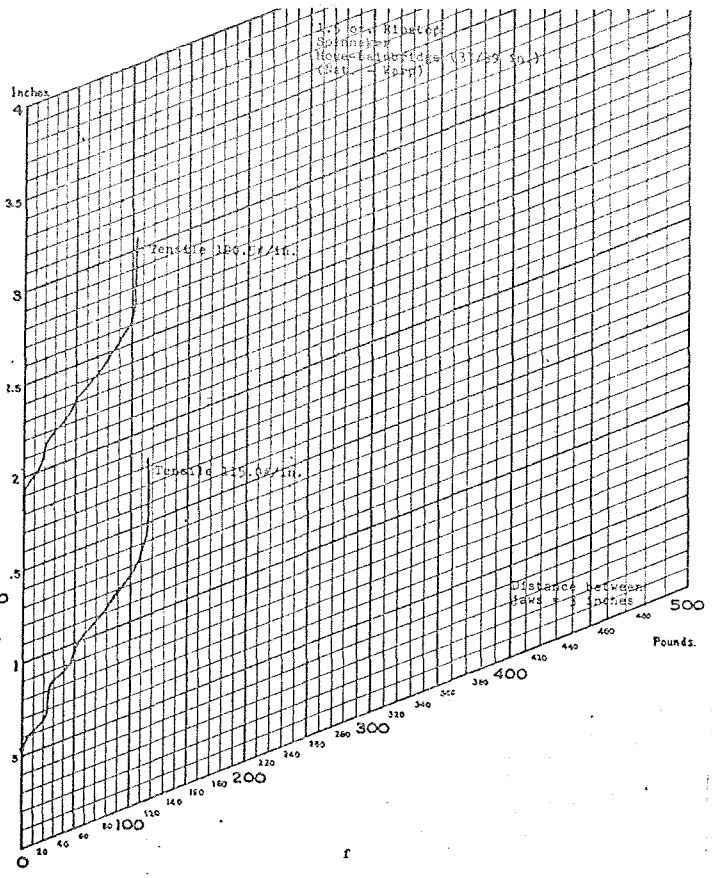

f

SCOTT MODEL J-3

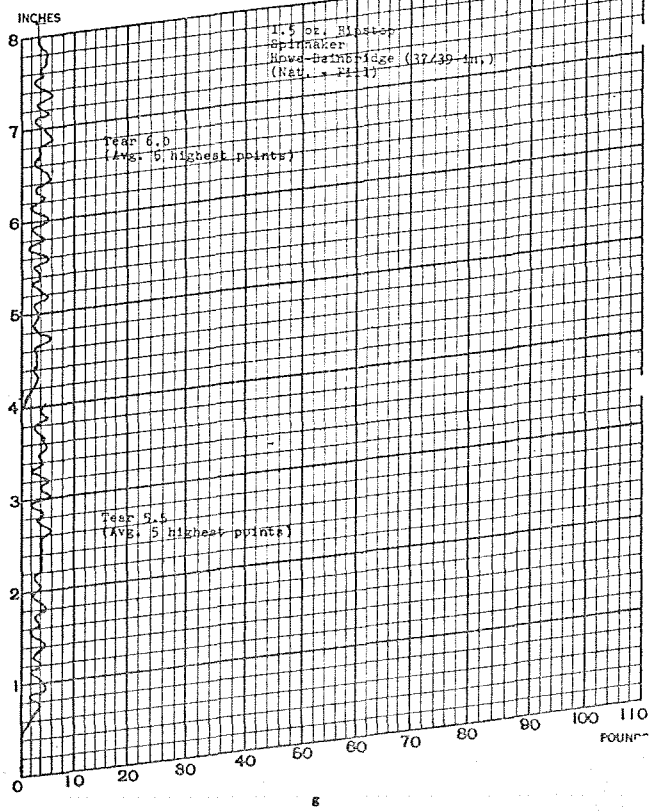

g

SCOTT MODEL J-3

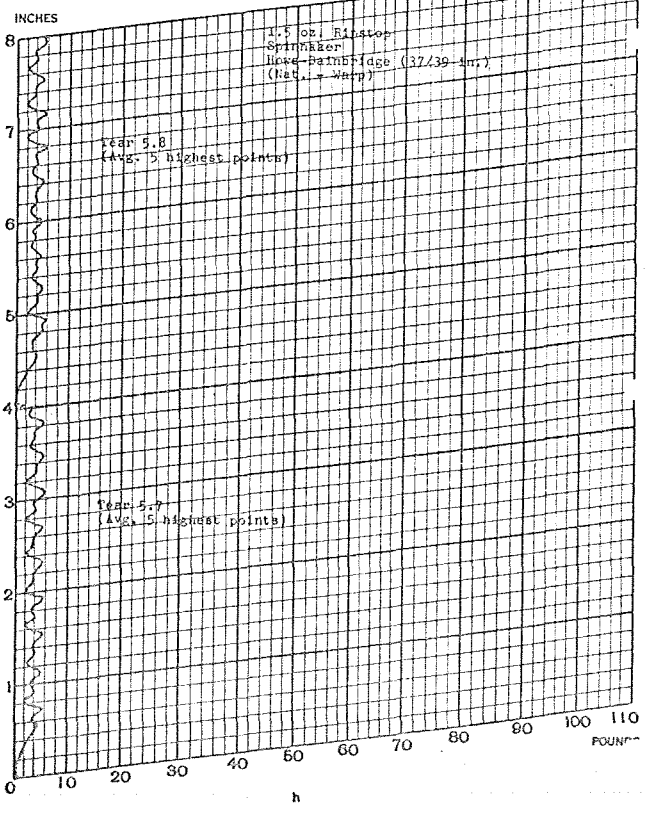

h

SCOTT MODEL J-3

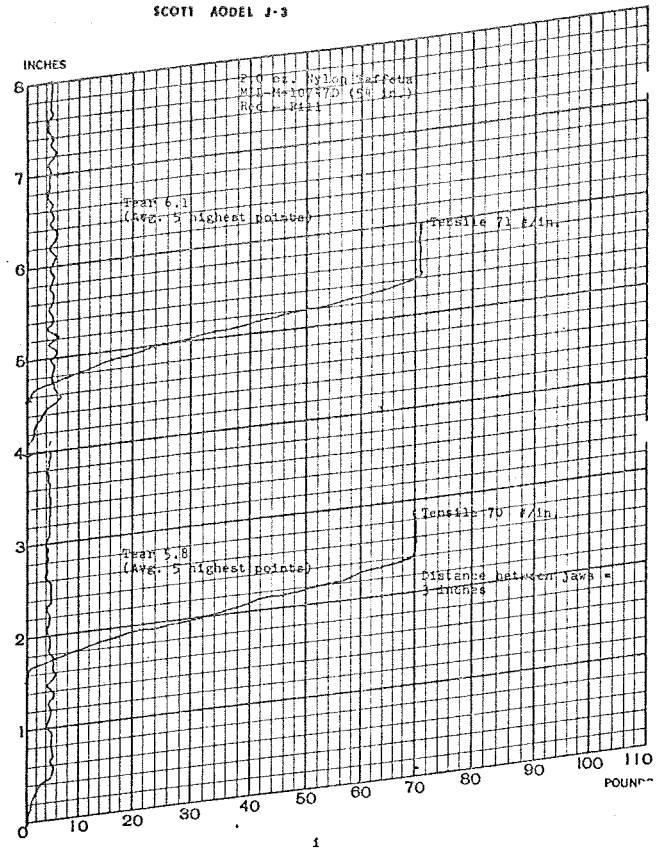

i

SCOTT MODEL J-3

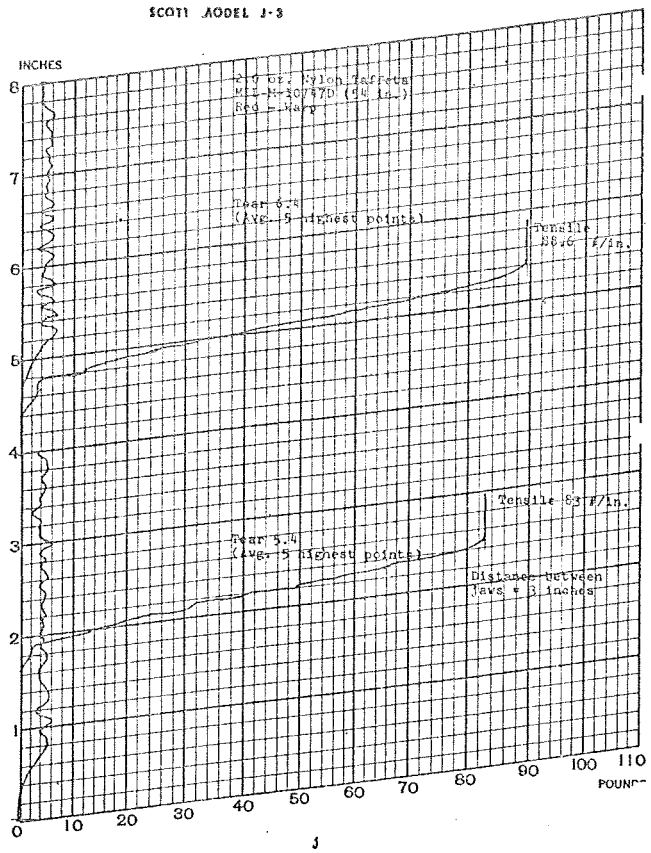

j

SCOTT MODEL J-3

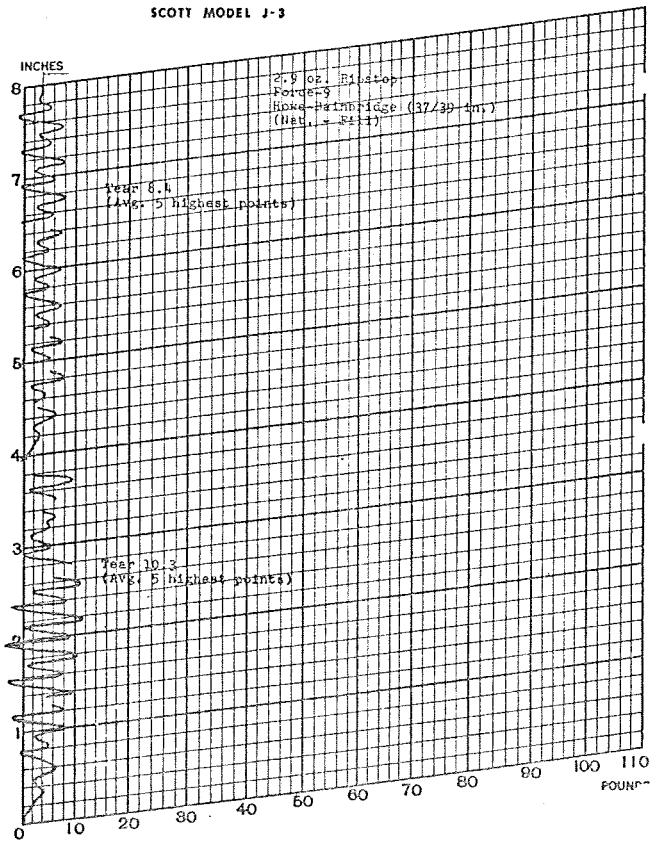

k

SCOTT MODEL J-3

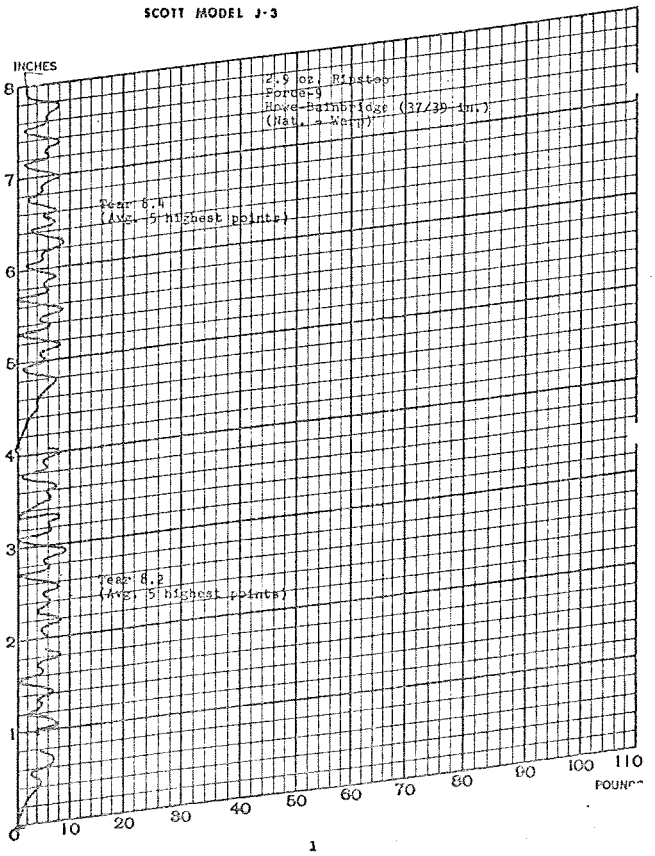

l

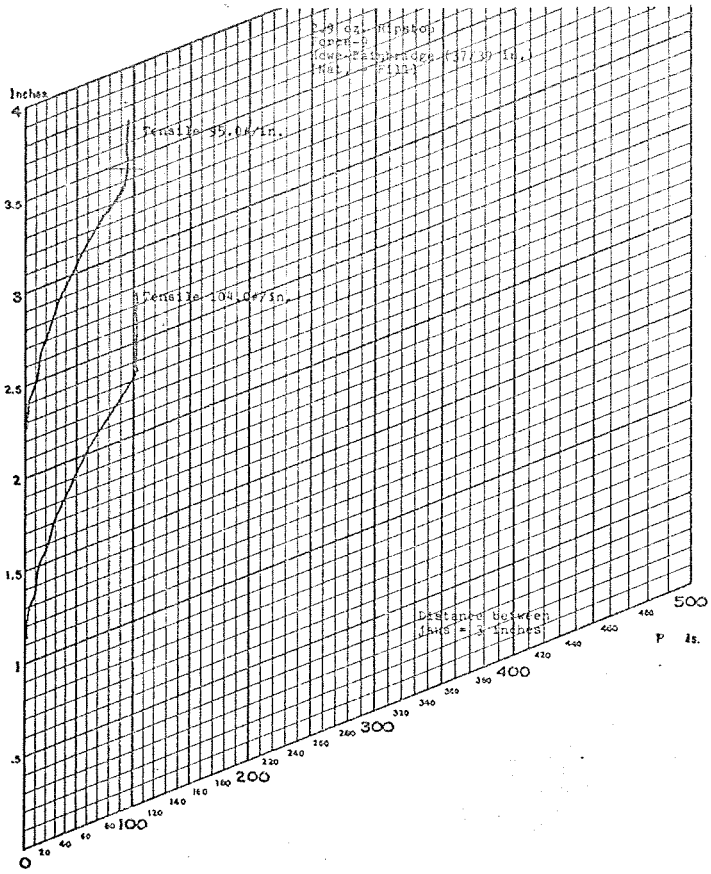
Inches
Tensile 35.0#/in.
Tensile 104.0#/in.
Distance between jaws = 3 inches
Pounds.

m

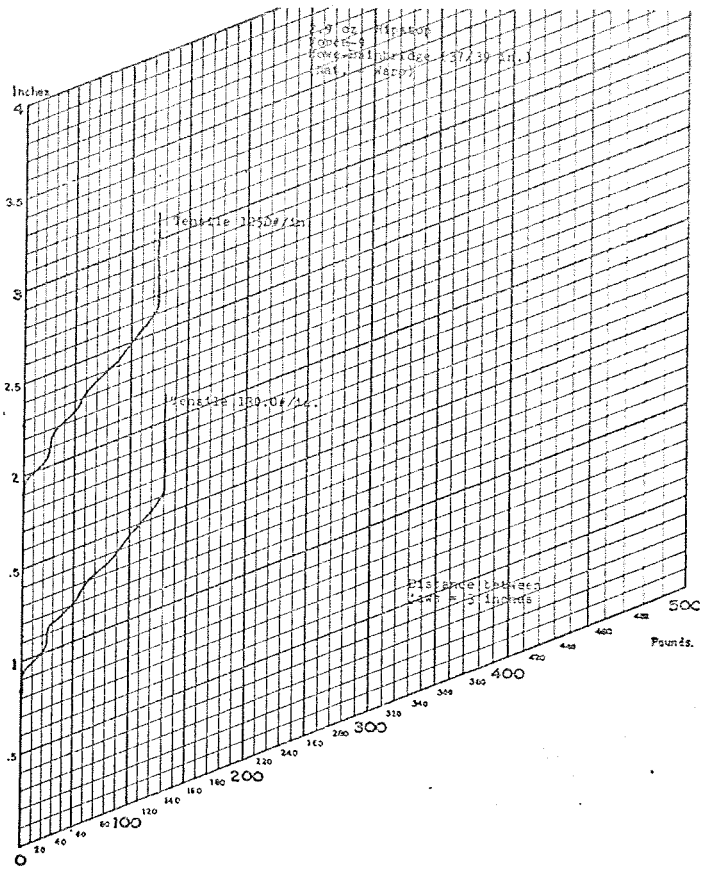
Inches
Tensile 135.0#/in
Tensile 180.0#/in.
Distance between jaws = 3 inches
Pounds.

n

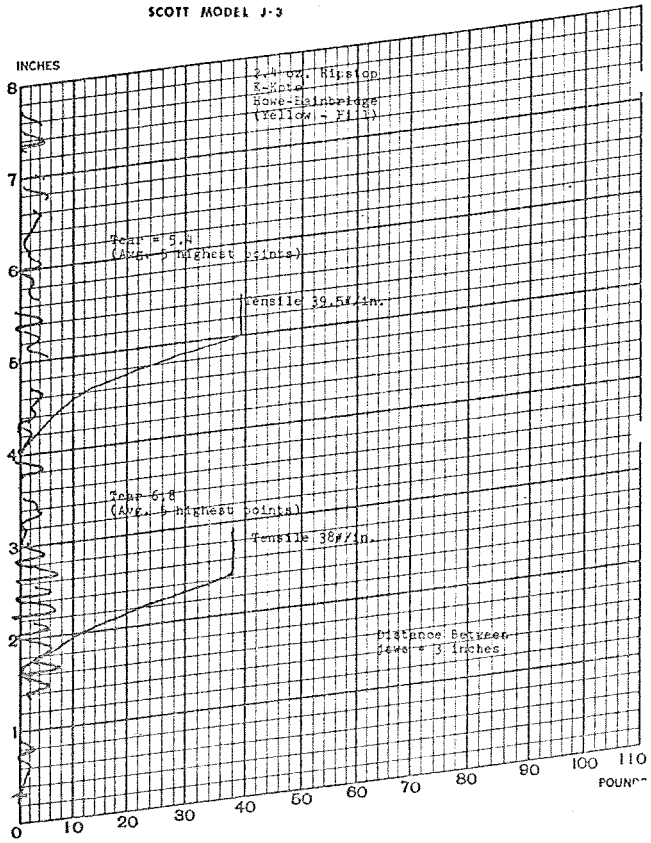
SCOTT MODEL J-3
INCHES
2.4 oz. Ripstop
K-Kote
Rowe-Rainbridge
(Yellow - Fill)
Tear = 5.4
(Avg. 5 highest points)
Tensile 39.5#/in.
Tear 6.8
(Avg. 5 highest points)
Tensile 38#/in.
Distance Between
Jaws = 3 Inches
POUNDS

o

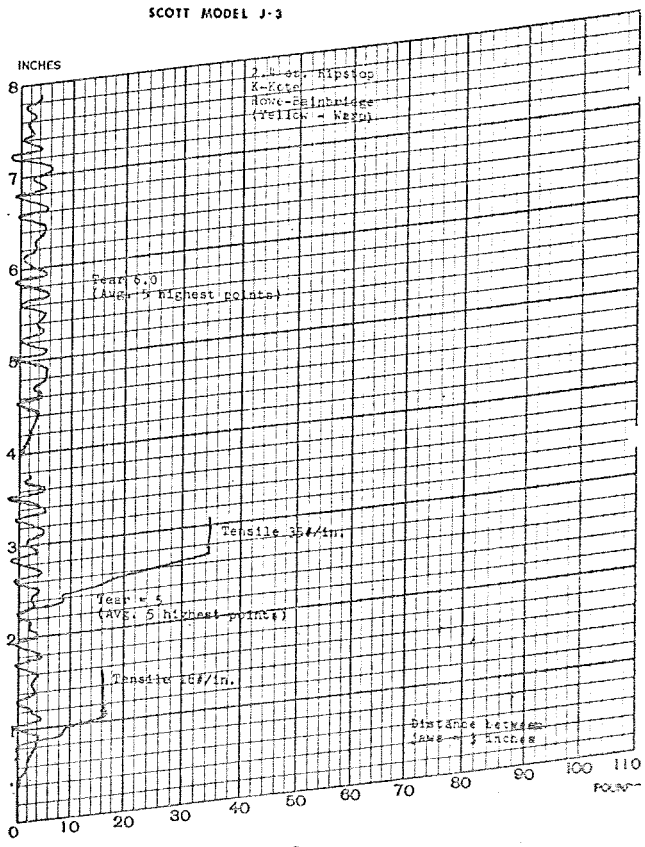
SCOTT MODEL J-3
INCHES
2.4 oz. Ripstop
K-Kote
Rowe-Rainbridge
(Yellow - Warp)
Tear 6.0
(Avg. 5 highest points)
Tensile 35#/in.
Tear = 5
(AVG. 5 highest points)
Tensile 16#/in.
Distance between
Jaws = 3 Inches
POUNDS

p

APPENDIX C

Static Test Results

TITLE: Connector Link Riser

PURPOSE: Three connector link risers were tested to destruction to determine the ultimate load that the riser and link could withstand before failure occurred, and at what point the failure took place.

METHOD: The tests were conducted using a Tinius Olsen Tension Testing Machine, the jaw separation speed was set at 4 inches per minute. The construction of the sample and the link used may be seen below.

RESULTS:

Specimen No.	Breaking Strength Lbs.	Remarks
1	9400	Link failed
2	9800	Link failed
3	9500	Link failed
	Avg. 9566	

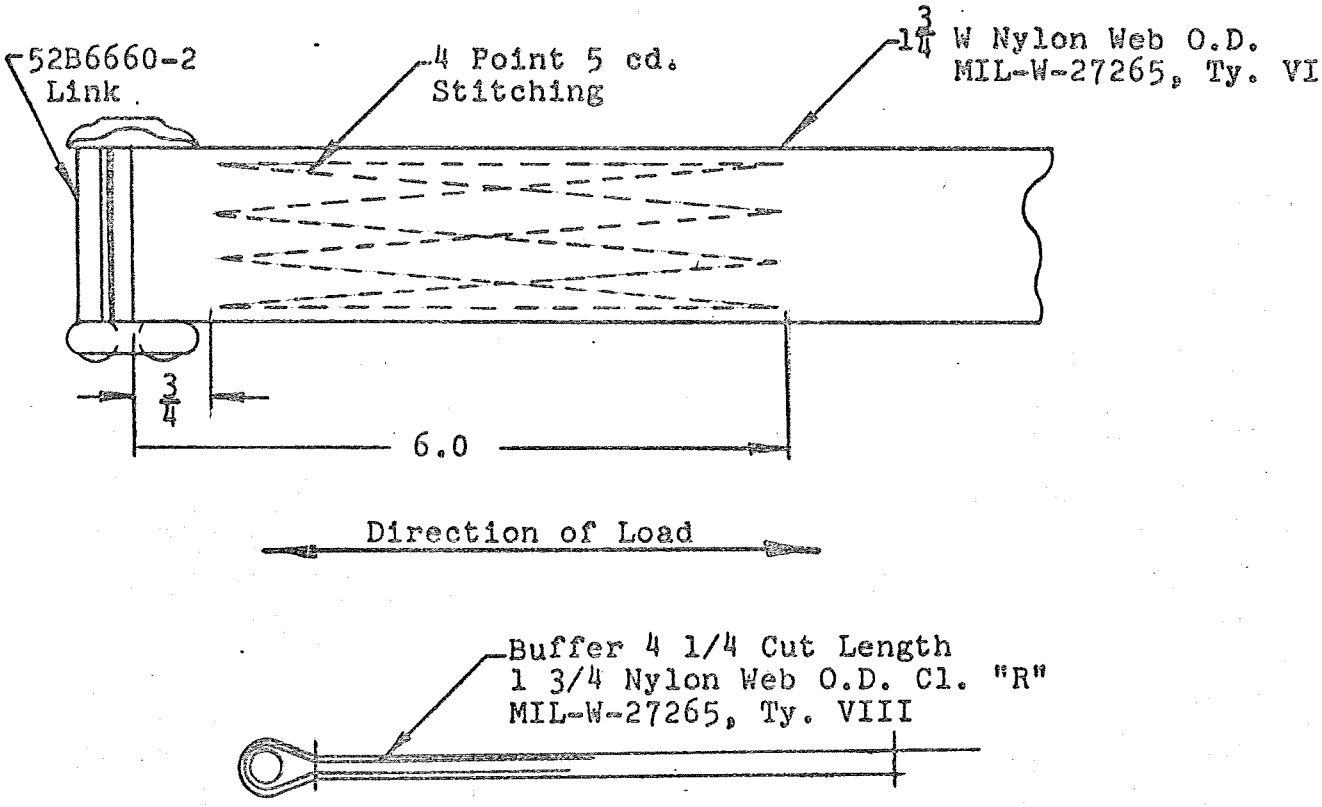

FIGURE - 1 -

J.S. Mansi
10 November 1964

TITLE: Suspension Line Attachment to Connector Link 750 lb.

PURPOSE: Three suspension lines were tested to destruction to determine the ultimate load that the lines could withstand before failure occurred. The tests were conducted using 750 lb. nylon cord.

METHOD: The tests were conducted using a Scott Cord Testing Machine with a jaw separation speed of 13 1/2 inches per minute. The construction of the samples and the method of test are shown below.

RESULTS:

Test No.	Breaking Strength Lbs.
1	760
2	744
3	758
Avg.	754

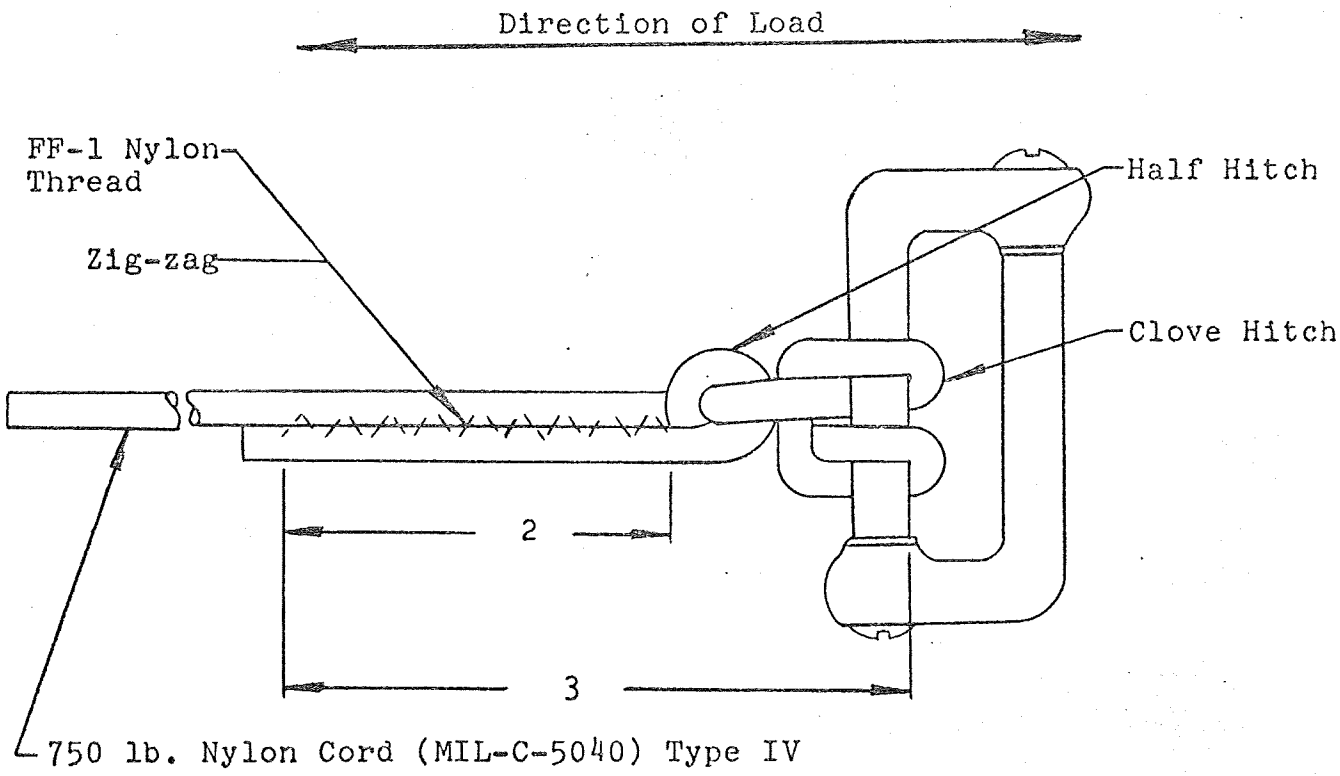

FIGURE - 2 -

J.S. Mansi
10 November 1964

TITLE: Suspension Line Attachment Connector Link 550 lb.

PURPOSE: Three suspension lines were tested to destruction to determine the ultimate load that the lines could withstand before failure occurred. The tests were conducted using 550 lb. nylon cord.

METHOD: The tests were conducted using a Scott Cord Testing Machine with a jaw separation speed of 13 1/2 inches per minute. The construction of the samples and the method used are shown below.

RESULTS:

Test No.	Breaking Strength Lbs.
1	598
2	590
3	560
Avg.	582.6

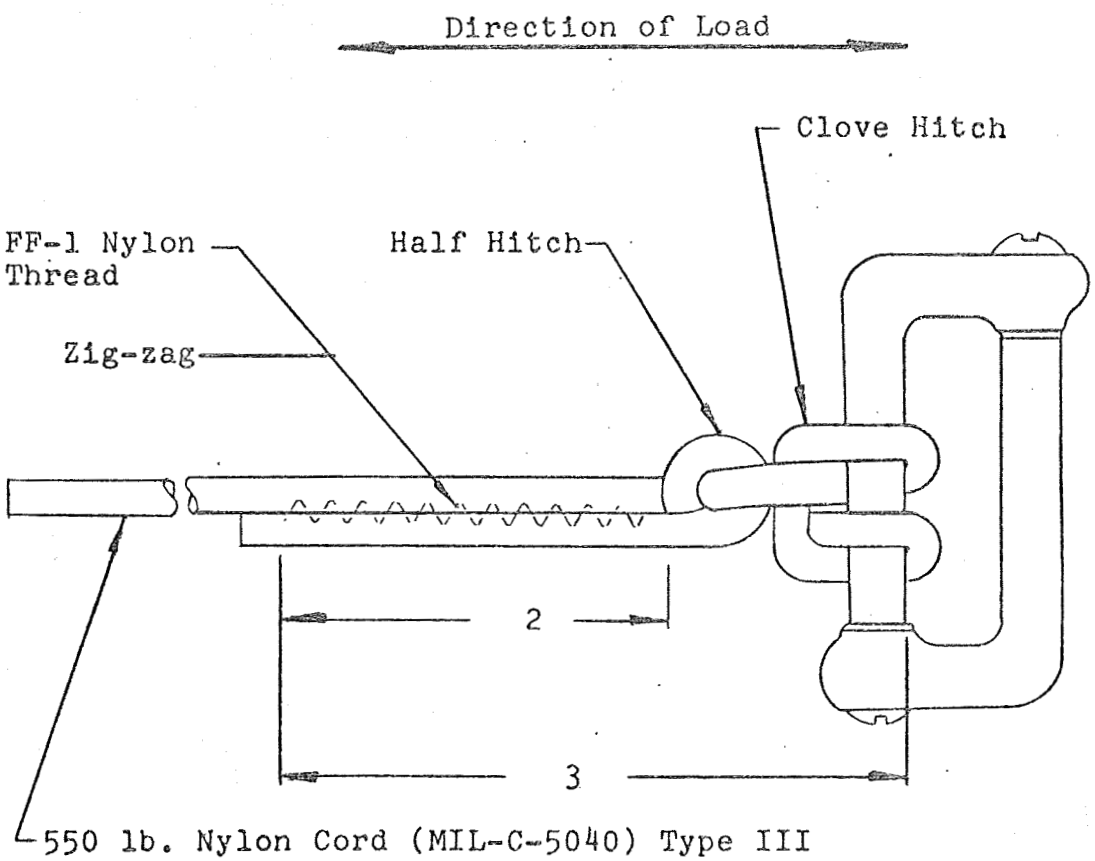

FIGURE - 3 -

J.S. Mansi
10 November 1964

TITLE: Suspension Line Attachment to Skirt 550 lb.

PURPOSE: Three test specimens were tested to destruction to determine the ultimate load that may be applied to the suspension line attachment before failure occurred, and at what point the failure took place.

METHOD: All tests were conducted using a Scott Cord Testing Machine with a jaw separation speed of 13 1/2 inches per minute. The construction of the sample may be seen below.

RESULTS:

Specimen No.	Breaking Strength Lbs.	Comments
1	500	Line failed above jaw
2	468	Main seam failed above line attachment
3	498	Main seam failed above line attachment
	Avg. 489	

CONTROL SAMPLES: Nylon Cord, MIL-C-5040, Ty. III, 550 lbs. t.s.
Average Breaking Strength = 568 lbs.

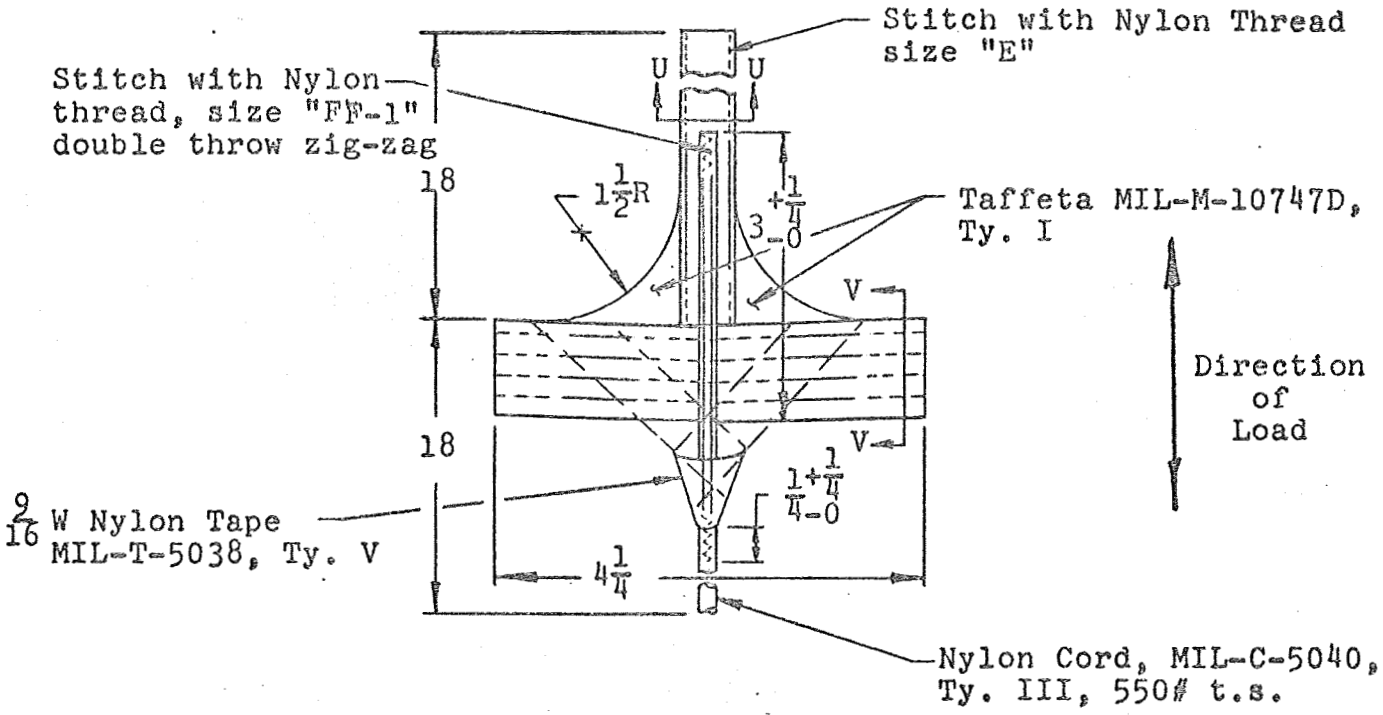

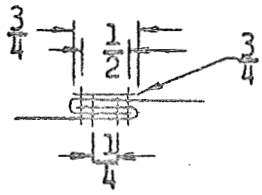

SECTION U-U

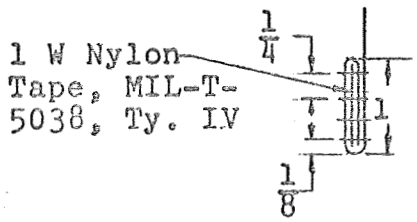

SECTION V-V

FIGURE - 4 -

J.S. Mansi
10 November 1964

TITLE: Stabilizer Panel Attachment with Skirt

PURPOSE: Three test specimens were tested to destruction to determine the ultimate load that the panel could withstand before failure occurred, and at what point the failure took place.

METHOD: The tests were conducted using a Scott Cord Testing Machine with a jaw separation speed of 13 1/2 inches per minute. The Construction of the sample may be seen below.

RESULTS:

Test No.	Breaking Strength Lbs.
1	510
2	500
3	522
Avg.	510

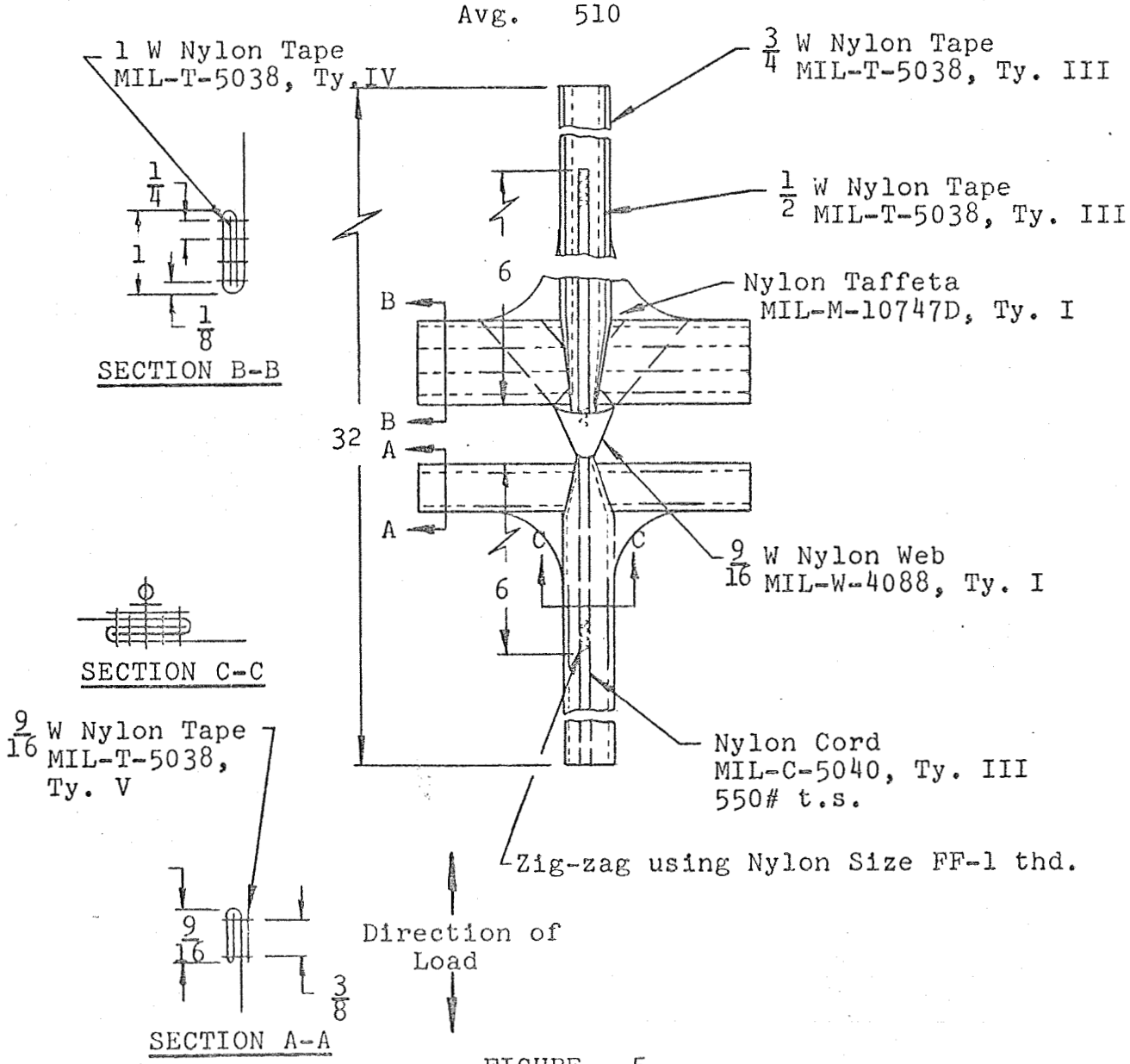

FIGURE - 5 -

J.S. Mansi
11 November 1964

TITLE: Skirt Band Joint

PURPOSE: Three skirt band joints were tested to destruction to determine the ultimate load the joint could withstand before failure occurred.

METHOD: The tests were conducted using a Tinius Olsen Tension Testing Machine with a jaw separation speed of four (4) inches per minute.

RESULTS:

Specimen No.	Breaking Strength Lbs.
1	1260
2	1200
3	1280
Avg.	1246.7

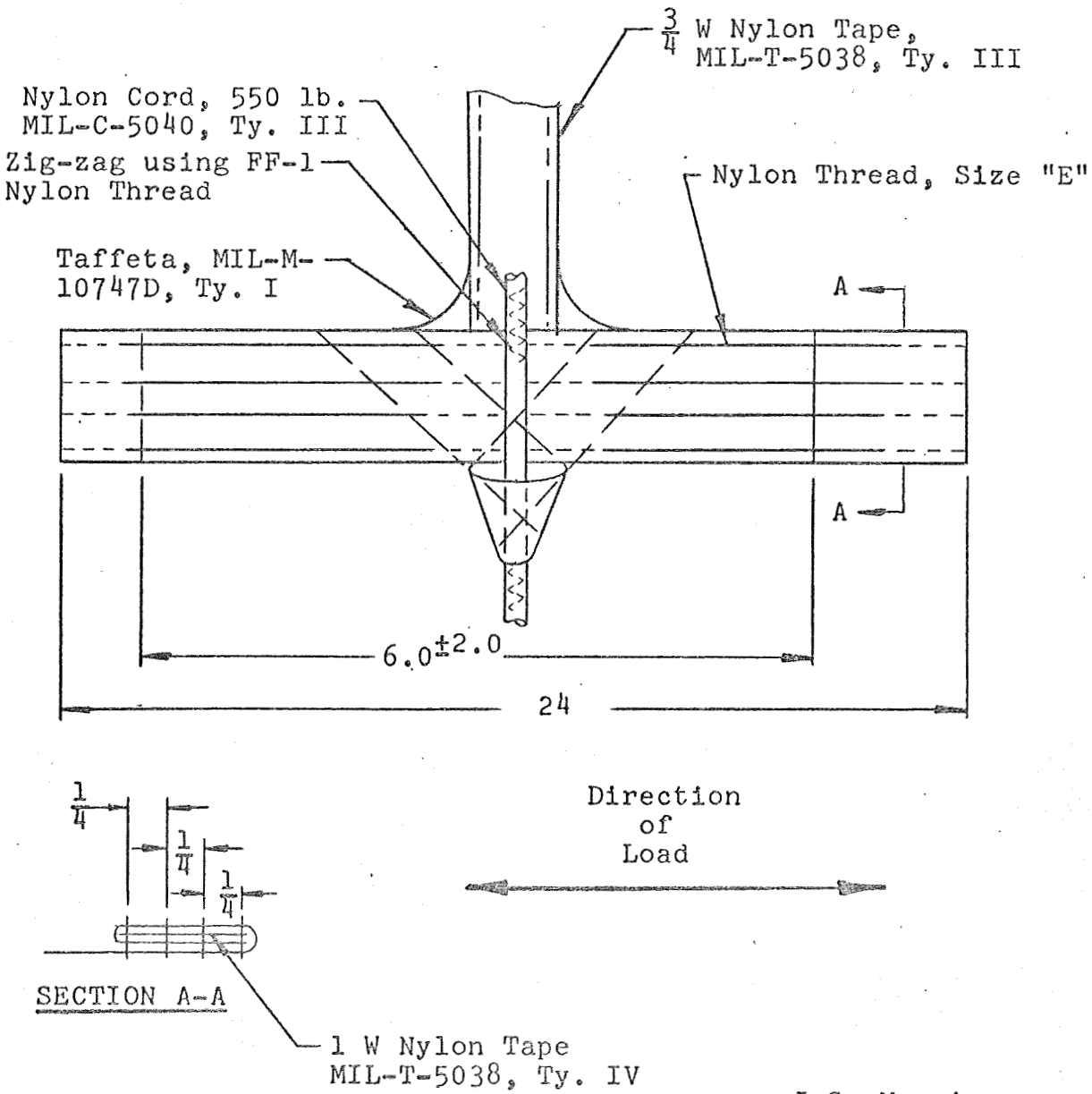

FIGURE - 6 -

J.S. Mansi
10 November 1964

Test No. 7

TITLE: Suspension Line Attachment to Skirt 750 lb.

PURPOSE: Three test specimens were tested to destruction to determine the ultimate load that may be applied to the suspension line attachment before failure occurred, and at what point the failure took place.

METHOD: All tests were conducted using a Scott Cord Testing Machine with a jaw separation speed of 13 1/2 inches per minute. The construction of the sample may be seen below.

RESULTS:

Specimen No.	Breaking Strength Lbs.	Comments
1	640	Lines failed at zig-zag sewing below V-tab.
2	595	
3	630	
	Avg. 621.7	

CONTROL SAMPLE: Nylon cord, MIL-C-5040, Ty. IV, 750 lbs. t.s.
Average breaking strength = 730 lbs.

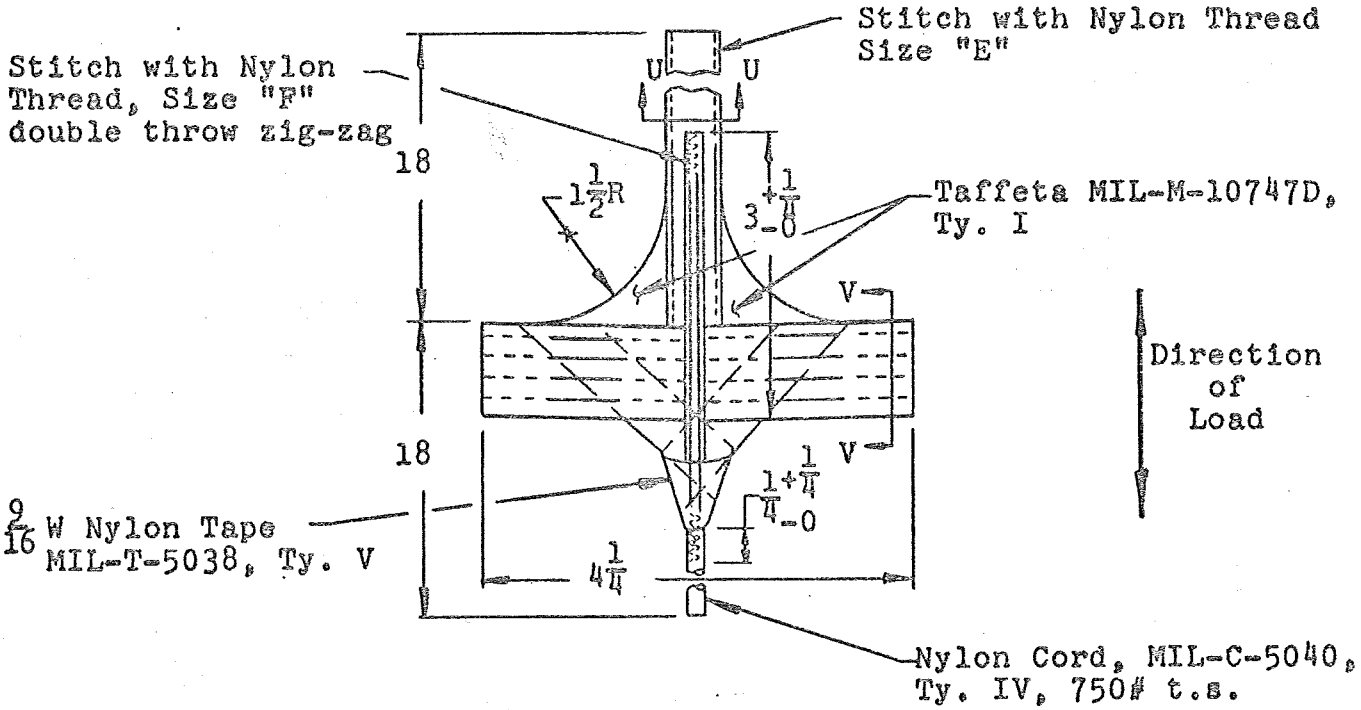

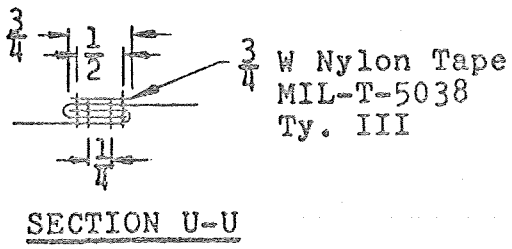

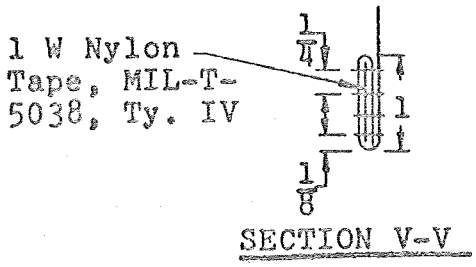

FIGURE - 7 -

J.S. Mansi
10 November 1964

TITLE: Radial Seam at Turn Scoop Edge

PURPOSE: Three test specimens were tested to destruction to determine the ultimate load that may be applied to the seam before failure occurred.

METHOD: The tests were conducted using a Scott Cord Testing Machine with a jaw separation speed of 13 1/2 inches per minute. The construction of the sample may be seen below.

RESULTS:

Test No.	Breaking Strength Lbs.
1	626
2	620
3	620
Avg.	622

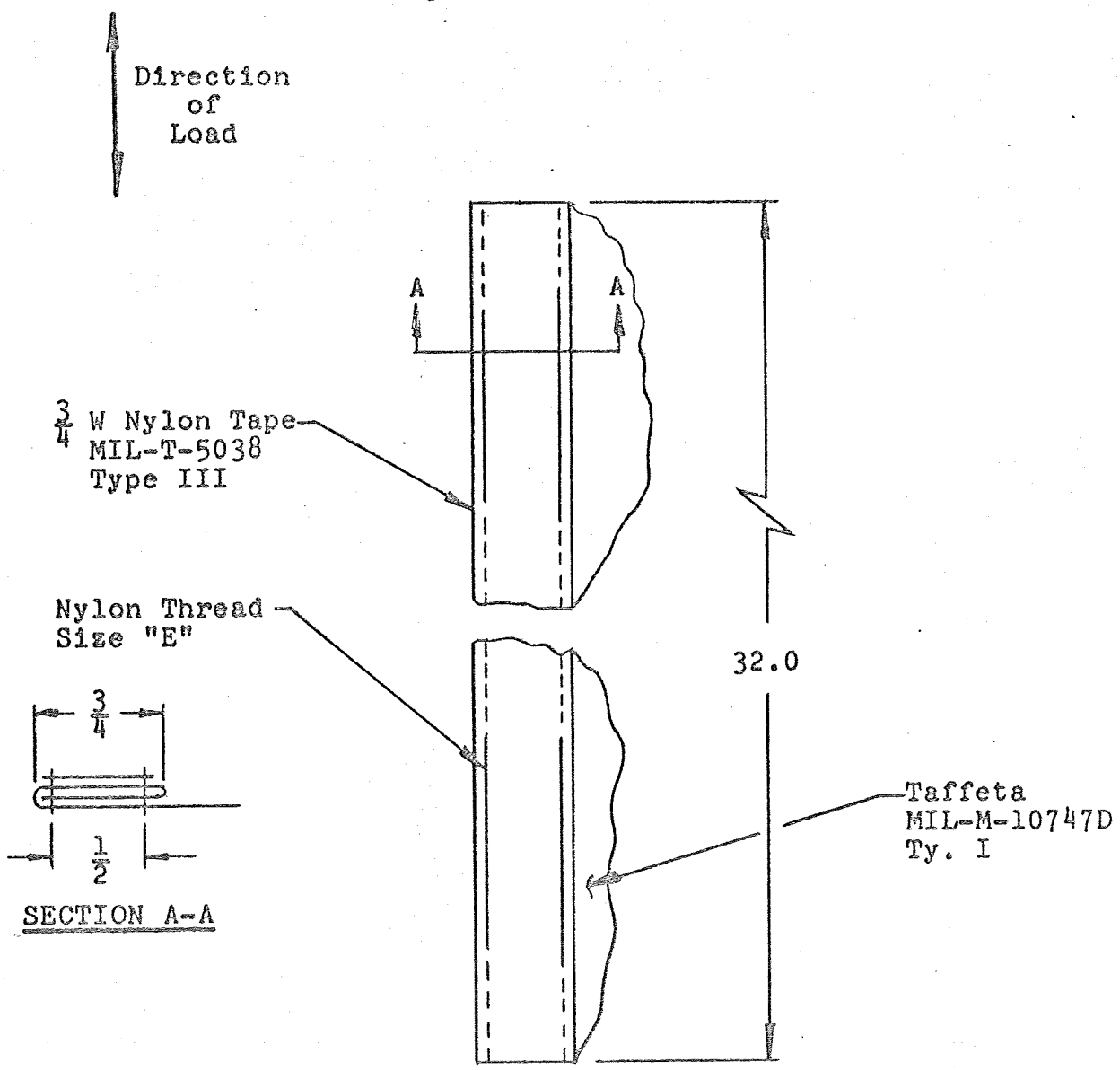

FIGURE - 8 -

J.S. Mansi
10 November 1964

TITLE: Reefing Ring Attachment

PURPOSE: Three reefing ring attachment samples were tested to destruction to determine the ultimate load that they may withstand before failure occurred.

METHOD: The tests were conducted using a Tinius Olsen Tension Testing Machine, with a jaw separation speed of four (4) inches per minute. The construction of the samples may be seen below.

RESULTS:

Test No.	Breaking Strength Lbs.
1	820
2	840
3	820
Avg.	826.6

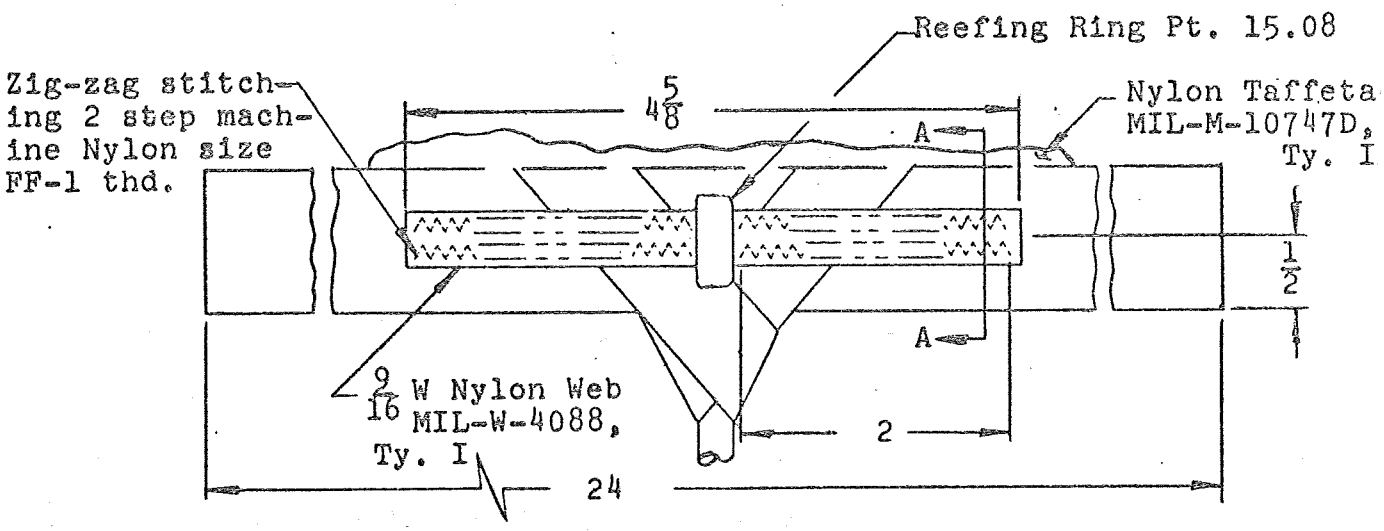

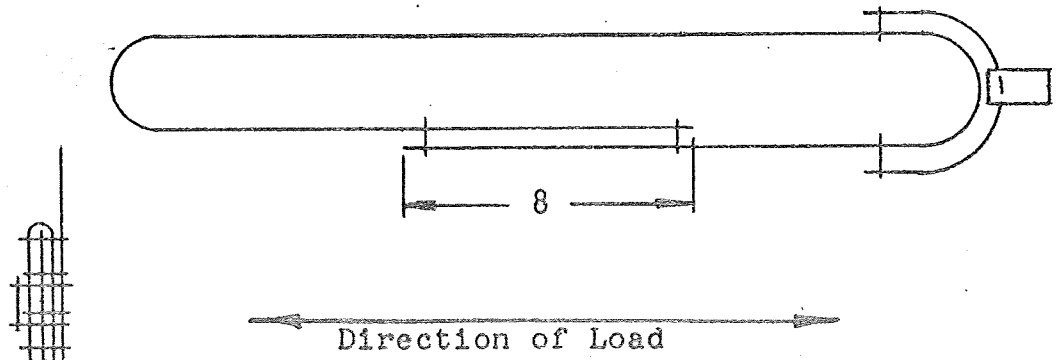

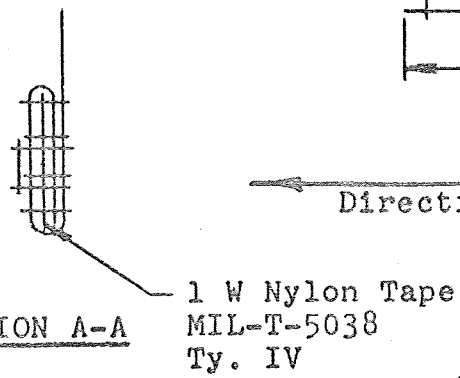

SECTION A-A

J.S. Mansi
10 November 1964

FIGURE - 9 -

TITLE: Radial Seam Single Ply

PURPOSE: Three test specimens were tested to destruction to determine the ultimate load that may be applied to the seam before failure occurred.

METHOD: The tests were conducted using a Scott Cord Testing Machine with a jaw separation speed of 13 1/2 inches per minute. The construction of the sample may be seen below.

RESULTS:

Test No.	Breaking Strength Lbs.
1	730
2	706
3	730
Avg.	722

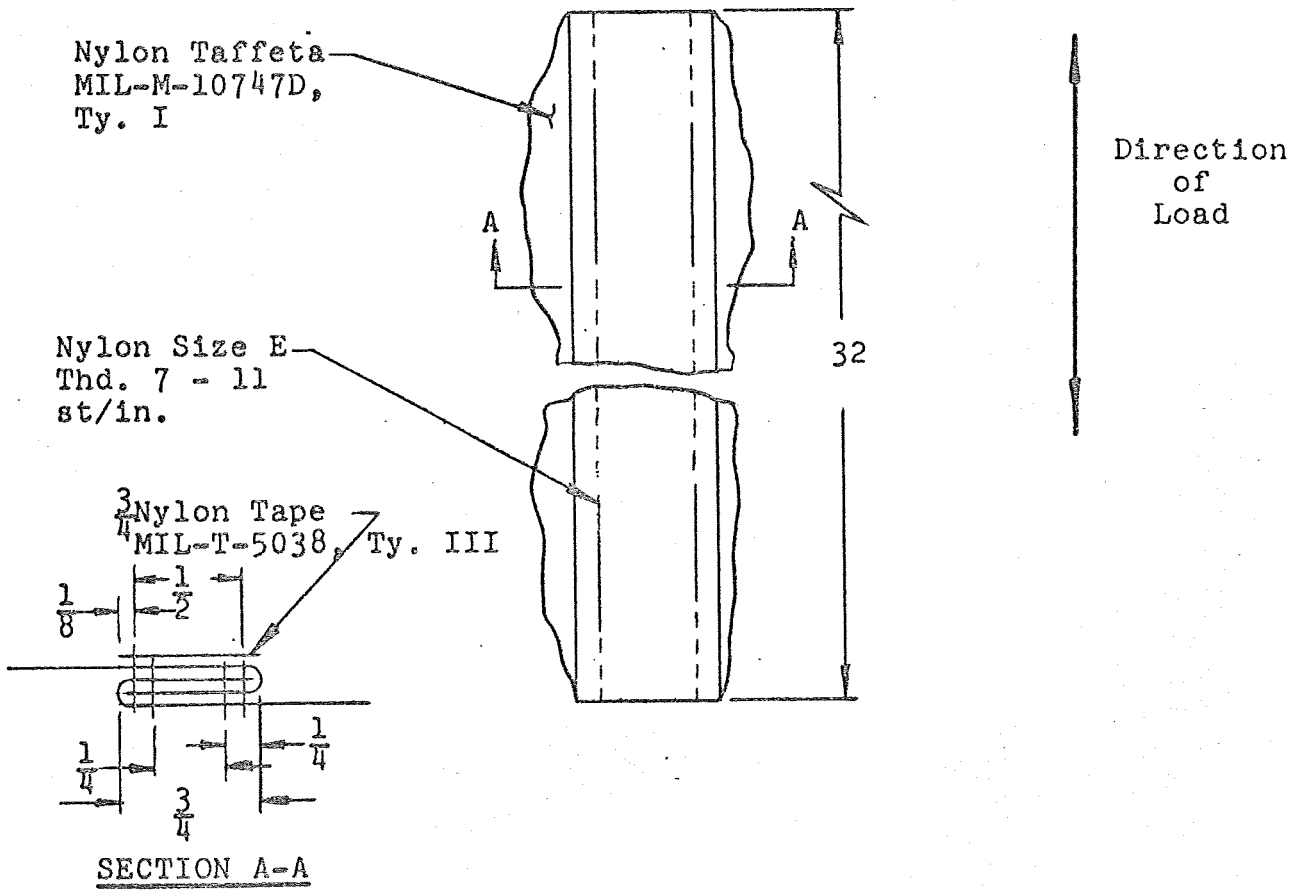

FIGURE - 10 -

J.S. Mansi
10 November 1964

TITLE: Main Seam Longitudinal

PURPOSE: This report covers the longitudinal main seams for gores 1 - 11 and 62 - 72. These samples were tested to destruction to determine the ultimate load the seam could withstand before failure occurred.

METHOD: The tests were conducted using a Scott Cord Testing Machine with a jaw separation speed of 13 1/2 inches per minute. The construction of the sample may be seen below.

RESULTS:

Test No.	Breaking Strength Lbs.
1	960
2	984
3	970
Avg.	971

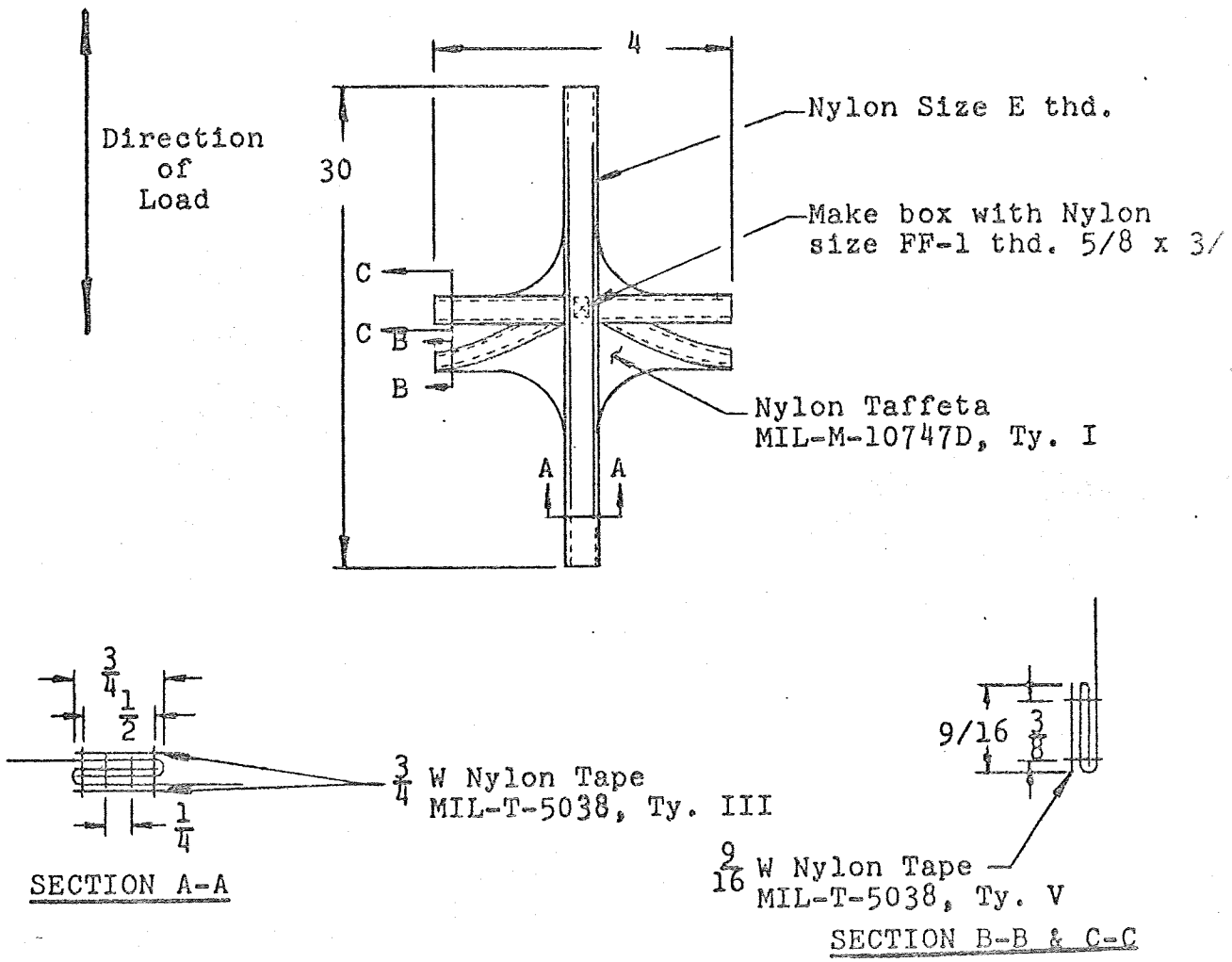

FIGURE - 11 -

J.S. Mansi
11 November 1964

TITLE: Main Seam Taffeta - Single Ply

PURPOSE: Two types of main seams were tested to destruction to determine the ultimate load that may be applied before failure occurs. The two types of main seams are constructed of single ply, 2.0 ounce taffeta material and of 3/4" wide, 400 lb., tensile strength, nylon tape, MIL-T-5038, Type III.

METHOD: The samples were tested on a Scott Tensile Testing Machine with a jaw separation speed of 12 inches per minute and a jaw separation distance of one inch, using three inch jaws. The construction of the samples may be seen below.

RESULTS:

Test No.	Direction of Pull	Breaking Strength Lbs./In.	Direction of Pull	Breaking Strength Lbs.
1	Warp	68	Fill	55
2	Warp	76	Fill	57
3	Warp	70	Fill	60
	Avg.	71.3	Avg.	57.3

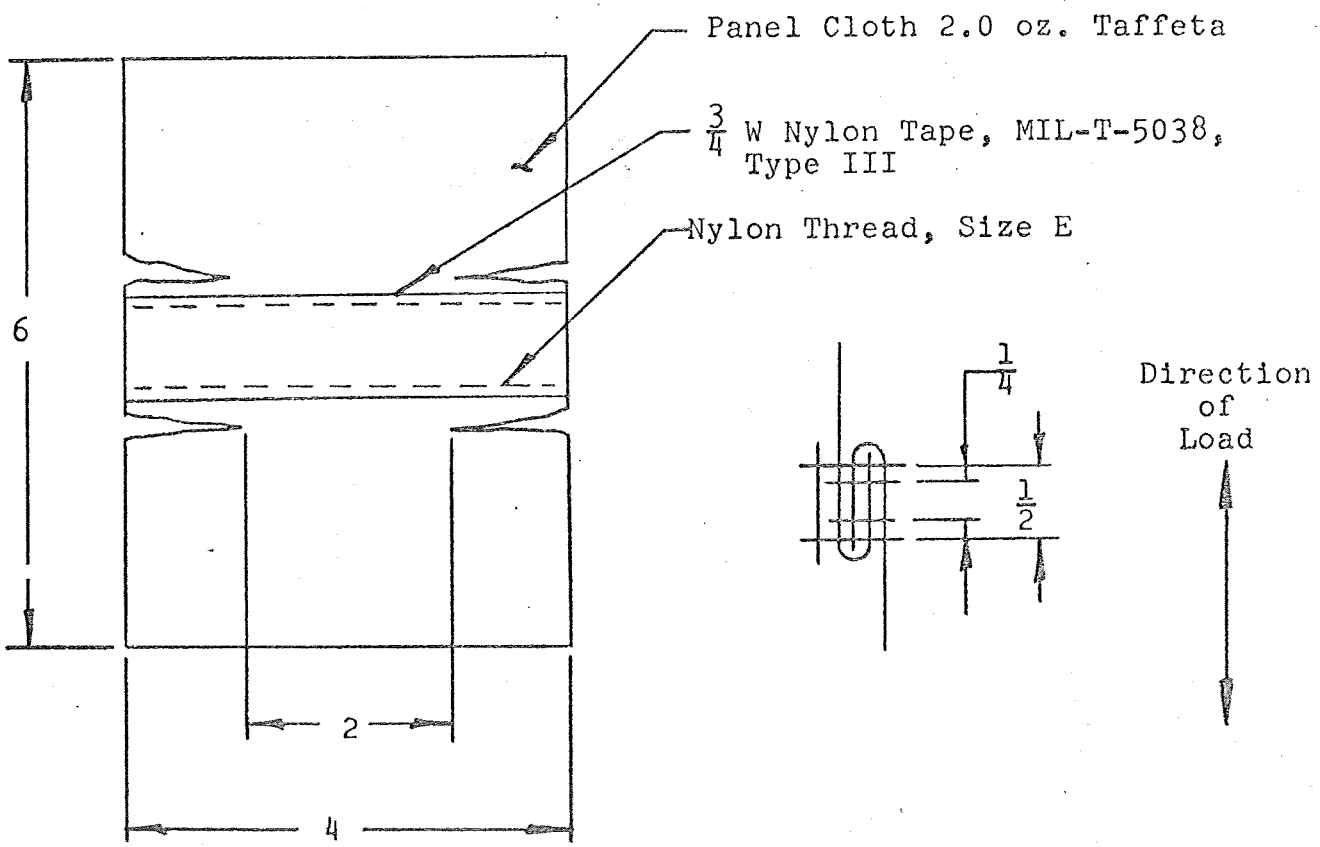

FIGURE - 12 -

J.S. Mansi
12 November 1964

TITLE: Main Seam Taffeta - Double Ply

PURPOSE: Two types of main seams were tested to destruction to determine the ultimate load that may be applied before failure occurs. The two types of main seams are constructed of double ply, 2.0 ounce taffeta material, 3/4" wide, 400 lb., tensile strength, nylon tape, MIL-T-5038, Type III.

METHOD: The samples were tested on a Scott Tensile Testing Machine with a jaw separation speed of 12 inches per minute and a jaw separation distance of one inch, using three inch jaws. The construction of the samples may be seen below.

RESULTS:

Test No.	Direction of Pull	Breaking Strength Lbs./In.	Direction of Pull	Breaking Strength Lbs.
1	Warp	55	Fill	57
2	Warp	67	Fill	55
3	Warp	72	Fill	55
		Avg. 64.3		Avg. 55.3

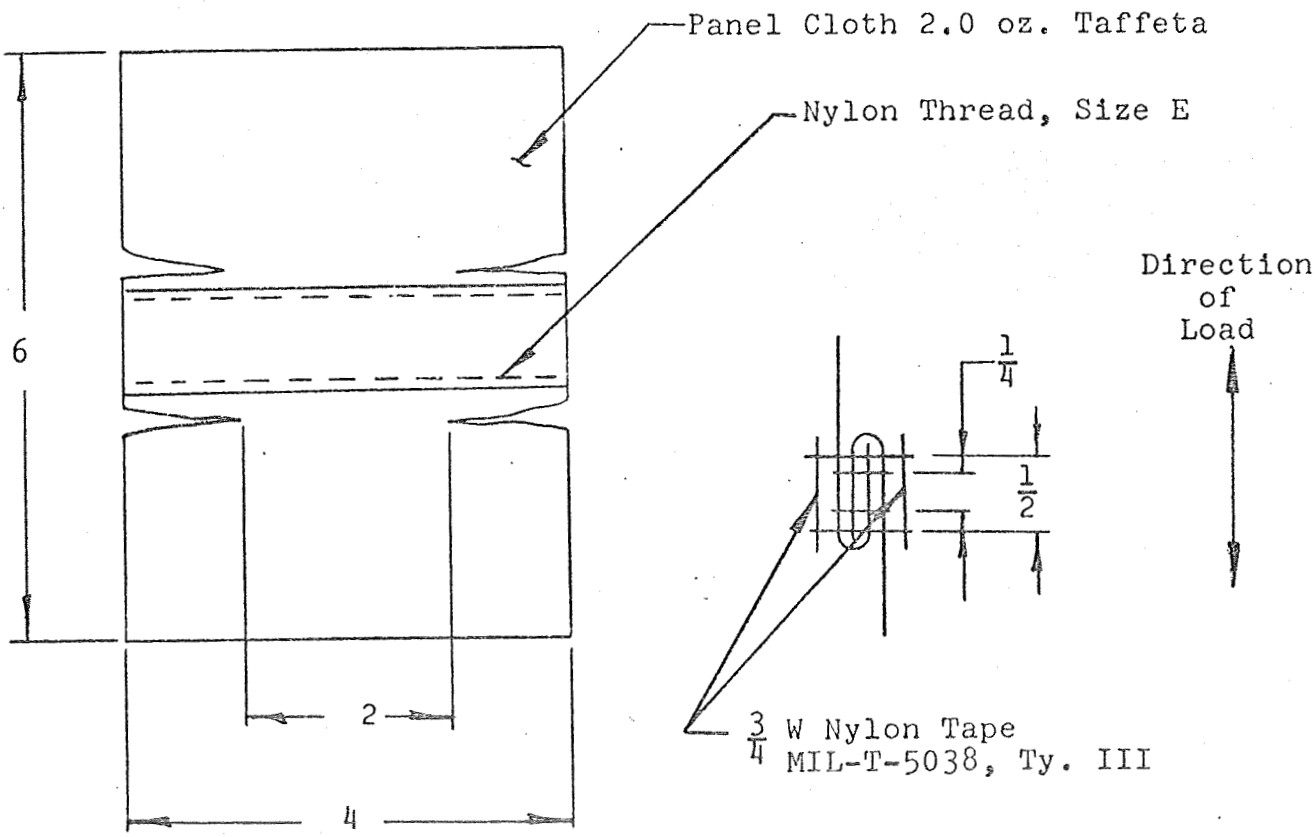

FIGURE - 13 -

J.S. Mansi
12 November 1964

TITLE: Main Seam 2.25 oz. MIL-C-7350, Ty. I - Single Ply

PURPOSE: Two types of main seams were tested to destruction to determine the ultimate load that may be applied before failure occurs. The two types of main seams are constructed of single ply 2.25 ounce, MIL-C-7350, Type I nylon material and of 3/4" wide, 400 lb., tensile strength nylon tape, MIL-T-5038, Type III.

METHOD: The samples were tested on a Scott Tensile Testing Machine with a jaw separation of 12 inches per minute and a jaw separation distance of one inch, using three inch jaws.

RESULTS:

Test No.	Direction of Pull	Breaking Strength Lbs./In.	Direction of Pull	Breaking Strength Lbs.
1	Warp	76	Fill	68
2	Warp	88	Fill	76
3	Warp	85	Fill	70
		Avg. 83		Avg. 71.3

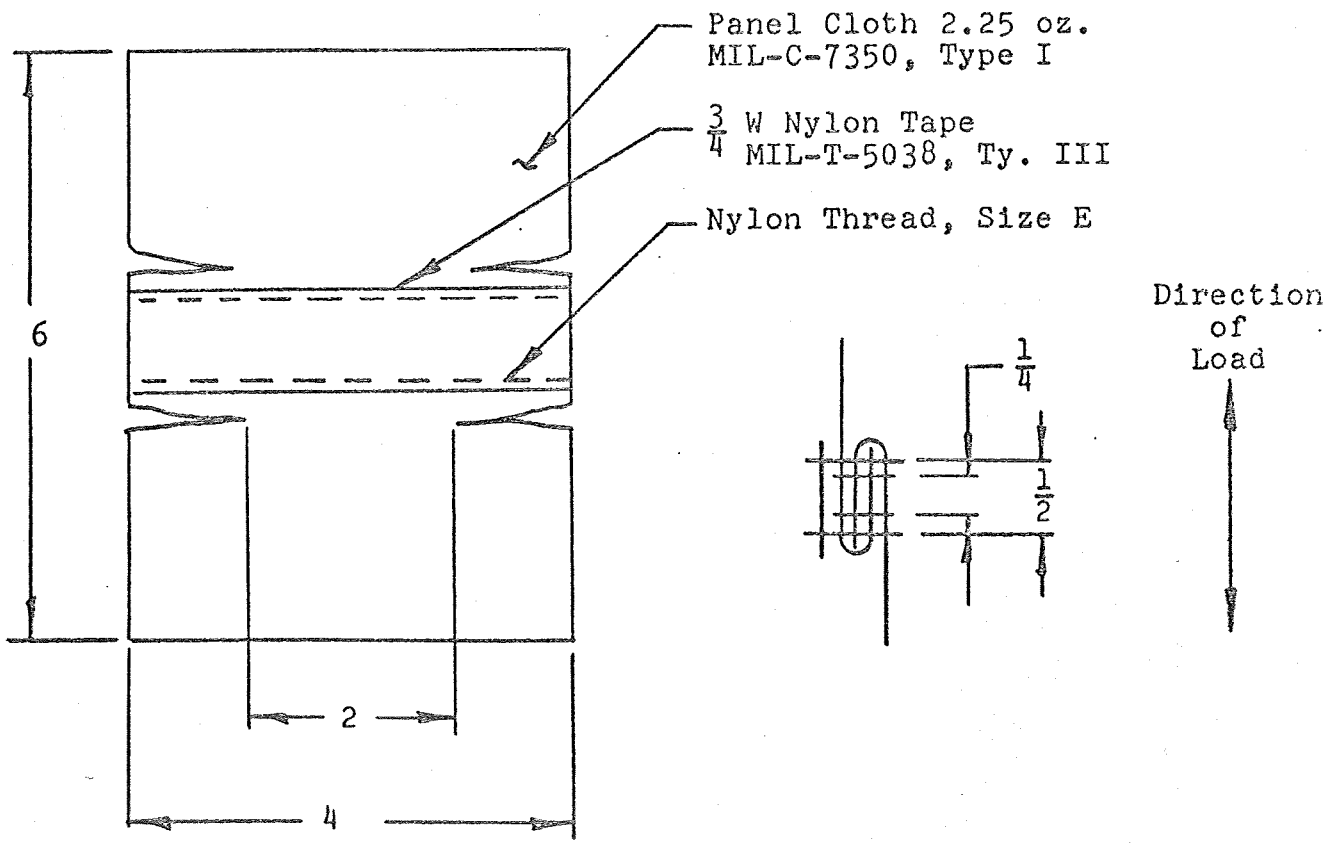

FIGURE - 14 -

J.S. Mansi
12 November 1964

TITLE: Main Seam 2.25 oz. MIL-C-7350, Ty. I - Double Ply

PURPOSE: Two types of main seams were tested to destruction to determine the ultimate load that may be applied before failure occurs. The two types of main seams are constructed of double ply, 2.25 oz., MIL-C-7350, Type I nylon material, 3/4" wide, 400 lb., tensile strength nylon tape, MIL-T-5038, Type III.

METHOD: The samples were tested on a Scott Tensile Testing Machine with a jaw separation of 12 inches per minute and a jaw separation distance of one inch, using three inch jaws.

RESULTS:

Test No.	Direction of Pull	Breaking Strength Lbs./In.	Direction of Pull	Breaking Strength Lbs.
1	Warp	72	Fill	76
2	Warp	79	Fill	70
3	Warp	80	Fill	73
	Avg.	77	Avg.	73

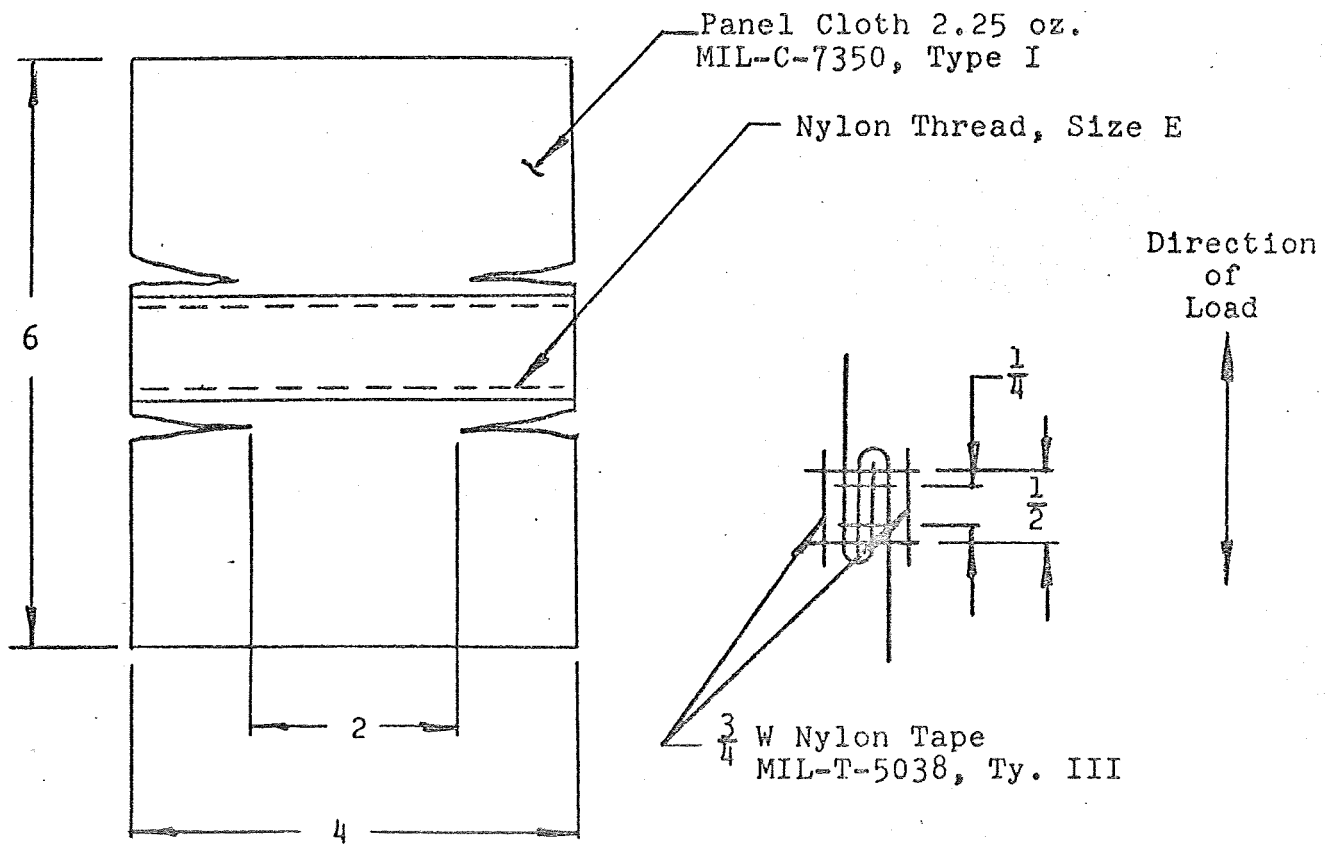

FIGURE - 15 -

J.S. Mansi
12 November 1964

TITLE: Vent Line Attachment

PURPOSE: Three specimens were tested to destruction to determine the ultimate load that the vent line attachment could withstand before failure occurred, and at what point the failure took place.

METHOD: The tests were conducted using a Scott Cord Testing Machine with a jaw separation speed of 13 1/2 inches per minute. The construction of the sample may be seen below.

RESULTS:

Test No.	Breaking Strength Lbs.
1	538
2	580
3	560
Avg.	558

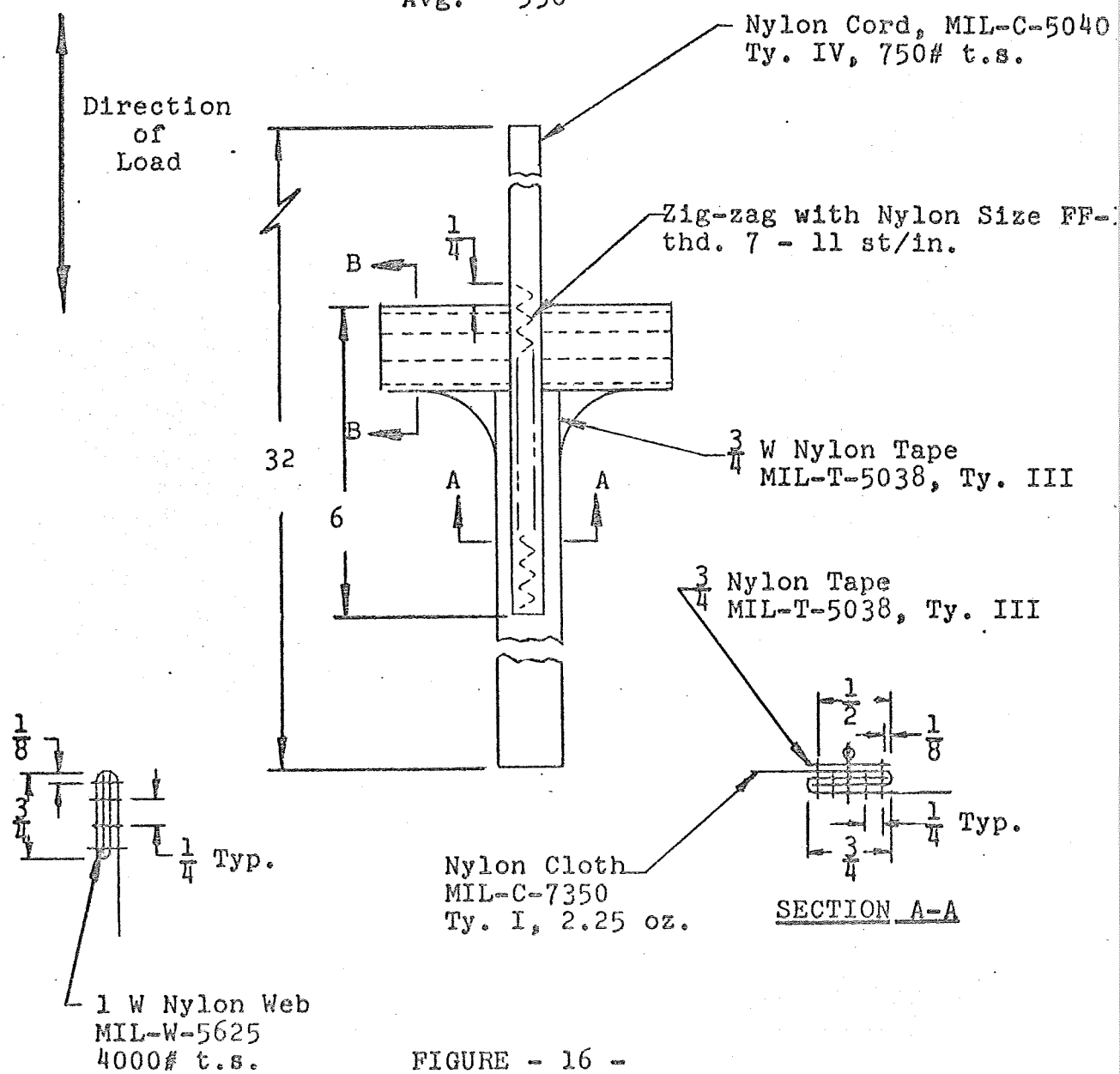

FIGURE - 16 -

J.S. Mansi
11 November 1964

TITLE: Vent Band Joint

PURPOSE: Three vent band joints were tested to destruction to determine the ultimate loads the joint could withstand before failure occurred.

METHOD: The tests were conducted using a Tinius Olsen Tension Testing Machine with a jaw separation speed of four (4) inches per minute.

RESULTS:

Test No.	Breaking Strength Lbs.
1	3840
2	4100
3	3860
Avg.	3933

Direction of Load

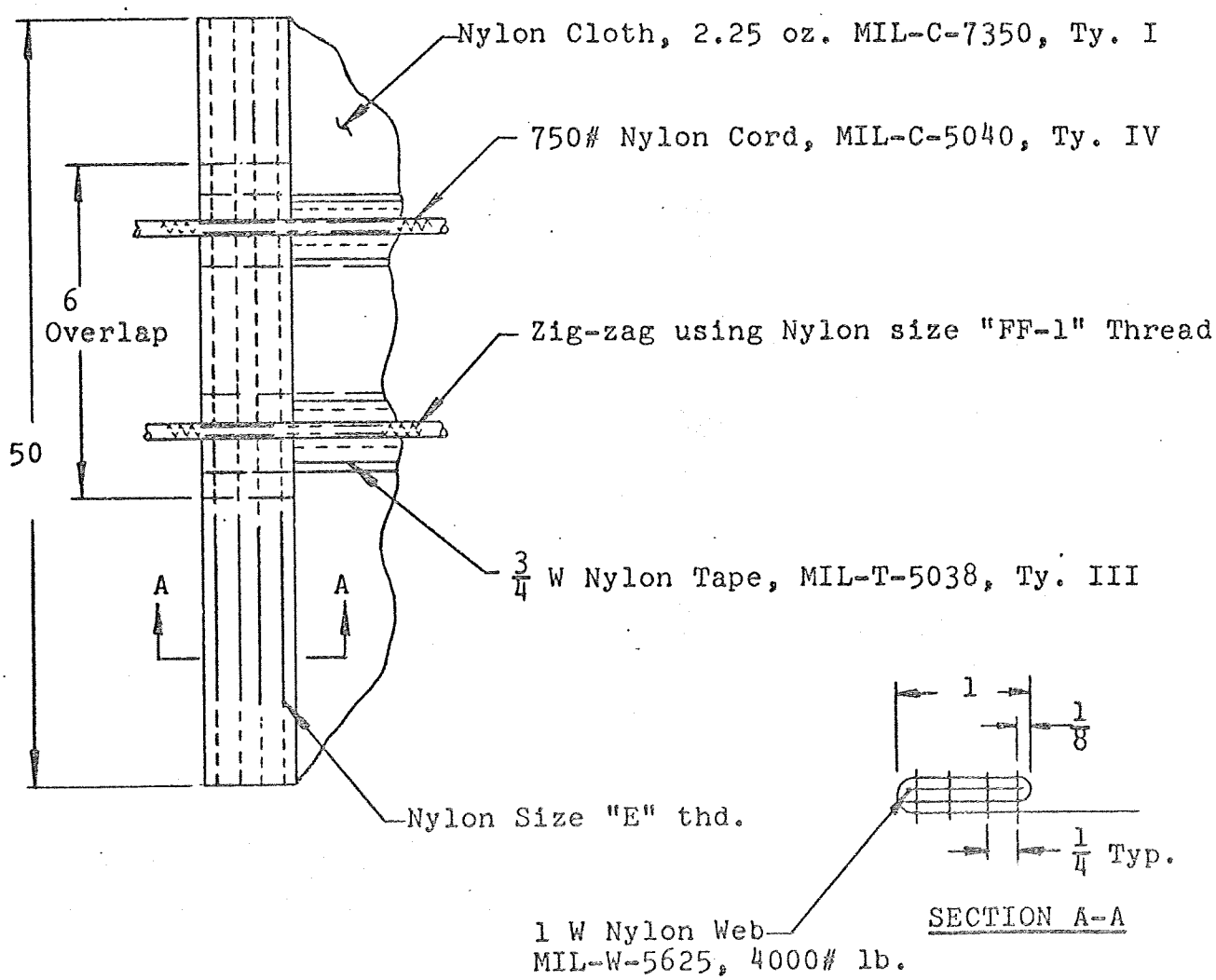

FIGURE - 17 -

J.S. Mansi
11 November 1964

TITLE: Bridle/Bridle Loop/Vent Line

PURPOSE: Three test specimens were tested to destruction to determine the ultimate load that may be applied before failure occurred and at what point the failure took place.

METHOD: The tests were conducted using a Tinius Olsen Tension Testing Machine. The jaw separation speed was set at four (4) inches per minute. The construction of the sample may be seen below.

RESULTS:

Test No.	Breaking Strength Lbs.	Remarks
1	5000 lbs.	Used 20 vent lines. Lines failed
2	7566 lbs.	Bridle failed at cow hitch
3	7320 lbs.	Bridle failed at cow hitch
Avg. Tests Nos. 2 & 3	7443 lbs.	

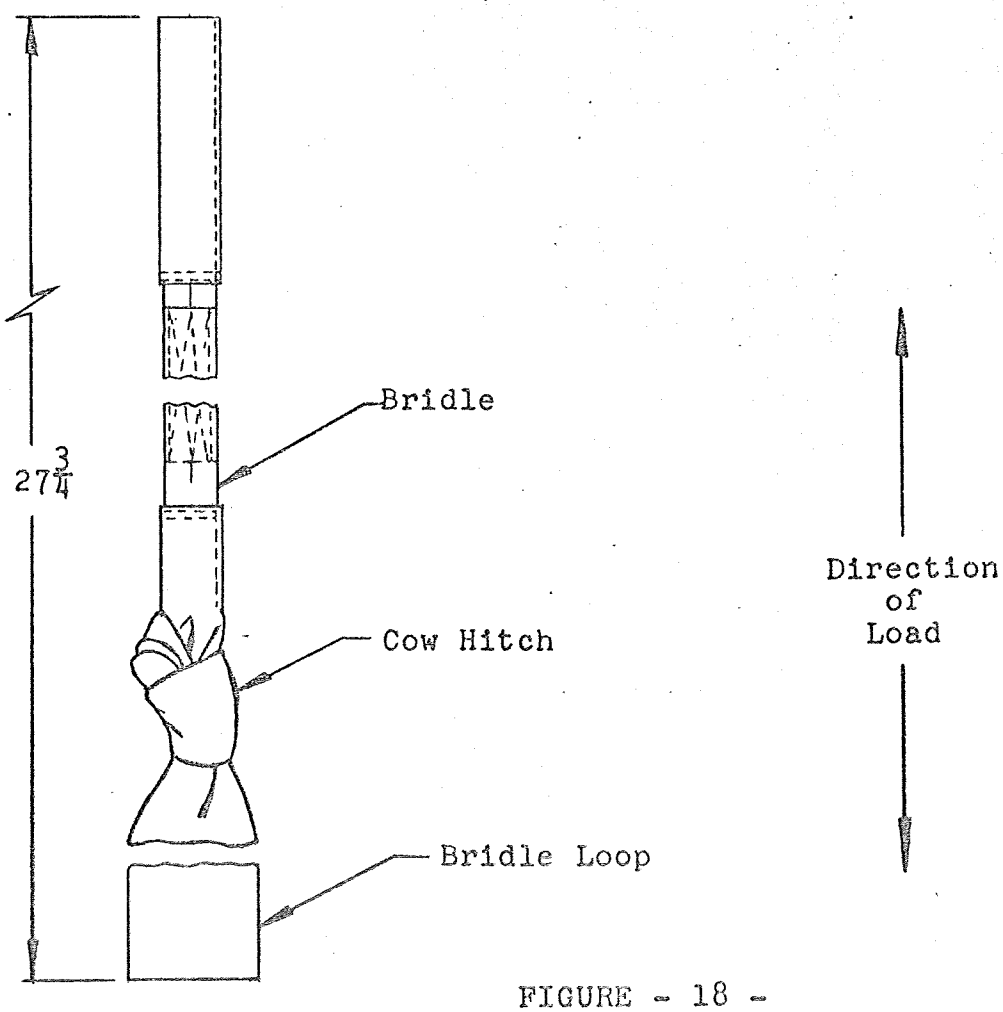

FIGURE - 18 -

J.S. Mansi
18 November 1964

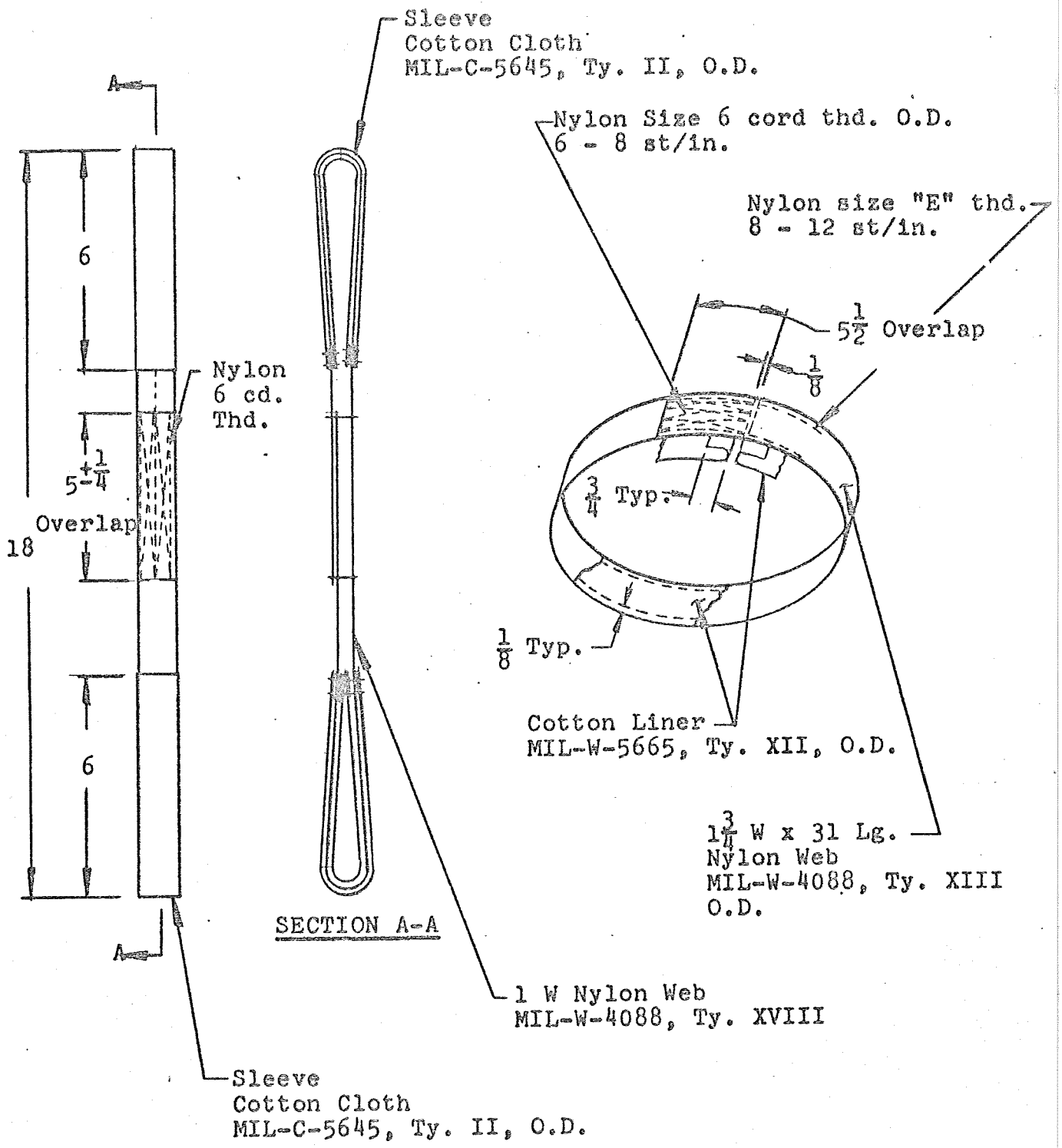

FIGURE - 19 -

J.S. Mansi
18 November 1964

TITLE: Stabilization/Pilot Chute Confluence

PURPOSE: Three test specimens were tested to destruction to determine the ultimate load that may be applied before failure occurred and at what point the failure took place.

METHOD: The tests were conducted using a Tinius Olsen Tension Testing Machine. The jaw separation speed was set at four (4) inches per minute. The construction of the sample may be seen below.

RESULTS:

Test No.	Breaking Strength Lbs.	Remarks
1	7400	Failed riser loop
2	7760	Failed riser loop
3	8100	Failed riser loop
Avg.	7753	

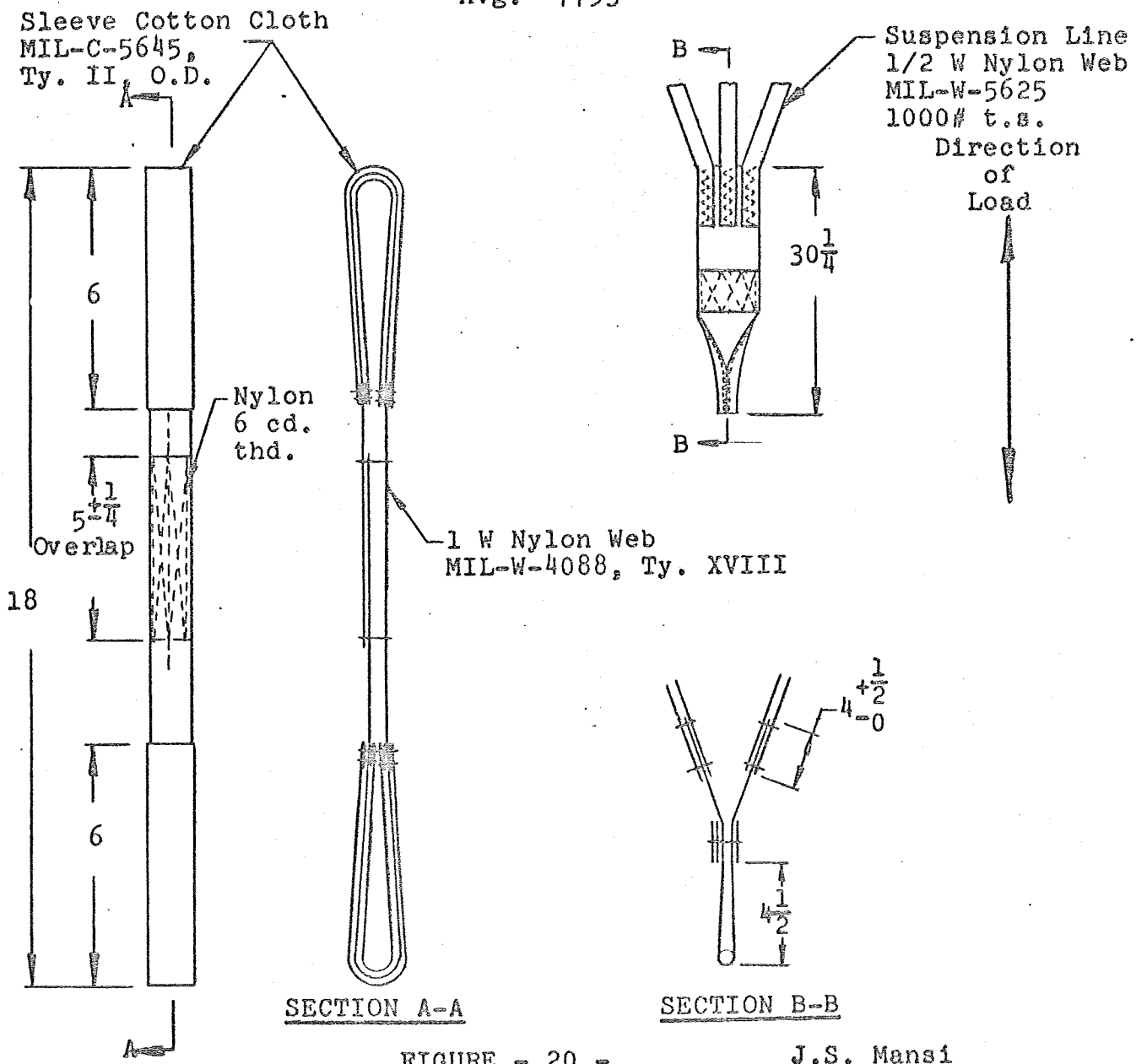

FIGURE - 20 -

J.S. Mansi
11 November 1964

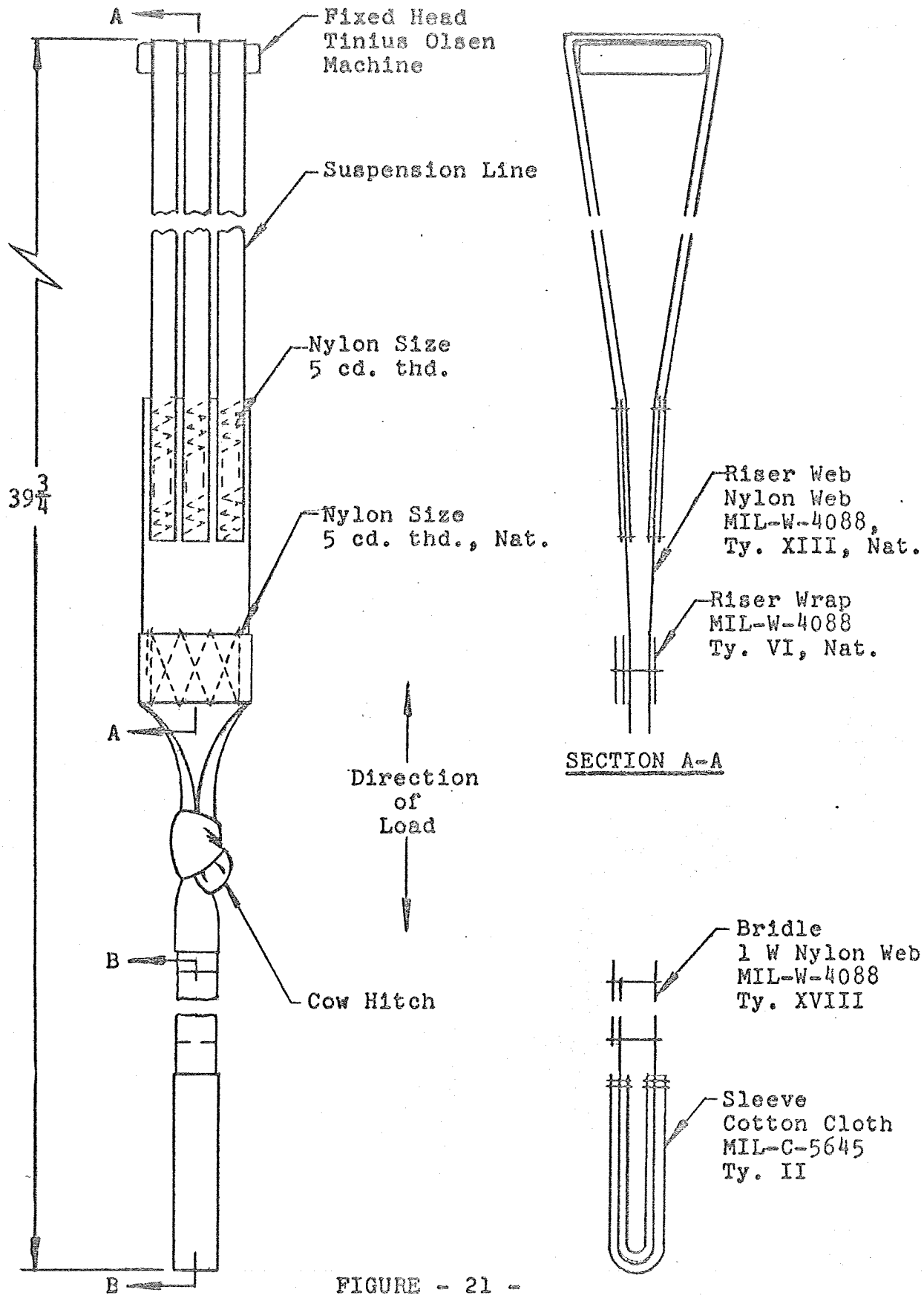

FIGURE - 21 -

J.S. Mansi
11 November 1964

TITLE: Internal Parachute Confluence

PURPOSE: Three specimens were tested to destruction to determine the ultimate load that the confluence and center line attachment could withstand before failure occurred, and at what point the failure took place.

METHOD: The tests were conducted using a Tinius Olsen Tension Testing Machine with a jaw separation speed of four (4) inches per minute. The construction of the sample may be seen below.

RESULTS:

Specimen No.	Breaking Strength Lbs.	Remarks
1	5580	Zig-zag stitching failed on 750# cord
2	6260	" " "
3	6200	" " "
Avg.	6013	

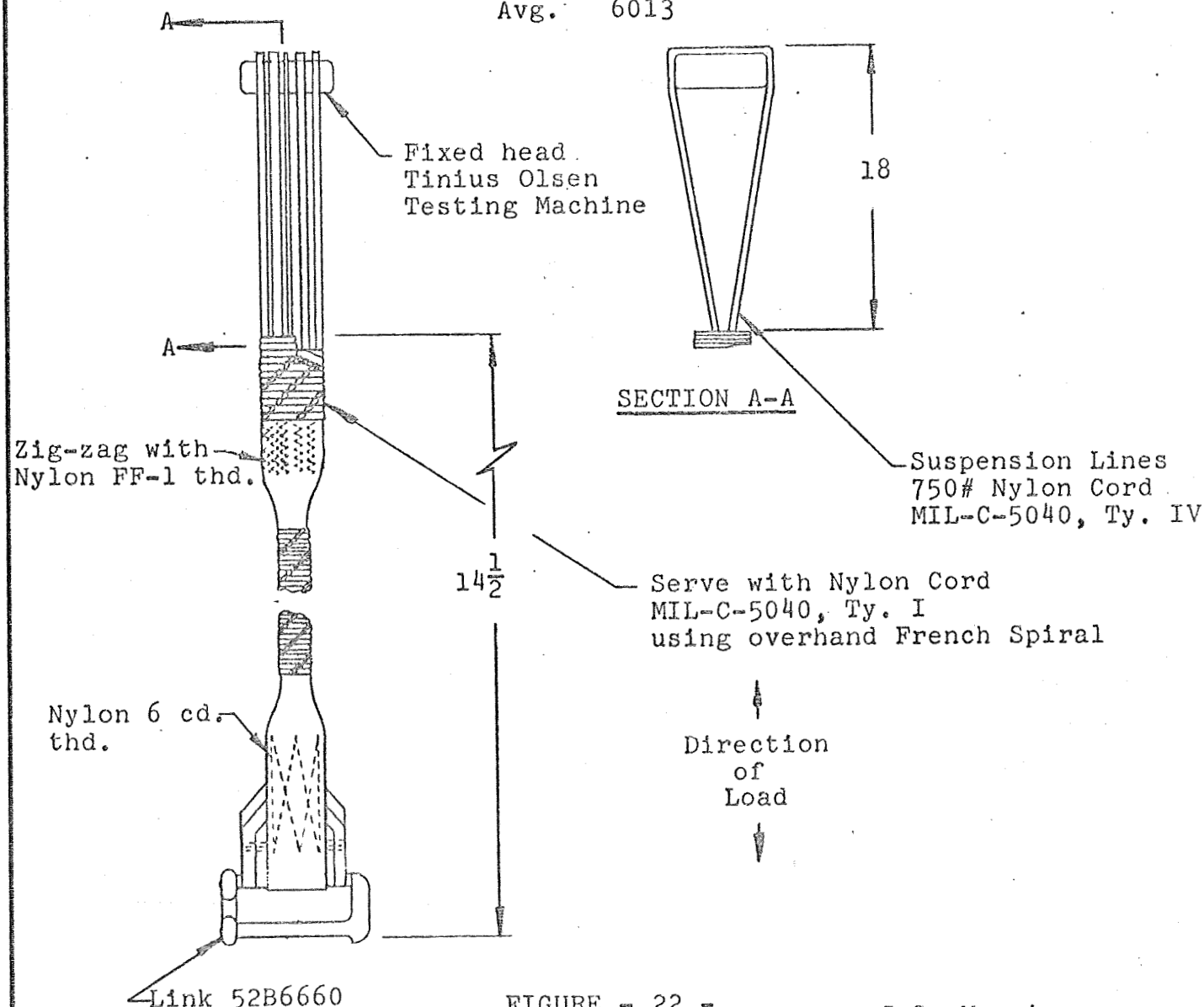

FIGURE - 22 -

J.S. Mansi
10 November 1964

APPENDIX D

Para-Sail Damage Charts

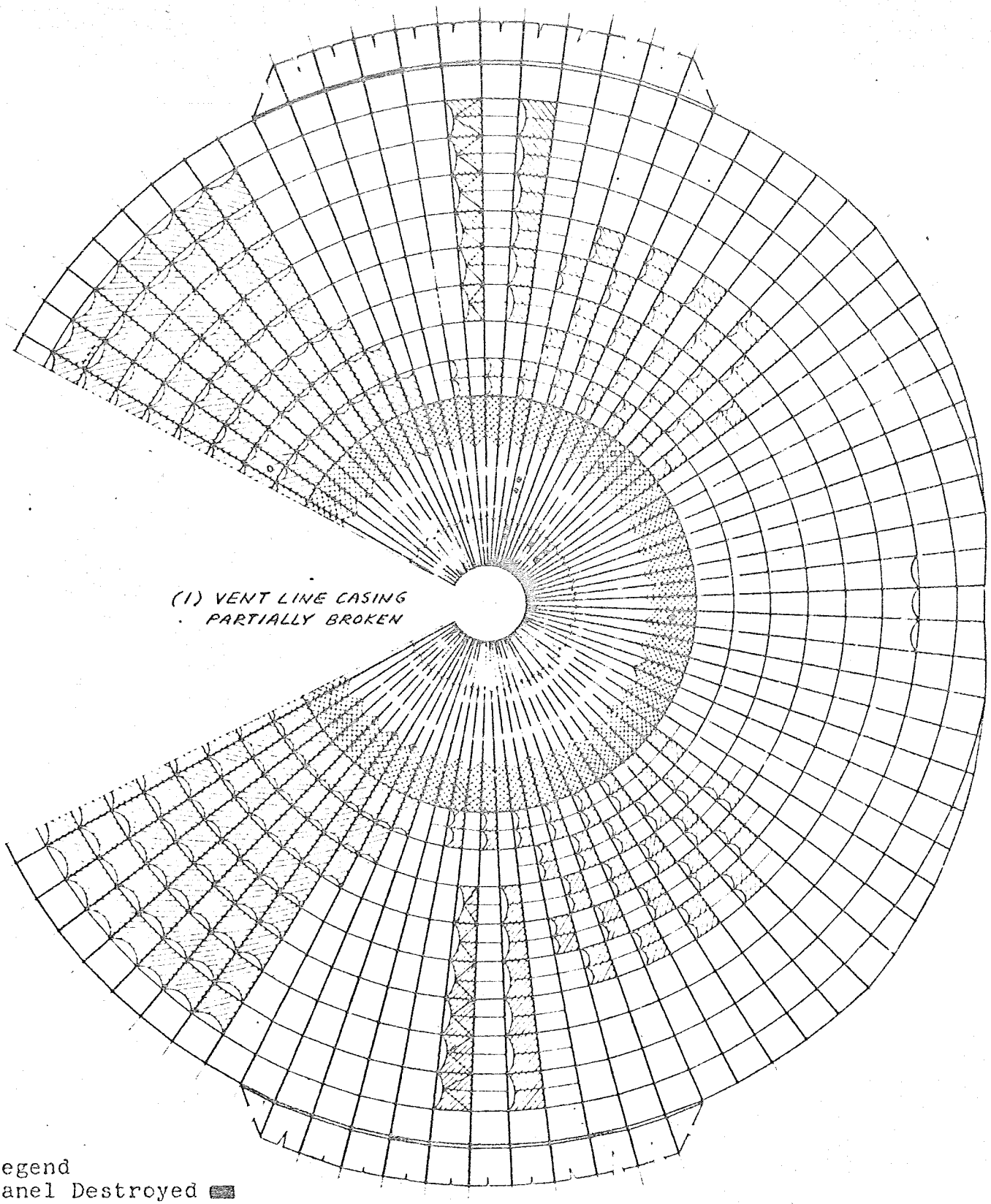

Legend
Panel Destroyed
Burns
Tears - - -

Drop Test No. 5
25 September 1963
Configuration 80A-1
Serial No. PS 6339

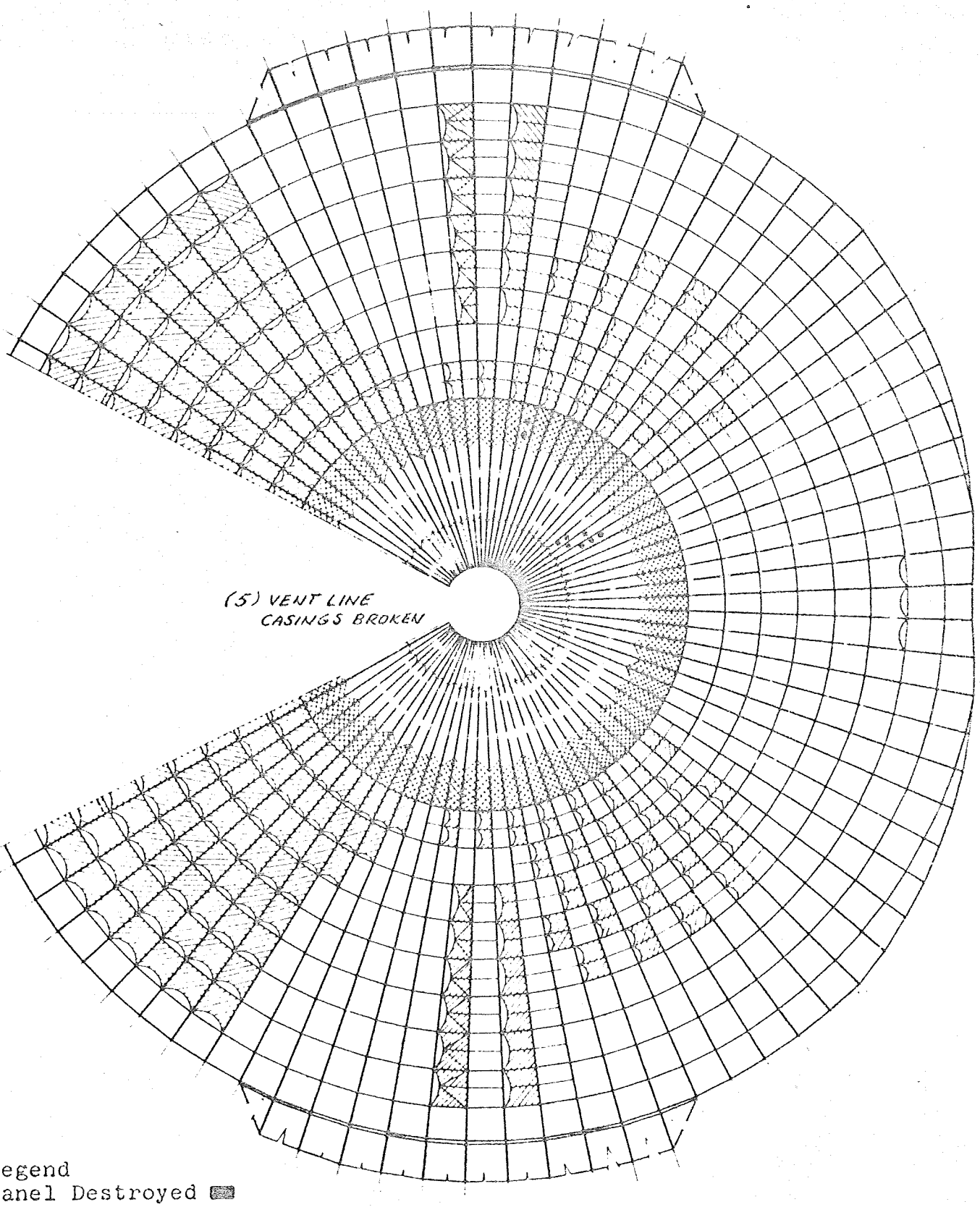

Legend
Panel Destroyed
Burns
Tears

Drop Test No. 6
2 October 1963
Configuration 80A-1
Serial No. PS 6339

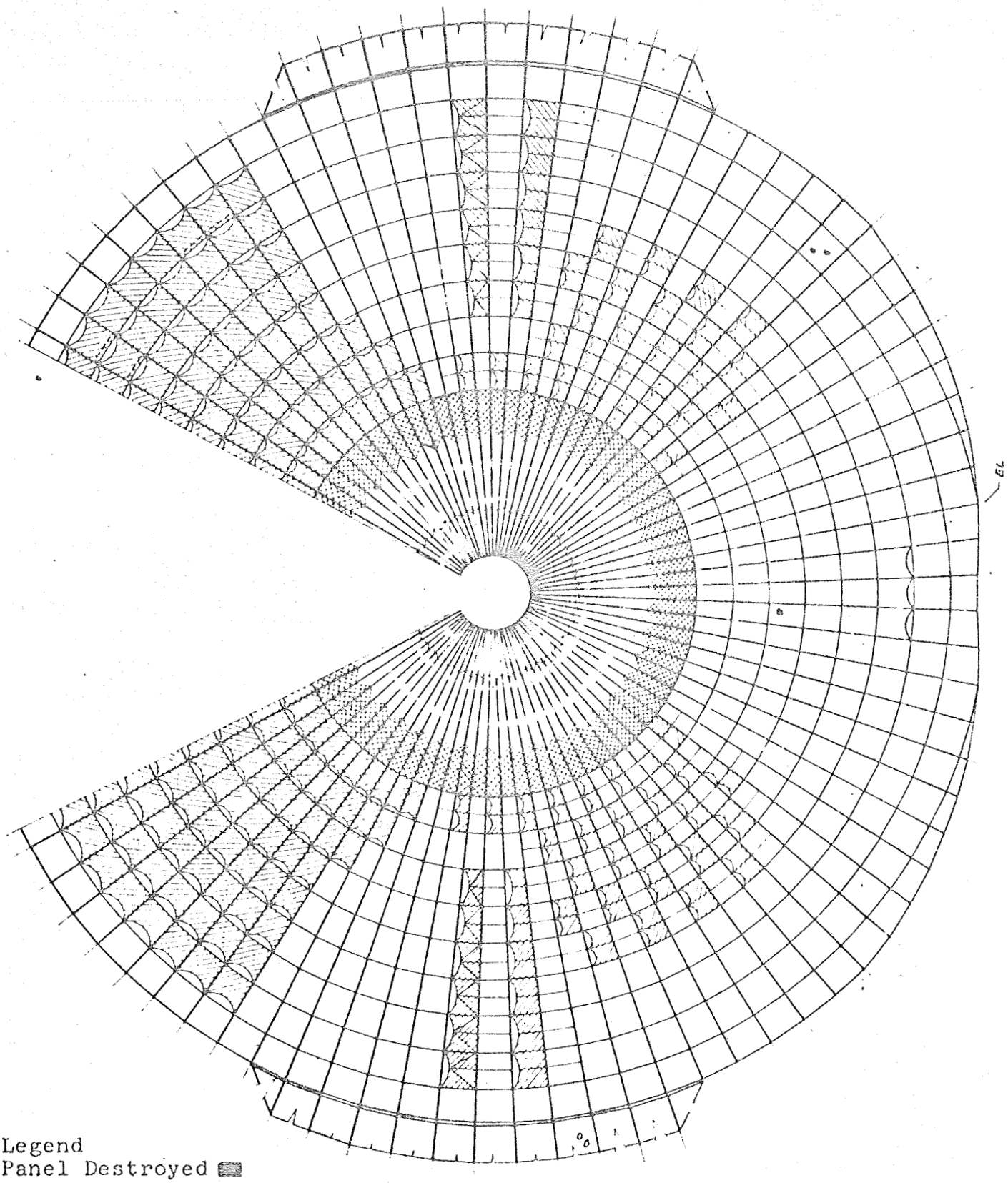

Legend
Panel Destroyed
Burns
Tears

Drop Test No. 7
8 October 1963
Configuration 80A-2
Serial No. PS 6339

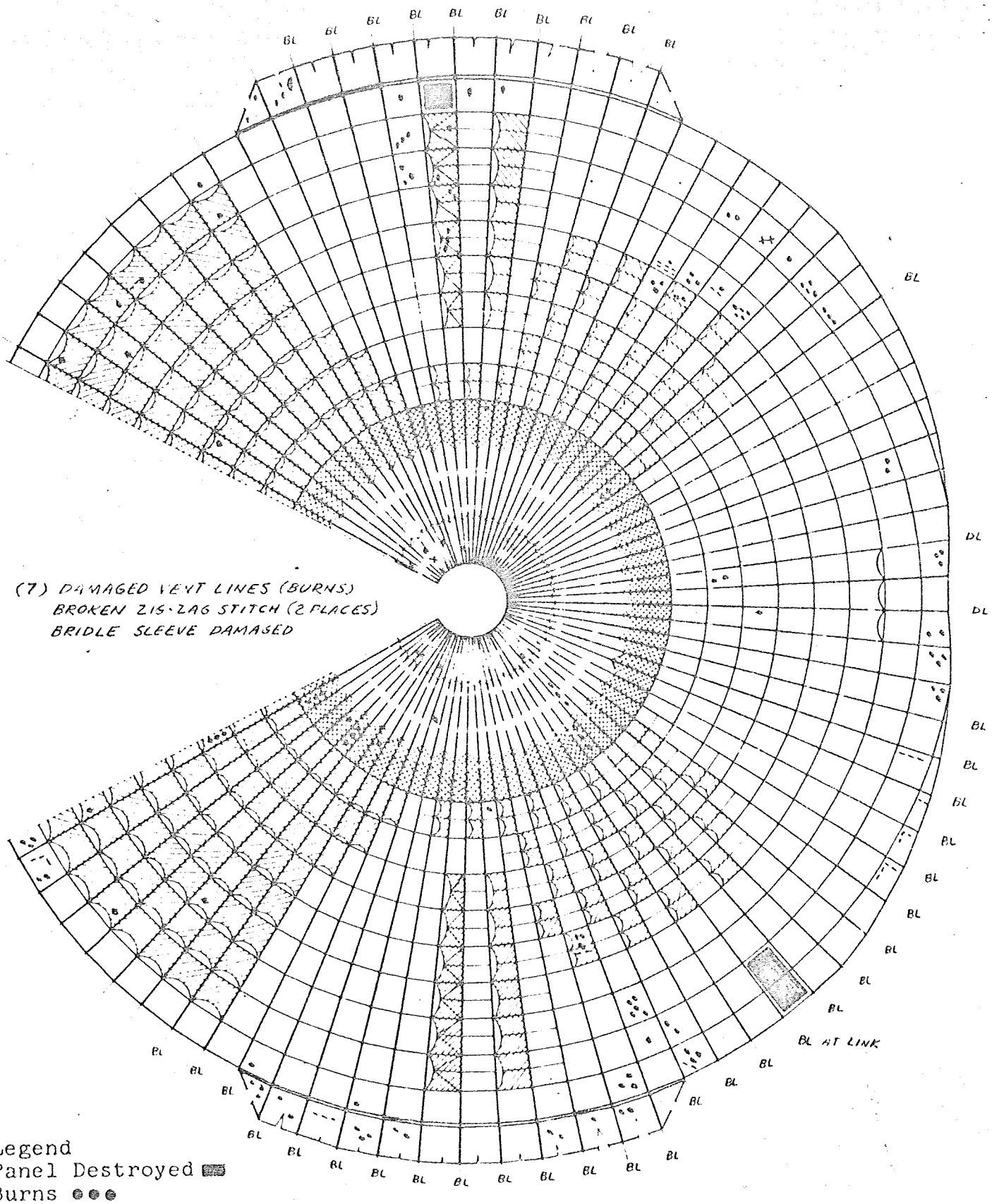

Legend
Panel Destroyed
Burns
Tears ---

Drop Test No. 9
29 October 1963
Configuration 80A-1
Serial No. PS 6339

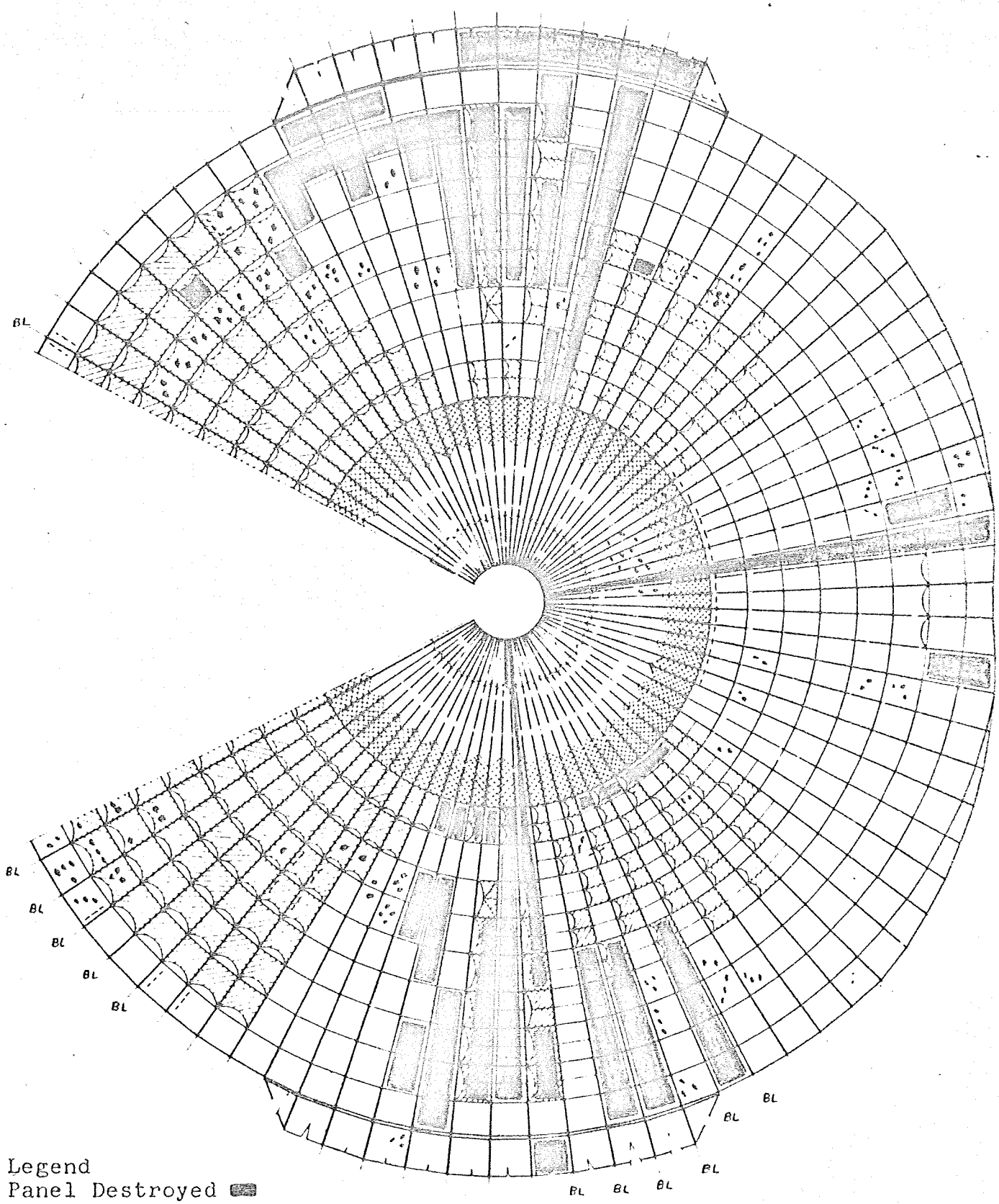

Legend
Panel Destroyed
Burns
Tears - - -

Drop Test No. 11
27 November 1963
Configuration 80A-3
Serial No. PS 63109

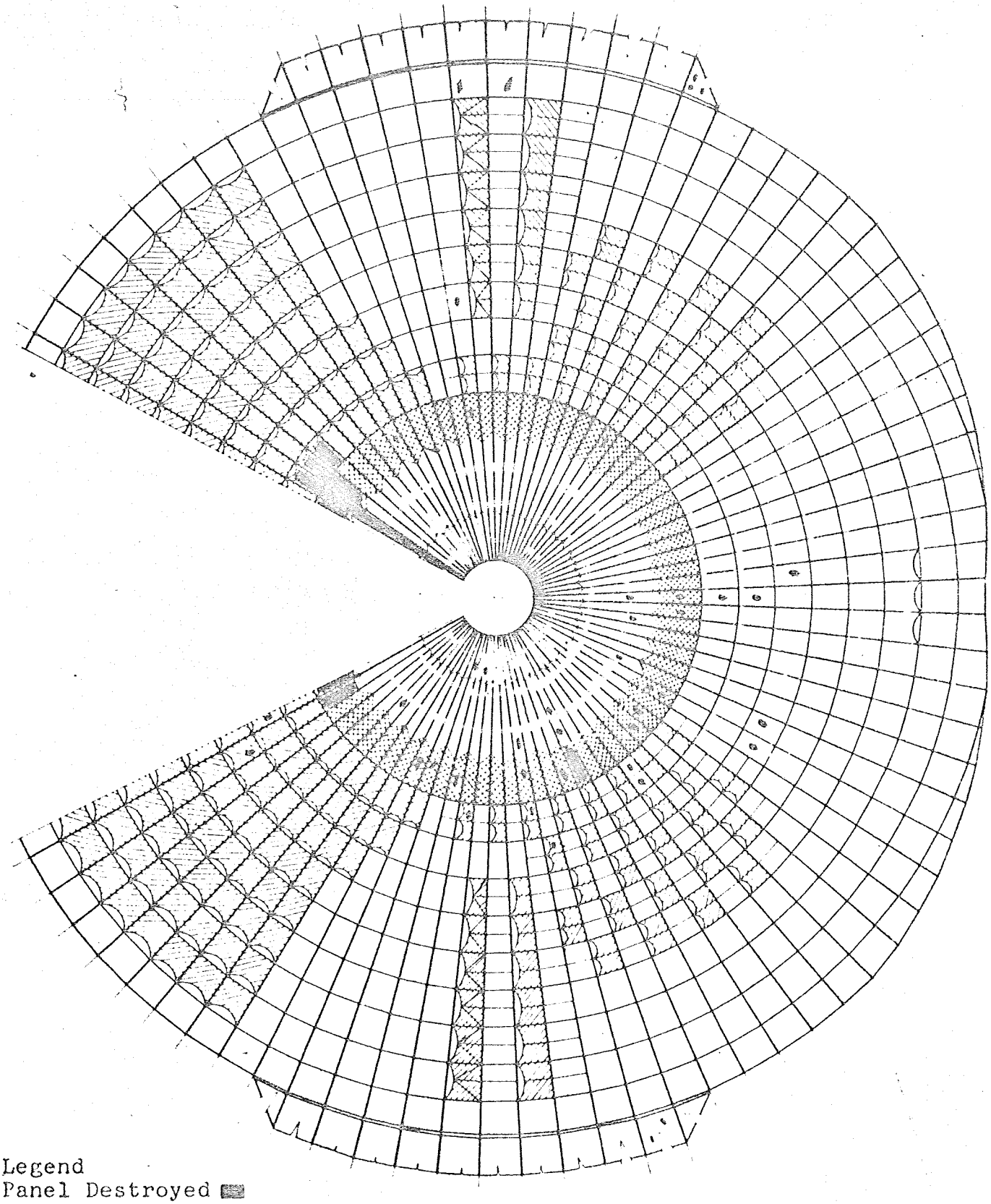

Legend
Panel Destroyed
Burns
Tears ---

Drop Test No. 15
29 January 1964
Configuration 80A-7
Serial No. PS 63114

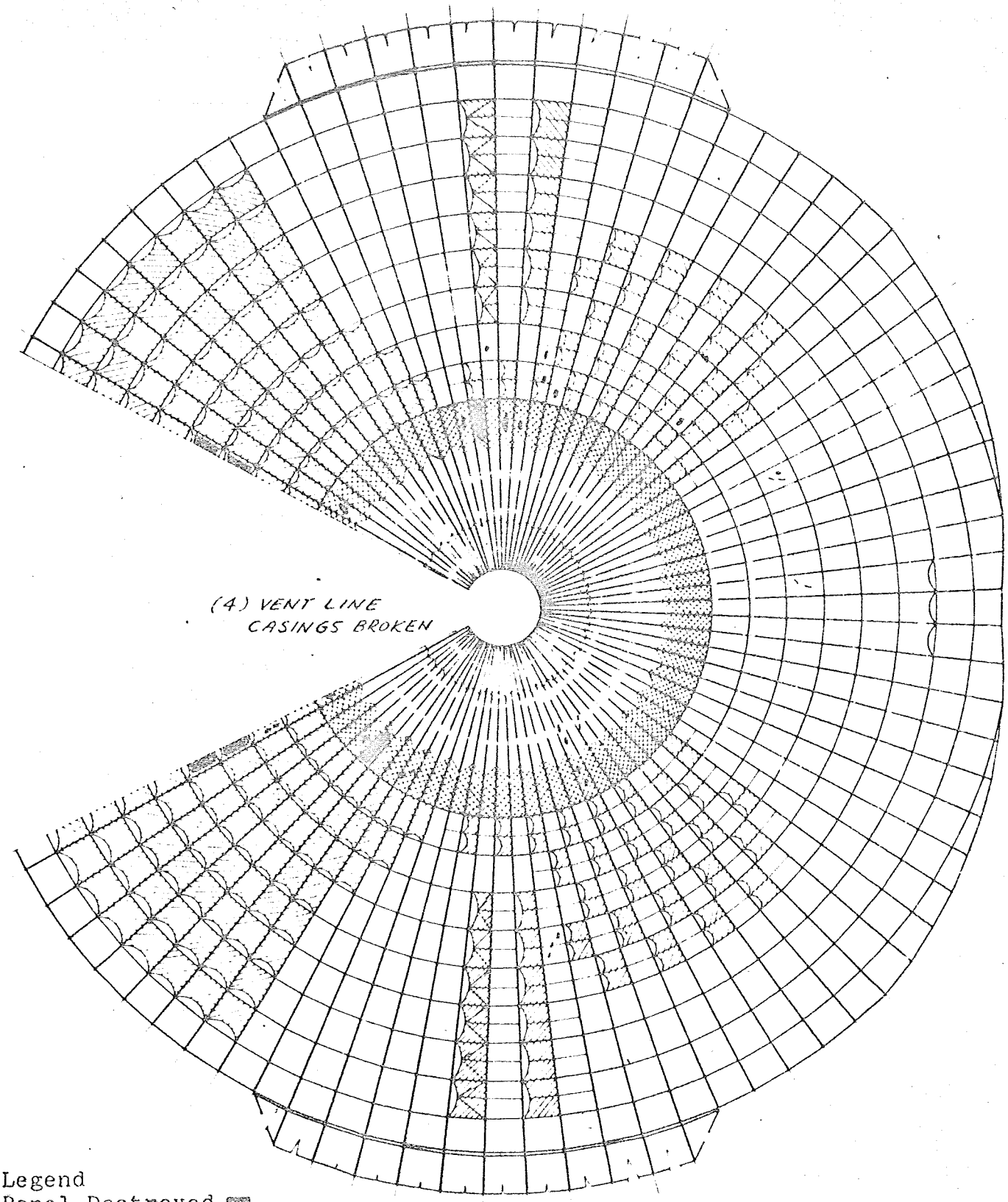

Legend
Panel Destroyed
Burns
Tears - - -

Drop Test No. 17
4 March 1964
Configuration 80A-9
Serial No. PS 64130

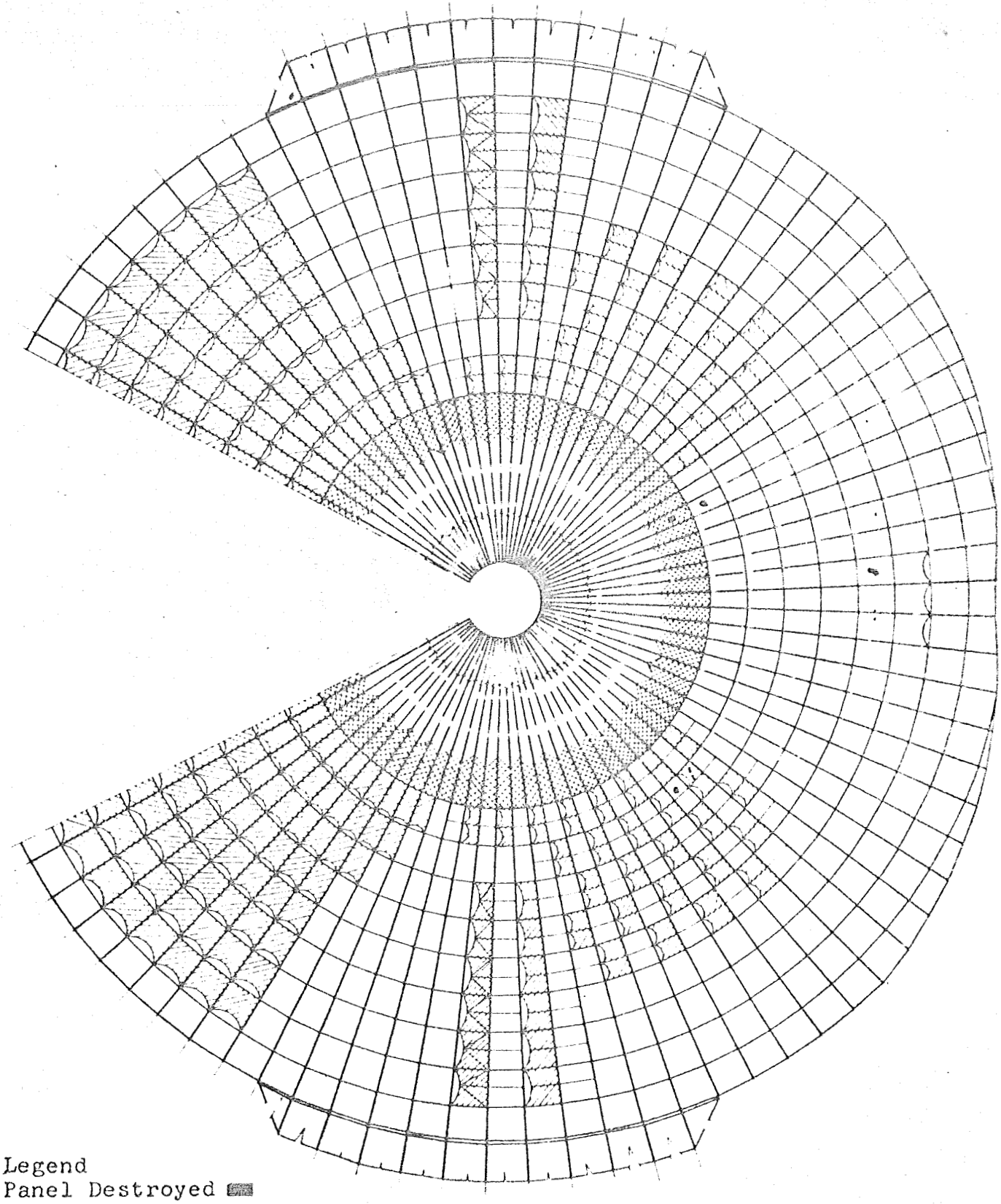

Legend
Panel Destroyed
Burns
Tears

Drop Test No. 18
9 March 1964
Configuration 80A-9
Serial No. PS 63114

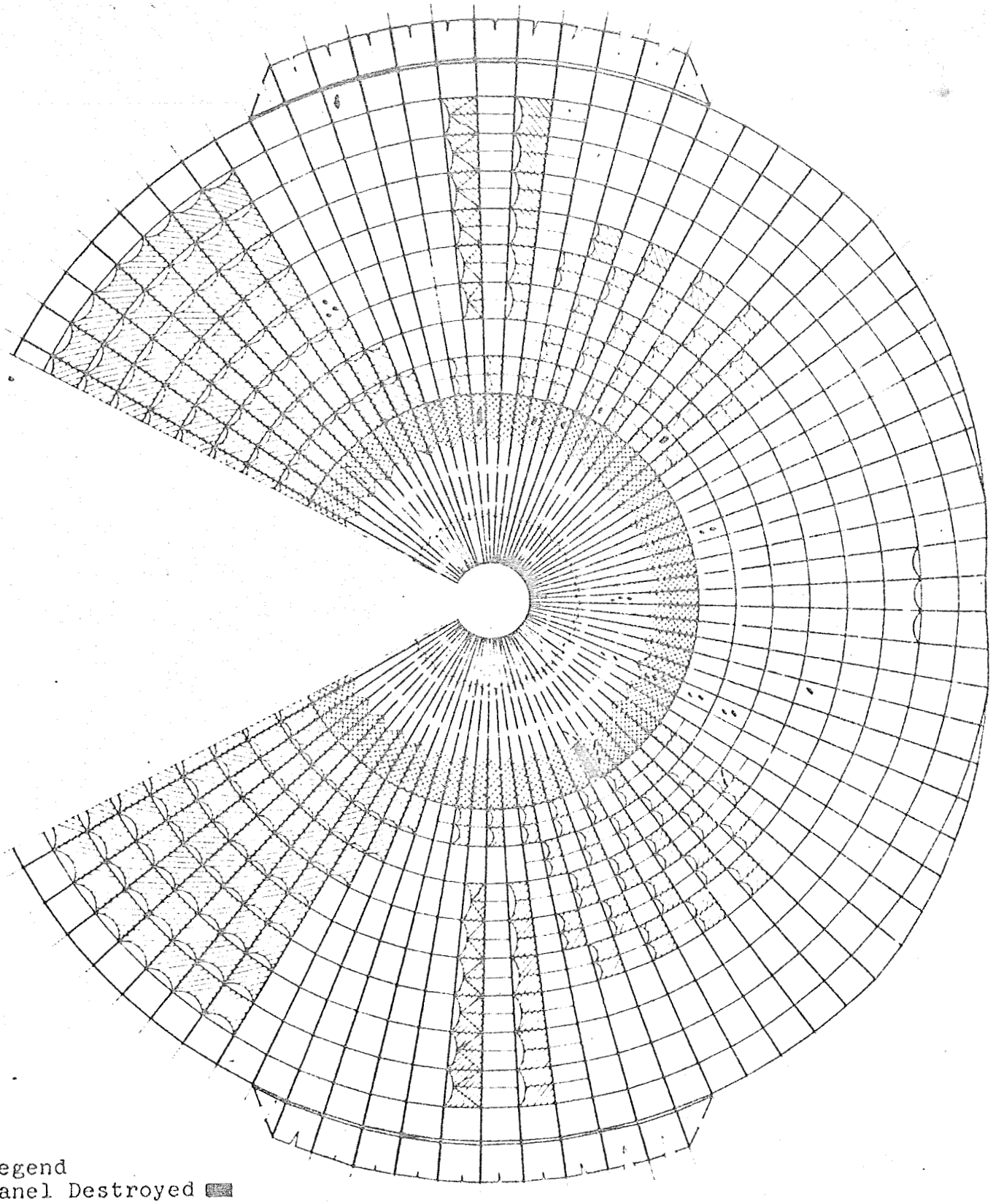

Legend
Panel Destroyed
Burns
Tears ---

Drop Test No. 19
13 March 1964
Configuration 80A-9
Serial No. PS 64130

APPENDIX E

Para-Sail Force Histories

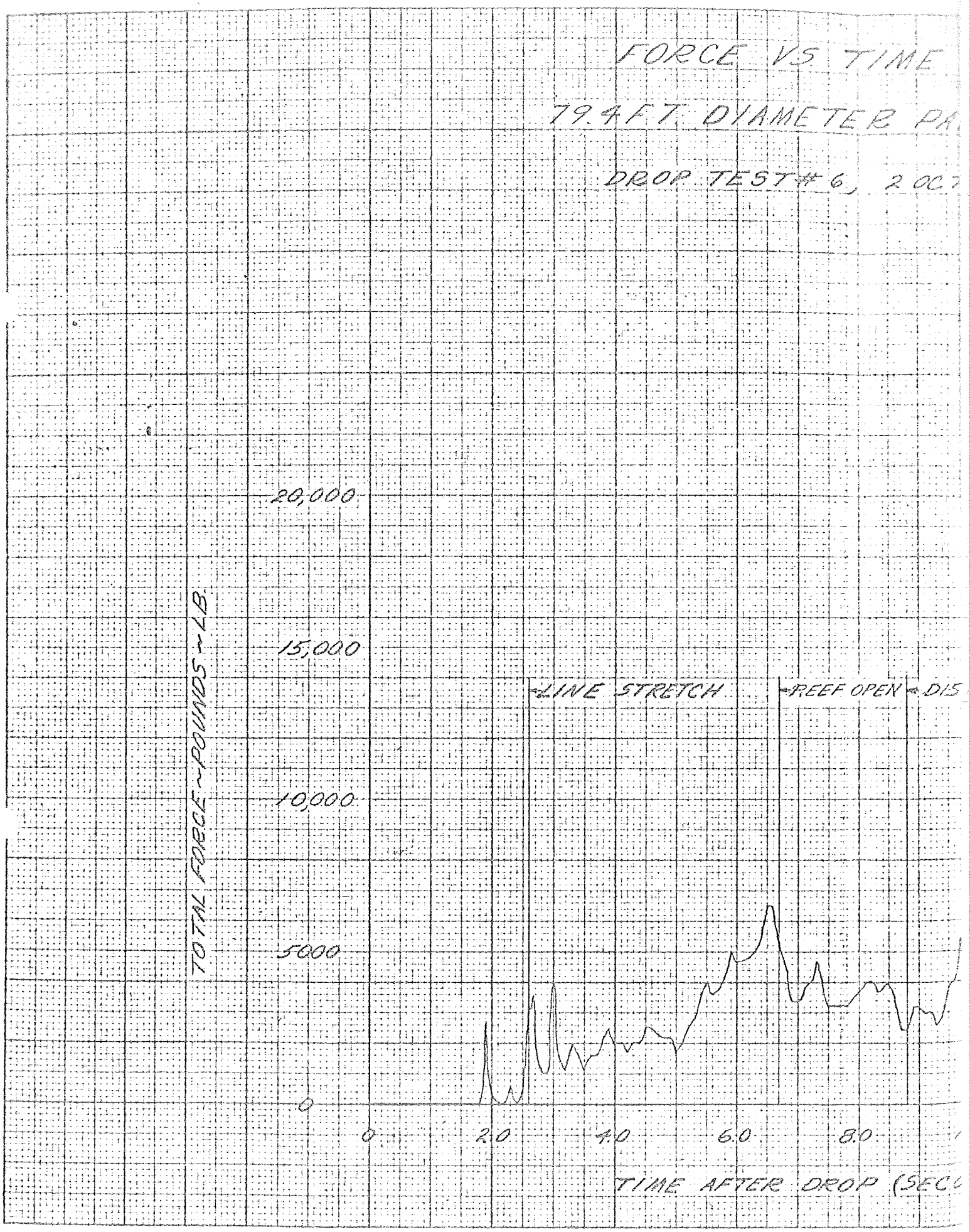
FORCE VS TIME
79.4 FT. DIAMETER PA
DROP TEST #6, 2 OC
20,000
15,000
10,000
5000
0
TOTAL FORCE ~ POUNDS ~ LB.
LINE STRETCH
REEF OPEN
DIS
0
2.0
4.0
6.0
8.0
TIME AFTER DROP (SEC

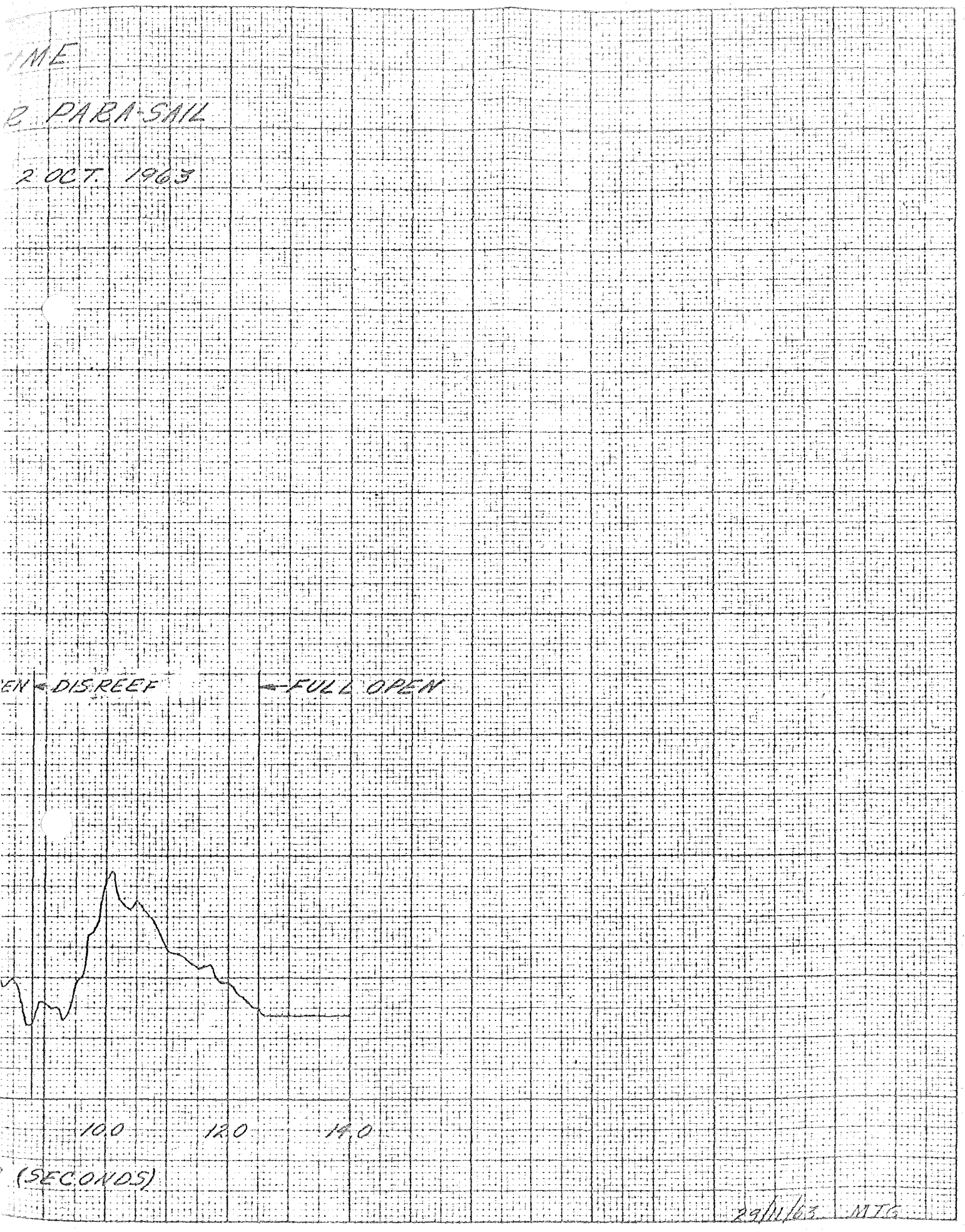
ME
PARA-SAIL
2 OCT. 1963
EN
DISREEF
FULL OPEN
10.0
12.0
14.0
(SECONDS)
29/11/63 MTG

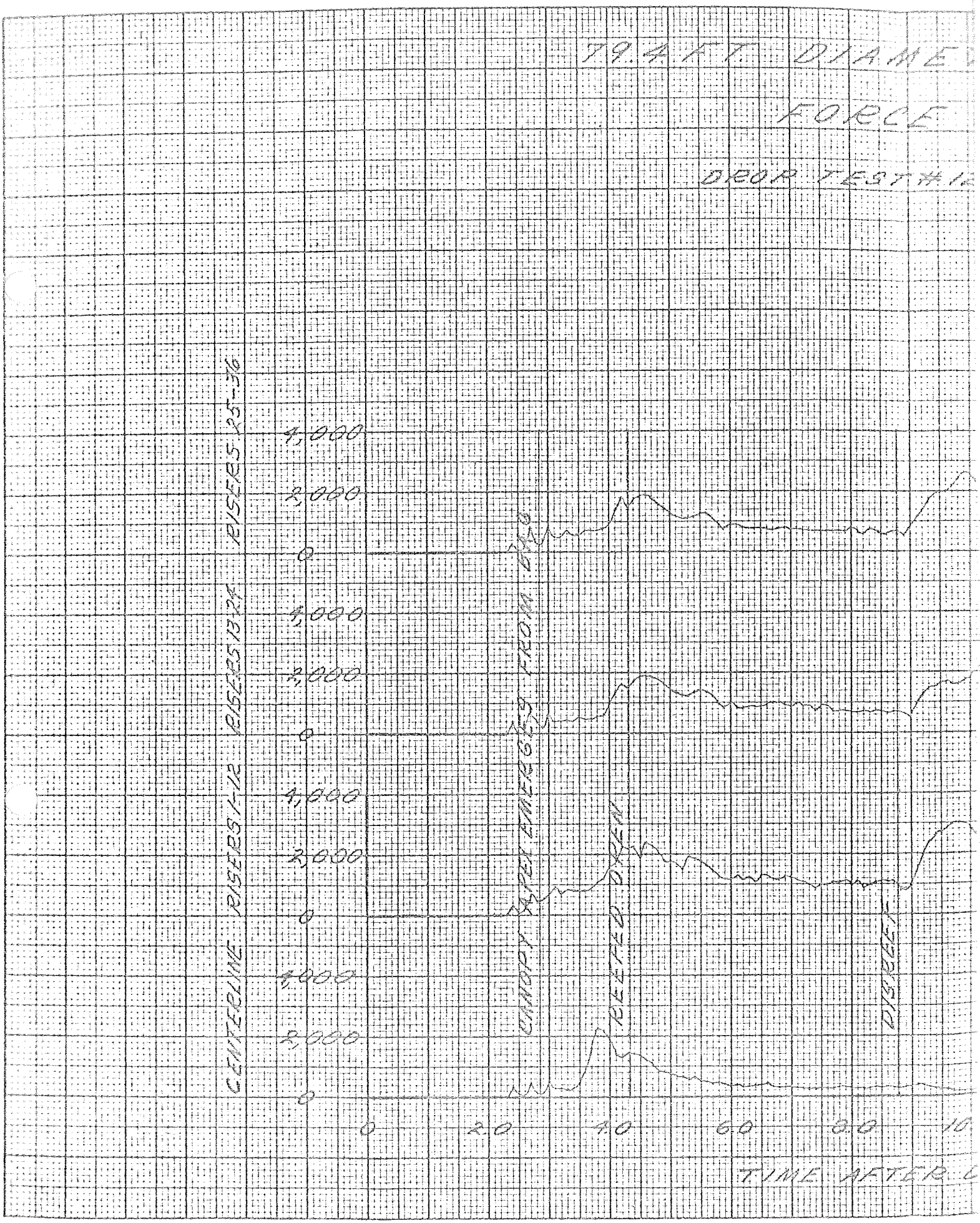

79.4 FT. DIAME
FORCE
DROP TEST #12
CENTERLINE RISERS 1-12 RISERS 13-24 RISERS 25-36
4,000
2,000
0
CANOPY APEX EMERGES FROM BAG
REEFED OPEN
DISREEF
0
2.0
4.0
6.0
8.0
10
TIME AFTER

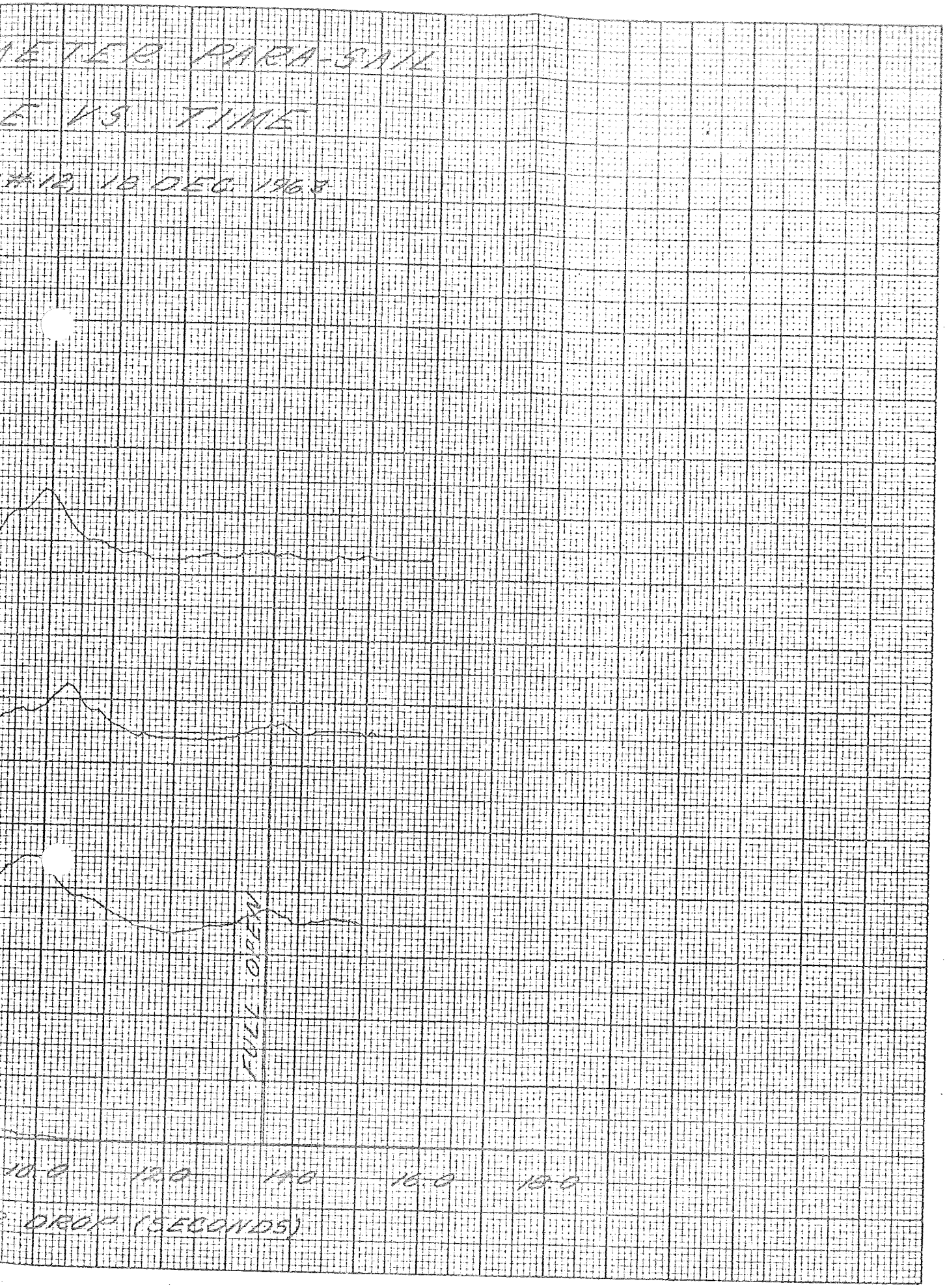
TE TEG PARA-SAIL
E VS TIME
#13 12 DEC. 1965
FULL OPEN
10.0
12.0
14.0
16.0
18.0
DROP (SECONDS)

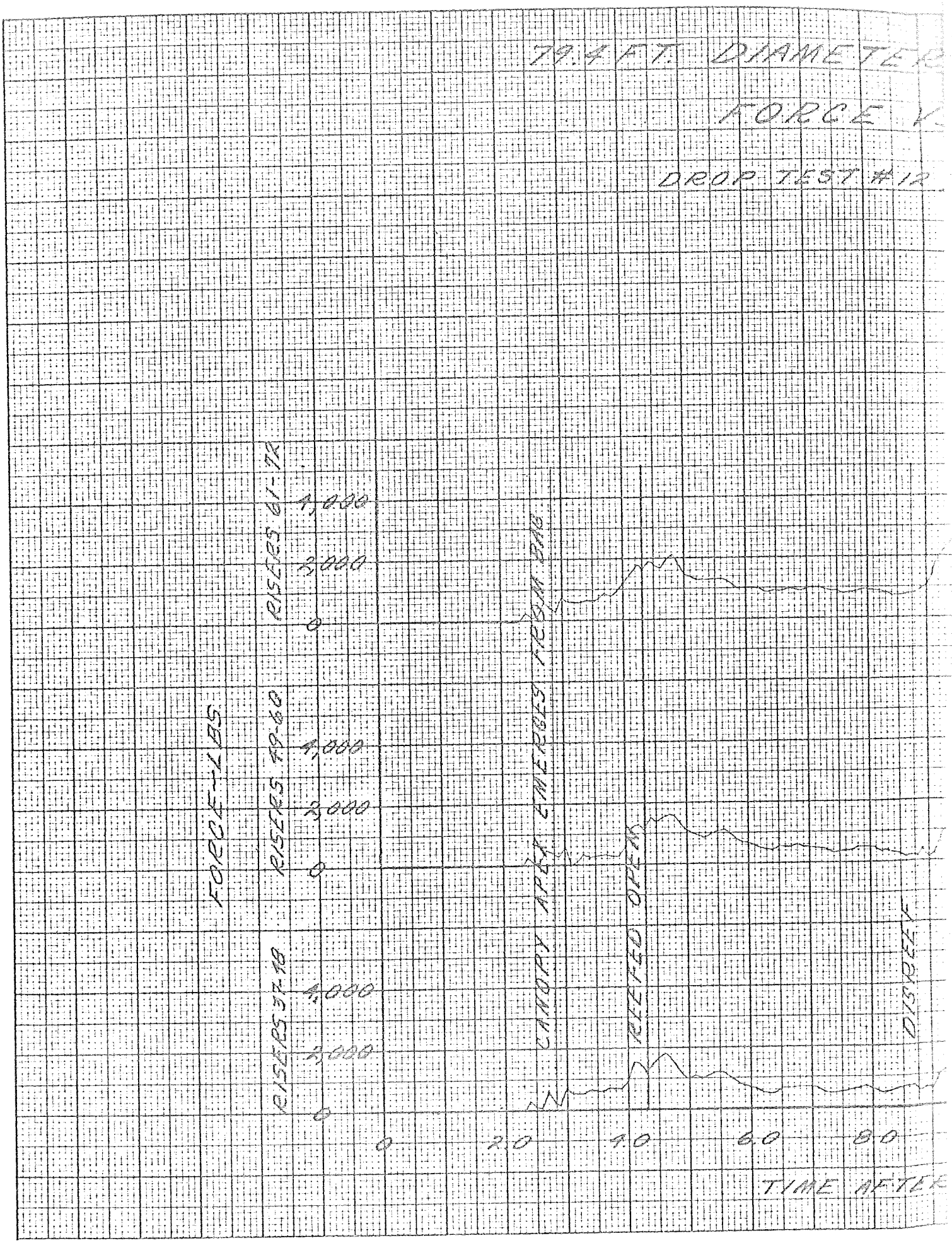
79.4 FT. DIAMETER
FORCE V
DROP TEST #12
FORCE-LBS
RISERS 61-72
RISERS 49-60
RISERS 37-18
4,000
2,000
0
CANOPY APEX EMERGES FROM BAG
REEFED OPEN
DISREEF
0
2.0
4.0
6.0
8.0
TIME AFTER

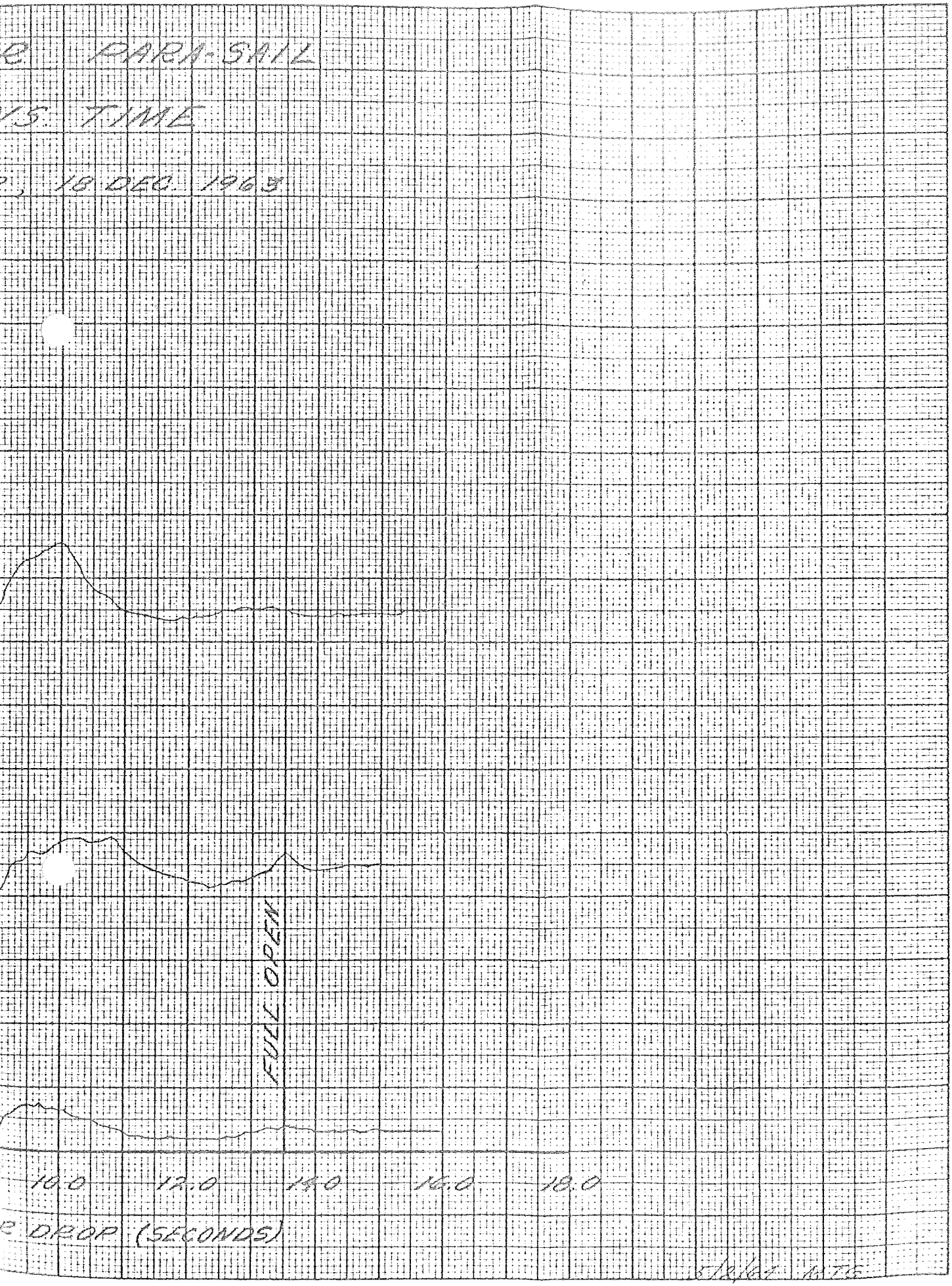
E PARA-SAIL
VS. TIME
, 18 DEC. 1963
FULL OPEN
10.0
12.0
14.0
16.0
18.0
E DROP (SECONDS)

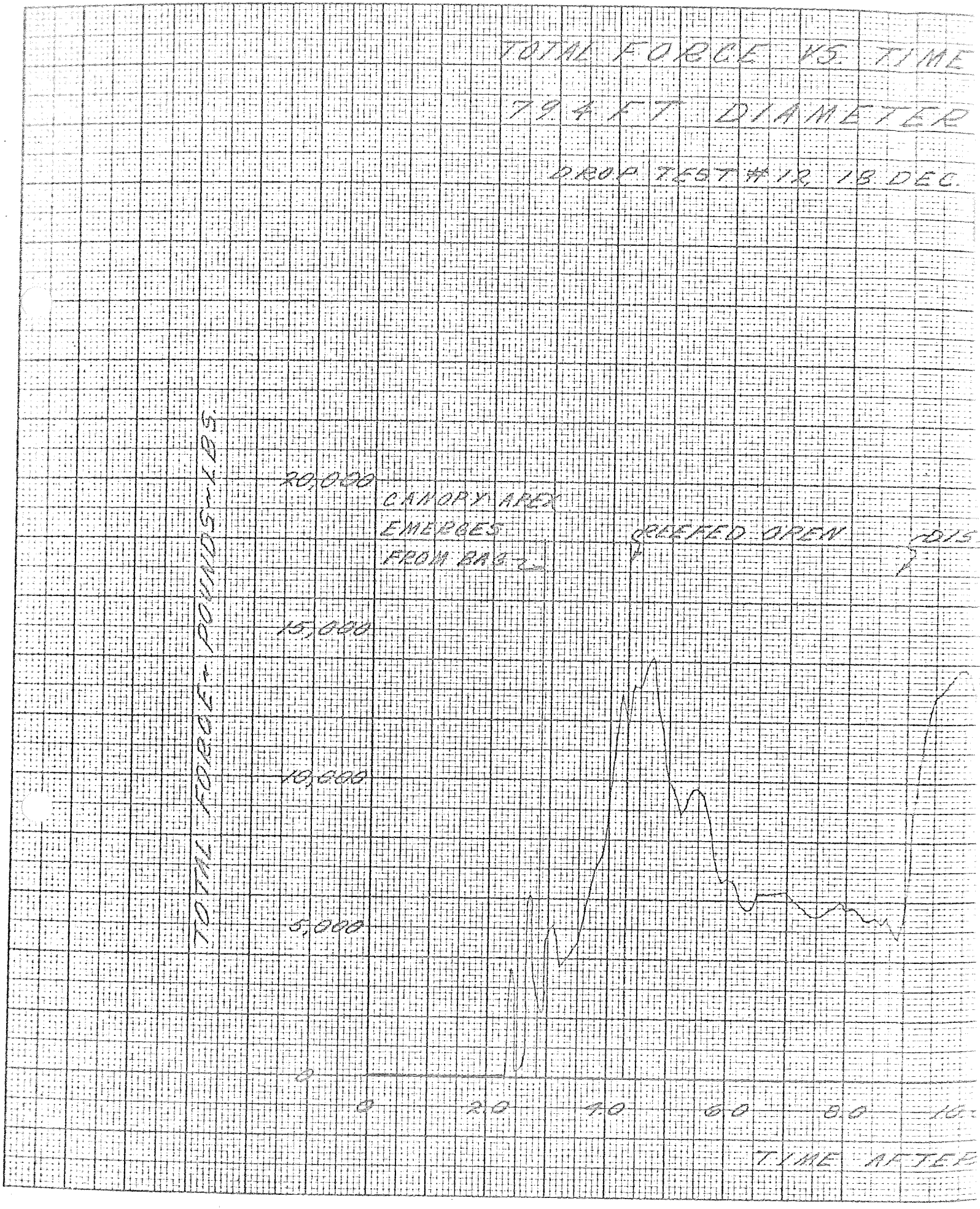
TOTAL FORCE VS. TIME
79.4 FT. DIAMETER
DROP TEST #12, 18 DEC.
TOTAL FORCE - POUNDS ~ LBS.
20,000
15,000
10,000
5,000
0
CANOPY APEX
EMERGES
FROM BAG
REEFED OPEN
0
2.0
4.0
6.0
8.0
TIME AFTER

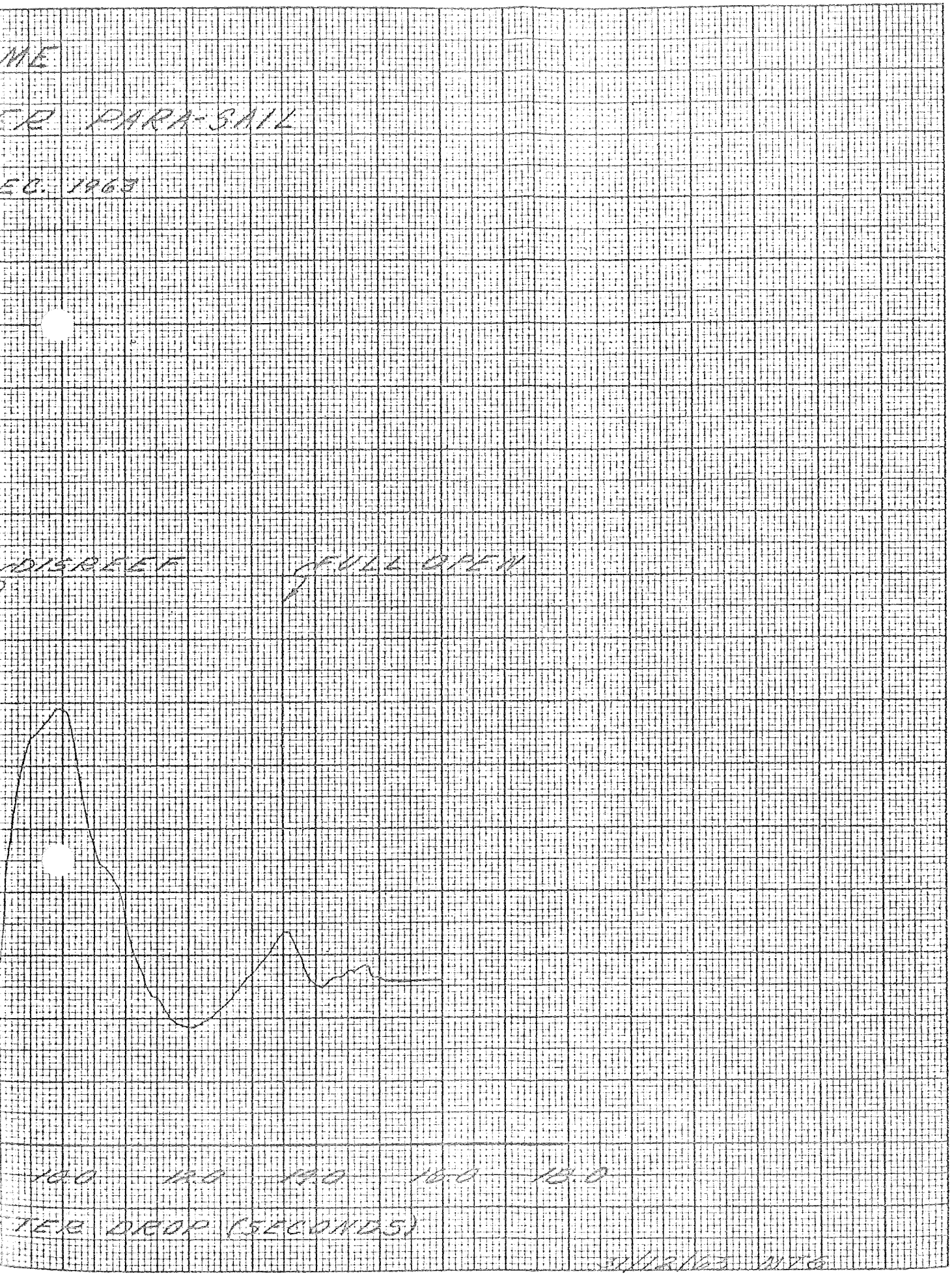
ME
ER PARA-SAIL
EC. 1963
DISREEF
FULL OPEN
10.0
12.0
14.0
16.0
18.0
TER DROP (SECONDS)

K&E AUTOTIME 4 INCH 359-11L KEUFFEL & ESSER CO. MADE IN U.S.A.

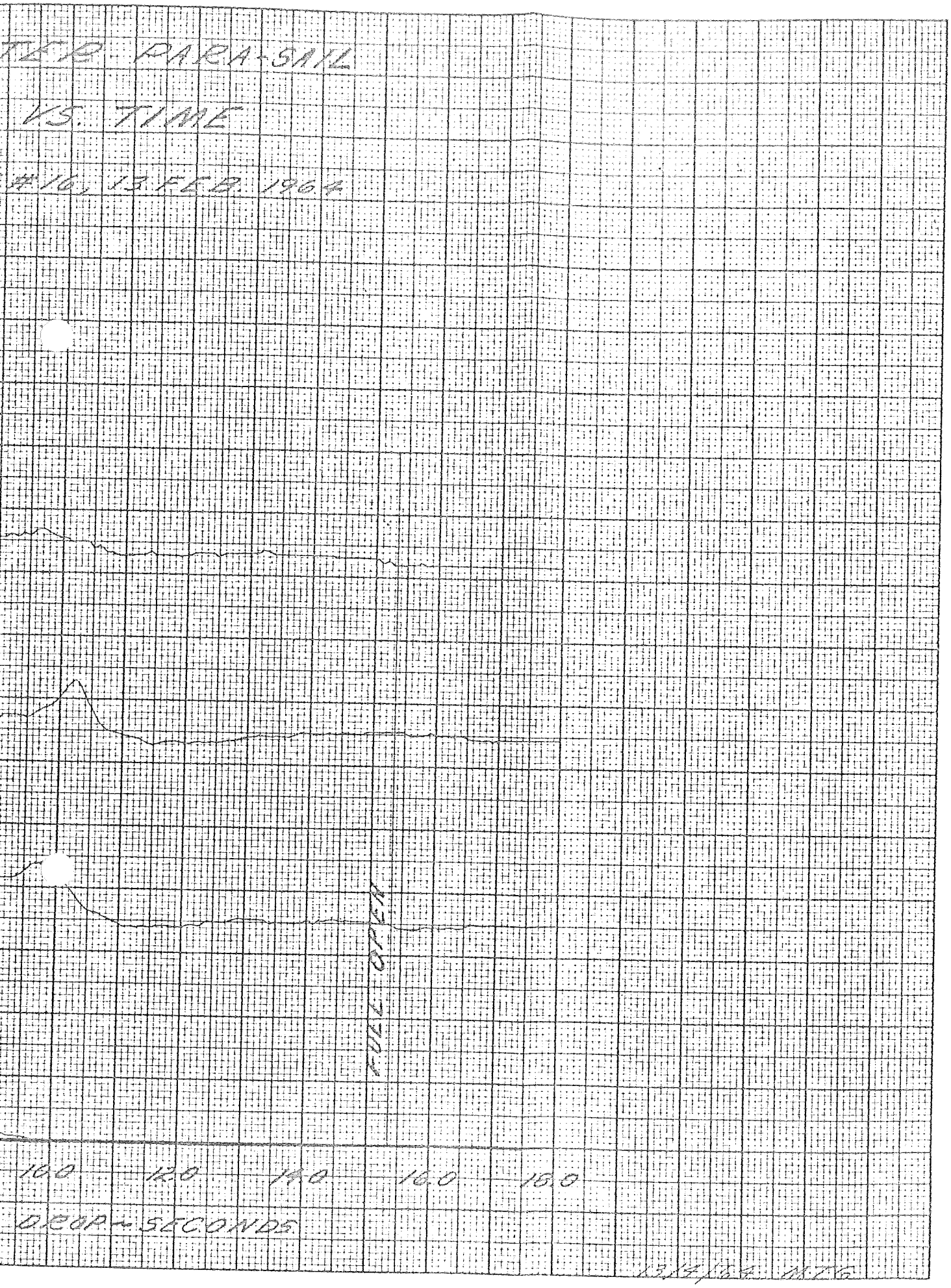
TER PARA-SAIL
VS. TIME
#16, 13 FEB. 1964
FULL OPEN
10.0
12.0
14.0
16.0
18.0
DECAP - SECONDS

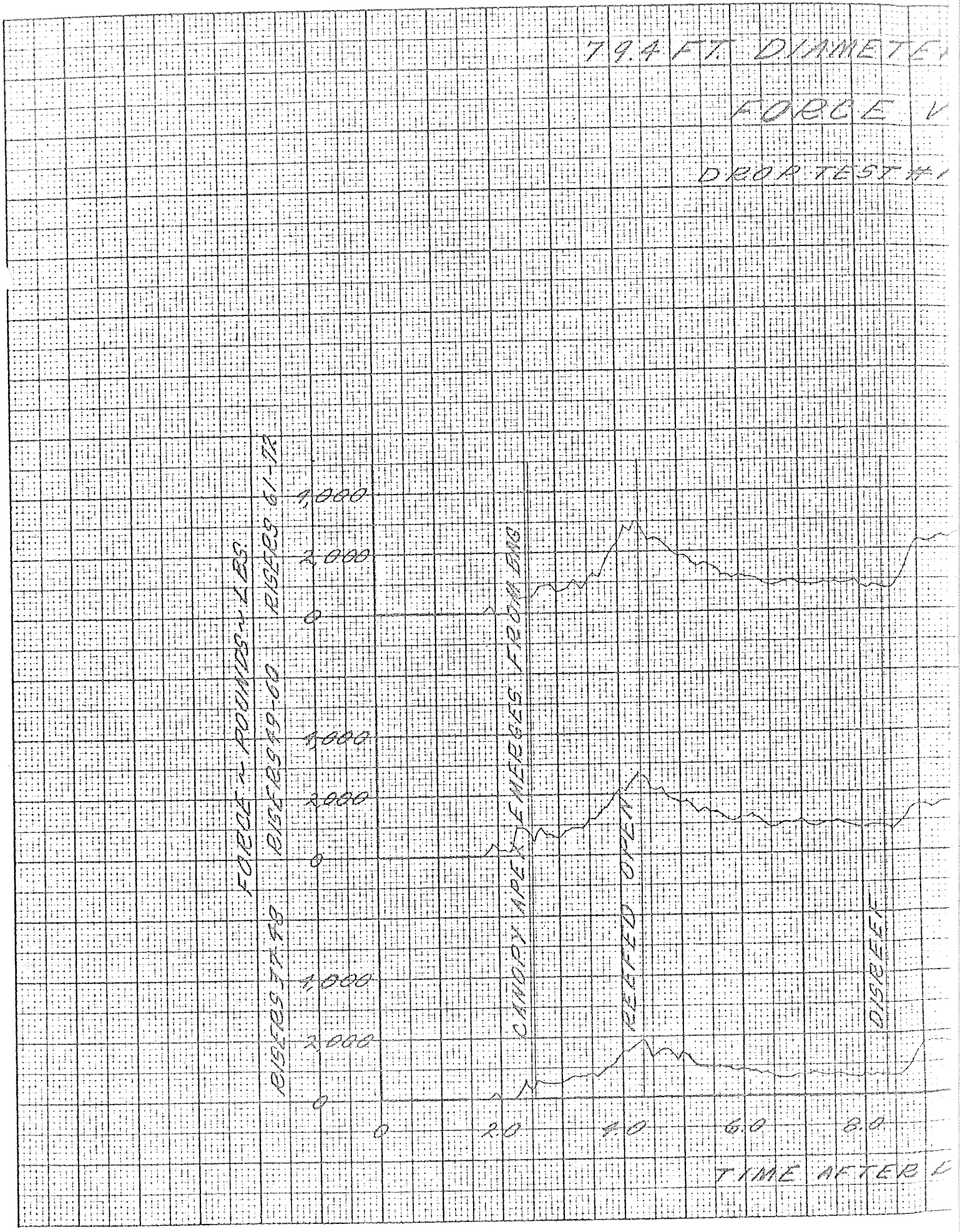

79.4 FT. DIAMETE
FORCE V
DROP TEST #
FORCE ~ POUNDS ~ LBS.
RISERS 61-72
RISERS 49-60
RISERS 37-48
4,000
2,000
0
CANOPY APEX EMERGES FROM BAG
REEFED OPEN
DISREEF
0
2.0
4.0
6.0
8.0
TIME AFTER

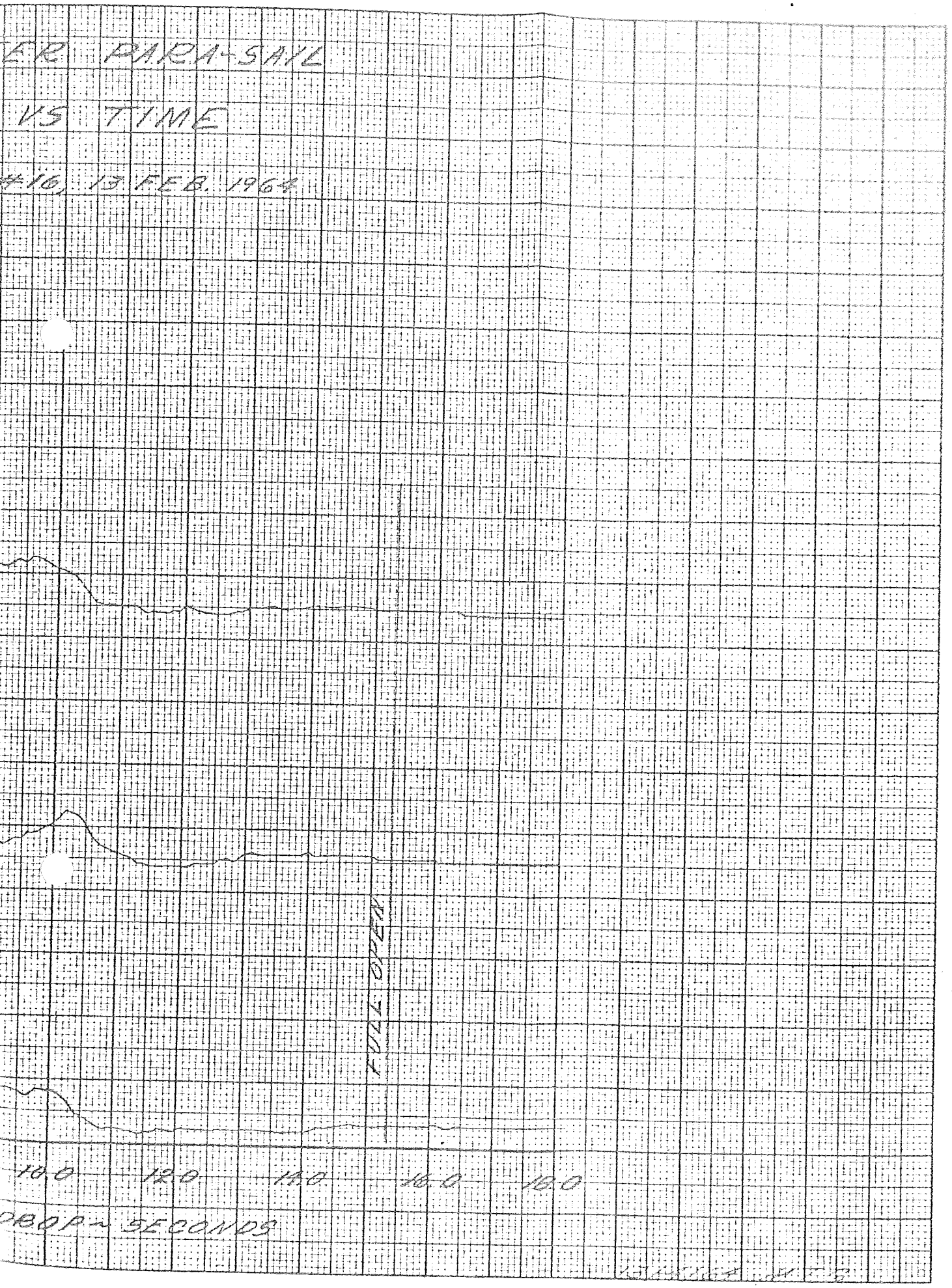
ER PARA-SAIL
VS TIME
#16, 13 FEB. 1964
FULL OPEN
10.0
12.0
14.0
16.0
18.0
OBOP ~ SECONDS

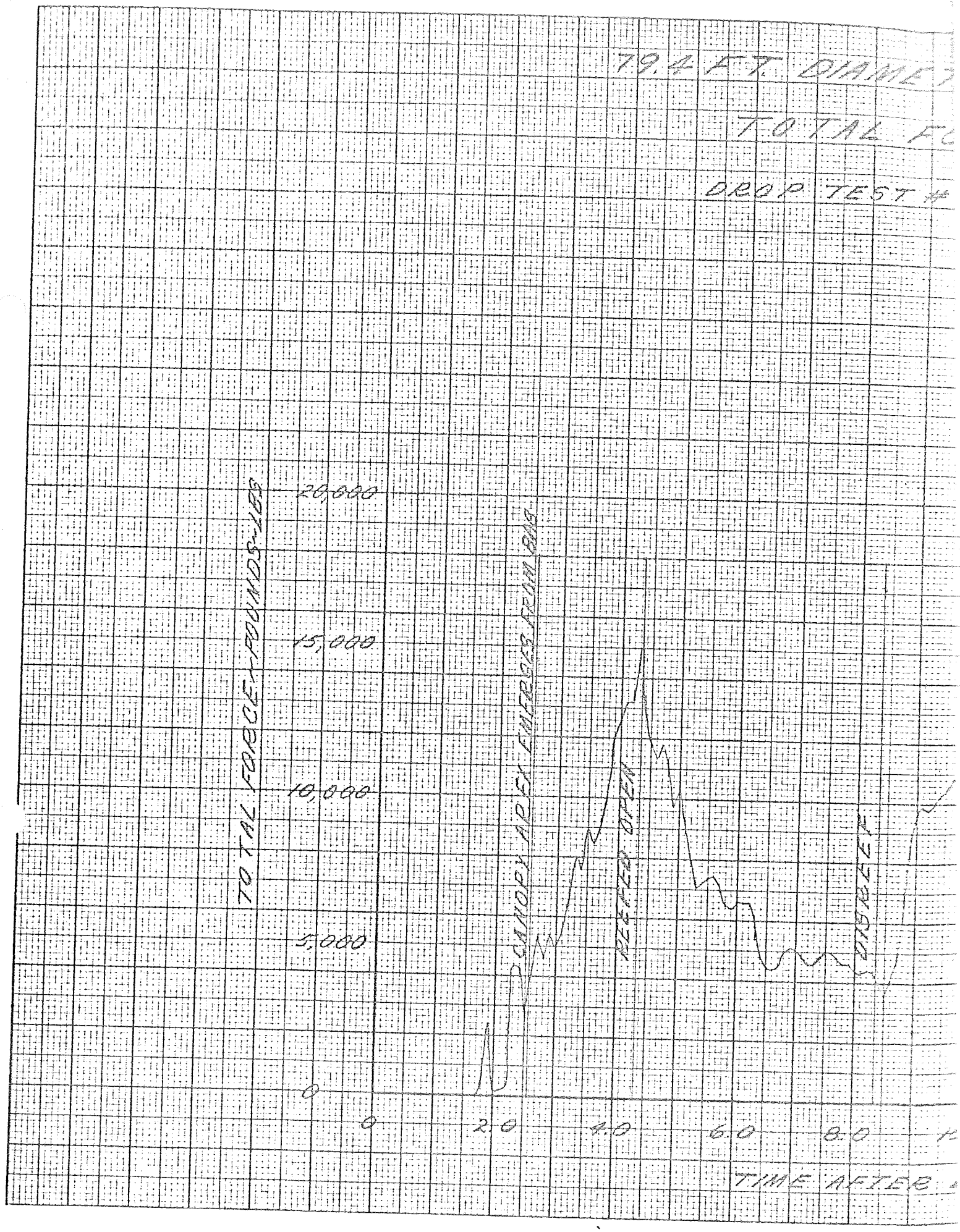

79.4 FT. DIAMET
TOTAL FO
DROP TEST #
TOTAL FORCE-POUNDS-LBS
20,000
15,000
10,000
5,000
0
0
2.0
4.0
6.0
8.0
CANOPY AREA EMERGES FROM BAG
REEFED OPEN
DISREEF
TIME AFTER

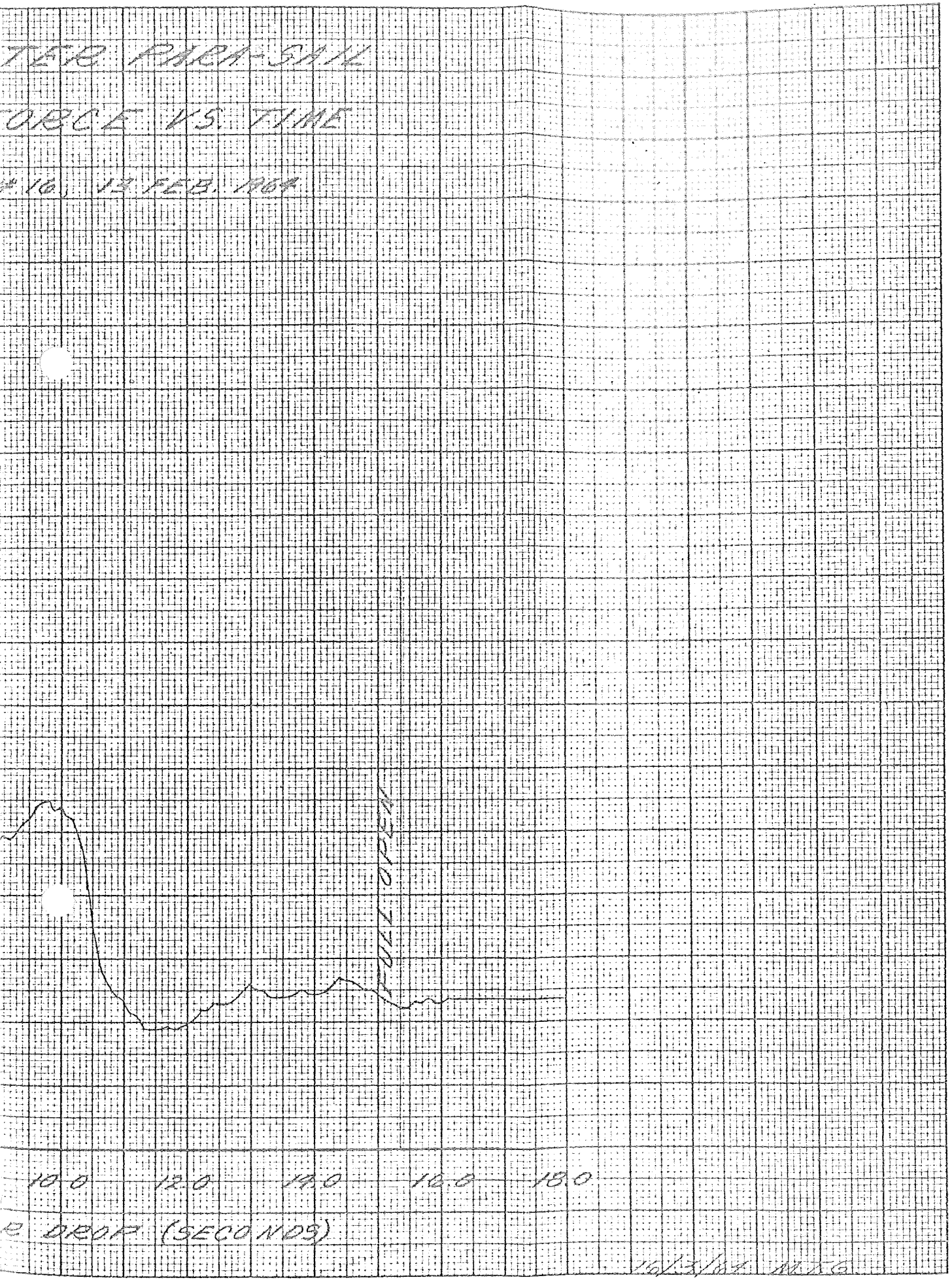
TER PARA-SAIL
ORCE VS. TIME
#16, 13 FEB. 1964
FULL OPEN
10.0
12.0
14.0
16.0
18.0
R DROP (SECONDS)
16/3/64 M.T.G.

79.4 FT. DIAMETE
FORCE V
DROP TEST #18.
FORCE ~ POUNDS
CENTERLINE RISERS 1-12 RISERS 13-24 RISERS 25-36
4,000
2,000
0
4,000
2,000
0
4,000
2,000
0
4,000
2,000
0
CANOPY MOST EMERGES FROM BAG
REEFED OPEN
DISREEF
0
2.0
4.0
6.0
8.0
10.
TIME AFTER

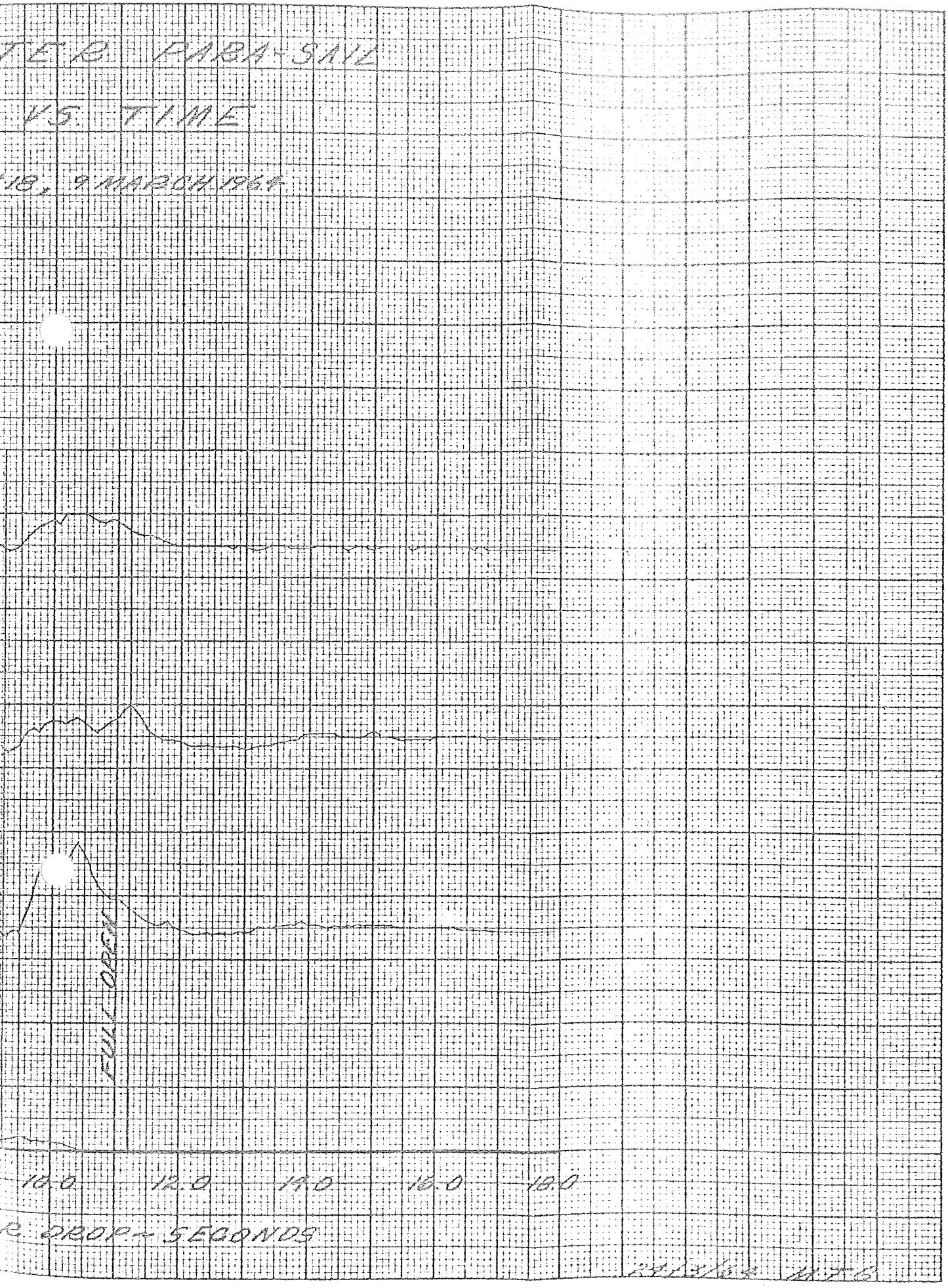
TE R PARA-SAIL
VS. TIME
18, 9 MARCH 1965
FULL DROP
10.0
12.0
14.0
16.0
18.0
DROP-SECONDS

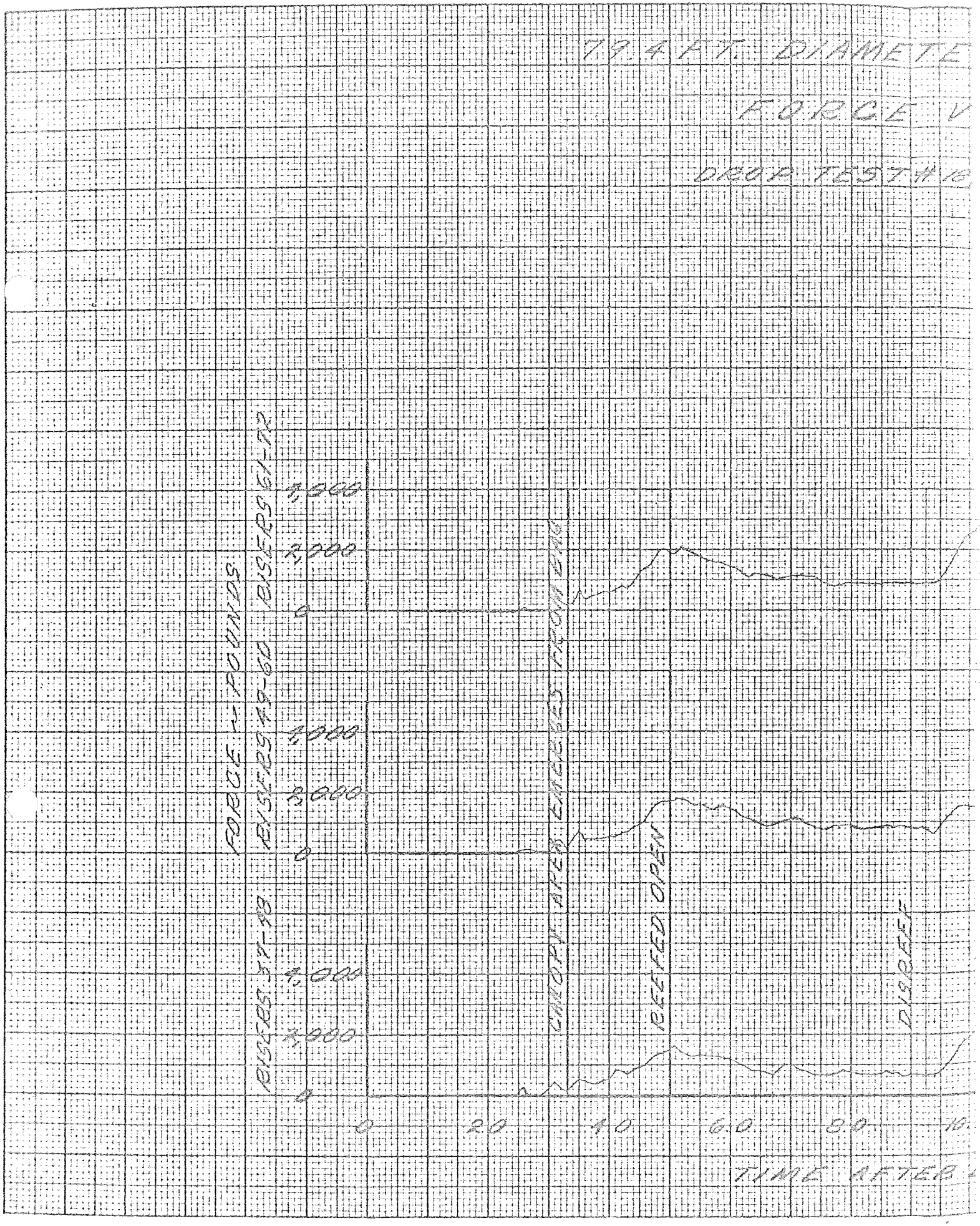

79.4 FT. DIAMETE
FORCE V
DROP TEST # 18
FORCE ~ POUNDS
RISERS 37-48
RISERS 49-60
RISERS 61-72
4,000
2,000
0
CANOPY APEX EMERGES FROM BAG
REEFED OPEN
DISREEF
0
20
40
60
80
10
TIME AFTER

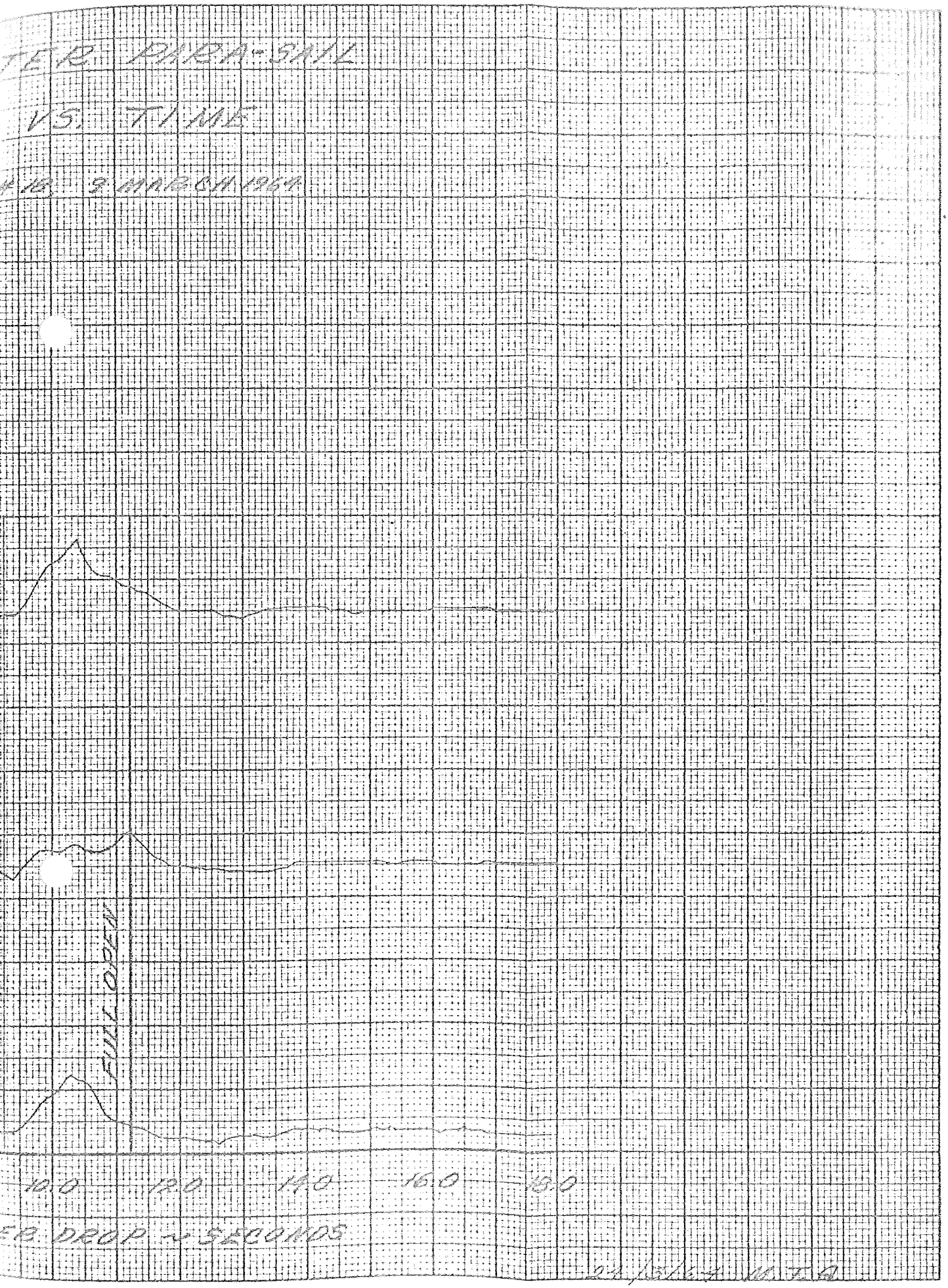
TER PARA-SAIL
VS. TIME
#18, 9 MARCH 1964
FULL OPEN
10.0
12.0
14.0
16.0
18.0
ER DROP ~ SECONDS

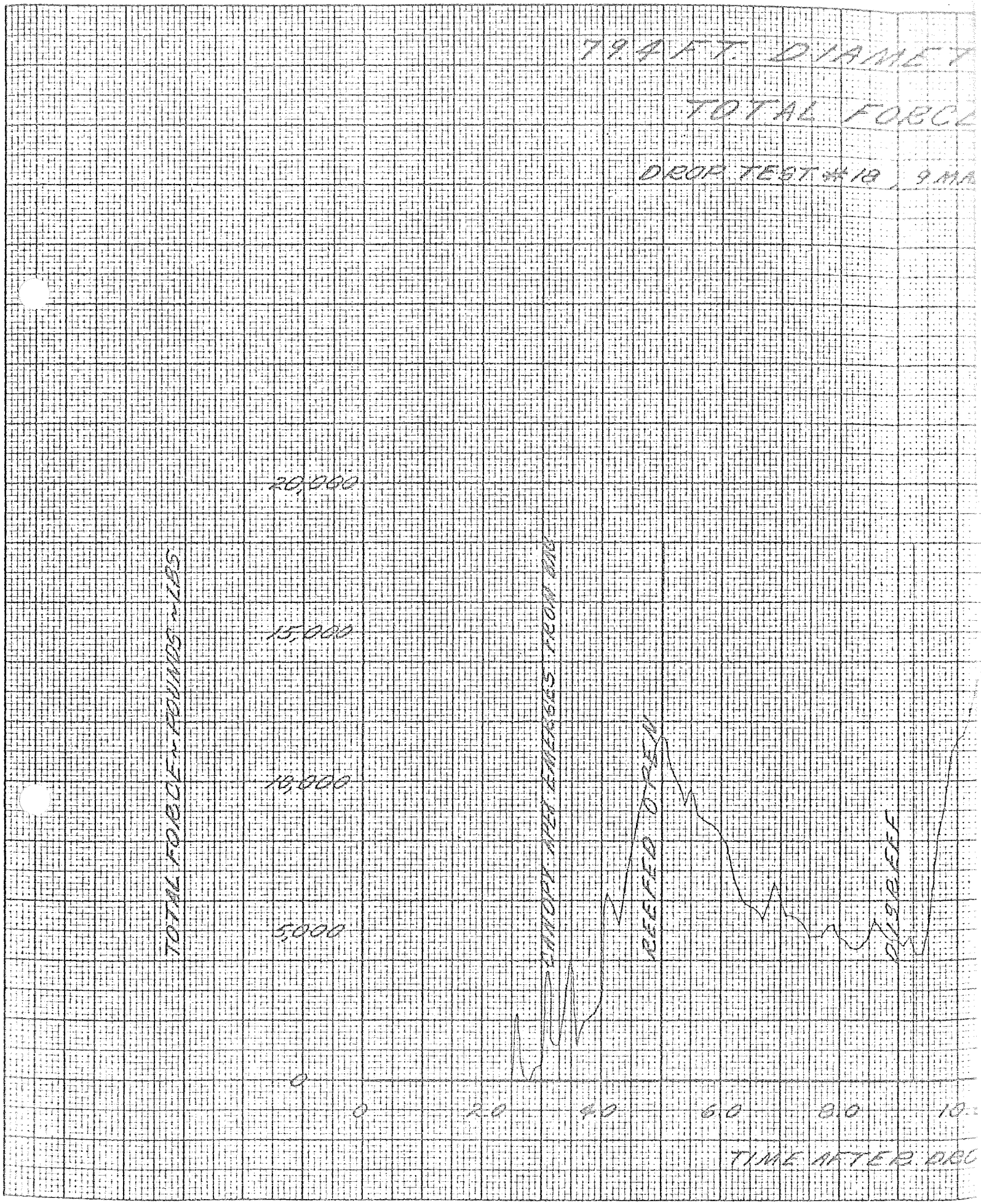

79.4 FT. DIAMET
TOTAL FORCE
DROP TEST #18, 9 MA
TOTAL FORCE ~ POUNDS ~ LBS
20,000
15,000
10,000
5,000
0
CANOPY APEX EMERGES FROM BAG
REEFED OPEN
DISREEF
0
2.0
4.0
6.0
8.0
10.
TIME AFTER DRO

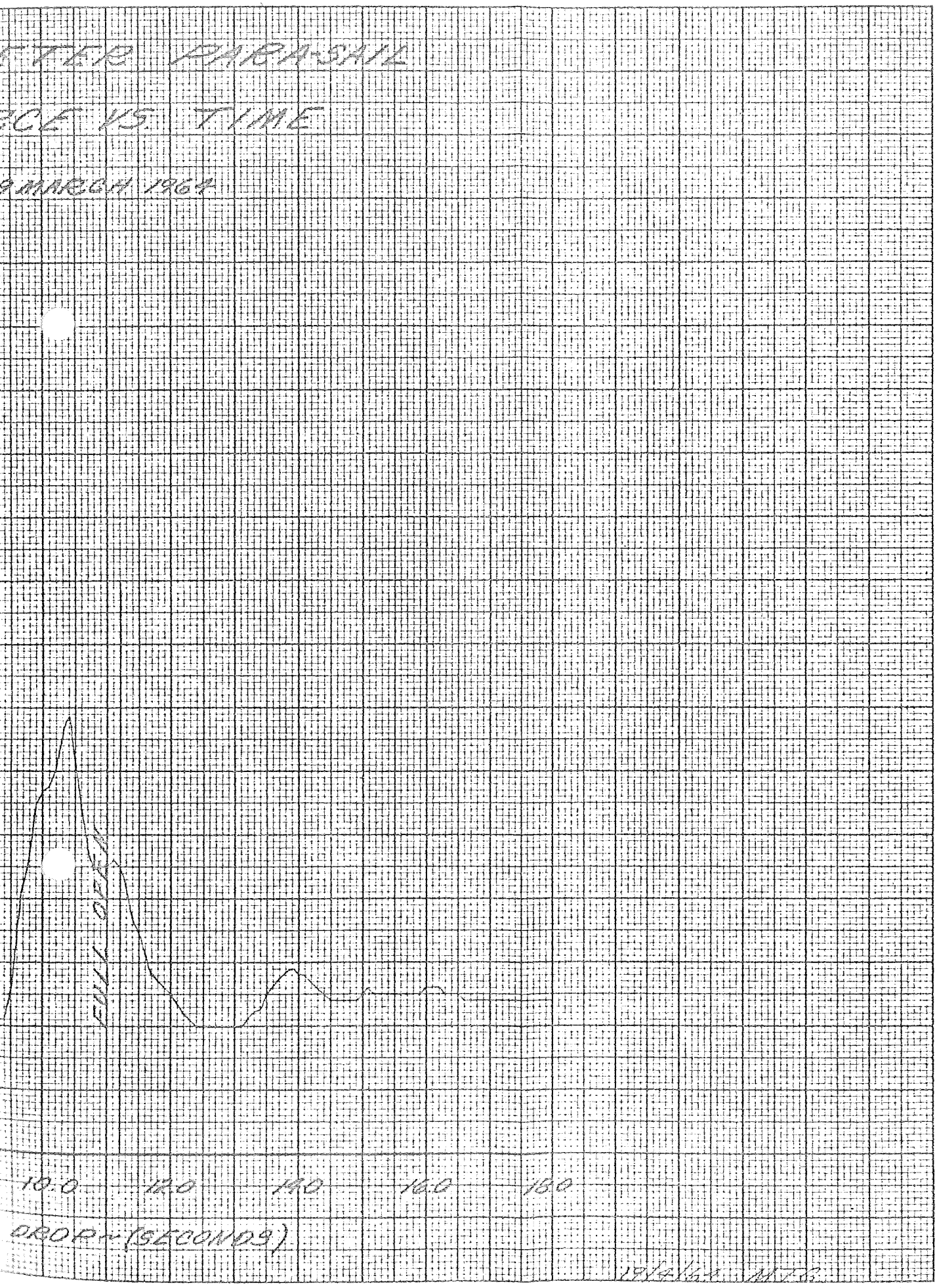
TTER PARA-SAIL
CE VS TIME
9 MARCH 1964
10.0
12.0
14.0
16.0
18.0
DROP - (SECONDS)

APPENDIX F

Para-Sail Drag Area Histories

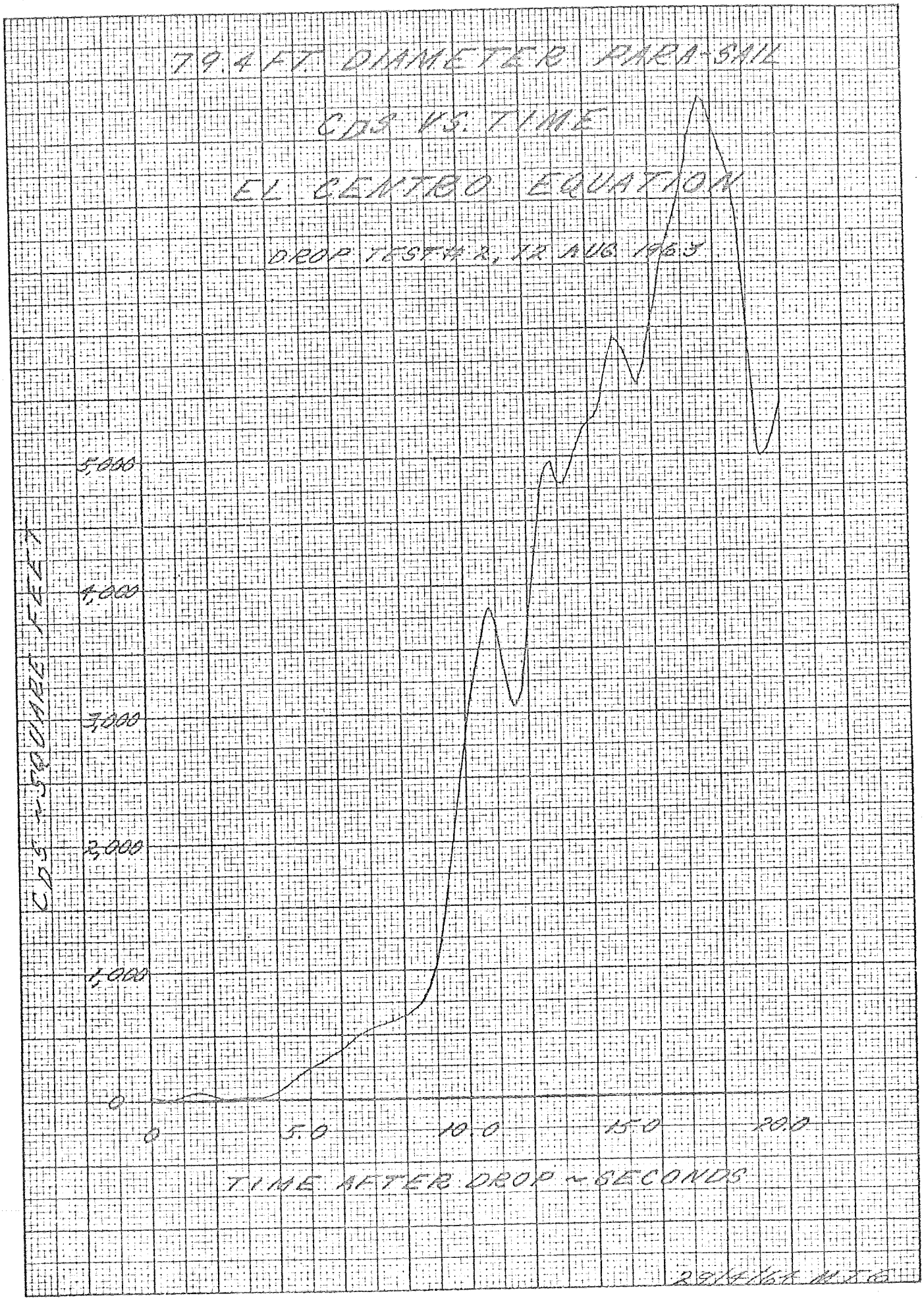

K+E 10 X 10 TO ½ INCH 46 1323
7 X 10 INCHES MADE IN U.S.A.
KEUFFEL & ESSER CO.

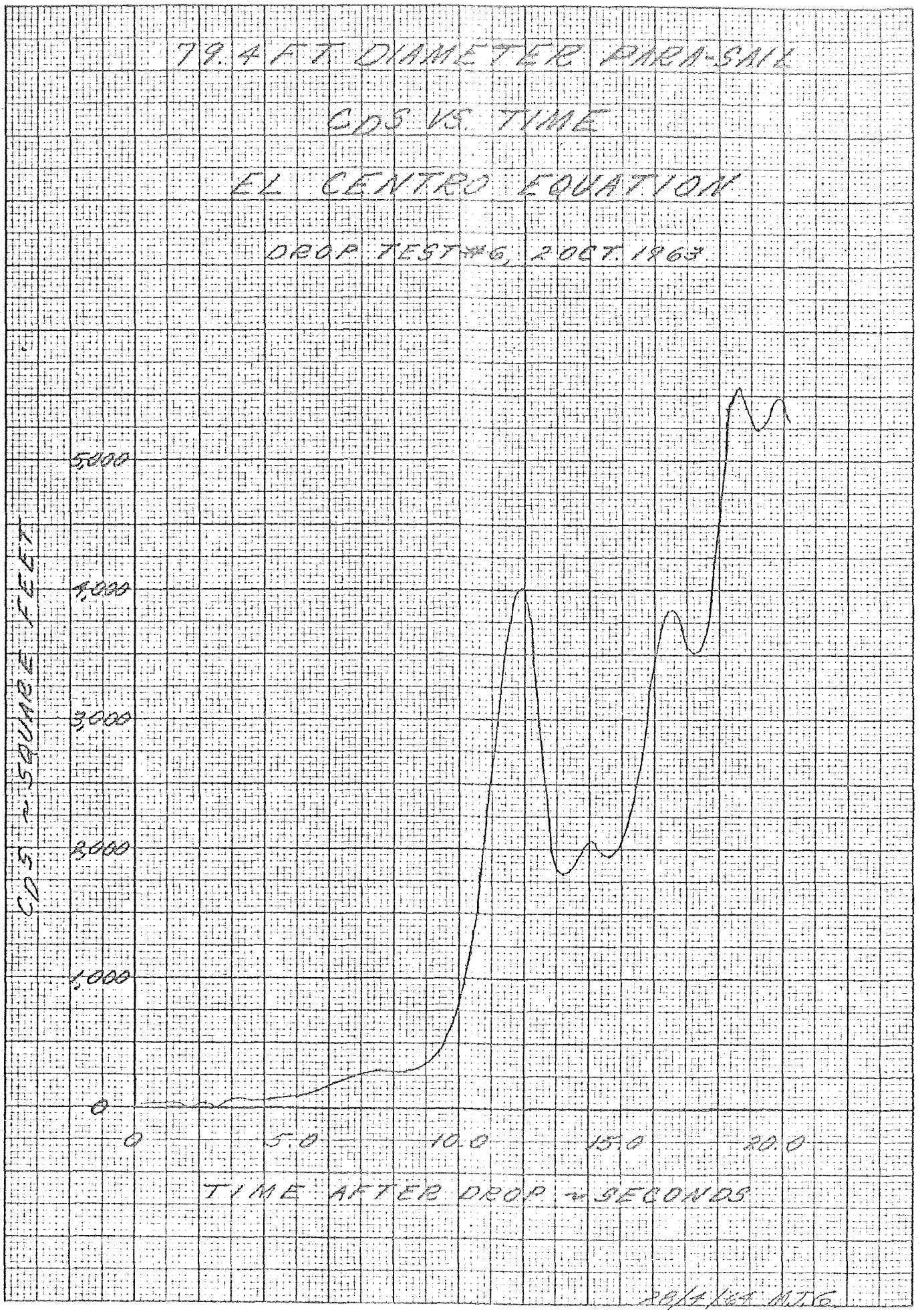

K+E 10 X 10 TO ½ INCH 46 1323
7 X 10 INCHES MADE IN U.S.A.
KEUFFEL & ESSER CO.

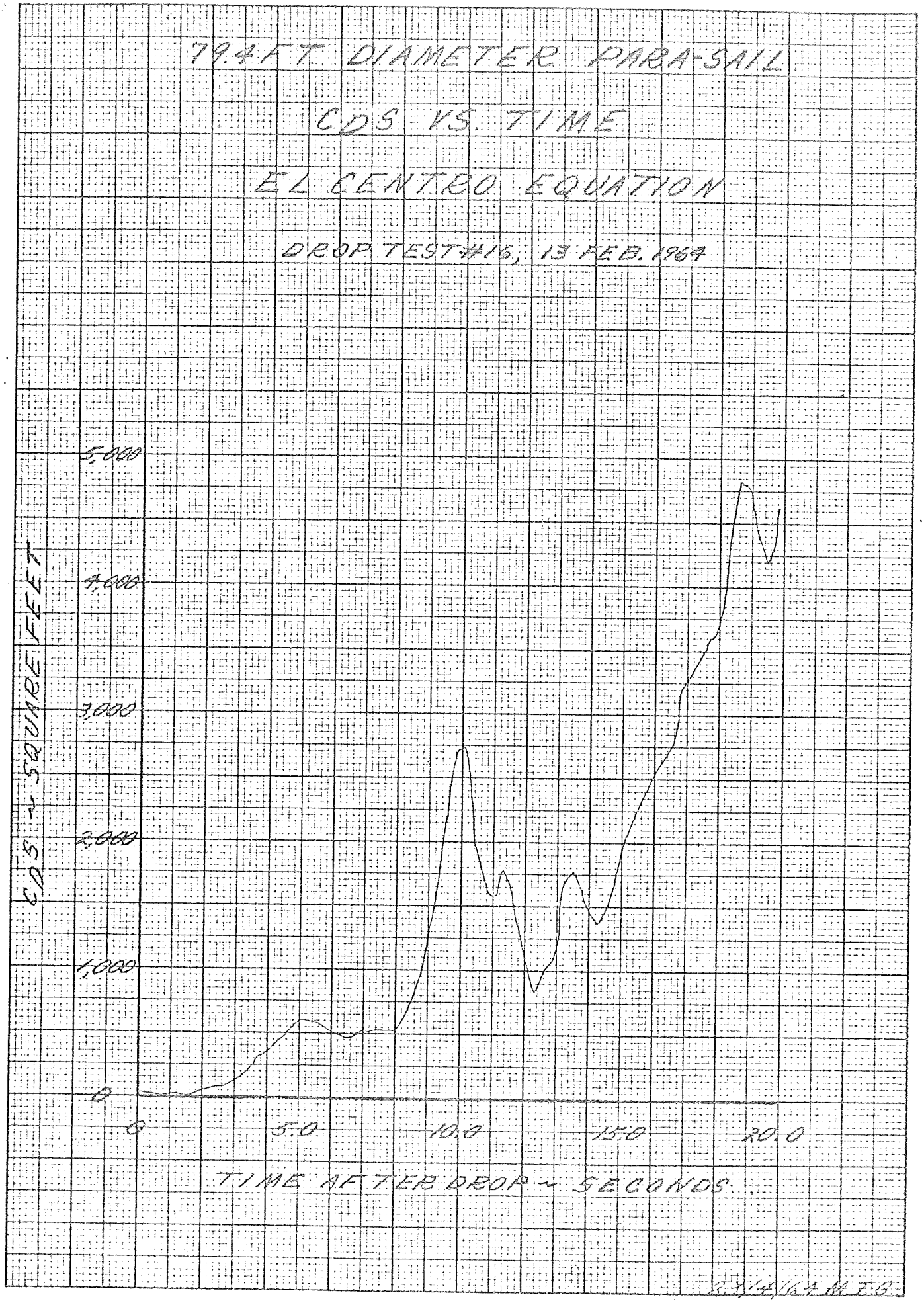
79.4 FT. DIAMETER PARA-SAIL
CDS VS. TIME
EL CENTRO EQUATION
DROP TEST #16, 13 FEB. 1964
CDS ~ SQUARE FEET
5,000
4,000
3,000
2,000
1,000
0
0
5.0
10.0
15.0
20.0
TIME AFTER DROP ~ SECONDS

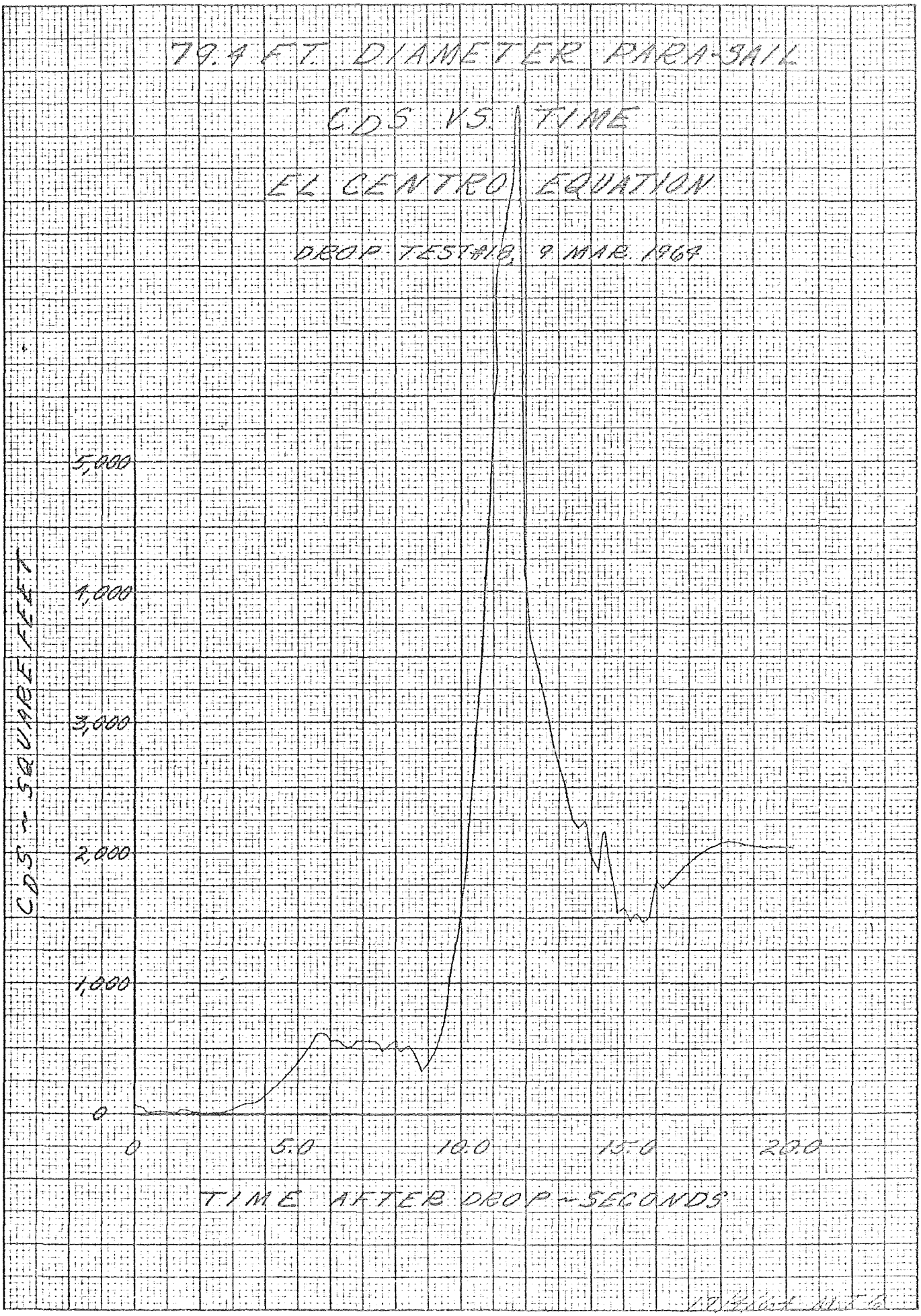
79.4 FT. DIAMETER PARA-SAIL
CDS VS. TIME
EL CENTRO EQUATION
DROP TEST #18, 9 MAR. 1967
CDS - SQUARE FEET
5,000
4,000
3,000
2,000
1,000
0
0
5.0
10.0
15.0
20.0
TIME AFTER DROP - SECONDS

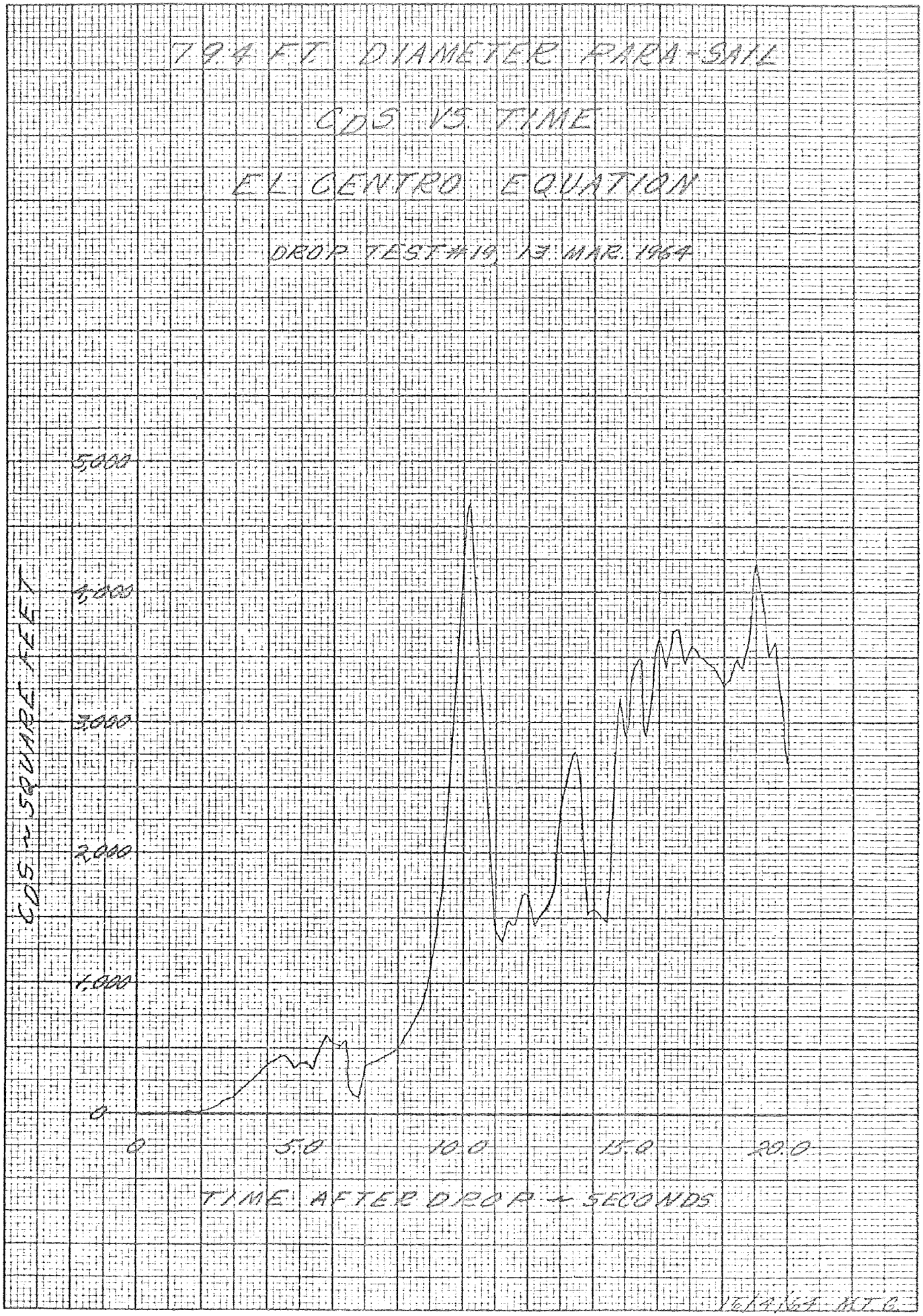
79.4 FT. DIAMETER PARA-SAIL
CDS VS. TIME
EL CENTRO EQUATION
DROP TEST #19, 13 MAR. 1964
CDS ~ SQUARE FEET
5,000
4,000
3,000
2,000
1,000
0
0
5.0
10.0
15.0
20.0
TIME AFTER DROP ~ SECONDS
16/4/64 MTC

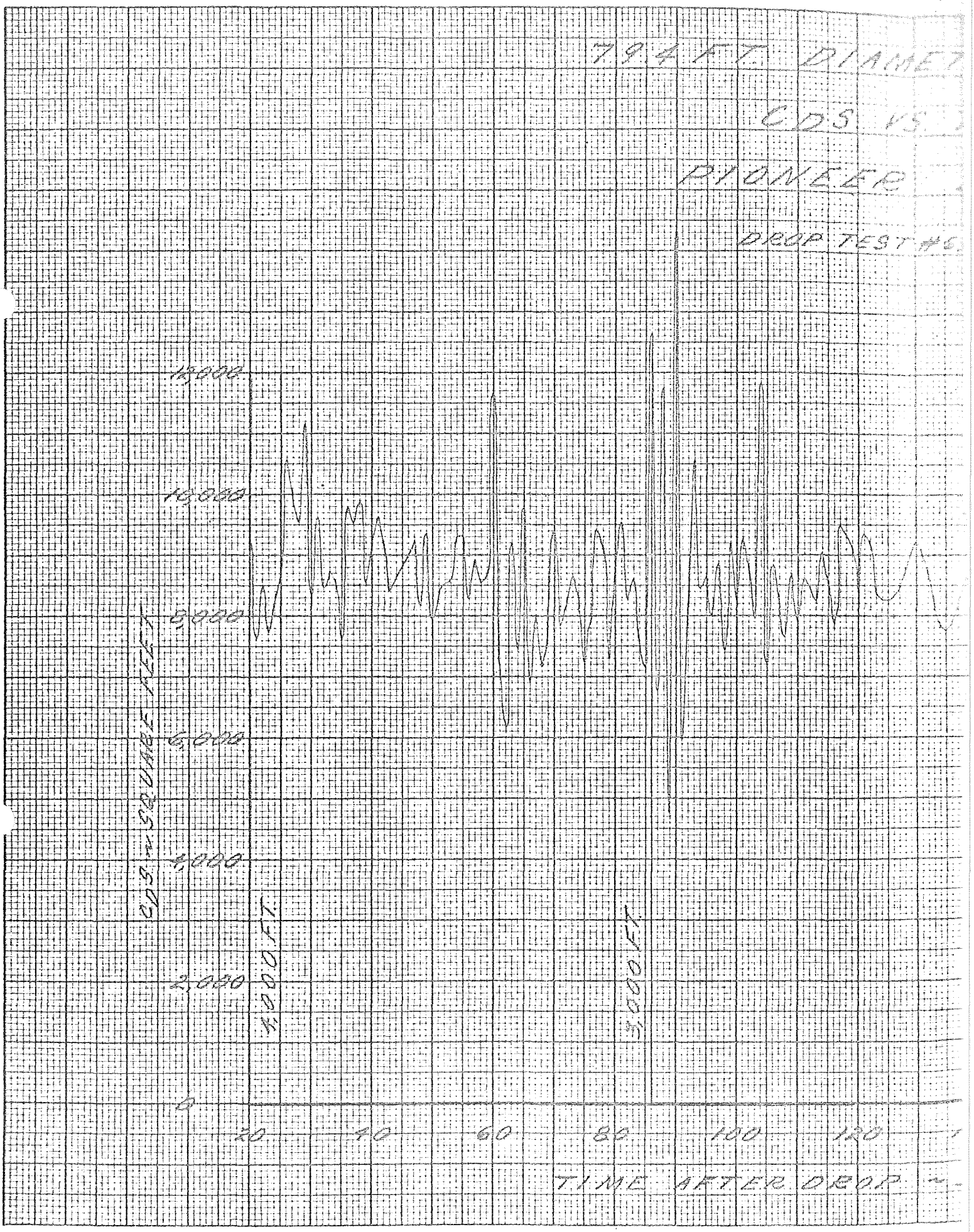
7.94 FT. DIAMET
CDS VS
PIONEER
DROP TEST #5
12,000
10,000
8,000
6,000
4,000
2,000
0
CDS - SQUARE FEET
8,000 FT.
3,000 FT.
20
40
60
80
100
120
TIME AFTER DROP

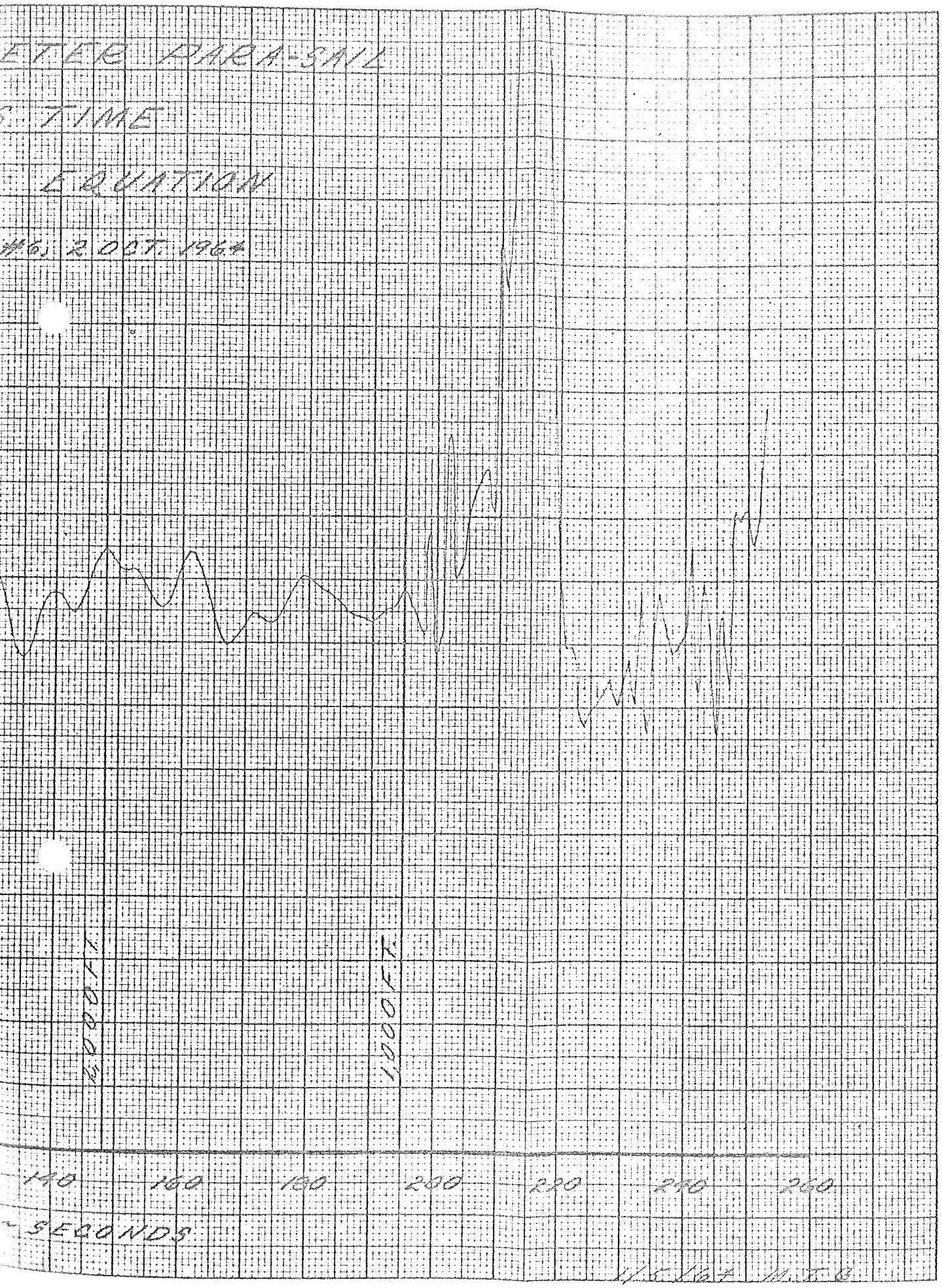
ETER PARA-SAIL
S TIME
EQUATION
#6, 2 OCT. 1964
2,000 FT.
1,000 FT.
140
160
180
200
220
240
260
SECONDS

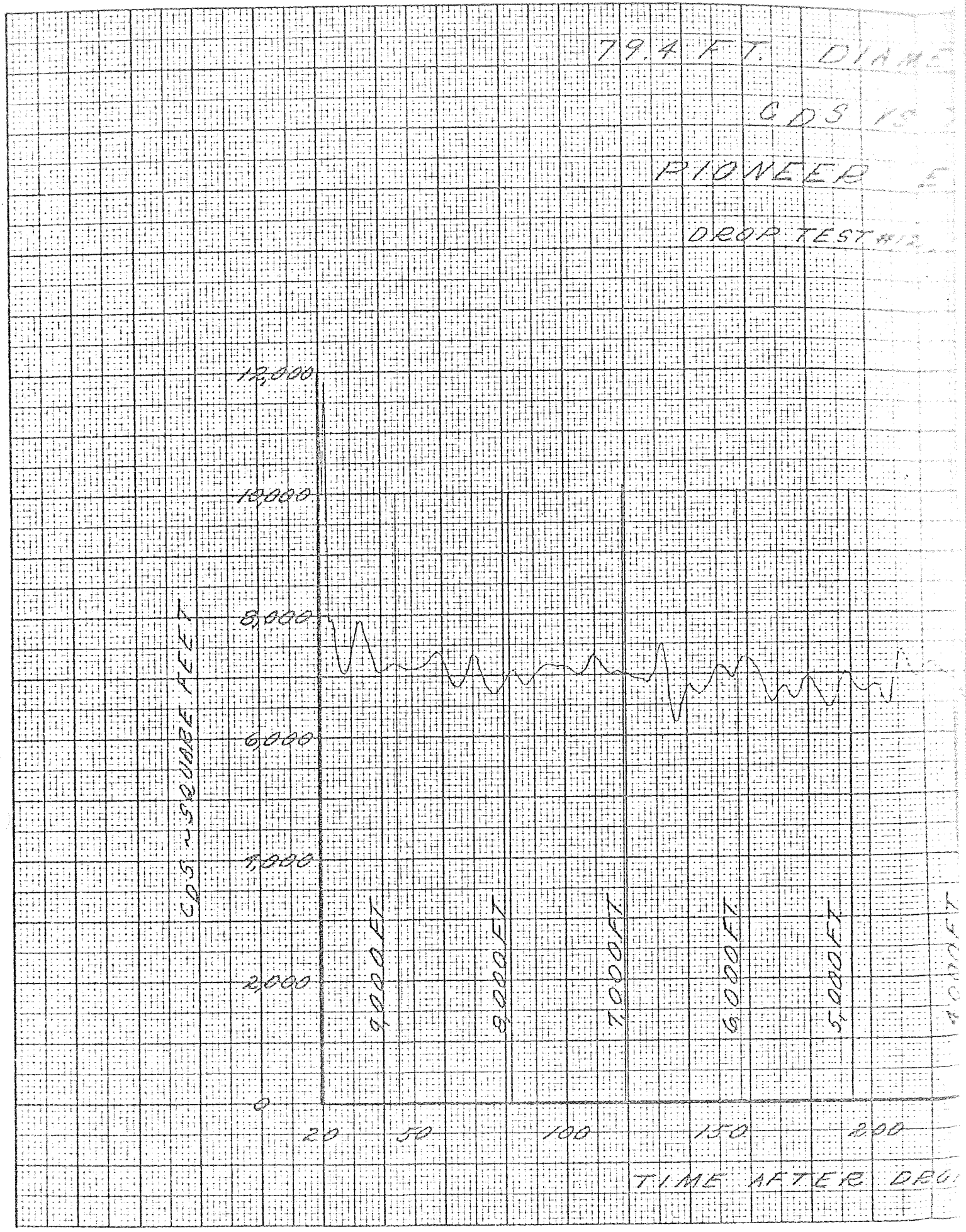

79.4 FT. DIAME
CDS VS
PIONEER E
DROP TEST #12
12,000
10,000
8,000
6,000
4,000
2,000
0
CDS ~ SQUARE FEET
9,000 FT
8,000 FT
7,000 FT
6,000 FT
5,000 FT
20
50
100
150
200
TIME AFTER DRO

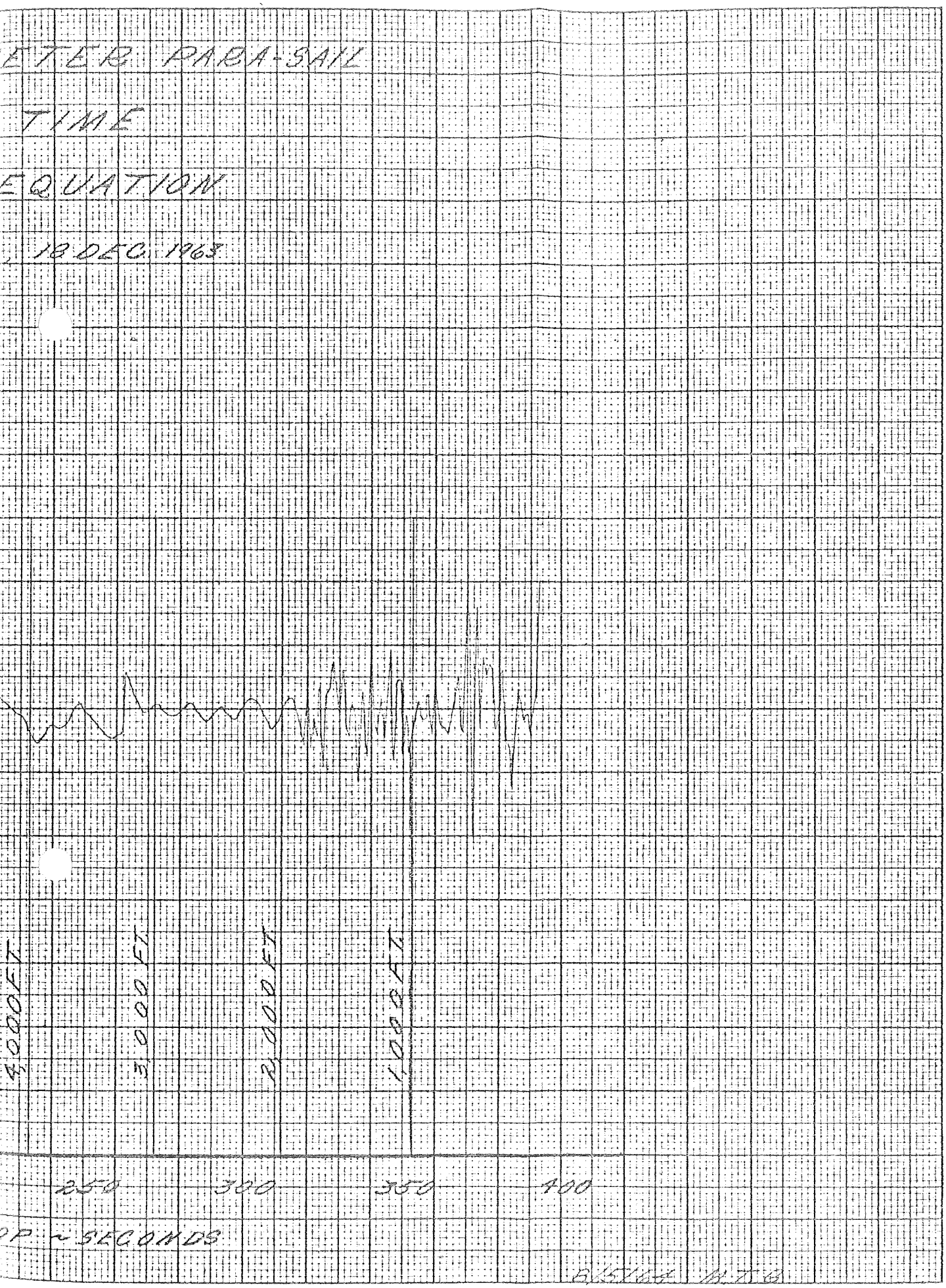
ETER PARA-SAIL
TIME
EQUATION
18 DEC 1963
4000 FT
3000 FT
2000 FT
1000 FT
250
300
350
400
P ~ SECONDS

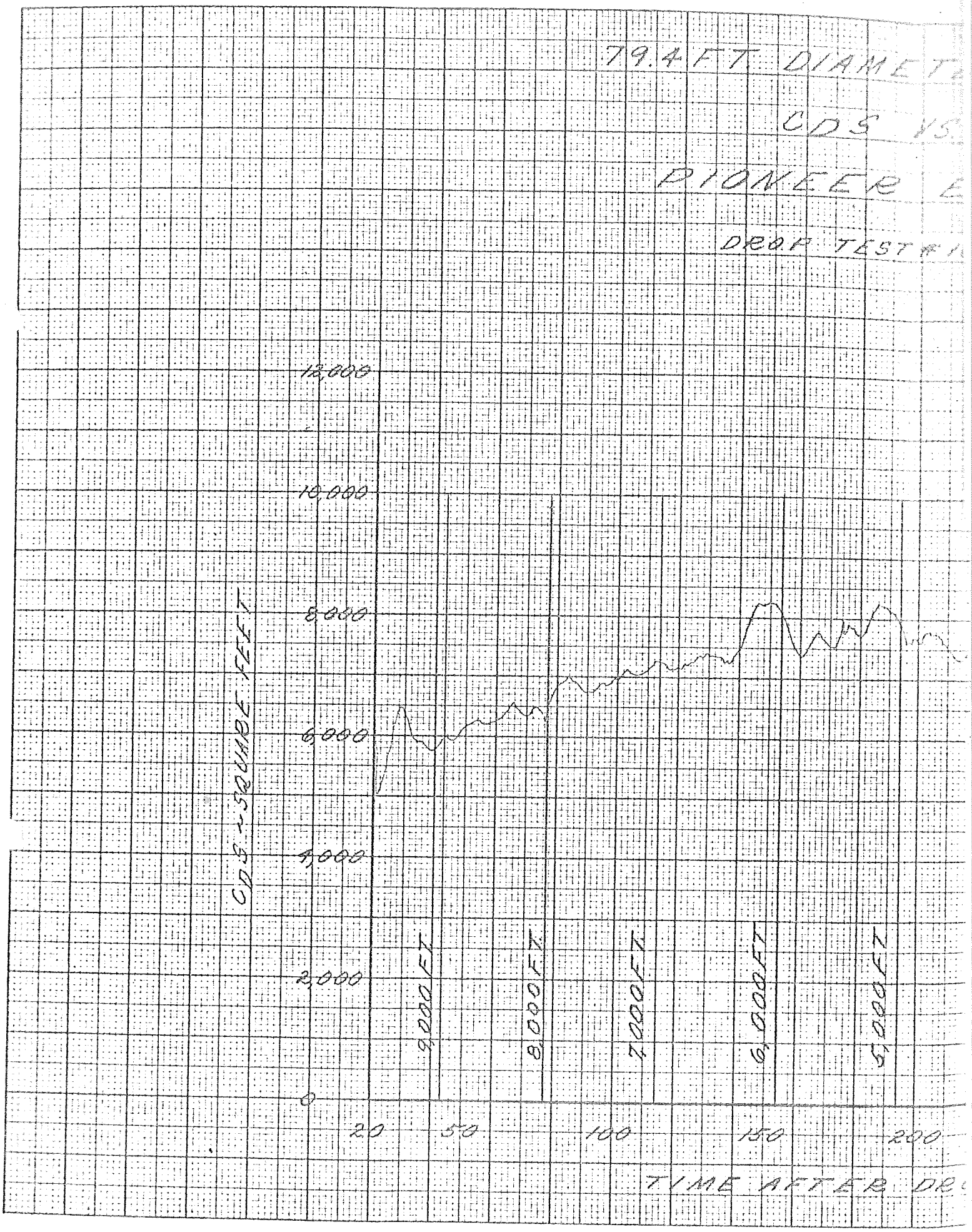
79.4 FT DIAMETE
CDS VS
PIONEER
DROP TEST #
12,000
10,000
8,000
6,000
4,000
2,000
0
CDS ~ SQUARE FEET
9,000 FT
8,000 FT
7,000 FT
6,000 FT
5,000 FT
20
50
100
150
200
TIME AFTER DR

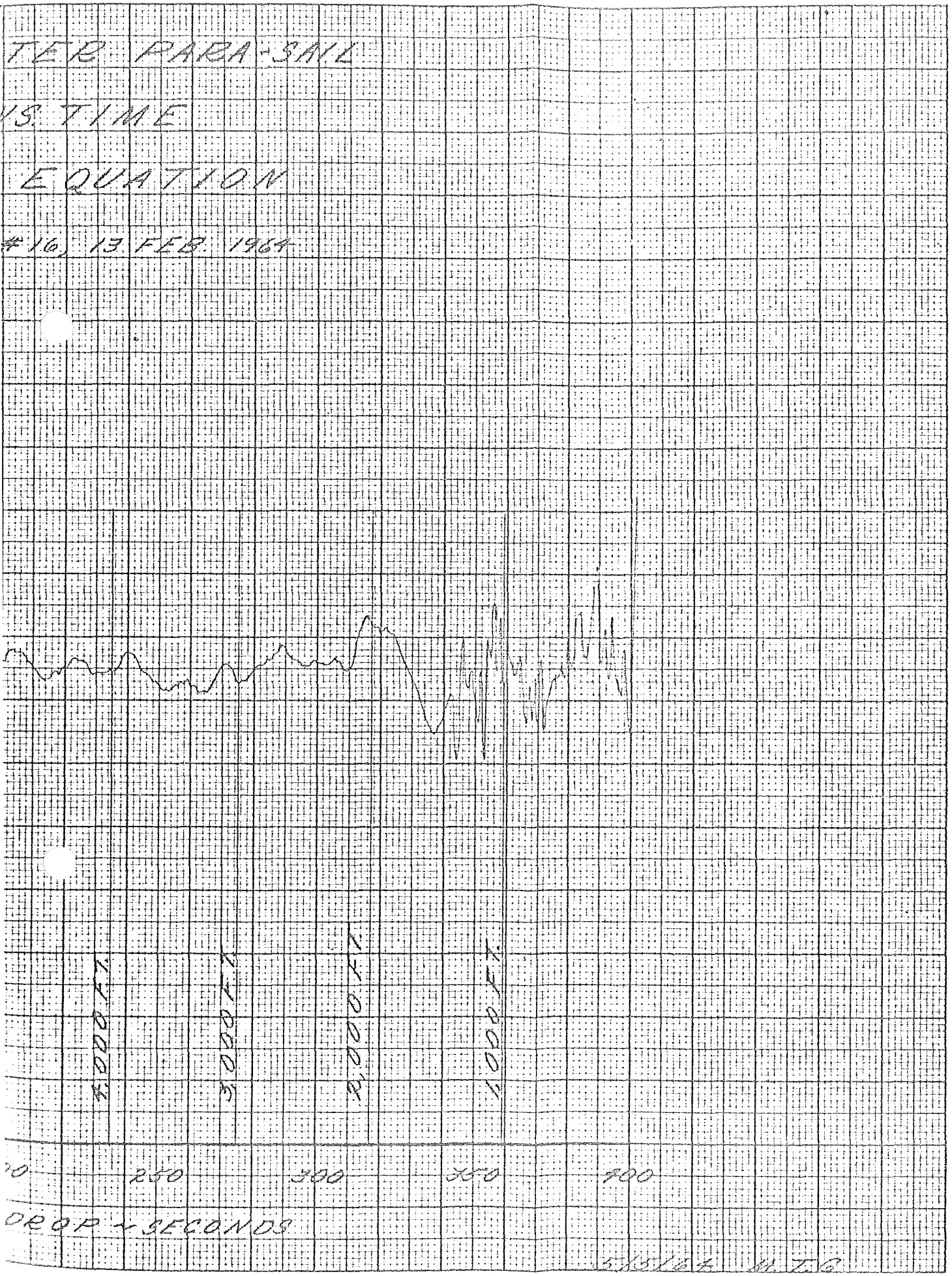
TER PARA-SAIL
VS. TIME
EQUATION
#16, 13 FEB. 1964
4,000 FT.
3,000 FT.
2,000 FT.
1,000 FT.
250
300
350
400
DROP - SECONDS

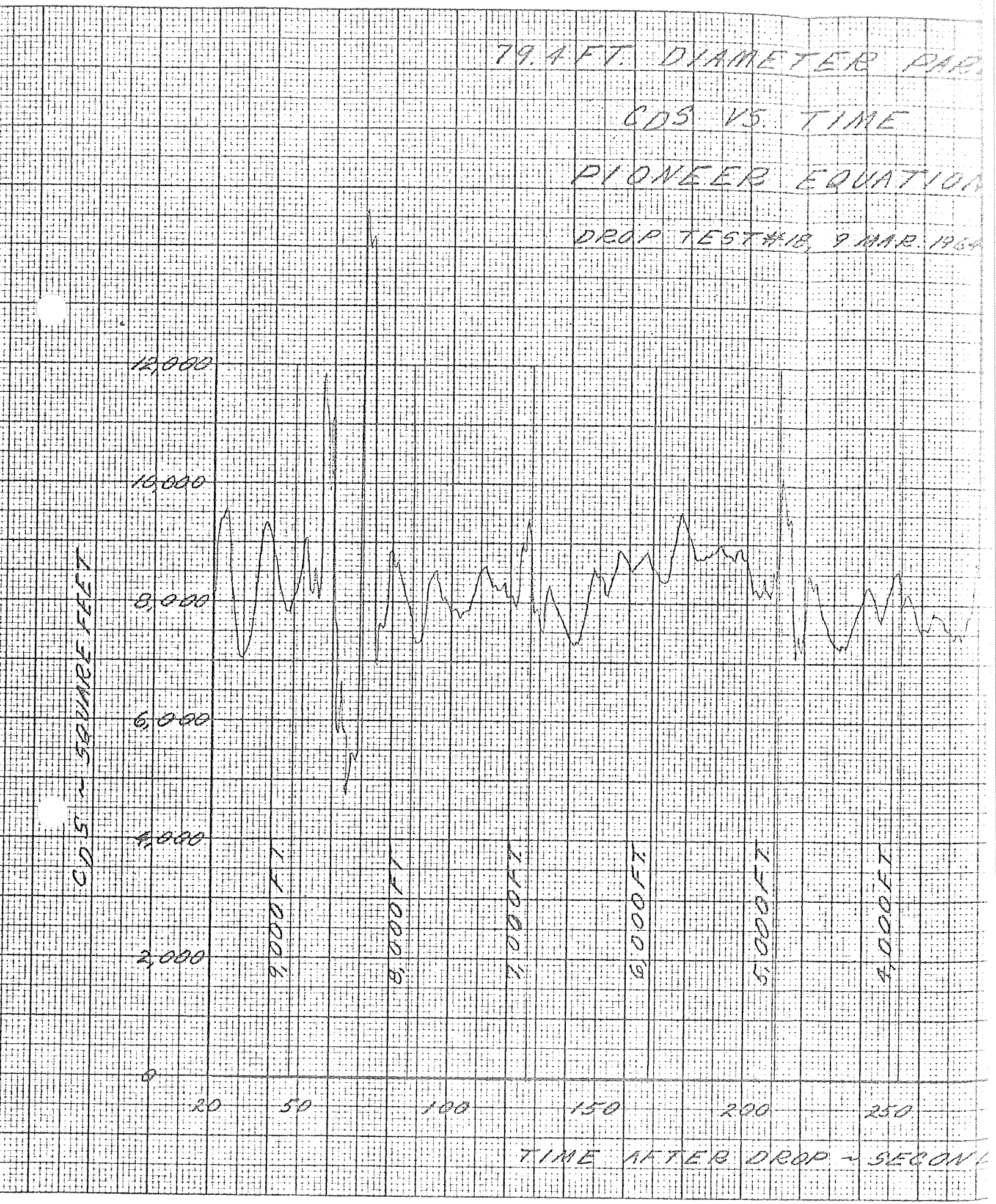
79.4 FT. DIAMETER PAR
CDS VS. TIME
PIONEER EQUATION
DROP TEST #18, 9 MAR. 196
12,000
10,000
8,000
6,000
4,000
2,000
0
CDS ~ SQUARE FEET
9,000 FT
8,000 FT
7,000 FT
6,000 FT
5,000 FT
4,000 FT
20
50
100
150
200
250
TIME AFTER DROP ~ SECON

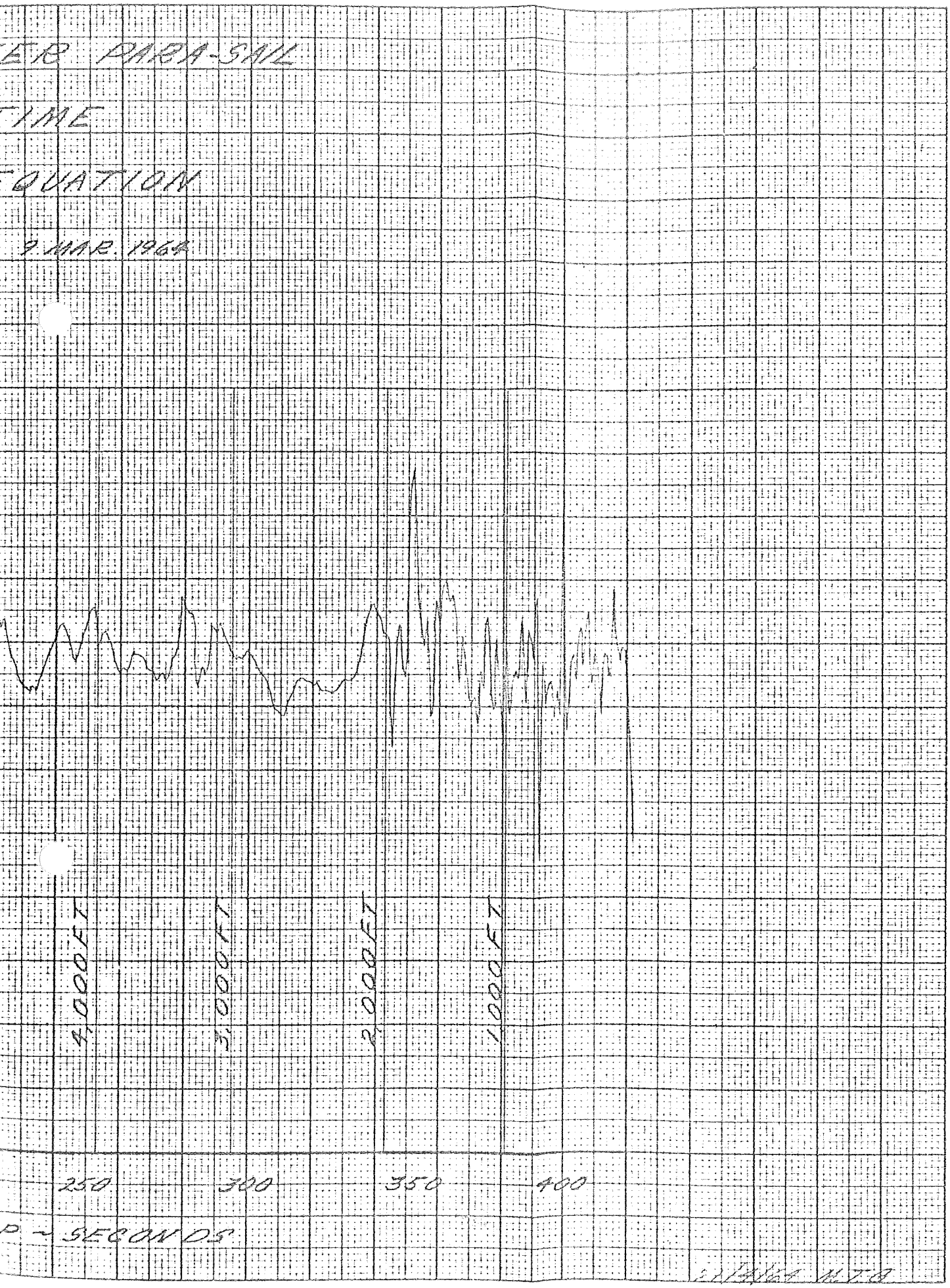
ER PARA-SAIL
TIME
QUATION
9 MAR. 1964
4,000 FT
3,000 FT
2,000 FT
1,000 FT
250
300
350
400
P - SECONDS

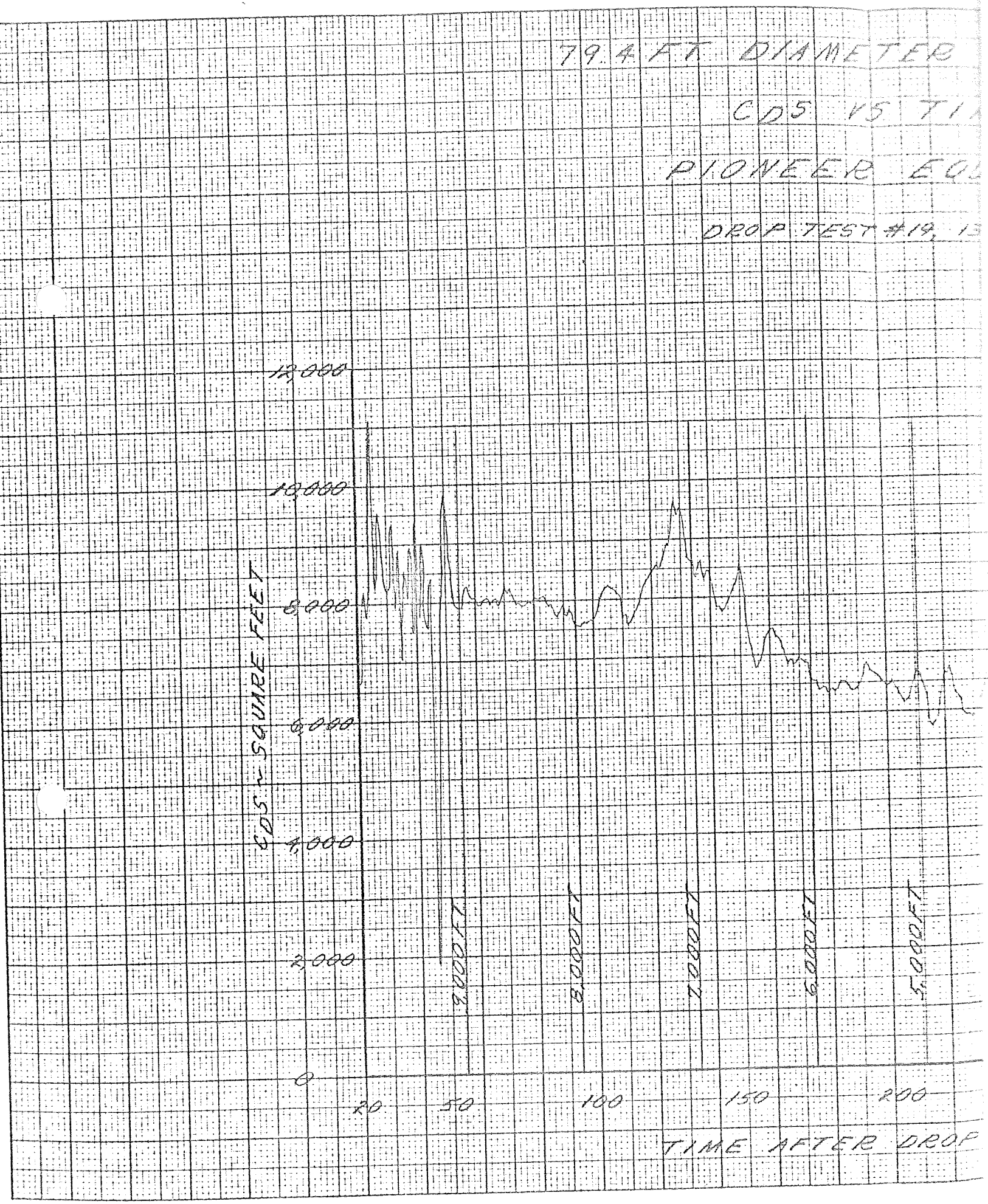
79.4 FT DIAMETER
CD5 VS TI
PIONEER EQ
DROP TEST #19, 1
12,000
10,000
8,000
6,000
4,000
2,000
0
CD5 ~ SQUARE FEET
9,000 FT
8,000 FT
7,000 FT
6,000 FT
5,000 FT
20
50
100
150
200
TIME AFTER DROP

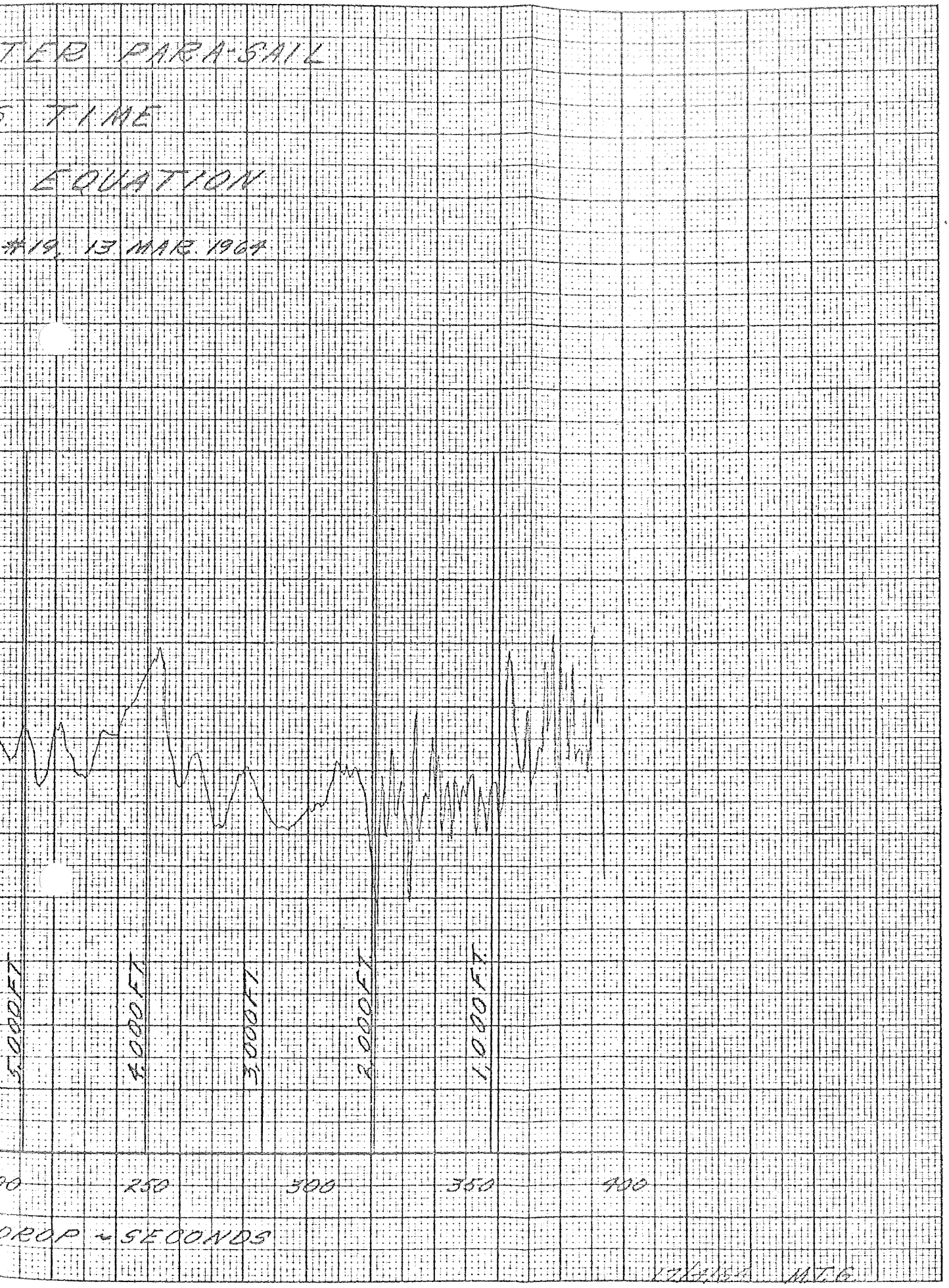
TER PARA-SAIL
S TIME
EQUATION
#19. 13 MAR. 1964
5,000 FT
4,000 FT
3,000 FT
2,000 FT
1,000 FT
250
300
350
400
ROP ~ SECONDS
M.T.G.

APPENDIX G

Para-Sail Lift/Drag Histories

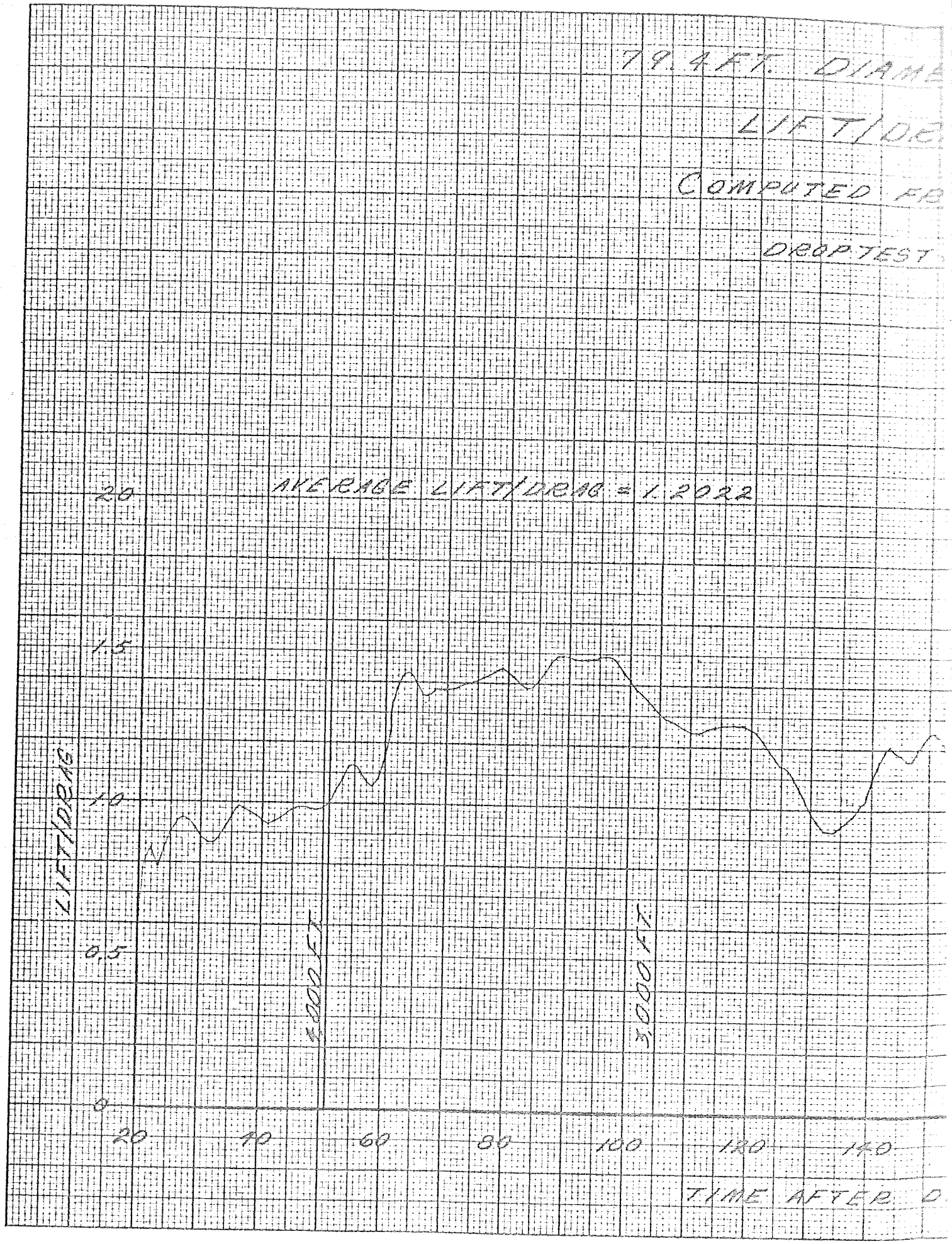
79.4 FT. DIAME
LIFT/DR
COMPUTED FR
DROP TEST
AVERAGE LIFT/DRAG = 1.2022
LIFT/DRAG
2.0
1.5
1.0
0.5
0
20
40
60
80
100
120
140
TIME AFTER D
2,000 FT.
3,000 FT.

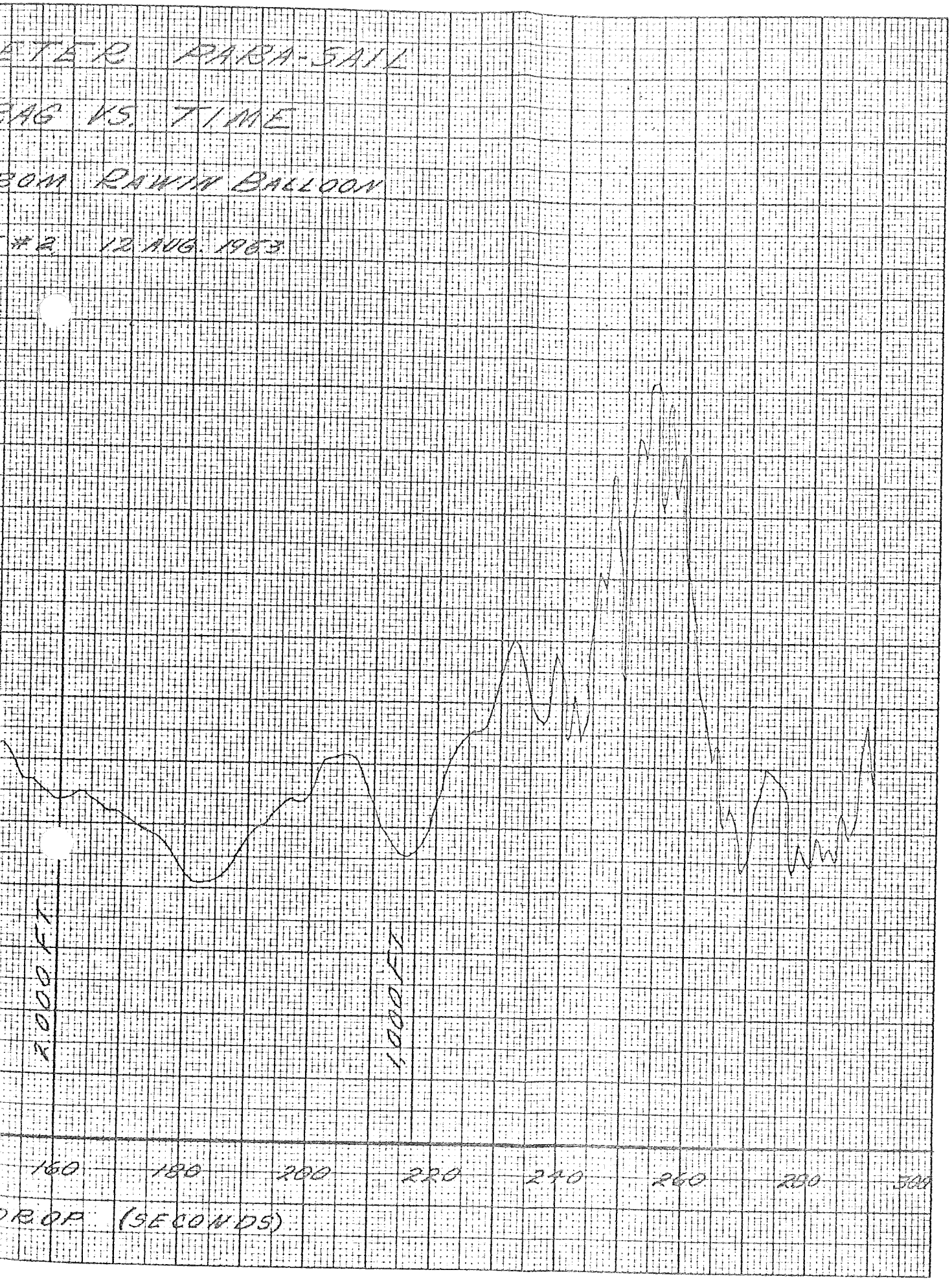
ATER PARA-SAIL
AG VS. TIME
OM RAWIN BALLOON
#2 12 AUG. 1963
2,000 FT
1,000 FT
160
180
200
220
240
260
280
300
ROP (SECONDS)

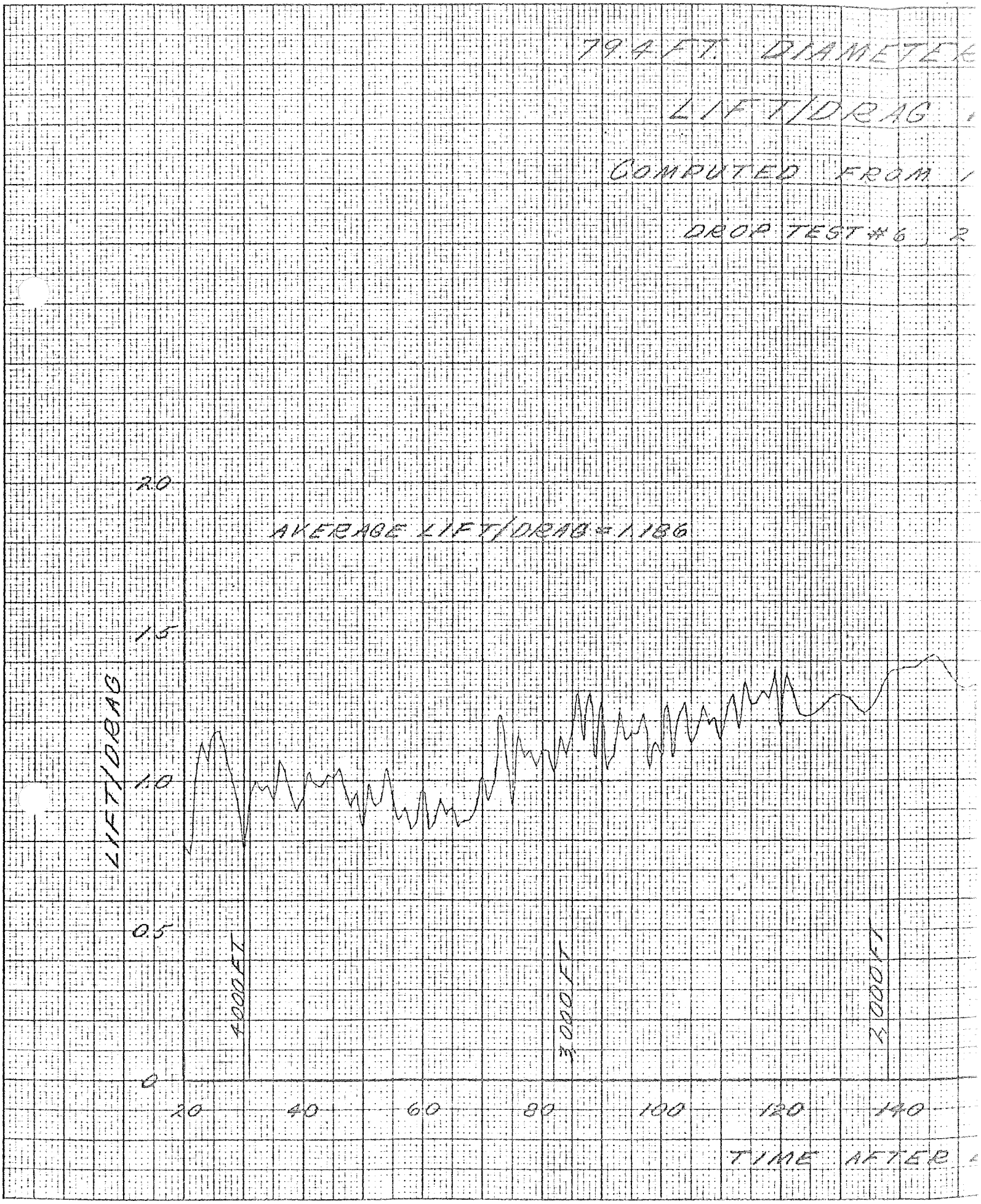
79.4 FT. DIAMETER
LIFT/DRAG
COMPUTED FROM
DROP TEST #6
AVERAGE LIFT/DRAG = 1.186
LIFT/DRAG
2.0
1.5
1.0
0.5
0
1000 FT
3000 FT
2000 FT
20
40
60
80
100
120
140
TIME AFTER

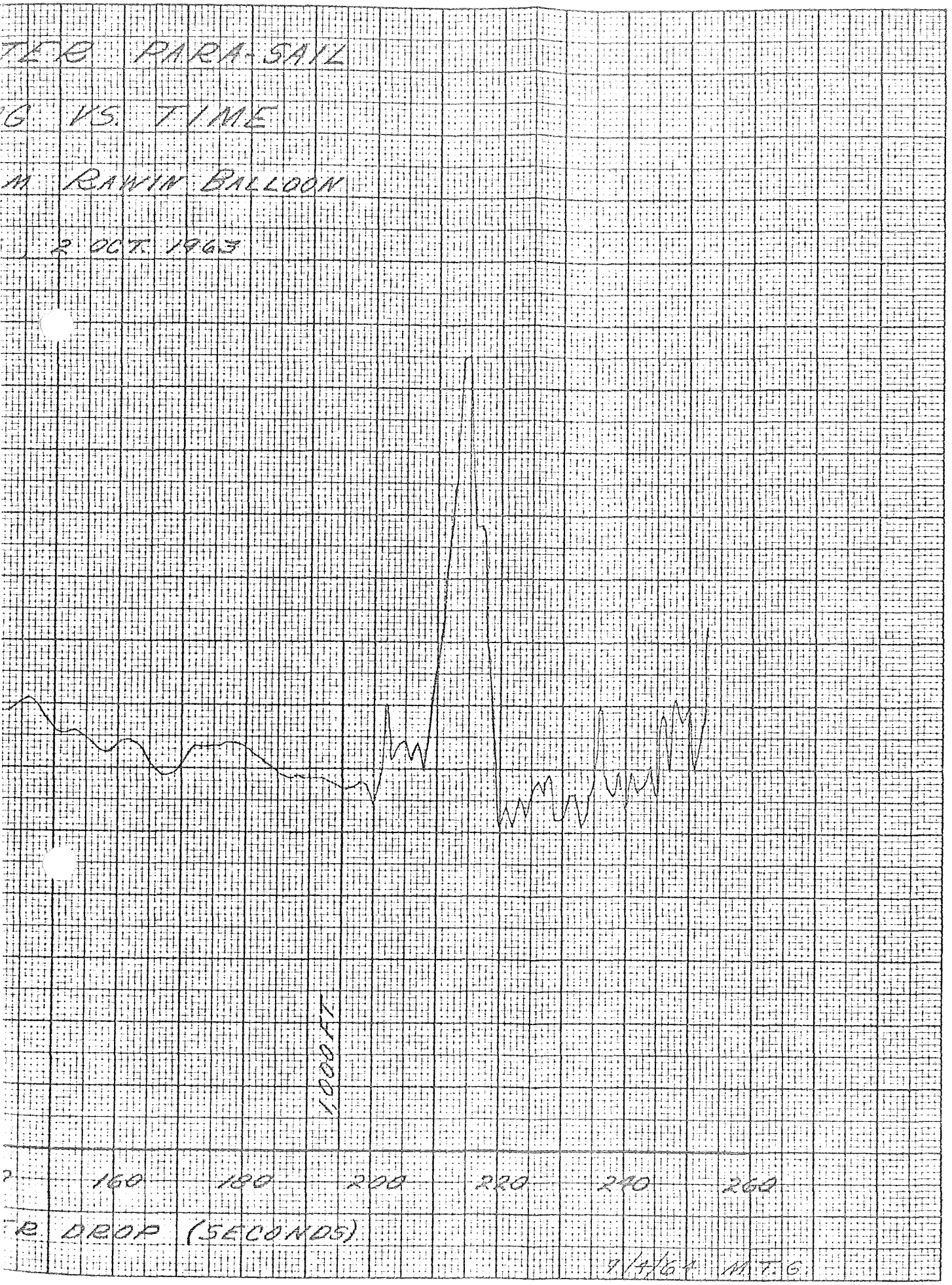
TER PARA-SAIL
G VS. TIME
M RAWIN BALLOON
2 OCT. 1963
1,000 FT
160
180
200
220
240
260
E DROP (SECONDS)
7/4/64 M.T.G.

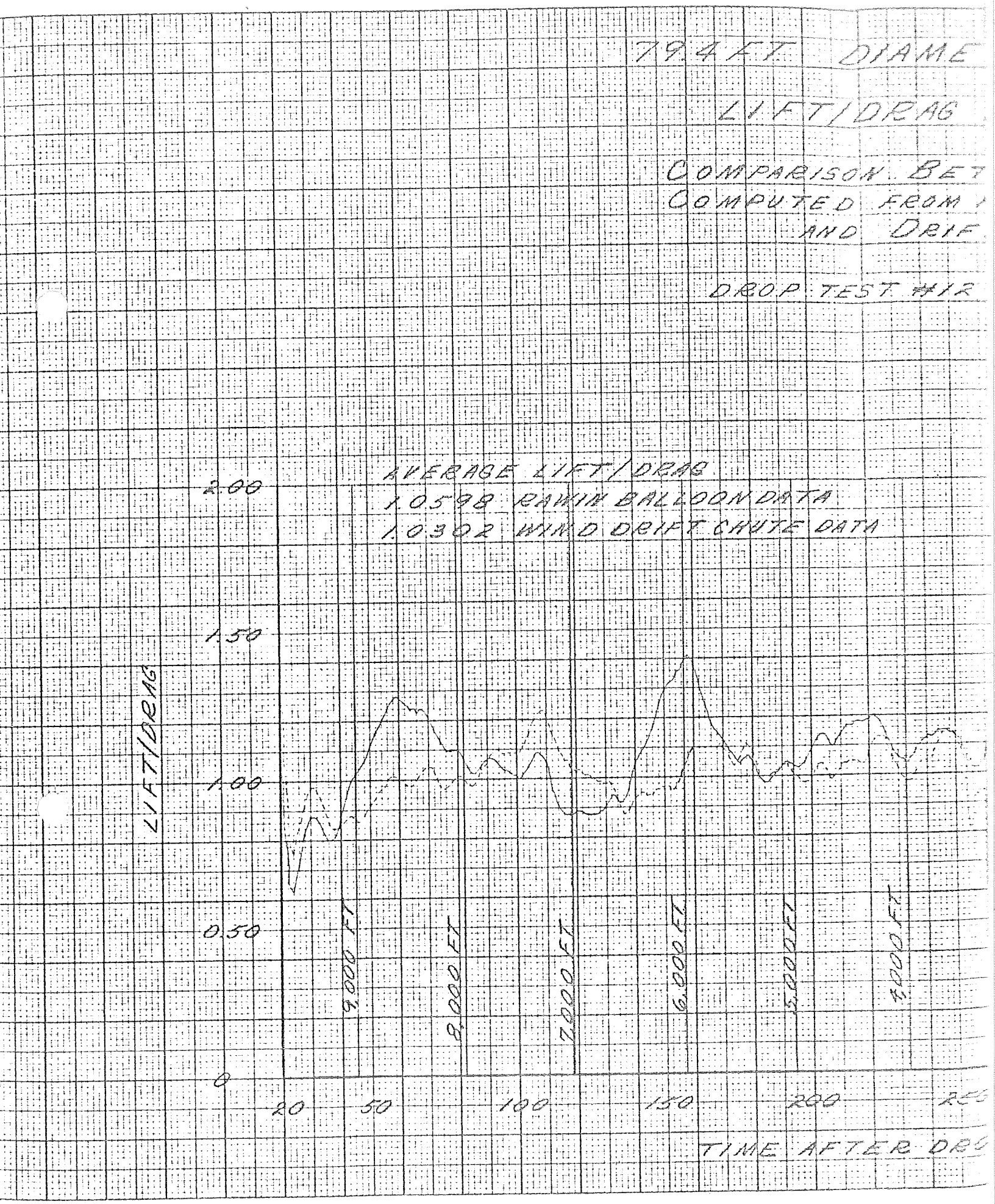
79.4 FT. DIAME
LIFT/DRAG
COMPARISON BET
COMPUTED FROM
AND DRIF
DROP TEST #12
AVERAGE LIFT/DRAG
1.0598 RAWIN BALLOON DATA
1.0302 WIND DRIFT CHUTE DATA
2.00
1.50
1.00
0.50
0
LIFT/DRAG
9,000 FT
8,000 FT
7,000 FT
6,000 FT
5,000 FT
4,000 FT
20
50
100
150
200
TIME AFTER DRO

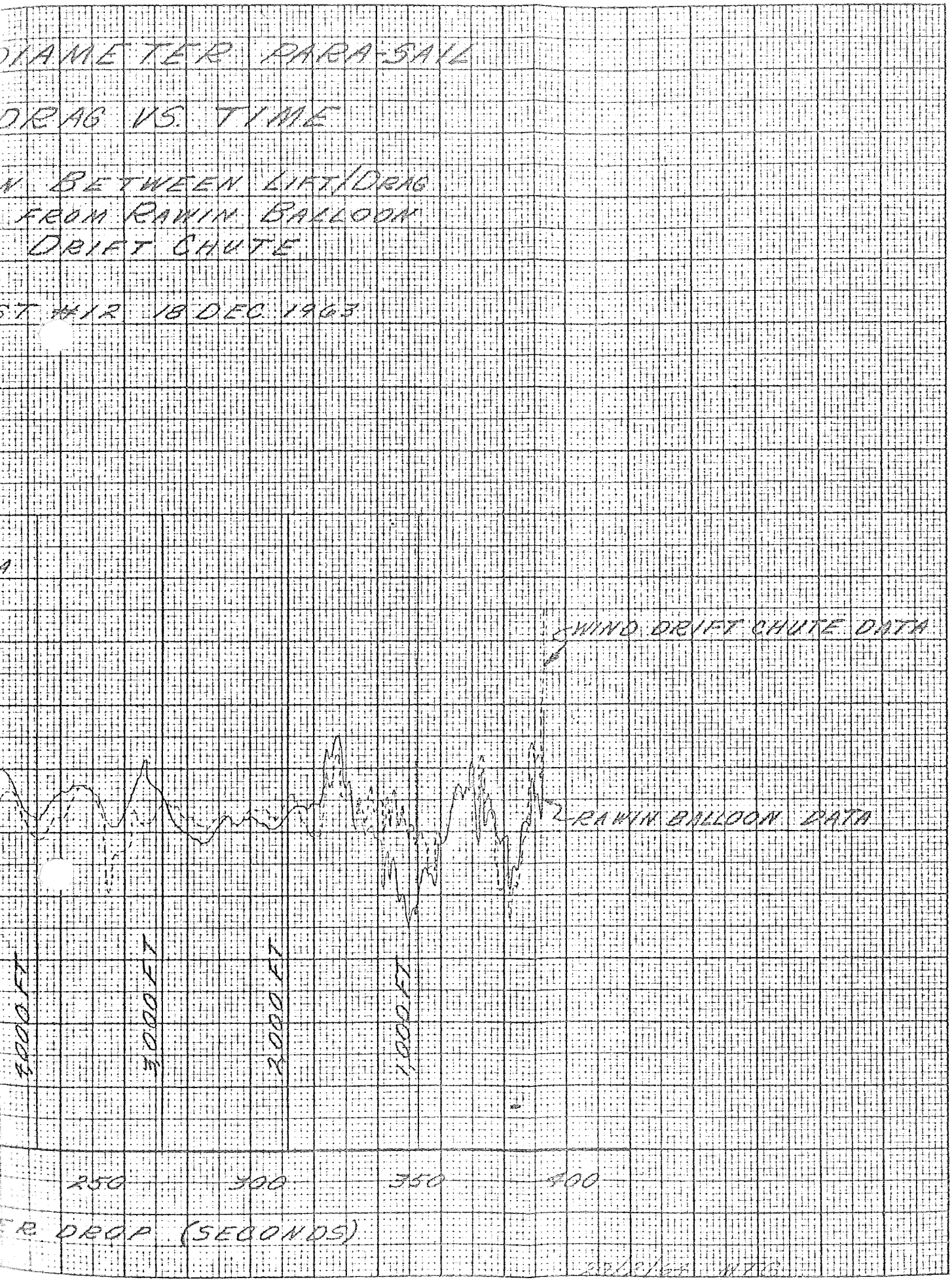
DIAMETER PARA-SAIL
DRAG VS. TIME
N BETWEEN LIFT/DRAG
FROM RAWIN BALLOON
DRIFT CHUTE
ST #12 18 DEC 1963
WIND DRIFT CHUTE DATA
RAWIN BALLOON DATA
4000 FT
3000 FT
2000 FT
1000 FT
250
300
350
400
R DROP (SECONDS)

79.4 FT. DIAMETER P

LIFT/DRAG VS. T

COMPUTED FROM RAWIN B

DROP TEST #16, 15 FE

AVERAGE LIFT/DRAG = 1.2156

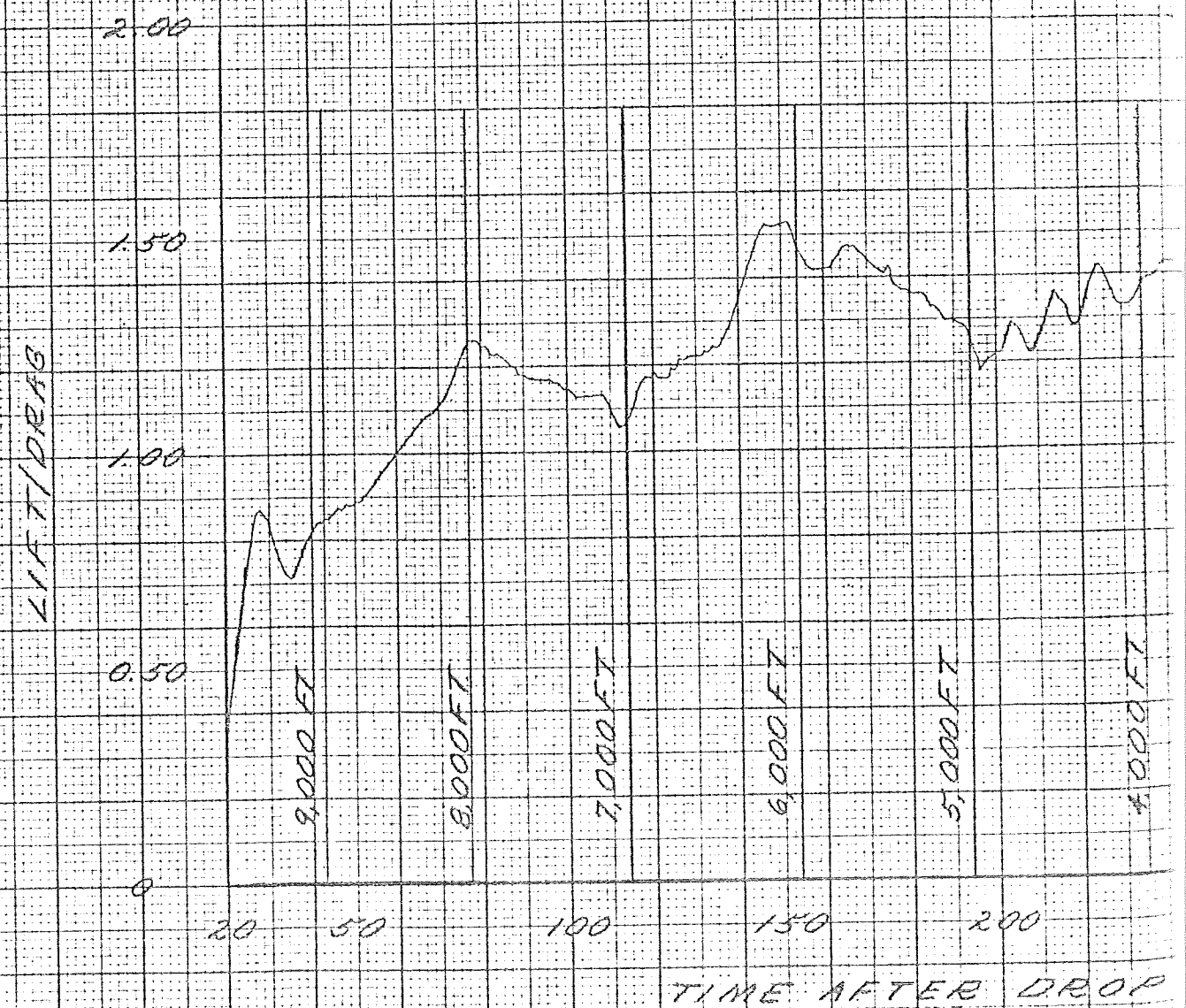

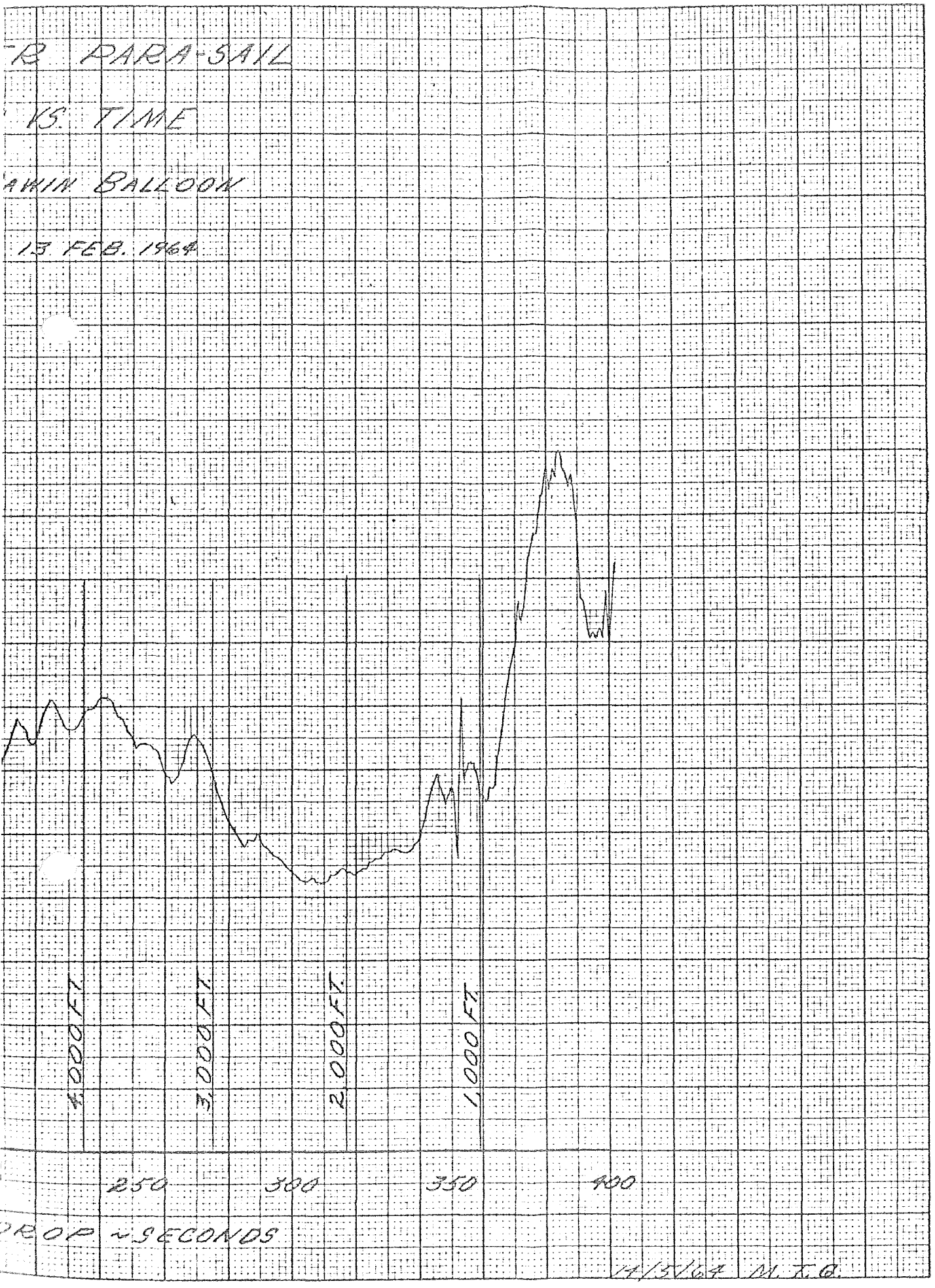
-R PARA-SAIL
KS. TIME
AKIN BALLOON
13 FEB. 1964
4,000 FT
3,000 FT
2,000 FT.
1,000 FT
250
300
350
400
ROP ~SECONDS
14/3/64 M.T.G.

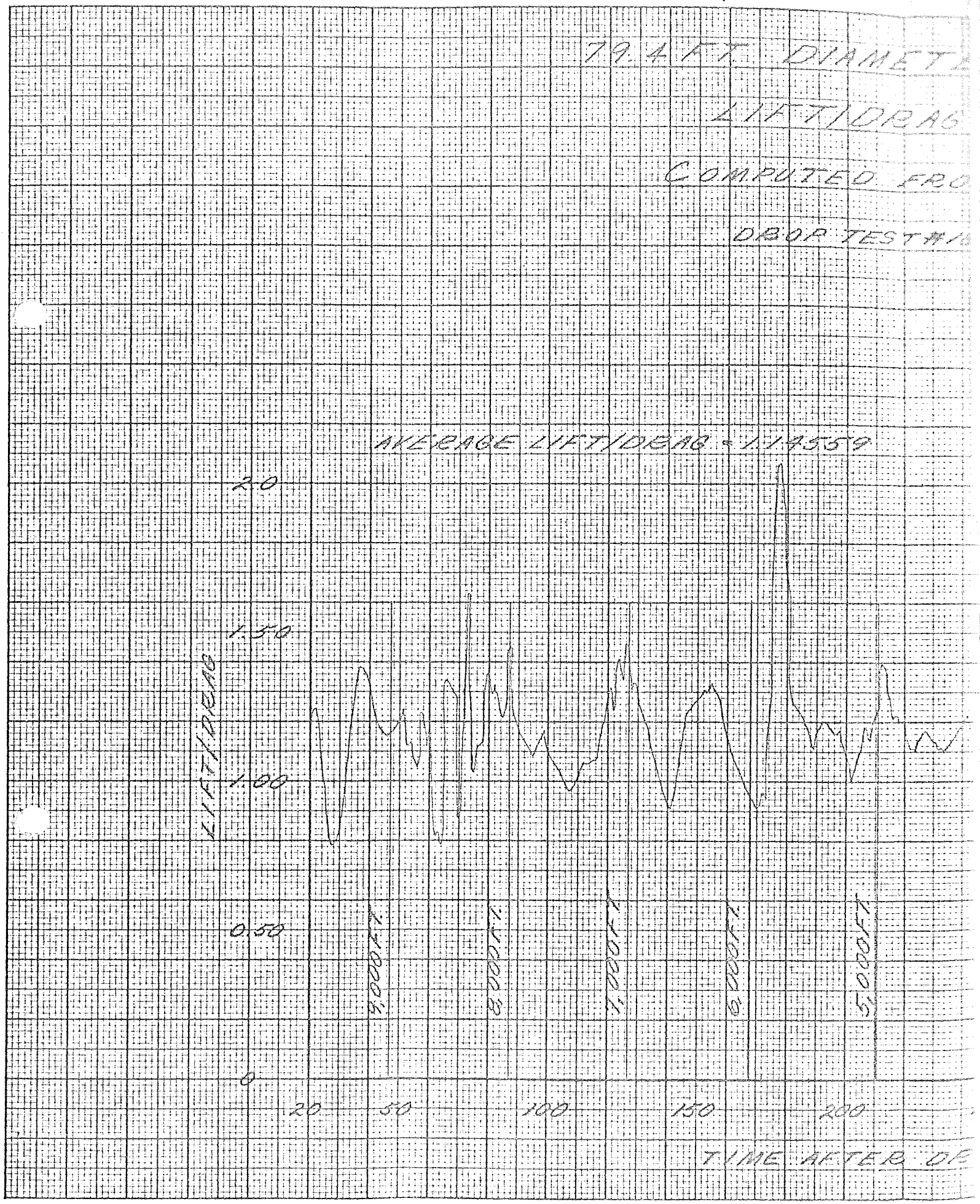
79.4 FT. DIAMETE
LIFT/DRAG
COMPUTED FRO
DROP TEST #1
AVERAGE LIFT/DRAG = 1.19559
2.0
1.50
1.00
0.50
0
LIFT/DRAG
9,000 FT.
8,000 FT.
7,000 FT.
6,000 FT.
5,000 FT.
20
50
100
150
200
TIME AFTER DR

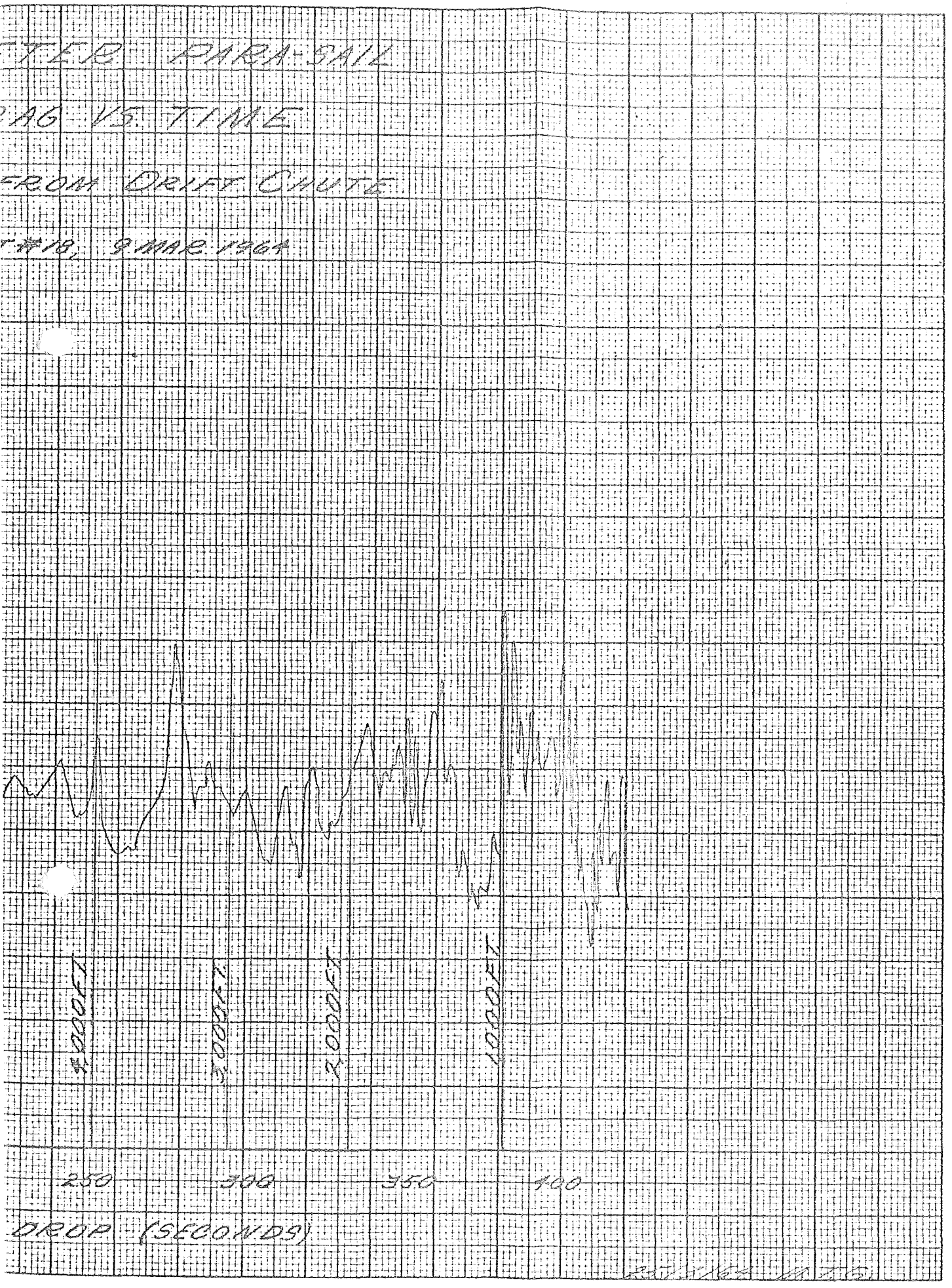
TFB PARA-SAIL
AG VS. TIME
FROM DRIFT CHUTE
T#18, 9 MAR 1964
4000FT
3000FT
2000FT
1000FT
250
300
350
400
DROP (SECONDS)

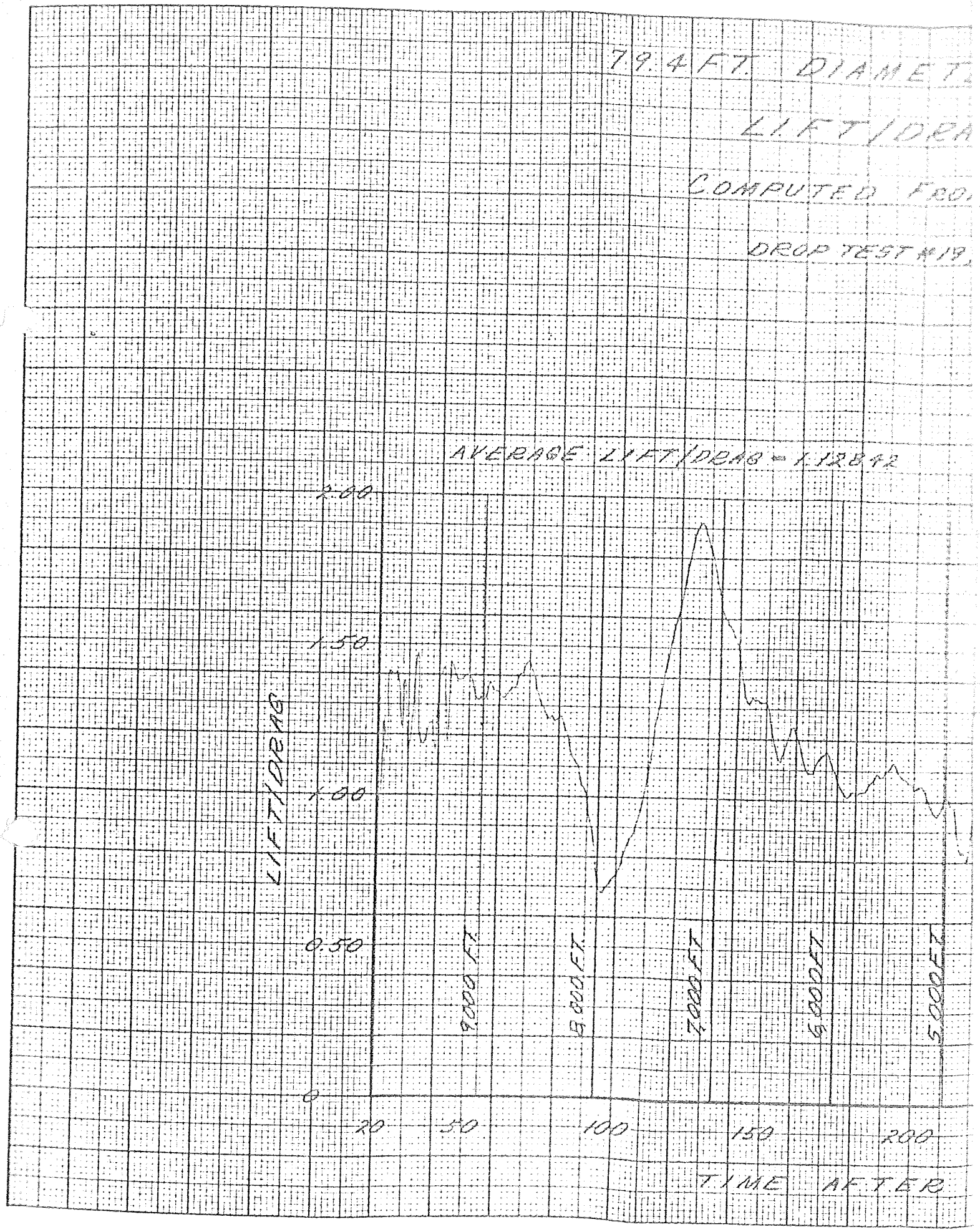
79.4 FT. DIAMET
LIFT/DRA
COMPUTED FRO
DROP TEST #19
AVERAGE LIFT/DRAG = 1.12842
2.00
1.50
1.00
0.50
0
LIFT/DRAG
9000 FT.
8000 FT.
7000 FT.
6000 FT.
5000 FT.
20
50
100
150
200
TIME AFTER

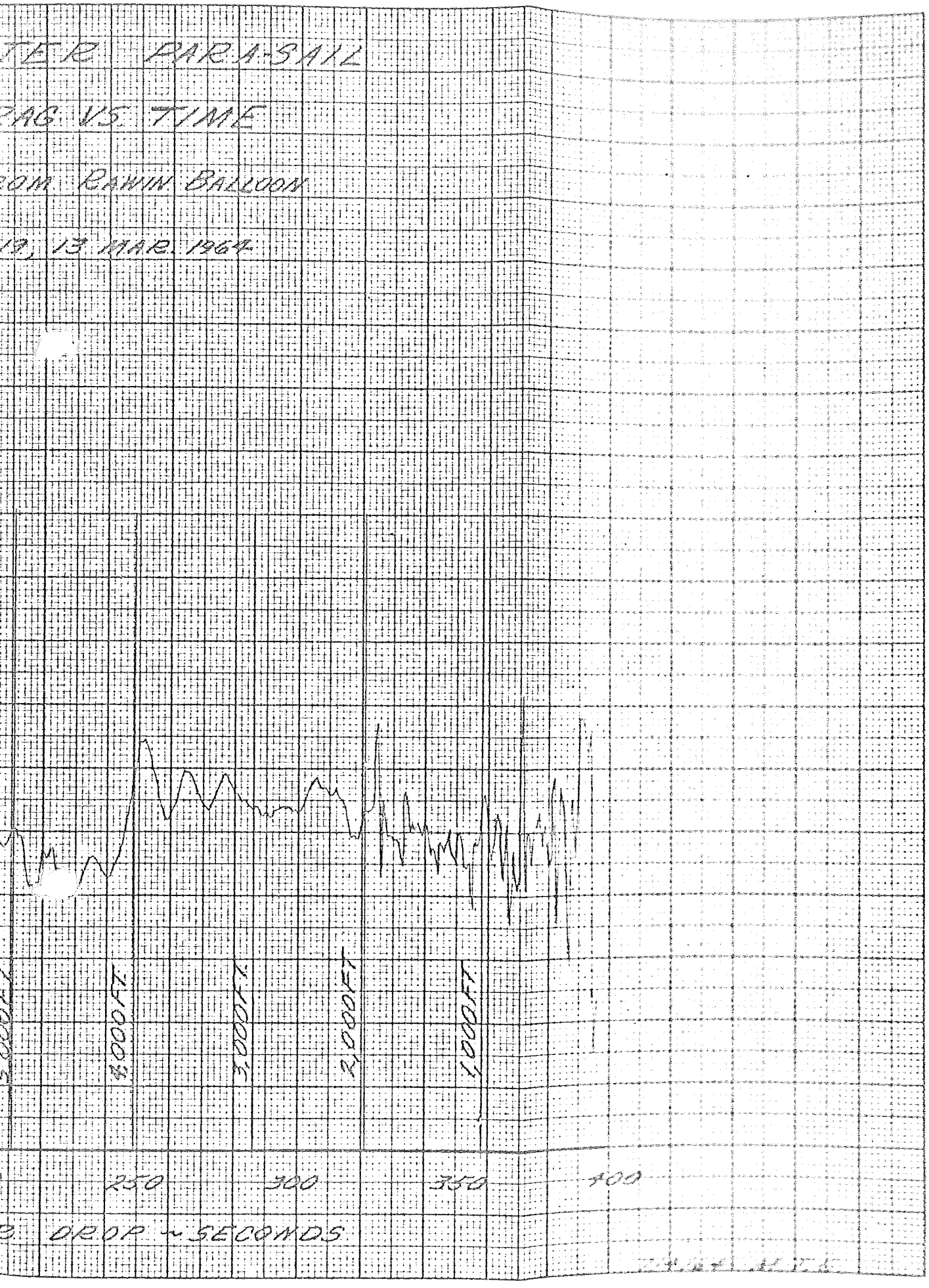
TER PARA-SAIL
PAG. VS TIME
OM RAWIN BALLOON
19, 13 MAR. 1964
4,000 FT.
3,000 FT.
2,000 FT.
1,000 FT.
250
300
350
400
DROP ~5 SECONDS